

WL-TR-91-3023

AD-A251 015



A FINITE ELEMENT PROCEDURE FOR ANALYSIS OF LAMINATED COMPOSITE PLATES

M. Moazzami, R.S. Sandhu and W.E. Wolfe
Department of Civil Engineering
The Ohio State University

June 18, 1991

Final Report for Period July 1985 - June 1990

Approved for public release; distribution unlimited

FLIGHT DYNAMICS DIRECTORATE
WRIGHT LABORATORY
AIR FORCE SYSTEMS COMMAND
WRIGHT-PATTERSON AIR FORCE BASE, OHIO 45433-6553

20070919069

NOTICE

When Government drawings, specifications, or other data are used for any purpose other than in connection with a definitely Government-related procurement, the United States Government incurs no responsibility or any obligation whatsoever. The fact that the Government may have formulated or in any way supplied the said drawings, specifications, or other data, is not to be regarded by implication, or otherwise in any manner construed, as licensing the holder, or any other person or corporation; or as conveying any rights or permission to manufacture, use, or sell any patented invention that may in any way be related thereto.

This report is releasable to the National Technical Information Service (NTIS). At NTIS, it will be available to the general public, including foreign nations.

This technical report has been reviewed and is approved for publication.

George A. Sendeckyj
GEORGE A. SENDECKYJ, Project Engineer
Fatigue, Fracture and Reliability Group
Structural Integrity Branch

John K. Ryde
JOHN K. RYDER, Capt, USAF
Technical Manager
Fatigue, Fracture and Reliability Group
Structural Integrity Branch

FOR THE COMMANDER

James L. Rudd

JAMES L. RUDD, Chief
Structural Integrity Branch
Structures Division

If your address has changed, if you wish to be removed from our mailing list, or if the addressee is no longer employed by your organization, please notify WL/FIBEC, WPAFB, OH 45433-6553 to help us maintain a current mailing list.

Copies of this report should not be returned unless return is required by security considerations, contractual obligations, or notice on a specific document.

UNCLASSIFIED

SECURITY CLASSIFICATION OF THIS PAGE

Form Approved
OMB No. 0704-0188

REPORT DOCUMENTATION PAGE

1a. REPORT SECURITY CLASSIFICATION Unclassified		1b. RESTRICTIVE MARKINGS None													
2a. SECURITY CLASSIFICATION AUTHORITY		3. DISTRIBUTION/AVAILABILITY OF REPORT Available for public release; distribution unlimited													
2b. DECLASSIFICATION/DOWNGRADING SCHEDULE															
4. PERFORMING ORGANIZATION REPORT NUMBER(S) RF Project 764779/717297		5. MONITORING ORGANIZATION REPORT NUMBER(S) WL-TR-91-3023													
6a. NAME OF PERFORMING ORGANIZATION The Ohio State University Research Foundation	6b. OFFICE SYMBOL (If applicable) OSURF	7a. NAME OF MONITORING ORGANIZATION Flight Dynamics Directorate (WL/FIBEC) Wright Laboratory													
6c. ADDRESS (City, State, and ZIP Code) 1960 Kenny Road Columbus, Ohio 43212		7b. ADDRESS (City, State, and ZIP Code) Wright-Patterson Air Force Base Dayton, Ohio 45433-6553													
8a. NAME OF FUNDING/SPONSORING ORGANIZATION Flight Dynamics Directorate	8b. OFFICE SYMBOL (If applicable) WL/FIBEC	9. PROCUREMENT INSTRUMENT IDENTIFICATION NUMBER Contract No. F33615-85-C-3213													
8c. ADDRESS (City, State, and ZIP Code) Wright-Patterson Air Force Base Dayton, Ohio 45433-6553		10. SOURCE OF FUNDING NUMBERS <table border="1"><tr><td>PROGRAM ELEMENT NO. 61102F</td><td>PROJECT NO. 2302</td><td>TASK NO. N1</td><td>WORK UNIT ACCESSION NO. 02</td></tr></table>		PROGRAM ELEMENT NO. 61102F	PROJECT NO. 2302	TASK NO. N1	WORK UNIT ACCESSION NO. 02								
PROGRAM ELEMENT NO. 61102F	PROJECT NO. 2302	TASK NO. N1	WORK UNIT ACCESSION NO. 02												
11. TITLE (Include Security Classification) A Finite Element Procedure for Analysis of Laminated Composite Plates															
12. PERSONAL AUTHOR(S) R.S. Sandhu, W.E. Wolfe and M. Moazzami															
13a. TYPE OF REPORT Final	13b. TIME COVERED FROM 7/1/85 TO 6/30/90	14. DATE OF REPORT (Year, Month, Day) 1991, June 18	15. PAGE COUNT 143												
16. SUPPLEMENTARY NOTATION															
17. COSATI CODES <table border="1"><tr><th>FIELD</th><th>GROUP</th><th>SUB-GROUP</th></tr><tr><td></td><td></td><td></td></tr><tr><td></td><td></td><td></td></tr><tr><td></td><td></td><td></td></tr></table>		FIELD	GROUP	SUB-GROUP										18. SUBJECT TERMS (Continue on reverse if necessary and identify by block number) Composite Laminates Delamination Discrete Plate Theory Finite Element Method Free-Edge Delamination	
FIELD	GROUP	SUB-GROUP													
19. ABSTRACT (Continue on reverse if necessary and identify by block number) <p>A variational formulation and finite-element implementation of the well-known discrete laminate theory of laminated composite plates is presented. To allow for varying properties of different layers with respect to the fixed reference frame used in the analysis, a linear variation of 'in-plane' displacements over each layer is assumed. The rate of variation can be different for each layer. The coupling between 'in-plane' and 'transverse' deformation is allowed for as is deformation due to shear. The mathematical model essentially assumes the laminated plate to be a stacking of Mindlin's orthotropic plates allowing for interfacial continuity of displacement. A finite element scheme implementing the foregoing concepts is described. Through the thickness, nodal points are used to reduce the problem to one of two-dimensional geometry. Three different interpolation schemes viz., the eight-point serendipity, the nine-point Lagrangian and the four-point Lagrangian are used in the isoparametric elements and their effectiveness is compared. The numerical procedure</p>															
20. DISTRIBUTION/AVAILABILITY OF ABSTRACT <input checked="" type="checkbox"/> UNCLASSIFIED/UNLIMITED <input type="checkbox"/> SAME AS RPT. <input type="checkbox"/> DTIC USERS		21. ABSTRACT SECURITY CLASSIFICATION Unclassified													
22a. NAME OF RESPONSIBLE INDIVIDUAL George P. Sendeckyj		22b. TELEPHONE (Include Area Code) 513-255-6104	22c. OFFICE SYMBOL WL/FIBEC												

UNCLASSIFIED

SECURITY CLASSIFICATION OF THIS PAGE

19. ABSTRACT (continued)

is verified against available solutions and then applied to analysis of stresses in a multi-ply free-edge delamination specimen. The procedure does not satisfy the traction-free edge condition and, therefore, the approach cannot be used to predict delamination and its growth.

FOREWORD

This report covers part of the work done during the period July 1, 1985 to June 30, 1990 under U.S. Air Force Systems Command/Wright Laboratory Grant F33615-85-C-3213 to The Ohio State University. The Program Manager was Dr. George P. Sendeckyj of the Flight Dynamics Directorate(WL/FIBEC). The research was carried out at The Ohio State University by Mr. Mehdi Moazzami under the supervision of Drs. Ranbir S. Sandhu and William E. Wolfe, Professors of Civil Engineering.

The Ohio State University Instruction and Research Computer Center provided the computational as well as documentation facilities.

CONTENTS

FOREWORD	iii
Section I: INTRODUCTION	1
Section II: BENDING AND STRETCHING OF LAMINATED PLATES	3
INTRODUCTION	3
EQUATIONS GOVERNING BENDING AND STRETCHING OF LAMINATED PLATES	4
Introduction	4
Kinematics	5
Equilibrium Equations	7
Constitutive Equations	10
Stress-Strain Relations for Linear Elastic Materials	10
Constitutive Relations for Force and Moment Resultants	12
The Interlaminar Continuity Equations	13
Summary of Field Equations in Convolution Form	13
Self-adjointness of the Operator Matrix	17
Consistent Boundary Conditions	18
VARIATIONAL FORMULATION OF THE PROBLEM	20
The Basic Variational Formulation	20
Extended Variational Formulation	26
Some Specialization	33
Section III: FINITE ELEMENT FORMULATION	41
INTRODUCTION	41
FINITE ELEMENT DISCRETIZATION	41
SOLUTION PROCESS	49
Section IV: VERIFICATION AND APPLICATIONS	51
PROBLEM DESCRIPTION	51
Analysis of Plates	53
Analysis of Four-Ply Free-Edge Delamination Specimens	56
Results of the Analysis	58
Analysis of 22-Layer Free-Edge Delamination Specimen	96
Summary and Conclusions	121

Section V: DISCUSSION	122
REFERENCES	126
Appendix A: VARIATIONAL FORMULATION	128
PRELIMINARIES	128
Boundary Value Problem	128
Bilinear Mapping	129
Self-Adjoint Operator	129
Gateaux Differential	130
THEOREM	130
LINEAR COUPLED PROBLEMS	131
Appendix B: SOLUTION OF SANDWICH PLATE	132
PRELIMINARIES	132
METHOD OF SOLUTION	133

FIGURES

1.	Configuration of a multilayer composite plate.	6
2.	Four, eight, and nine-noded quadrilateral element used.	52
3.	Mesh configuration and boundary conditions for a quarter plate.	55
4.	Configuration for laminated coupon under uniaxial tension.	57
5.	Sequence of mesh refinement across the width.	59
6.	Sequence of refinement across the width with a thinner edge element. . . .	60
7.	Sequence of refinements over the thickness.	61
8.	Number of subdomains along each side vs central deflection of a square isotropic simply supported plate with No. of elements =	62
9.	CPU time vs error in central deflection with mesh refinement-isotropic layers.	63
10.	Central deflection of a square orthotropic simply supported sandwich plate.	64
11.	CPU time vs error in central deflection with mesh refinement-orthotropic layers.	65
12.	X-stress at the mid-surface of the top lamina with refinement in y-direction; Angle-ply specimen.	70
13.	X-stress at the mid-surface of the top lamina with refinement in x-direction; Angle-ply specimen.	71
14.	X-stress at midsurface of the top layer with refinement in x-direction; Angle-ply specimen, using edge elements.	72
15.	X-stress at midsurface of top layer with thickness refinement; Angle-ply specimen.	73
16.	XY-stress at midsurface of top layer with refinement in y-direction; Angle-ply specimen.	74
17.	XY-stress at midsurface of top layer with refinement in x-direction; Angle-ply specimen.	75
18.	XY-stress at midsurface of top layer with refinement in x-direction; Angle-ply specimen.	76
19.	XZ-stress at z=h with refinement in y-direction; Angle-ply specimen.	77
20.	XZ-stress at z=h with refinement in x-direction; Angle-ply specimen.	78

21.	XZ-stress at z=h with refinement in x-direction; Angle-ply specimen.	79
22.	XY-stress at the mid-surface of the top layer with thickness refinement; Angle-ply specimen.	80
23.	XZ-stress at z=h with thickness refinement; Angle-ply specimen.	81
24.	X-stress for N=2, Q4, Q8, and Q9 elements.	84
25.	X-stress for N=6, Q4, Q8, and Q9 elements.	85
26.	X-stress for N=10, Q4, Q8, and Q9 elements.	86
27.	XY-stress for N=2, Q4, Q8, and Q9 elements.	87
28.	XY-stress for N=6, Q4, Q8, and Q9 elements.	88
29.	XY-stress for N=10, Q4, Q8, and Q9 elements.	89
30.	XZ-stress at z=h for N=2, Q4, Q8, and Q9 elements.	90
31.	XZ-stress at z=h for N=6, Q4, Q8, and Q9 elements.	91
32.	XZ-stress at z=h for N=10, Q4, Q8, and Q9 elements.	92
33.	Longitudinal displacement at U(L/2,y,2h) of Q8 element, N=2,6 and 10.	93
34.	Longitudinal displacement at U(L/2,y,2h) of Q9 element, N=2, and 6.	94
35.	Longitudinal displacement at U(L/2,y,2h) of Q4 element, N=2, and 6.	95
36.	YZ-stress at z=h with mesh refinement in y-direction; Cross-ply specimen.	97
37.	YZ-stress at z=h with mesh refinement in x-direction; Cross-ply specimen.	98
38.	YZ-stress at z=h for (11x17) mesh in case of N=2, N=6, and N=10; Cross-ply specimen.	99
39.	Cross-section of the upper half of the 22-layer coupon.	102
40.	Y-stress at R1 for 22-layer coupon.	103
41.	Y-stress at R5 for 22-layer coupon.	104
42.	X-stress at R1 for 22-layer coupon.	105
43.	XY-stress at R11 for 22-layer coupon.	106
44.	ZX-stress at R1 for 22-layer coupon.	107
45.	ZX-stress at R5 for 22-layer coupon.	108

46.	ZX-stress at R6 for 22-layer coupon.	109
47.	ZX-stress at R11 for 22-layer coupon.	110
48.	YZ-stress at R5 for 22-layer coupon.	111
49.	YZ-stress at R6 for 22-layer coupon.	112
50.	YZ-stress at R11 for 22-layer coupon.	113
51.	Through the thickness distribution of Z-stress at $y/b=0.995$ for the 22-layer coupon.	114
52.	Through the thickness distribution of XZ-stress at $y/b=0.995$ for the 22-layer coupon.	115
53.	Through the thickness distribution of YZ-stress at $y/b=0.995$ for the 22-layer coupon.	116
54.	Z-stress at R1 for 22-layer coupon.	117
55.	Z-stress at R5 for 22-layer coupon.	118
56.	Z-stress at R6 for 22-layer coupon.	119
57.	Z-stress at R11 for 22-layer coupon.	120

TABLES

1. Numerical values for maximum deflection and the corresponding CPU time for different types of elements.(Isotropic case) 66
2. Numerical values for maximum deflection and the corresponding CPU time for different types of elements.(Orthotropic case) 67
3. Comparison of CPU time on X-MP/28 for Q4, Q8, and Q9 elements. 83

Section I

INTRODUCTION

An objective of the present research program was to develop a finite-element based procedure for analysis of free-edge delamination specimens using through-the-thickness elements and including both stretching and bending effects. This necessitates the use of multilayer plate theories which can simultaneously consider bending and stretching. Multilayer plate theories have been developed using assumptions on displacements or on stresses. The former class of theories may be classified into two groups, viz.,

1. Theories based upon assumed variation of displacement as a polynomial in the transverse coordinate over the entire thickness.
2. Theories based on assumption of piecewise linear variation of displacements over the thickness with 'nodes' at the interfacial surfaces.

The first group of the displacement theories has been found to be inadequate for representation of behavior of composite laminates where the material properties along fiber are significantly different from those in the directions across fiber. The second group of theories, called the discrete laminate theories, apparently is a better candidate for further consideration. These discrete laminate theories have been described by Srinivas [1] and Sun and Whitney [2], among others, and solution schemes have been proposed. However, for arbitrary geometry and a large number of layers one has to resort to numerical procedures. The finite element method has been extensively used for the analysis of plates (e.g. Reddy [3] and [4], Davis [5] among others).

Davis and Mawenya [5] proposed a general finite element formulation using quadratic, isoparametric, multilayer plate elements which allowed layers to deform

locally with no restriction imposed on the relative properties of the constituent layers. Since this formulation considers the transverse shear deformation in all layers, it is applicable to any arbitrarily layered plate. However, the stresses are discontinuous across the interfaces.

As a starting point in the present research program, Davis and Mawenya's approach was used to develop a finite element solution for analysis of laminated plates. Davis and Mawenya did not give details of the theoretical and numerical formulation they used. In this report, the theory is restated in variational form, and an extension of the general variational theory is specialized for implementation in a finite element computer program. Its effectiveness for analysis of plates and also its inadequacy in modelling stresses in free-edge delamination specimens are noted.

Section II contains a summary of the equations governing bending and stretching of laminated plates. In this section, the kinematic, equilibrium, and constitutive equations for a lamina are derived based on an extension of Mindlin's theory of plates. The displacement field is assumed such that the rotation of each lamina is an additional variable independent of transverse deflection. The set of coupled field equations and interlaminar continuity conditions is written as a self-adjoint matrix of operators. Consistent boundary conditions are identified, and a general variational formulation for the purpose of finite element approximation to the problem is developed. Section III discusses the finite element formulation and computer implementation of the theory. Some illustrative examples and comparisons of results against some alternative solution schemes are discussed in section IV. This section also includes application of the procedure developed to analyse a multi-layer free-edge delamination specimen.

Section II

BENDING AND STRETCHING OF LAMINATED PLATES

2.1 INTRODUCTION

Structural elements composed of an arbitrary number of orthotropic layers can be approximated by finite element procedures. In these composite elements, each layer may have different thickness and/or elastic properties and different orientation of axes of material symmetry. In the following, we summarize the governing equations for bending of plates based on the following assumptions.

1. Loads are carried primarily by bending and stretching of the plate.
2. Sliding of one layer past another is impossible.
3. Plane sections normal to the undeformed surface of each layer remain plane but not necessarily normal in the deformed configuration and the in-plane displacements vary linearly over each layer.
4. The transverse displacement is independent of the transverse coordinate i.e. the transverse strain vanishes.
5. Deformations and rotations are small and the material is linear elastic so that the linear theory of elasticity is applicable.

Since the neutral axis is a priori unknown, bending and stretching are coupled with respect to an arbitrary plane of reference.

With the above assumptions, using the rectangular Cartesian reference frame, the kinematic field variables consist of three displacement components for an arbitrary point on a reference surface defined by a constant value of the transverse coordinate in the reference (undeformed) configuration along with the values of the rotations of

segments of the ray along the transverse axis through this point defined by intersection with interlaminar surfaces. The number of field variables, therefore, is $2m+3$ where m is the total number of layers.

2.2 EQUATIONS GOVERNING BENDING AND STRETCHING OF LAMINATED PLATES

2.2.1 Introduction

The generalized equilibrium equations represent the integral, over the thickness, of the three-dimensional equilibrium equations and of the first moment of the equilibrium equation. The constitutive equations are stated for a linear elastic monoclinic material. For implementation in a Ritz type finite element approximation procedure, the problem is formulated as a set of self-adjoint field equations with consistent boundary operators. The index notation is used throughout. Latin indices take on the range of values 1, 2, and 3 whereas Greek indices take values 1 and 2. Subscripts following a subscripted comma denote partial differentiation with respect to the coordinates defined by the subscripts. Summation on repeated indices is implied except where indicated otherwise. A pair of indices within parentheses denotes the symmetric part of the tensor described by the subscripts and a single super- or subscript within parentheses denotes 'no sum' on that index.

The actual displacement vector at any point is a function of the coordinates (x_i) of the plate. Assumption of transverse displacement being independent of the transverse coordinate x_3 makes it a function of (x_α) only.

2.2.2 Kinematics

Components of the displacement vector for each lamina, assuming linear variation of inplane displacement over the thickness of the lamina (Fig. 1), can be stated in the form:

$$u_{\alpha}^{(k)}(x_i) = v_{\alpha}^{(k)}(x_{\beta}) + x_3^{(k)} \phi_{\alpha}^{(k)}(x_{\beta}) \quad (1)$$

$$u_3^{(k)}(x_i) = u_3^{(k)}(x_{\alpha}) = u_3(x_{\alpha})$$

Here a rectangular Cartesian frame of reference is used. $u_i^{(k)}$ are components of the displacement vector, and $v_{\alpha}^{(k)}$ are the 'inplane' displacements at the kth interface. $\phi_{\alpha}^{(k)}$ are the components of the rotation of the kth layer in the $\alpha-3$ planes. For infinitesimal elastic deformation i.e., $\frac{\partial u_i}{\partial x_j} \ll 1$, the strain-displacement relationship is:

$$\epsilon_{ij} = \frac{1}{2}(u_{i,j} + u_{j,i}) = u_{(i,j)} \quad (2)$$

Therefore,

$$\begin{aligned} \epsilon_{\alpha\beta}^{(k)} &= v_{(\alpha,\beta)}^{(k)} + x_3^{(k)} \phi_{(\alpha,\beta)}^{(k)} = e_{\alpha\beta}^{(k)} + x_3^{(k)} \kappa_{\alpha\beta}^{(k)} \\ \epsilon_{\alpha 3}^{(k)} &= \frac{1}{2}(u_{3,\alpha}^{(k)} + \phi_{\alpha}^{(k)}) \\ \epsilon_{33}^{(k)} &= \epsilon_{33} = 0 \end{aligned} \quad (3)$$

where

$$\begin{aligned} e_{\alpha\beta}^{(k)} &= v_{(\alpha,\beta)}^{(k)} = \frac{1}{2}(v_{\alpha,\beta}^{(k)} + v_{\beta,\alpha}^{(k)}) \\ \kappa_{\alpha\beta}^{(k)} &= \phi_{(\alpha,\beta)}^{(k)} = \frac{1}{2}(\phi_{\alpha,\beta}^{(k)} + \phi_{\beta,\alpha}^{(k)}) \end{aligned} \quad (4)$$

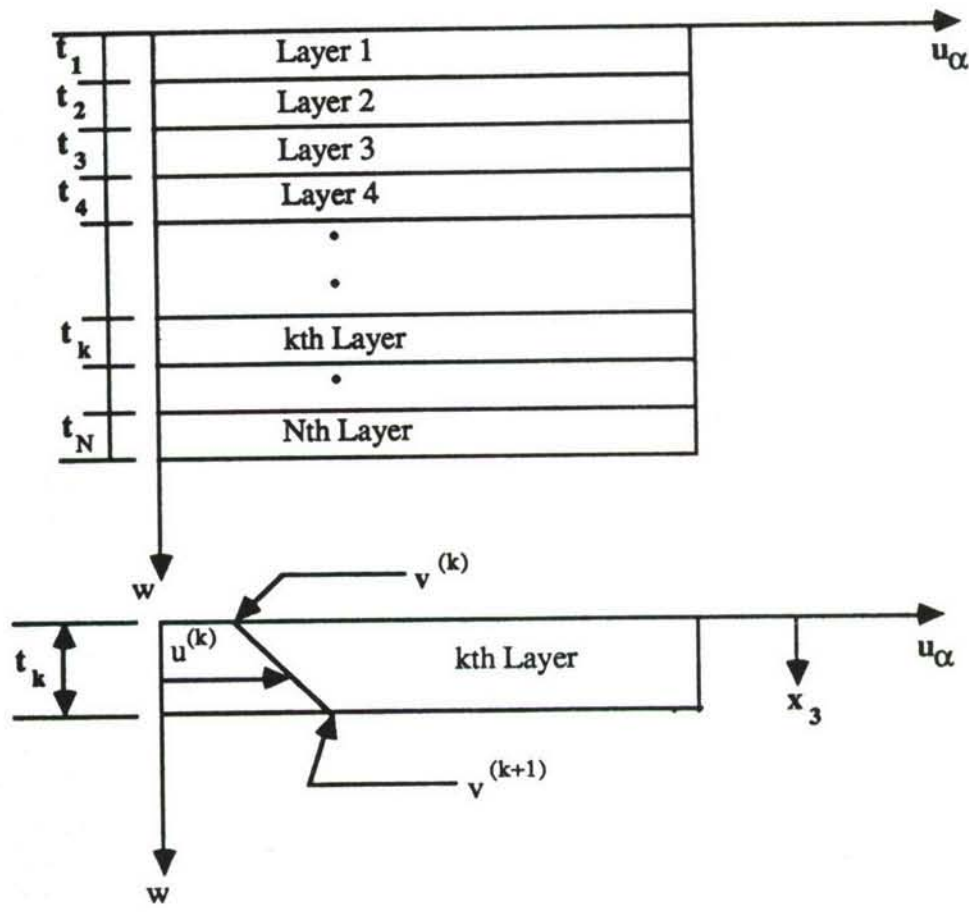


Figure 1: Configuration of a multilayer composite plate.

2.2.3 Equilibrium Equations

The three-dimensional equations of motion including body forces are:

$$\sigma_{ij,j}^{(k)} + f_i^{(k)} = \rho^{(k)} \dot{u}_i^{(k)} \quad (5)$$

where σ_{ij} are components of the Cauchy stress tensor and f_i those of the body force per unit volume. Equation (5) is difficult to satisfy exactly. To eliminate the dependence on the coordinate x_3 , (5) can be restated in the form

$$\int_0^{l_k} (\sigma_{ij,j}^{(k)} + f_i^{(k)} - \rho^{(k)} \dot{u}_i^{(k)}) (x_3^{(k)})^n dx_3^{(k)} = 0, \quad n = 0, 1, \dots \infty. \quad (6)$$

As an approximation, in general, (6) is enforced only for $n=0,1$. Higher order theories would use higher values on n as well. Equation(6) for $n=0$ is:

a. For $i=1,2$, setting $u_a^{(k)}(x_i) = v_a^{(k)}(x_3) + x_3^{(k)} \phi_a^{(k)}(x_3)$ following (1):

$$\int_0^{l_k} (\sigma_{\alpha\beta,\beta}^{(k)} + \sigma_{\alpha 3,3}^{(k)} + f_\alpha^{(k)} - \rho^{(k)} \dot{v}_\alpha^{(k)} - \rho^{(k)}(x_3^{(k)}) \dot{\phi}_\alpha^{(k)}) dx_3^{(k)} = 0$$

or

$$N_{\alpha\beta,\beta}^{(k)} + (\sigma_{\alpha 3}^{(k)} - \sigma_{3\alpha}^{(k)}) + F_\alpha^{(k)} - P^{(k)} \dot{v}_\alpha^{(k)} - R^{(k)} \dot{\phi}_\alpha^{(k)} = 0 \quad (7)$$

where

$$N_{\alpha\beta}^{(k)} = \int_0^{l_k} \sigma_{\alpha\beta}^{(k)} dx_3^{(k)} \quad (8)$$

$$F_\alpha^{(k)} = \int_0^{l_k} f_\alpha^{(k)} dx_3^{(k)} \quad (9)$$

and

$$(P^{(k)}, R^{(k)}) = \int_0^{l_k} \rho^{(k)}(1, x_3^{(k)}) dx_3^{(k)} \quad (10)$$

b. For $i=3$.

$$\int_0^{r_k} (\sigma_{\alpha 3, \alpha}^{(k)} + \sigma_{33, 3}^{(k)} + f_3^{(k)} - \rho^{(k)} \ddot{w}_3^{(k)}) dx_3^{(k)} = 0$$

or

$$Q_{\alpha, \alpha}^{(k)} + (\sigma_{33}^{+(k)} - \sigma_{33}^{-(k)}) + F_3^{(k)} - P^{(k)} \ddot{w}_3^{(k)} = 0 \quad (11)$$

where

$$Q_{\alpha}^{(k)} = \int_0^{r_k} \sigma_{\alpha 3}^{(k)} dx_3^{(k)} \quad (12)$$

$$F_3^{(k)} = \int_0^{r_k} f_3^{(k)} dx_3^{(k)} \quad (13)$$

For $n=1$, i.e., taking the first moment, considering $i=1, 2$.

$$\int_0^{r_k} (\sigma_{\alpha \beta, \beta}^{(k)} + \sigma_{\alpha 3, 3}^{(k)} + f_{\alpha}^{(k)} - \rho^{(k)} \dot{v}_{\alpha}^{(k)} - \rho^{(k)}(x_3^{(k)}) \dot{\phi}_{\alpha}^{(k)})(x_3^{(k)}) dx_3^{(k)} = 0$$

or

$$M_{\alpha \beta, \beta}^{(k)} + t_k \sigma_{\alpha 3}^{+(k)} - Q_{\alpha}^{(k)} + G_{\alpha}^{(k)} - R^{(k)} \dot{v}_{\alpha}^{(k)} - I^{(k)} \dot{\phi}_{\alpha}^{(k)} = 0 \quad (14)$$

where

$$M_{\alpha \beta}^{(k)} = \int_0^{r_k} \sigma_{\alpha \beta}^{(k)} x_3^{(k)} dx_3^{(k)} \quad (15)$$

$$G_{\alpha}^{(k)} = \int_0^{r_k} f_{\alpha}^{(k)} x_3^{(k)} dx_3^{(k)} \quad (16)$$

and

$$I^{(k)} = \int_0^{r_k} \rho^{(k)} (x_3^{(k)})^2 dx_3^{(k)} \quad (17)$$

In the approximate theory considered, the first moment equation for $i=3$ is ignored.

To eliminate the time derivatives in (7), (11), and (14) and to include the initial conditions, convolution of both sides of the equations with, $g(t)=t$, a function of time is performed [8] and [9]. Equations (7), (11), and (14) can then be written in the following form:

$$g^* N_{\alpha\beta,\beta}^{(k)} + g^*(\sigma_{\alpha 3}^{+(k)} - \sigma_{\alpha 3}^{-(k)}) + g^* F_\alpha^{(k)} - P^{(k)} g^* \ddot{v}_\alpha^{(k)} - R^{(k)} g^* \ddot{\phi}_\alpha^{(k)} = 0 \quad (18)$$

$$g^* Q_{\alpha,\alpha}^{(k)} + g^*(\sigma_{33}^{+(k)} - \sigma_{33}^{-(k)}) + g^* F_3^{(k)} - P^{(k)} g^* \ddot{w}^{(k)} = 0 \quad (19)$$

$$g^* M_{\alpha\beta,\beta}^{(k)} + t_k g^* \sigma_{\alpha 3}^{+(k)} - g^* Q_\alpha^{(k)} + g^* G_\alpha^{(k)} - R^{(k)} g^* \ddot{v}_\alpha^{(k)} - I^{(k)} g^* \ddot{\phi}_\alpha^{(k)} = 0 \quad (20)$$

where (*) represents the convolution product. Evaluating the convolution integrals for terms involving time derivatives

$$\begin{aligned} g^* \ddot{w}^{(k)} &= \int_0^{t_{(time)}} g(t-\tau) \ddot{w}^{(k)}(x_\beta, \tau) d\tau \\ &= \int_0^t (t-\tau) \ddot{w}^{(k)} d\tau \\ &= -t \dot{w}^{(k)}(x_\beta, 0) + w^{(k)}(x_\beta, t) - w^{(k)}(x_\beta, 0) \end{aligned} \quad (21)$$

where $\dot{w}^{(k)}(x_\beta, 0)$ and $w^{(k)}(x_\beta, 0)$ are, respectively, the initial conditions for transverse velocity and displacement. Similarly,

$$g^* \ddot{v}_\alpha^{(k)} = -t \dot{v}_\alpha^{(k)}(x_\beta, 0) - v_\alpha^{(k)}(x_\beta, 0) + v_\alpha^{(k)}(x_\beta, t) \quad (22)$$

$$g^* \ddot{\phi}_\alpha^{(k)} = -t \dot{\phi}_\alpha^{(k)}(x_\beta, 0) - \phi_\alpha^{(k)}(x_\beta, 0) + \phi_\alpha^{(k)}(x_\beta, t) \quad (23)$$

Let

$$X^{(k)} = -P^{(k)} [-t \dot{w}^{(k)}(x_\beta, 0) - w^{(k)}(x_\beta, 0)] \quad (24)$$

$$Y^{(k)} = -P^{(k)} [-t \dot{v}_\alpha^{(k)}(x_\beta, 0) - v_\alpha^{(k)}(x_\beta, 0)] - R^{(k)} [-t \dot{\phi}_\alpha^{(k)}(x_\beta, 0) - \phi_\alpha^{(k)}(x_\beta, 0)] \quad (25)$$

$$Z^{(k)} = -R^{(k)} [-t \dot{v}_\alpha^{(k)}(x_\beta, 0) - v_\alpha^{(k)}(x_\beta, 0)] - I^{(k)} [-t \dot{\phi}_\alpha^{(k)}(x_\beta, 0) - \phi_\alpha^{(k)}(x_\beta, 0)] \quad (26)$$

Substituting (24) through (26) into (18) through (20):

$$g^* Q_{\alpha,\alpha}^{(k)} + g^*(\sigma_{33}^{+(k)} - \sigma_{33}^{-(k)}) + g^* I_3^{(k)} - P^{(k)} w^{(k)} + X^{(k)} = 0 \quad (27)$$

$$g^* N_{\alpha\beta,\beta}^{(k)} + g^*(\sigma_{\alpha 3}^{+(k)} - \sigma_{\alpha 3}^{-(k)}) + g^* F_\alpha^{(k)} - P^{(k)} v_\alpha^{(k)} - R^{(k)} \phi_\alpha^{(k)} + Y^{(k)} = 0 \quad (28)$$

$$g^* M_{\alpha\beta,\beta}^{(k)} + t_k g^* \sigma_{\alpha 3}^{+(k)} - g^* Q_\alpha^{(k)} + g^* G_\alpha^{(k)} - R^{(k)} v_\alpha^{(k)} - I^{(k)} \phi_\alpha^{(k)} + Z^{(k)} = 0 \quad (29)$$

Eqs. (27) through (29) are the spatial equilibrium equations for the motion of each lamina of the laminated plate in terms of laminar force resultants.

2.2.4 Constitutive Equations

2.2.4.1 Stress-Strain Relations for Linear Elastic Materials

A material is said to be ideally elastic if the material completely recovers its original shape upon the removal of the forces causing the deformation. The generalized Hooke's law relates the nine components of stress and the nine components of strain by a linear relation. Assuming an initially unstressed reference configuration, and a rectangular Cartesian reference frame, this can be expressed as:

$$\sigma_{ij} = E_{ijkl} \epsilon_{kl} \quad (30)$$

where E_{ijkl} are components of fourth rank isothermal elasticity tensor. Owing to symmetry of σ_{ij} , i.e., in the absence of body couples, we have:

$$E_{ijkl} = E_{jikl} \quad (31)$$

Furthermore since $\epsilon_{kl} = \epsilon_{lk}$:

$$E_{ijkl} = E_{ijlk} \quad (32)$$

If a strain energy function exists then

$$E_{ijkl} = E_{klji} \quad (33)$$

For a monoclinic system with two orthogonal planes of symmetry the stress-strain relations for any layer k in the reduced form with respect to a global plane of reference (second rank tensors written in vector form) are:

$$\begin{array}{c|ccccc|c} \sigma_{11}^{(k)} & E_{1111}^{(k)} & E_{1122}^{(k)} & E_{1133}^{(k)} & 0 & 0 & E_{1112}^{(k)} \\ \sigma_{22}^{(k)} & E_{2211}^{(k)} & E_{2222}^{(k)} & E_{2233}^{(k)} & 0 & 0 & E_{2212}^{(k)} \\ \sigma_{33}^{(k)} & E_{3311}^{(k)} & E_{3322}^{(k)} & E_{3333}^{(k)} & 0 & 0 & E_{3312}^{(k)} \\ \sigma_{23}^{(k)} & 0 & 0 & 0 & E_{2323}^{(k)} & E_{2313}^{(k)} & 0 \\ \sigma_{13}^{(k)} & 0 & 0 & 0 & E_{1323}^{(k)} & E_{1313}^{(k)} & 0 \\ \sigma_{12}^{(k)} & E_{1211}^{(k)} & E_{1222}^{(k)} & E_{1233}^{(k)} & 0 & 0 & E_{1212}^{(k)} \end{array} \left| \begin{array}{c} \epsilon_{11}^{(k)} \\ \epsilon_{22}^{(k)} \\ \epsilon_{33}^{(k)} \\ 2\epsilon_{23}^{(k)} \\ 2\epsilon_{13}^{(k)} \\ 2\epsilon_{12}^{(k)} \end{array} \right. \quad (34)$$

Equation (34) can be written in the indicial form as:

$$\sigma_{\alpha\beta}^{(k)} = E_{\alpha\beta\gamma\delta}^{(k)} \epsilon_{\gamma\delta}^{(k)} + E_{\alpha\beta 33}^{(k)} \epsilon_{33}^{(k)} \quad (35)$$

$$\sigma_{\alpha 3}^{(k)} = 2E_{\alpha 3\gamma 3}^{(k)} \epsilon_{\gamma 3}^{(k)} \quad (36)$$

$$\sigma_{33}^{(k)} = E_{33\gamma\delta}^{(k)} \epsilon_{\gamma\delta}^{(k)} + E_{3333}^{(k)} \epsilon_{33}^{(k)} \quad (37)$$

Solving (37) for $\epsilon_{33}^{(k)}$ and substituting into (35)

$$\sigma_{\alpha\beta}^{(k)} = \bar{E}_{\alpha\beta\gamma\delta}^{(k)} \epsilon_{\gamma\delta}^{(k)} + \bar{E}_{\alpha\beta 33}^{(k)} \sigma_{33}^{(k)} \quad (38)$$

where

$$\bar{E}_{\alpha\beta\gamma\delta}^{(k)} = E_{\alpha\beta\gamma\delta}^{(k)} - \frac{E_{\alpha\beta 33}^{(k)}}{E_{3333}^{(k)}} E_{33\gamma\delta}^{(k)} \quad (39)$$

and

$$\bar{E}_{\alpha\beta 33}^{(k)} = \frac{E_{\alpha\beta 33}^{(k)}}{E_{3333}^{(k)}} \quad (40)$$

Substituting (3) into (38), (36), and (37):

$$\sigma_{\alpha\beta}^{(k)} = \bar{E}_{\alpha\beta\gamma\delta}^{(k)} \epsilon_{\gamma\delta}^{(k)} + \bar{E}_{\alpha\beta\gamma\delta}^{(k)} x_3^{(k)} \kappa_{\alpha\beta}^{(k)} + \bar{E}_{\alpha\beta 33}^{(k)} \sigma_{33}^{(k)} \quad (41)$$

$$\sigma_{\alpha 3}^{(k)} = \bar{E}_{\alpha 3\gamma 3}^{(k)} (\omega_{,\alpha}^{(k)} + \phi_{\alpha}^{(k)}) \quad (42)$$

$$\sigma_{33}^{(k)} = \bar{E}_{33\gamma\delta}^{(k)} \epsilon_{\gamma\delta}^{(k)} + \bar{E}_{33\gamma\delta}^{(k)} x_3^{(k)} \kappa_{\gamma\delta}^{(k)} + \bar{E}_{3333}^{(k)} \epsilon_{33}^{(k)} \quad (43)$$

We note here that the assumption of $u_3^{(k)}$ constant over the thickness of each lamina,

implies $u_3^{(k)}(x_i) = w^{(k)}(x_i)$, $\epsilon_{33}^{(k)} = 0$. This would result in the terms containing $\epsilon_{33}^{(k)}$ dropping from (43). We also note that this would mean that (37) and (35) would not contain $\epsilon_{33}^{(k)}$ and, therefore, there would be no question of eliminating $\epsilon_{33}^{(k)}$ between these two equations. However, most plate theories suffer from this defect viz. $\epsilon_{33}^{(k)}$ is eliminated in the constitutive equations (35) through (37) but is set equal to zero in the equation for σ_{33} i.e., (43).

2.2.4.2 Constitutive Relations for Force and Moment Resultants

Substituting $\sigma_{\alpha\beta}^{(k)}$ from (35) into (8) and (15) and carrying out the integration, the following equations are obtained:

$$N_{\alpha\beta}^{(k)} = A_{\alpha\beta\gamma\delta}^{(k)} e_{\gamma\delta}^{(k)} + B_{\alpha\beta\gamma\delta}^{(k)} K_{\gamma\delta}^{(k)} \quad (44)$$

$$M_{\alpha\beta}^{(k)} = B_{\alpha\beta\gamma\delta}^{(k)} e_{\gamma\delta}^{(k)} + D_{\alpha\beta\gamma\delta}^{(k)} K_{\gamma\delta}^{(k)} \quad (45)$$

where

$$(A_{\alpha\beta\gamma\delta}^{(k)}, B_{\alpha\beta\gamma\delta}^{(k)}, D_{\alpha\beta\gamma\delta}^{(k)}) = \int_0^{r_k} E_{\alpha\beta\gamma\delta}^{(k)} [1, (x_3^{(k)}), (x_3^{(k)})^2] dx_3^{(k)} \quad (46)$$

Substituting $\sigma_{\alpha 3}^{(k)}$ from (42) into (12), and carrying out the integration gives:

$$Q_\alpha^{(k)} = G_{\alpha 3 \gamma 3}^{(k)} (w_{,\alpha}^{(k)} + \phi_\alpha^{(k)}) \quad (47)$$

where

$$G_{\alpha 3 \gamma 3}^{(k)} = \int_0^{r_k} E_{\alpha 3 \gamma 3}^{(k)} dx_3^{(k)} \quad (48)$$

The quantities $M_{\alpha\beta}^{(k)}, Q_\alpha^{(k)}, N_{\alpha\beta}^{(k)}$ are the 'laminar' resultants. It is to be noticed that whereas corresponding quantities for the entire laminate are obtained by simple addition of $Q_\alpha^{(k)}$ and $N_{\alpha\beta}^{(k)}$, $M_{\alpha\beta}$ is the total moment including contribution due to $N_{\alpha\beta}^{(k)}$, i.e.,

$$Q_\alpha = \sum_{k=1}^n Q_\alpha^{(k)} \quad (49)$$

$$N_{\alpha\beta} = \sum_{k=1}^n N_{\alpha\beta}^{(k)} \quad (50)$$

$$M_{\alpha\beta} = \sum_{k=1}^n M_{\alpha\beta}^{(k)} + \sum_{k=1}^n N_{\alpha\beta}^{(k)} T_{(k)} \quad (51)$$

where $T_{(k)}$ is the distance of the center of the k th layer from the point of application of the resultant $N_{\alpha\beta}$.

2.2.5 The Interlaminar Continuity Equations

For the continuity of tractions and displacements to be satisfied

$$\sigma_{\alpha 3}^{+(k)} = \sigma_{\alpha 3}^{-(k+1)} \quad (52)$$

$$v_{\alpha}^{(k)} + t_k \phi_{\alpha}^{(k)} = v_{\alpha}^{(k+1)} \quad (53)$$

$$w^{(k)} = w^{(k+1)} \quad (54)$$

and

$$\sigma_{33}^{+(k)} = \sigma_{33}^{-(k+1)} \quad (55)$$

where

$\sigma_{\alpha 3}^{+(k)}$ = components of the shearing stress at the top of the k th layer.

$\sigma_{\alpha 3}^{-(k+1)}$ = components of the shearing stress at the bottom of the $(k+1)$ th layer.

$v_{\alpha}^{(k)}$ = components of the in-plane displacement for the k th interface.

$\phi_{\alpha}^{(k)}$ = components of the rotation of the k th layer.

2.2.6 Summary of Field Equations in Convolution Form

For self-adjointness of the set of operators consisting of those appearing in the kinematics equations, the constitutive relations, the equilibrium equations, and the continuity equations, noting that the equilibrium equations had to be transformed (27) through (29), it is necessary to express the remaining field equations in convolution form as well. i.e.,

a. Equilibrium Equations ((27) through (29)):

$$g^* Q_{\alpha,\alpha}^{(k)} + g^* (\sigma_{33}^{+(k)} - \sigma_{33}^{-(k-1)}) + g^* F_3^{(k)} - P^{(k)} w^{(k)} + X^{(k)} = 0 \quad (56)$$

$$g^* N_{\alpha\beta,\beta}^{(k)} + g^* (\sigma_{\alpha 3}^{+(k)} - \sigma_{\alpha 3}^{-(k)}) + g^* F_\alpha^{(k)} - P^{(k)} v_\alpha^{(k)} - R^{(k)} \phi_\alpha^{(k)} + Y^{(k)} = 0 \quad (57)$$

$$g^* M_{\alpha\beta,\beta}^{(k)} + t_k g^* \sigma_{\alpha 3}^{+(k)} - g^* Q_\alpha^{(k)} + g^* G_\alpha^{(k)} - R^{(k)} v_\alpha^{(k)} - I^{(k)} \phi_\alpha^{(k)} + Z^{(k)} = 0 \quad (58)$$

b. Kinematic Relations ((2) through (4))

$$g^* e_{\alpha\beta}^{(k)} = \frac{1}{2} g^* (v_{\alpha,\beta}^{(k)} + v_{\beta,\alpha}^{(k)}) \quad (59)$$

$$g^* \kappa_{\alpha\beta}^{(k)} = \frac{1}{2} g^* (\phi_{\alpha,\beta}^{(k)} + \phi_{\beta,\alpha}^{(k)}) \quad (60)$$

$$2g^* \epsilon_{\alpha 3}^{(k)} = g^* (w_{\alpha}^{(k)} + \phi_\alpha^{(k)}) \quad (61)$$

c. Constitutive Equations ((44), (45) and (47))

$$g^* N_{\alpha\beta}^{(k)} = g^* A_{\alpha\beta\gamma\delta}^{(k)} e_{\gamma\delta}^{(k)} + g^* B_{\alpha\beta\gamma\delta}^{(k)} \kappa_{\gamma\delta}^{(k)} \quad (62)$$

$$g^* M_{\alpha\beta}^{(k)} = g^* B_{\alpha\beta\gamma\delta}^{(k)} e_{\gamma\delta}^{(k)} + g^* D_{\alpha\beta\gamma\delta}^{(k)} \kappa_{\gamma\delta}^{(k)} \quad (63)$$

$$g^* Q_\alpha^{(k)} = g^* G_{\alpha 3\gamma 3}^{(k)} (2\epsilon_{\gamma 3}^{(k)}) \quad (64)$$

d. Continuity Equations ((52) through (55))

$$g^* \sigma_{\alpha 3}^{+(k)} = g^* \sigma_{\alpha 3}^{-(k+1)} \quad (65)$$

$$g^* v_\alpha^{(k)} + t_k g^* \phi_\alpha^{(k)} = g^* v_\alpha^{(k+1)} \quad (66)$$

$$g^* w^{(k)} = g^* w^{(k+1)} \quad (67)$$

$$g^* \sigma_{33}^{+(k)} = g^* \sigma_{33}^{-(k+1)} \quad (68)$$

The field operators, for layer k, in self-adjoint form are:

$$[A]^{(k)} = \begin{pmatrix} -P^{(k)} & 0 & g^*L & -R^{(k)} & 0 & 0 & 0 & 0 \\ 0 & -g^*A_{\alpha\beta\gamma b}^{(k)} & g^* & 0 & -g^*B_{\alpha\beta\gamma b}^{(k)} & 0 & 0 & 0 \\ -g^*L & g^* & 0 & 0 & 0 & 0 & 0 & 0 \\ -R^{(k)} & 0 & 0 & -I^{(k)} & 0 & g^*L & 0 & -g^* \\ 0 & -g^*B_{\alpha\beta\gamma\delta}^{(k)} & 0 & 0 & -g^*D_{\alpha\beta\gamma\delta}^{(k)} & g^* & 0 & 0 \\ 0 & 0 & 0 & -g^*L & g^* & 0 & 0 & 0 \\ 0 & 0 & 0 & 0 & 0 & 0 & -P^{(k)} & 0 \\ 0 & 0 & 0 & 0 & 0 & 0 & 0 & -g^*G_{\alpha 3\gamma 3}^{(k)} & g^* \\ 0 & 0 & 0 & -g^* & 0 & 0 & -g^*\frac{\partial}{\partial\alpha} & g^* & 0 \end{pmatrix} \quad (69)$$

where

$$L = \frac{1}{2}(\delta_{\gamma\alpha}\frac{\partial}{\partial\beta} + \delta_{\gamma\beta}\frac{\partial}{\partial\alpha})$$

The domain of the operators is the direct-sum space, under the convolution product, of the spaces consisting of admissible $v_\gamma^{(k)}, e_{\alpha\beta}^{(k)}, N_{\alpha\beta}^{(k)}, \phi_\alpha^{(k)}, \kappa_{\alpha\beta}^{(k)}, M_{\alpha\beta}^{(k)}, w^{(k)}, 2\epsilon_{\alpha 3}^{(k)}, Q_\alpha^{(k)}$, in that order. The operators in (69) are the ones in (57), (62), (59), (58), (63), (60), (56), (64), and (61) excluding those associated with interlaminar tractions. The displacement continuity (66) and (67) can be directly incorporated in the system of equations. At the same time, addition of operators associated with the interlaminar traction completes the set of field equations for the system. Traction continuity ((65) and (68)) is implicitly satisfied by using only one set of tractions for each interface. The system set of field equations then has the form:

$$\begin{matrix} [A^{(1)}] & [B^{(1)}] \\ [B^{(1)}]^T & [0] \\ [C^{(2)}]^T & [A^{(2)}] \\ [C^{(2)}]^T & [B^{(2)}] \\ \cdot & \cdot \\ \cdot & \cdot \\ [0] & [B^{(N-1)}]^T \\ & [C^{(N)}]^T \end{matrix} \begin{matrix} [0] \\ \vdots \\ \cdot \\ [0] \\ \vdots \\ \cdot \\ [0] \end{matrix} = \begin{matrix} \{u^{(1)}\} \\ \{\sigma^{(1)}\} \\ \{u^{(2)}\} \\ \{P\}^{(2)} \\ \{0\} \\ \{P\}^{(N-1)} \\ \{0\} \\ \{P\}^{(N)} + \{\sigma^{(N)}\} \end{matrix} \quad (70)$$

or, symbolically,

$$[X]\{y\} = \{z\}$$

Here

$$[B^{(k)}]^T = \begin{bmatrix} g^* & 0 & 0 & t_k g^* & 0 & 0 & 0 & 0 \\ 0 & 0 & 0 & 0 & 0 & g^* & 0 & 0 \end{bmatrix} \quad (71)$$

$$[C^{(k)}] = \begin{bmatrix} -g^* & 0 & 0 & 0 & 0 & 0 & 0 & 0 \\ 0 & 0 & 0 & 0 & 0 & 0 & -g^* & 0 & 0 \end{bmatrix} \quad (72)$$

$$\{u^{(k)}\}^T = \langle v_{\alpha}^{(k)}, e_{\alpha\beta}^{(k)}, N_{\alpha\beta}^{(k)}, \phi_{\alpha}^{(k)}, \kappa_{\alpha\beta}^{(k)}, M_{\alpha\beta}^{(k)}, w^{(k)}, 2\epsilon_{\alpha 3}^{(k)}, Q_{\alpha}^{(k)} \rangle \quad (73)$$

$$\{\sigma^{(k)}\}^T = \langle \sigma_{\alpha 3}^{+(k)}, \sigma_{33}^{-(k)} \rangle \quad (74)$$

$$\{P^{(k)}\}^T = \langle -g^* F_{\alpha}^{(k)} - Y^{(k)}, 0, 0, -g^* G_{\alpha}^{(k)} - Z^{(k)}, 0, 0, -g^* F_3^{(k)} - X^{(k)}, 0, 0 \rangle \quad (75)$$

$$\{0\}^T = \langle 0, 0 \rangle \quad (76)$$

$$\{\sigma^{(0)}\}^T = \langle g^* \sigma_{\alpha 3}^{-(1)}, 0, 0, 0, 0, 0, g^* \sigma_{33}^{-(1)}, 0, 0 \rangle \quad (77)$$

$$\{\sigma^{(N)}\}^T = \langle -g^* \sigma_{\alpha 3}^{+(N)}, 0, 0, -t_N g^* \sigma_{\alpha 3}^{+(N)}, 0, 0, -g^* \sigma_{33}^{+(N)}, 0, 0 \rangle \quad (78)$$

$$[0] = \begin{bmatrix} 0 & 0 \\ 0 & 0 \end{bmatrix} \quad (79)$$

Continuity of tractions is ensured explicitly by using the interfacial traction as the field variable $[\sigma^{(k)}]$ in the manner expressed by (70), i.e., $\sigma_{i3}^{+(k)} \equiv \sigma_{i3}^{-(k+1)}$ and $\sigma_{i3}^{-(k)}$ do not appear as field variables. The operators $[B^{(k)}], [C^{(k)}]$ and their adjoints $[B^{(k)}]^T, [C^{(k)}]^T$ represent coupling between field equations for the layers and the continuity of interlayer displacements. Explicitly, for the interface between the k th and the $(k+1)$ th layer; these have the form

2.2.7 Self-adjointness of the Operator Matrix

For the operator matrix $[X]$ to be self-adjoint, a sufficient condition is that the elements of X satisfy the relationship

$$\langle f_i, X_{ij} g_j \rangle_R = \langle g_i, X_{ji} f_j \rangle_R + \text{Boundary terms}$$

where $\langle \cdot, \cdot \rangle_R$ is a bilinear mapping over the space of functions defined over the region R . The elements of X satisfy this requirement in the sense of inner product defined as

$$\langle f, g \rangle = \int_R f(\underline{x}) g(\underline{x}) dR$$

Specifically, if the operator matrix $A^{(k)}$ is self-adjoint and $([B^{(k)}], [B^{(k)}]^T); ([C^{(k)}], [C^{(k)}]^T)$ constitute adjoint pairs, $[X]$ is self-adjoint. Considering A_{13} and A_{31} for the k th layer,

based on Green's theorem (Kreyszig [1979]):

$$\begin{aligned} & \langle v_{\alpha}^{(k)}, g^* N_{\alpha\beta, \beta}^{(k)} \rangle_{R^{(k)}} = - \langle N_{\alpha\beta}^{(k)}, g^* v_{(\alpha, \beta)}^{(k)} \rangle_{R^{(k)}} \\ & + \langle N_{\alpha\beta}^{(k)} \eta_{\beta}, g^* v_{\alpha}^{(k)} \rangle_{S_2^{(k)}} + \langle v_{\alpha}^{(k)}, g^* N_{\alpha\beta}^{(k)} \eta_{\beta} \rangle_{S_1^{(k)}} \\ & + \langle N_{\alpha\beta}^{(k)} \eta_{\beta}, g^* (v_{\alpha}^{(k)})' \rangle_{S_2^{(k)}} + \langle v_{\alpha}^{(k)}, g^* (N_{\alpha\beta}^{(k)})' \eta_{\beta} \rangle_{S_1^{(k)}} \end{aligned} \quad (80)$$

Similarly for A_{46} and A_{64} :

$$\begin{aligned} & \langle \phi_{\alpha}^{(k)}, g^* M_{\alpha\beta, \beta}^{(k)} \rangle_{R^{(k)}} = - \langle M_{\alpha\beta}^{(k)}, g^* \phi_{(\alpha, \beta)}^{(k)} \rangle_{R^{(k)}} \\ & + \langle M_{\alpha\beta}^{(k)} \eta_{\beta}, g^* \phi_{\alpha}^{(k)} \rangle_{S_4^{(k)}} + \langle \phi_{\alpha}^{(k)}, g^* M_{\alpha\beta}^{(k)} \eta_{\beta} \rangle_{S_3^{(k)}} \\ & + \langle M_{\alpha\beta}^{(k)} \eta_{\beta}, g^* (\phi_{\alpha}^{(k)})' \rangle_{S_4^{(k)}} + \langle \phi_{\alpha}^{(k)}, g^* (M_{\alpha\beta}^{(k)})' \eta_{\beta} \rangle_{S_3^{(k)}} \end{aligned} \quad (81)$$

and for A_{79} and A_{97} :

$$\begin{aligned} & \langle w^{(k)}, g^* Q_{\alpha, \alpha}^{(k)} \rangle_{R^{(k)}} = - \langle Q_{\alpha}^{(k)}, g^* w_{,\alpha}^{(k)} \rangle_{R^{(k)}} \\ & + \langle Q_{\alpha}^{(k)} \eta_{\alpha}, g^* w^{(k)} \rangle_{S_6} + \langle w^{(k)}, g^* Q_{\alpha}^{(k)} \eta_{\alpha} \rangle_{S_5^{(k)}} \\ & + \langle Q_{\alpha}^{(k)} \eta_{\alpha}, g^* (w^{(k)})' \rangle_{S_6^{(k)}} + \langle w^{(k)}, g^* (Q_{\alpha}^{(k)})' \eta_{\alpha} \rangle_{S_5^{(k)}} \end{aligned} \quad (82)$$

The remaining elements of $[A]^{(k)}$ constitute algebraic operators which are self-adjoint or consist of adjoint pairs. The adjointness of $[B^{(k)}]$ and $[B^{(k)}]^T$, and of $[C^{(k)}]$ and $[C^{(k)}]^T$ is obvious.

2.2.8 Consistent Boundary Conditions

Referring to Sandhu [1975], consistent boundary conditions for the problem are:

$$\begin{aligned} & g^* C_1^{(k)} N_{\alpha\beta}^{(k)} = -g^* \hat{N}_{\alpha\beta}^{(k)} \eta_{\beta} \quad \text{on} \quad S_1^{(k)} \\ & g^* C_3^{(k)} M_{\alpha\beta}^{(k)} = -g^* \hat{M}_{\alpha\beta}^{(k)} \eta_{\beta} \quad \text{on} \quad S_3^{(k)} \\ & g^* C_5^{(k)} Q_{\alpha}^{(k)} = -g^* \hat{Q}_{\alpha}^{(k)} \eta_{\alpha} \quad \text{on} \quad S_5^{(k)} \\ & g^* C_2^{(k)} v_{\alpha}^{(k)} = g^* \hat{v}_{\alpha}^{(k)} \eta_{\beta} \quad \text{on} \quad S_2^{(k)} \end{aligned} \quad (83)$$

$$g^* C_4^{(k)} \phi_{\alpha}^{(k)} = g^* \phi_{\alpha}^{(k)} \eta_{\beta} \quad \text{on} \quad S_4^{(k)}$$

$$g^* C_6^{(k)} w^{(k)} = g^* w^{(k)} \eta_{\alpha} \quad \text{on} \quad S_6^{(k)}$$

where $C_1^{(k)}, C_2^{(k)}, C_3^{(k)}, C_4^{(k)}, C_5^{(k)},$ and $C_6^{(k)}$ are the consistent boundary operators and

$$S_1^{(k)} \cup S_2^{(k)} = S_3^{(k)} \cup S_4^{(k)} = S_5^{(k)} \cup S_6^{(k)} = S^{(k)}$$

$$S_1^{(k)} \cap S_2^{(k)} = S_3^{(k)} \cap S_4^{(k)} = S_5^{(k)} \cap S_6^{(k)} = \phi$$

Explicitly,

$$C_1^{(k)} = C_3^{(k)} = C_5^{(k)} = -\eta_{\beta}$$

$$C_2^{(k)} = C_4^{(k)} = C_6^{(k)} = \eta_{\beta}$$

Corresponding internal jump discontinuity conditions are:

$$\begin{aligned} g^*(C_1^{(k)} N_{\alpha\beta}^{(k)})' &= -g^*(g'_1) \quad \text{on} \quad S_{1i}^{(k)} \\ g^*(C_3^{(k)} M_{\alpha\beta}^{(k)})' &= -g^*(g'_3) \quad \text{on} \quad S_{3i}^{(k)} \\ g^*(C_5^{(k)} Q_{\alpha}^{(k)})' &= -g^*(g'_5) \quad \text{on} \quad S_{5i}^{(k)} \\ g^*(C_2^{(k)} v_{\alpha}^{(k)})' &= g^*(g'_2) \quad \text{on} \quad S_{2i}^{(k)} \\ g^*(C_4^{(k)} \phi_{\alpha}^{(k)})' &= g^*(g'_4) \quad \text{on} \quad S_{4i}^{(k)} \\ g^*(C_6^{(k)} w^{(k)})' &= g^*(g'_6) \quad \text{on} \quad S_{6i}^{(k)} \end{aligned} \tag{84}$$

Here $S_{1i}^{(k)}, S_{2i}^{(k)}, \dots, S_{6i}^{(k)}$ represent surfaces imbedded in the interior of the region R. A prime over any quantity denotes the jump in that quantity across the surface of interest, e.g.

$$f' = f^+ - f^-$$

where \pm denote the two sides of the interior surface. Quantities $g_i^{(k)}$, $i=1, 2, \dots, 6$, denote the specified values of the jump discontinuities.

2.3 VARIATIONAL FORMULATION OF THE PROBLEM

2.3.1 The Basic Variational Formulation

Based on (A.20), the self-adjoint form of the field equations given in (70) the boundary conditions (83), and the jump discontinuity conditions (84), the governing function for the variational principle is:

$$\begin{aligned} \Omega = & \sum_{k=1}^N \left\langle u^{(k)}, A^{(k)} u^{(k)} - 2 p^{(k)} \right\rangle_{R^{(k)}} \\ & + \sum_{k=1}^{N-1} \left\langle u^{(k)}, B^{(k)} \sigma^{(k)} \right\rangle_{R^{(k)}} + \sum_{k=2}^N \left\langle u^{(k)}, C^{(k)T} \sigma^{(k-1)} \right\rangle_{R^{(k)}} \\ & + \sum_{k=1}^{N-1} \left\langle \sigma^{(k)}, B^{(k)T} u^{(k)} + C^{(k+1)} u^{(k+1)} \right\rangle_{R^{(k)}} \\ & - 2 \left\langle u^{(1)}, \sigma^{(0)} \right\rangle - 2 \left\langle u^{(N)}, \sigma^{(N)} \right\rangle + \text{Boundary terms} \end{aligned} \quad (2.85)$$

Substituting (70), (83), and (84) into (85), the explicit form of the function including the boundary and the discontinuity conditions is:

$$\begin{aligned} \Omega = & \sum_{k=1}^N \left\{ \left\langle v_\alpha^{(k)}, -P^{(k)} v_\alpha^{(k)} + g^* N_{\alpha\beta,\beta}^{(k)} - R^{(k)} \phi_\alpha^{(k)} + 2g^* F_\alpha^{(k)} + 2Y^{(k)} \right\rangle_{R^{(k)}} \right. \\ & + \left. \left\langle e_{\alpha\beta}^{(k)}, -g^* A_{\alpha\beta\gamma\delta}^{(k)} e_{\gamma\delta}^{(k)} + g^* N_{\alpha\beta}^{(k)} - g^* B_{\alpha\beta\gamma\delta}^{(k)} \kappa_{\gamma\delta}^{(k)} \right\rangle_{R^{(k)}} \right. \\ & + \left. \left\langle N_{\alpha\beta}^{(k)}, -g^* v_{(\alpha,\beta)}^{(k)} + g^* e_{\alpha\beta}^{(k)} \right\rangle_{R^{(k)}} \right. \\ & + \left. \left\langle \phi_\alpha^{(k)}, -R^{(k)} v_\alpha^{(k)} - I^{(k)} \phi_\alpha^{(k)} + g^* M_{\alpha\beta,\beta}^{(k)} - g^* Q_\alpha^{(k)} + 2g^* G_\alpha^{(k)} + 2Z^{(k)} \right\rangle_{R^{(k)}} \right. \\ & + \left. \left\langle \kappa_{\alpha\beta}^{(k)}, -g^* B_{\alpha\beta\gamma\delta}^{(k)} e_{\gamma\delta}^{(k)} - g^* D_{\alpha\beta\gamma\delta}^{(k)} \kappa_{\gamma\delta}^{(k)} + g^* M_{\alpha\beta}^{(k)} \right\rangle_{R^{(k)}} \right. \\ & + \left. \left\langle M_{\alpha\beta}^{(k)}, -g^* \phi_{(\alpha,\beta)}^{(k)} + g^* \kappa_{\alpha\beta}^{(k)} \right\rangle_{R^{(k)}} \right. \\ & + \left. \left\langle w^{(k)}, -P^{(k)} w^{(k)} + g^* Q_{\alpha,\alpha}^{(k)} + 2g^* F_3^{(k)} + 2X^{(k)} \right\rangle_{R^{(k)}} \right. \\ & + \left. \left\langle 2\epsilon_{\alpha 3}^{(k)}, -g^* G_{\alpha 3\gamma 3}^{(k)} (2\epsilon_{\gamma 3}^{(k)}) + g^* Q_\alpha^{(k)} \right\rangle_{R^{(k)}} \right. \end{aligned} \quad (2.86)$$

$$\begin{aligned}
& + \langle Q_{\alpha}^{(k)}, -g^* \phi_{\alpha}^{(k)} - g^* w_{,\alpha}^{(k)} + g^*(2\epsilon_{\alpha 3}^{(k)}) \rangle_{R^{(k)}} \\
& + \sum_{k=1}^{N-1} \{ \langle v_{\alpha}^{(k)}, g^* \sigma_{\alpha 3}^{+(k)} \rangle_{R^{(k)}} + \langle \phi_{\alpha}^{(k)}, t_k g^* \sigma_{\alpha 3}^{+(k)} \rangle_{R^{(k)}} + \langle w^{(k)}, g^* \sigma_{33}^{+(k)} \rangle_{R^{(k)}} \} \\
& + \sum_{k=2}^N \{ \langle v_{\alpha}^{(k)}, -g^* \sigma_{\alpha 3}^{-(k)} \rangle_{R^{(k)}} + \langle w^{(k)}, -g^* \sigma_{33}^{-(k)} \rangle_{R^{(k)}} \} \\
& + \sum_{k=1}^{N-1} \{ \langle \sigma_{\alpha 3}^{+(k)}, g^* v_{\alpha}^{(k)} + t_k g^* \phi_{\alpha}^{(k)} - g^* v_{\alpha}^{(k+1)} \rangle_{R^{(k)}} + \langle \sigma_{33}^{+(k)}, g^* w^{(k)} - g^* w^{(k+1)} \rangle_{R^{(k)}} \} \\
& - 2 \langle v_{\alpha}^{(1)}, g^* \sigma_{\alpha 3}^{-(1)} \rangle_{R^1} - 2 \langle w^{(1)}, g^* \sigma_{33}^{-(1)} \rangle_{R^1} \\
& - 2 \langle v_{\alpha}^{(N)}, -g^* \sigma_{\alpha 3}^{+(N)} \rangle_{R^{(N)}} - 2 \langle \phi_{\alpha}^{(N)}, -t_N g^* \sigma_{\alpha 3}^{+(N)} \rangle_{R^{(N)}} - 2 \langle w^{(N)}, -g^* \sigma_{33}^{+(N)} \rangle_{R^{(N)}} \\
& + \sum_{k=1}^N \{ \langle v_{\alpha}^{(k)}, g^*(C_1^{(k)} N_{\alpha\beta}^{(k)} + 2 \hat{N}_{\alpha\beta}^{(k)} \eta_{\beta}) \rangle_{S_1^{(k)}} + \langle N_{\alpha\beta}^{(k)}, g^*(C_2^{(k)} v_{\alpha}^{(k)} - 2 \phi_{\alpha}^{(k)} \eta_{\beta}) \rangle_{S_2^{(k)}} \\
& + \langle \phi_{\alpha}^{(k)}, g^*(C_3^{(k)} M_{\alpha\beta}^{(k)} + 2 \hat{M}_{\alpha\beta}^{(k)} \eta_{\beta}) \rangle_{S_3^{(k)}} + \langle M_{\alpha\beta}^{(k)}, g^*(C_4^{(k)} \phi_{\alpha}^{(k)} - 2 \phi_{\alpha}^{(k)} \eta_{\beta}) \rangle_{S_4^{(k)}} \\
& + \langle w^{(k)}, g^*(C_5^{(k)} Q_{\alpha}^{(k)} + 2 \hat{Q}_{\alpha}^{(k)} \eta_{\alpha}) \rangle_{S_5^{(k)}} + \langle Q_{\alpha}^{(k)}, g^*(C_6^{(k)} w^{(k)} - 2 \hat{w}^{(k)} \eta_{\alpha}) \rangle_{S_6^{(k)}} \} \\
& + \sum_{k=1}^N \{ \langle v_{\alpha}^{(k)}, g^*((C_1^{(k)} N_{\alpha\beta}^{(k)})' + 2 \hat{N}_{\alpha\beta}^{(k)} \eta_{\beta}) \rangle_{S_{1i}^{(k)}} + \langle N_{\alpha\beta}^{(k)}, g^*((C_2^{(k)} v_{\alpha}^{(k)})' - 2 \phi_{\alpha}^{(k)} \eta_{\beta}) \rangle_{S_{2i}^{(k)}} \\
& + \langle \phi_{\alpha}^{(k)}, g^*((C_3^{(k)} M_{\alpha\beta}^{(k)})' + 2 \hat{M}_{\alpha\beta}^{(k)} \eta_{\beta}) \rangle_{S_{3i}^{(k)}} + \langle M_{\alpha\beta}^{(k)}, g^*((C_4^{(k)} \phi_{\alpha}^{(k)})' - 2 \phi_{\alpha}^{(k)} \eta_{\beta}) \rangle_{S_{4i}^{(k)}} \\
& + \langle w^{(k)}, g^*((C_5^{(k)} Q_{\alpha}^{(k)})' + 2 \hat{Q}_{\alpha}^{(k)} \eta_{\alpha}) \rangle_{S_{5i}^{(k)}} + \langle Q_{\alpha}^{(k)}, g^*((C_6^{(k)} w^{(k)})' - 2 \hat{w}^{(k)} \eta_{\alpha}) \rangle_{S_{6i}^{(k)}} \}
\end{aligned}$$

Here we have used the notation $\sigma_{\beta}^{+(k)}$ for $\sigma_{\beta}^{-(k+1)}$ as explicitly stated in (52) and (55).

Theorem: The Gateaux differential of the function Ω defined by (86) vanishes if and only if (70) along with (83) and (84) are satisfied.

Proof.

Let $\{\bar{u}\} = \{\bar{v}_\alpha^{(k)}, \bar{e}_{\alpha\beta}^{(k)}, \bar{N}_{\alpha\beta}^{(k)}, \bar{\phi}_\alpha^{(k)}, \bar{\kappa}_{\alpha\beta}^{(k)}, \bar{M}_{\alpha\beta}^{(k)}, \bar{w}^{(k)}, \bar{\epsilon}_{\alpha 3}^{(k)}, \bar{Q}_\alpha^{(k)}, \bar{\sigma}_{\alpha 3}^{(k)}, \bar{\sigma}_{33}^{(k)}\}$ be an admissible state

corresponding to the set of field variables

$$\{u^{(k)}, \sigma^{(k)}\} = \{v_\alpha^{(k)}, e_{\alpha\beta}^{(k)}, N_{\alpha\beta}^{(k)}, \phi_\alpha^{(k)}, \kappa_{\alpha\beta}^{(k)}, M_{\alpha\beta}^{(k)}, w^{(k)}, \epsilon_{\alpha 3}^{(k)}, Q_\alpha^{(k)}, \sigma_{\alpha 3}^{(k)}, \sigma_{33}^{(k)}\}$$

Gateaux differential of the governing function (86) along the path \bar{u} , provided the limit exists, is

$$\begin{aligned} \delta_{\bar{u}} \Omega(u) = & \sum_{k=1}^N \left\{ \left\langle \bar{v}_\alpha^{(k)}, g^* N_{\alpha\beta,\beta}^{(k)} - P_k^{(k)} v_\alpha^{(k)} - R^{(k)} \phi_\alpha^{(k)} + 2 g^* F_\alpha^{(k)} + 2 Y^{(k)} \right\rangle_{R^{(k)}} \right. \\ & + \left\langle v_\alpha^{(k)}, g^* \bar{N}_{\alpha\beta,\beta}^{(k)} - P_k \bar{v}_\alpha^{(k)} - R^{(k)} \bar{\phi}_\alpha^{(k)} \right\rangle_{R^{(k)}} \\ & + \left\langle \bar{e}_{\alpha\beta}^{(k)}, g^* N_{\alpha\beta}^{(k)} - g^* A_{\alpha\beta\gamma\delta}^{(k)} g^* e_{\gamma\delta}^{(k)} - g^* B_{\alpha\beta\gamma\delta}^{(k)} \kappa_{\gamma\delta}^{(k)} \right\rangle_{R^{(k)}} \\ & + \left\langle e_{\alpha\beta}^{(k)}, g^* \bar{N}_{\alpha\beta}^{(k)} - g^* A_{\alpha\beta\gamma\delta}^{(k)} \bar{e}_{\gamma\delta}^{(k)} - g^* B_{\alpha\beta\gamma\delta}^{(k)} \bar{\kappa}_{\gamma\delta}^{(k)} \right\rangle_{R^{(k)}} \\ & + \left\langle \bar{N}_{\alpha\beta}^{(k)}, g^* e_{\alpha\beta}^{(k)} - g^* v_{(\alpha\beta)}^{(k)} \right\rangle_{R^{(k)}} + \left\langle N_{\alpha\beta}^{(k)}, g^* \bar{e}_{\alpha\beta}^{(k)} - g^* \bar{v}_{(\alpha\beta)}^{(k)} \right\rangle_{R^{(k)}} \\ & + \left\langle \bar{\phi}_\alpha^{(k)}, g^* M_{\alpha\beta,\beta}^{(k)} - g^* Q_\alpha^{(k)} - R^{(k)} v_\alpha^{(k)} - I^{(k)} \phi_\alpha^{(k)} + 2 g^* G_\alpha^{(k)} + 2 Z^{(k)} \right\rangle_{R^{(k)}} \\ & + \left\langle \phi_\alpha^{(k)}, g^* \bar{M}_{\alpha\beta,\beta}^{(k)} - g^* \bar{Q}_\alpha^{(k)} - R^{(k)} \bar{v}_\alpha^{(k)} - I^{(k)} \bar{\phi}_\alpha^{(k)} \right\rangle_{R^{(k)}} \\ & + \left\langle \bar{\kappa}_{\alpha\beta}^{(k)}, g^* M_{\alpha\beta}^{(k)} - g^* B_{\alpha\beta\gamma\delta}^{(k)} e_{\gamma\delta}^{(k)} - g^* D_{\alpha\beta\gamma\delta}^{(k)} \kappa_{\gamma\delta}^{(k)} \right\rangle_{R^{(k)}} \\ & + \left\langle \kappa_{\alpha\beta}^{(k)}, g^* \bar{M}_{\alpha\beta}^{(k)} - g^* B_{\alpha\beta\gamma\delta}^{(k)} \bar{e}_{\gamma\delta}^{(k)} - g^* D_{\alpha\beta\gamma\delta}^{(k)} \bar{\kappa}_{\gamma\delta}^{(k)} \right\rangle_{R^{(k)}} \\ & + \left\langle \bar{M}_{\alpha\beta}^{(k)}, g^* \kappa_{\alpha\beta}^{(k)} - g^* \phi_{(\alpha\beta)}^{(k)} \right\rangle_{R^{(k)}} + \left\langle M_{\alpha\beta}^{(k)}, g^* \bar{\kappa}_{\alpha\beta}^{(k)} - g^* \bar{\phi}_{(\alpha\beta)}^{(k)} \right\rangle_{R^{(k)}} \\ & + \left\langle \bar{w}^{(k)}, g^* Q_{\alpha,\alpha}^{(k)} - P^{(k)} w^{(k)} + 2 g^* F_3^{(k)} + 2 X^{(k)} \right\rangle_{R^{(k)}} + \left\langle w^{(k)}, g^* \bar{Q}_{\alpha,\alpha}^{(k)} - P^{(k)} \bar{w}^{(k)} \right\rangle_{R^{(k)}} \\ & + \left\langle 2 \bar{\epsilon}_{\alpha 3}^{(k)}, g^* Q_\alpha^{(k)} - g^* G_{\alpha 3 \gamma 3}^{(k)} (2 \bar{\epsilon}_{\gamma 3}^{(k)}) \right\rangle_{R^{(k)}} + \left\langle 2 \epsilon_{\alpha 3}^{(k)}, g^* \bar{Q}_\alpha^{(k)} - g^* G_{\alpha 3 \gamma 3}^{(k)} (2 \bar{\epsilon}_{\gamma 3}^{(k)}) \right\rangle_{R^{(k)}} \\ & + \left\langle \bar{Q}_\alpha^{(k)}, g^* (2 \bar{\epsilon}_{\alpha 3}^{(k)}) - g^* \phi_\alpha^{(k)} - g^* w_{,\alpha}^{(k)} \right\rangle_{R^{(k)}} \\ & + \left\langle Q_\alpha^{(k)}, g^* (2 \epsilon_{\alpha 3}^{(k)}) - g^* \bar{\phi}_\alpha^{(k)} - g^* \bar{w}_{,\alpha}^{(k)} \right\rangle_{R^{(k)}} \} \end{aligned} \quad (2.87)$$

$$\begin{aligned}
& + \sum_{k=1}^{N-1} \{ \langle \bar{v}_\alpha^{(k)}, g^* \sigma_{\alpha 3}^{+(k)} \rangle_{R^{(k)}} + \langle \bar{\phi}_\alpha^{(k)}, t_k g^* \sigma_{\alpha 3}^{+(k)} \rangle_{R^{(k)}} + \langle \bar{w}^{(k)}, g^* \sigma_{33}^{+(k)} \rangle_{R^{(k)}} \\
& \quad + \langle v_\alpha^{(k)}, g^* \bar{\sigma}_{\alpha 3}^{+(k)} \rangle_{R^{(k)}} + \langle \phi_\alpha^{(k)}, t_k g^* \bar{\sigma}_{\alpha 3}^{+(k)} \rangle_{R^{(k)}} + \langle w, g^* \bar{\sigma}_{33}^{+(k)} \rangle_{R^{(k)}} \} \\
& + \sum_{k=2}^N \{ \langle \bar{v}_\alpha^{(k)}, -g^* \sigma_{\alpha 3}^{-(k)} \rangle_{R^{(k)}} + \langle \bar{w}^{(k)}, -g^* \sigma_{33}^{-k} \rangle_{R^{(k)}} \\
& \quad + \langle v_\alpha^{(k)}, -g^* \bar{\sigma}_{\alpha 3}^{-(k)} \rangle_{R^{(k)}} + \langle w^{(k)}, -g^* \bar{\sigma}_{33}^{-(k)} \rangle_{R^{(k)}} \} \\
& + \sum_{k=1}^{N-1} \{ \langle \bar{\sigma}_{\alpha 3}^{+(k)}, g^* v_\alpha^{(k)} + t_k g^* \phi_\alpha^{(k)} - g^* v_\alpha^{(k+1)} \rangle_{R^{(k)}} + \langle \bar{\sigma}_{33}^{+(k)}, g^* w^{(k)} - g^* w^{(k+1)} \rangle_{R^{(k)}} \\
& \quad + \langle \sigma_{\alpha 3}^{+(k)}, g^* \bar{v}_\alpha^{(k)} + t_k g^* \bar{\phi}_\alpha^{(k)} - g^* \bar{v}_\alpha^{(k+1)} \rangle_{R^{(k)}} + \langle \sigma_{33}^{+(k)}, g^* \bar{w}^{(k)} - g^* \bar{w}^{(k+1)} \rangle_{R^{(k)}} \} \\
& - 2 \langle \bar{v}_\alpha^{(1)}, g^* \sigma_{\alpha 3}^{-(1)} \rangle_{R^1} - 2 \langle \bar{w}^{(1)}, g^* \sigma_{33}^{-(1)} \rangle_{R^1} \\
& - 2 \langle \bar{v}_\alpha^{(N)}, -g^* \sigma_{\alpha 3}^{+(N)} \rangle_{R^{(N)}} - 2 \langle \bar{\phi}_\alpha^{(N)}, -t_N g^* \sigma_{\alpha 3}^{+(N)} \rangle_{R^{(N)}} - 2 \langle \bar{w}^{(N)}, -g^* \sigma_{33}^{+(N)} \rangle_{R^{(N)}} \\
& + \sum_{k=1}^N \{ \langle \bar{v}_\alpha^{(k)}, g^* (-N_{\alpha\beta}^{(k)} \eta_\beta + 2 \hat{N}_{\alpha\beta}^{(k)} \eta_\beta) \rangle_{S_1^{(k)}} - \langle v_\alpha^{(k)}, g^* \bar{N}_{\alpha\beta}^{(k)} \eta_\beta \rangle_{S_1^{(k)}} \\
& \quad + \langle \bar{N}_{\alpha\beta}^{(k)}, g^* (v_\alpha^{(k)} \eta_\beta - 2 \vartheta_\alpha^{(k)} \eta_\beta) \rangle_{S_2^{(k)}} + \langle N_{\alpha\beta}^{(k)}, g^* \bar{v}_\alpha^{(k)} \eta_\beta \rangle_{S_2^{(k)}} \\
& \quad + \langle \bar{\phi}_\alpha^{(k)}, g^* (-M_{\alpha\beta}^{(k)} \eta_\beta + 2 \hat{M}_{\alpha\beta}^{(k)} \eta_\beta) \rangle_{S_3^{(k)}} - \langle \phi_\alpha^{(k)}, g^* \bar{M}_{\alpha\beta}^{(k)} \eta_\beta \rangle_{S_3^{(k)}} \\
& \quad + \langle \bar{M}_{\alpha\beta}^{(k)}, g^* (\phi_\alpha^{(k)} \eta_\beta - 2 \phi_\alpha^{(k)} \eta_\beta) \rangle_{S_4^{(k)}} + \langle M_{\alpha\beta}^{(k)}, g^* \bar{\phi}_\alpha^{(k)} \eta_\beta \rangle_{S_4^{(k)}} \\
& \quad + \langle \bar{w}^{(k)}, g^* (-Q_\alpha^{(k)} \eta_\alpha + 2 \hat{Q}_\alpha^{(k)} \eta_\alpha) \rangle_{S_5^{(k)}} - \langle w^{(k)}, g^* \bar{Q}_\alpha^{(k)} \eta_\alpha \rangle_{S_5^{(k)}} \\
& \quad + \langle \bar{Q}_\alpha^{(k)}, g^* (w^{(k)} \eta_\alpha - 2 \hat{w}^{(k)} \eta_\alpha) \rangle_{S_6^{(k)}} + \langle Q_\alpha^{(k)}, g^* \bar{w}^{(k)} \eta_\alpha \rangle_{S_6^{(k)}} \} \\
& + \sum_{k=1}^N \{ \langle \bar{v}_\alpha^{(k)}, g^* (-(\bar{N}_{\alpha\beta}^{(k)})' \eta_\beta + 2 (\hat{N}_{\alpha\beta}^{(k)})' \eta_\beta) \rangle_{S_{11}^{(k)}} - \langle v_\alpha^{(k)}, g^* (\bar{N}_{\alpha\beta}^{(k)})' \eta_\beta \rangle_{S_{11}^{(k)}} \\
& \quad + \langle \bar{N}_{\alpha\beta}^{(k)}, g^* ((v_\alpha^{(k)})' \eta_\beta - 2 (\vartheta_\alpha^{(k)} \eta_\beta) \rangle_{S_{21}^{(k)}} + \langle N_{\alpha\beta}^{(k)}, g^* (\bar{v}_\alpha^{(k)})' \eta_\beta \rangle_{S_{21}^{(k)}} \}
\end{aligned}$$

$$\begin{aligned}
& + \langle \bar{\phi}_{\alpha}^{(k)}, g^*(-(M_{\alpha\beta}^{(k)})' \eta_{\beta} + 2(\hat{M}_{\alpha\beta}^{(k)})' \eta_{\beta}) \rangle_{S_{3i}^{(k)}} - \langle \phi_{\alpha}^{(k)}, g^*(\bar{M}_{\alpha\beta}^{(k)})' \eta_{\beta} \rangle_{S_{3i}^{(k)}} \\
& + \langle \bar{M}_{\alpha\beta}^{(k)}, g^*(\phi_{\alpha}^{(k)})' \eta_{\beta} - 2(\phi_{\alpha}^{(k)})' \eta_{\beta} \rangle_{S_{4i}^{(k)}} + \langle M_{\alpha\beta}^{(k)}, g^*(\bar{\phi}_{\alpha}^{(k)})' \eta_{\beta} \rangle_{S_{4i}^{(k)}} \\
& + \langle \bar{w}^{(k)}, g^*(-(Q_{\alpha}^{(k)})' \eta_{\alpha} + 2(\hat{Q}_{\alpha}^{(k)})' \eta_{\alpha}) \rangle_{S_{5i}^{(k)}} - \langle w^{(k)}, g^*(\bar{Q}_{\alpha}^{(k)}) \eta_{\alpha} \rangle_{S_{5i}^{(k)}} \\
& + \langle \bar{Q}_{\alpha}^{(k)}, g^*((w^{(k)})' \eta_{\alpha} - 2(\hat{w}^{(k)})' \eta_{\alpha}) \rangle_{S_{6i}^{(k)}} + \langle Q_{\alpha}^{(k)}, g^*(\bar{w}^{(k)})' \eta_{\alpha} \rangle_{S_{6i}^{(k)}} \}
\end{aligned}$$

Similar to equations (80) through (82), the following relationships hold

$$\begin{aligned}
\langle v_{\alpha}^{(k)}, g^* \bar{N}_{\alpha\beta,\beta}^{(k)} \rangle_{R^{(k)}} &= - \langle v_{\alpha,\beta}^{(k)}, g^* \bar{N}_{\alpha\beta}^{(k)} \rangle_{R^{(k)}} + \langle v_{\alpha}^{(k)}, g^* \bar{N}_{\alpha\beta}^{(k)} \eta_{\beta} \rangle_{S^{(k)}} \\
\langle \phi_{\alpha}^{(k)}, g^* \bar{M}_{\alpha\beta,\beta}^{(k)} \rangle_{R^{(k)}} &= - \langle \phi_{\alpha,\beta}^{(k)}, g^* \bar{M}_{\alpha\beta}^{(k)} \rangle_{R^{(k)}} + \langle \phi_{\alpha}^{(k)}, g^* M_{\alpha\beta}^{(k)} \eta_{\beta} \rangle_{S^{(k)}} \\
\langle w^{(k)}, g^* \bar{Q}_{\alpha,\alpha}^{(k)} \rangle_{R^{(k)}} &= - \langle w_{\alpha}^{(k)}, g^* \bar{Q}_{\alpha}^{(k)} \rangle_{R^{(k)}} + \langle w^{(k)}, g^* \bar{Q}_{\alpha}^{(k)} \eta_{\alpha} \rangle_{S^{(k)}} \\
\langle N_{\alpha\beta}^{(k)}, g^* \bar{v}_{(\alpha,\beta)}^{(k)} \rangle_{R^{(k)}} &= - \langle N_{\alpha\beta,\beta}^{(k)}, g^* \bar{v}_{\alpha}^{(k)} \rangle_{R^{(k)}} + \langle N_{\alpha\beta}^{(k)}, g^* \bar{v}_{\alpha}^{(k)} \eta_{\beta} \rangle_{S^{(k)}} \\
\langle M_{\alpha\beta}^{(k)}, g^* \bar{\phi}_{(\alpha,\beta)}^{(k)} \rangle_{R^{(k)}} &= - \langle M_{\alpha\beta,\beta}^{(k)}, g^* \bar{\phi}_{\alpha}^{(k)} \rangle_{R^{(k)}} + \langle M_{\alpha\beta}^{(k)}, g^* \bar{\phi}_{\alpha}^{(k)} \eta_{\beta} \rangle_{S^{(k)}} \\
\langle Q_{\alpha}^{(k)}, g^* \bar{w}_{\alpha}^{(k)} \rangle_{R^{(k)}} &= - \langle Q_{\alpha,\alpha}^{(k)}, g^* \bar{w}^{(k)} \rangle_{R^{(k)}} + \langle Q_{\alpha}^{(k)}, g^* \bar{w}^{(k)} \eta_{\alpha} \rangle_{S^{(k)}}
\end{aligned}$$

where $S^{(k)}$ = Boundary of $R^{(k)}$ \cup internal surfaces in $R^{(k)}$. Using these to eliminate $\bar{v}_{(\alpha,\beta)}^{(k)}$, $\bar{\phi}_{(\alpha,\beta)}^{(k)}$, $\bar{w}_{\alpha}^{(k)}$, $\bar{N}_{\alpha\beta,\beta}^{(k)}$, $\bar{M}_{\alpha\beta,\beta}^{(k)}$, and $\bar{Q}_{\alpha,\alpha}^{(k)}$ from the Gateaux differential, one can write

$$\begin{aligned}
\delta_{\bar{u}} \Omega(u) &= 2 \sum_{k=1}^N \{ \langle \bar{v}_{\alpha}^{(k)}, g^* N_{\alpha\beta,\beta}^{(k)} - P^{(k)} v_{\alpha}^{(k)} - R^{(k)} \phi_{\alpha}^{(k)} + g^* F_{\alpha}^{(k)} + Y^{(k)} \rangle_{R^{(k)}} \\
&\quad + \langle \bar{e}_{\alpha\beta}^{(k)}, g^* N_{\alpha\beta}^{(k)} - g^* A_{\alpha\beta\gamma\delta}^{(k)} g^* e_{\gamma\delta}^{(k)} - g^* B_{\alpha\beta\gamma\delta}^{(k)} \kappa_{\gamma\delta}^{(k)} \rangle_{R^{(k)}} \\
&\quad + \langle \bar{N}_{\alpha\beta}^{(k)}, g^* e_{\alpha\beta}^{(k)} - g^* v_{(\alpha,\beta)}^{(k)} \rangle_{R^{(k)}} \\
&\quad + \langle \bar{\phi}_{\alpha}^{(k)}, g^* M_{\alpha\beta,\beta}^{(k)} - g^* Q_{\alpha}^{(k)} - R^{(k)} v_{\alpha}^{(k)} - I^{(k)} \phi_{\alpha}^{(k)} + g^* G_{\alpha}^{(k)} + Z^{(k)} \rangle_{R^{(k)}} \\
&\quad + \langle \bar{\kappa}_{\alpha\beta}^{(k)}, g^* M_{\alpha\beta}^{(k)} - g^* B_{\alpha\beta\gamma\delta}^{(k)} e_{\gamma\delta}^{(k)} - g^* D_{\alpha\beta\gamma\delta}^{(k)} \kappa_{\gamma\delta}^{(k)} \rangle_{R^{(k)}} \\
&\quad + \langle \bar{M}_{\alpha\beta}^{(k)}, g^* \kappa_{\alpha\beta}^{(k)} - g^* \phi_{(\alpha,\beta)}^{(k)} \rangle_{R^{(k)}}
\end{aligned} \tag{2.88}$$

$$\begin{aligned}
& + \langle \bar{w}^{(k)}, g^* Q_{\alpha,\alpha}^{(k)} - P^{(k)} w^{(k)} + g^* F_3^{(k)} + X^{(k)} \rangle_{R^{(k)}} \\
& + \langle 2\epsilon_{\alpha 3}^{(k)}, g^* Q_\alpha^{(k)} - g^* G_{\alpha 3 \gamma 3}^{(k)} (2\epsilon_{\gamma 3}^{(k)}) \rangle_{R^{(k)}} \\
& + \langle Q_\alpha^{(k)}, g^* (2\epsilon_{\alpha 3}^{(k)}) - g^* \phi_\alpha^{(k)} - g^* w_{,\alpha}^{(k)} \rangle_{R^{(k)}} \\
& + 2 \sum_{k=1}^{N-1} \{ \langle \bar{v}_\alpha^{(k)}, g^* \sigma_{\alpha 3}^{+(k)} \rangle_{R^{(k)}} + \langle \bar{\phi}_\alpha^{(k)}, t_k g^* \sigma_{\alpha 3}^{+(k)} \rangle_{R^{(k)}} + \langle \bar{w}^{(k)}, g^* \sigma_{33}^{+(k)} \rangle_{R^{(k)}} \} \\
& + 2 \sum_{k=2}^N \{ \langle \bar{v}_\alpha^{(k)}, -g^* \sigma_{\alpha 3}^{-(k)} \rangle_{R^{(k)}} + \langle \bar{w}^{(k)}, -g^* \sigma_{33}^{-k} \rangle_{R^{(k)}} \} \\
& + 2 \sum_{k=1}^{N-1} \{ \langle \bar{\sigma}_{\alpha 3}^{+(k)}, g^* v_\alpha^{(k)} + t_k g^* \phi_\alpha^{(k)} - g^* v_\alpha^{(k+1)} \rangle_{R^{(k)}} + \langle \bar{\sigma}_{33}^{+(k)}, g^* w^{(k)} - g^* w^{(k+1)} \rangle_{R^{(k)}} \\
& - 2 \langle \bar{v}_\alpha^{(1)}, g^* \sigma_{\alpha 3}^{-(1)} \rangle_{R^1} - 2 \langle \bar{w}^{(1)}, g^* \sigma_{33}^{-(1)} \rangle_{R^1} \\
& - 2 \langle \bar{v}_\alpha^{(N)}, -g^* \sigma_{\alpha 3}^{+(N)} \rangle_{R^{(N)}} - 2 \langle \bar{\phi}_\alpha^{(N)}, -t_N g^* \sigma_{\alpha 3}^{+(N)} \rangle_{R^{(N)}} - 2 \langle \bar{w}^{(N)}, -g^* \sigma_{33}^{+(N)} \rangle_{R^{(N)}} \\
& + 2 \sum_{k=1}^N \{ \langle \bar{v}_\alpha^{(k)}, g^* (-N_{\alpha\beta}^{(k)} \eta_\beta + \hat{N}_{\alpha\beta}^{(k)} \eta_\beta) \rangle_{S_1^{(k)}} \\
& + \langle \bar{N}_{\alpha\beta}^{(k)}, g^* (v_\alpha^{(k)} \eta_\beta - \bar{v}_\alpha^{(k)} \eta_\beta) \rangle_{S_2^{(k)}} \\
& + \langle \bar{\phi}_\alpha^{(k)}, g^* (-M_{\alpha\beta}^{(k)} \eta_\beta + \hat{M}_{\alpha\beta}^{(k)} \eta_\beta) \rangle_{S_3^{(k)}} \\
& + \langle \bar{M}_{\alpha\beta}^{(k)}, g^* (\phi_\alpha^{(k)} \eta_\beta - \bar{\phi}_\alpha^{(k)} \eta_\beta) \rangle_{S_4^{(k)}} \\
& + \langle \bar{w}^{(k)}, g^* (-Q_\alpha^{(k)} \eta_\alpha + \hat{Q}_\alpha \eta_\alpha) \rangle_{S_5^{(k)}} \\
& + \langle \bar{Q}_\alpha^{(k)}, g^* (w_\alpha^{(k)} \eta_\alpha - \bar{w}_\alpha^{(k)} \eta_\alpha) \rangle_{S_6^{(k)}} \\
& + 2 \sum_{k=1}^N \{ \langle \bar{v}_\alpha^{(k)}, g^* (-N_{\alpha\beta}^{(k)'} \eta_\beta + \hat{N}_{\alpha\beta}^{(k)'} \eta_\beta) \rangle_{S_{1i}^{(k)}} \\
& + \langle \bar{N}_{\alpha\beta}^{(k)}, g^* ((v_\alpha^{(k)'} \eta_\beta - \bar{v}_\alpha^{(k)'} \eta_\beta) \rangle_{S_{2i}^{(k)}} \}
\end{aligned}$$

$$+ \langle \phi_{\alpha}^{(k)}, g^*(-(M_{\alpha\beta}^{(k)})' \eta_{\beta} + (\hat{M}_{\alpha\beta}^{(k)})' \eta_{\beta}) \rangle_{S_{3i}^{(k)}}$$

$$+ \langle \bar{M}_{\alpha\beta}^{(k)}, g^*((\phi_{\alpha}^{(k)})' \eta_{\beta} - (\phi_{\alpha}^{(k)})' \eta_{\beta}) \rangle_{S_{4i}^{(k)}}$$

$$+ \langle \bar{w}^{(k)}, g^*(-(Q_{\alpha}^{(k)})' \eta_{\alpha} + (\hat{Q}_{\alpha}^{(k)})' \eta_{\alpha}) \rangle_{S_{5i}^{(k)}}$$

$$+ \langle \bar{Q}_{\alpha}^{(k)}, g^*((w^{(k)})' \eta_{\alpha} - (\hat{w}^{(k)})' \eta_{\alpha}) \rangle_{S_{6i}^{(k)}}$$

Linearity of the bilinear mapping $\langle \cdot, \cdot \rangle$ implies that $\delta_u \Omega(u)$ vanishes if all of equations (70), (83), and (84) are satisfied. Also, nondegenerateness of the bilinear mapping $\langle \cdot, \cdot \rangle$ implies that the Gateaux differential in equation (88) would vanish, along an arbitrary path $\{\bar{u}\}$, only if all the field and continuity equations and the corresponding boundary conditions are satisfied.

2.3.2 Extended Variational Formulation

The solution of (70) must belong to the admissible domain of the operators for the functional (86) to be meaningful. Using (A.21) along with (A.22) relaxation of the order of differentiability of either component of the following pairs is possible, viz., $(Q_{\alpha} \text{ or } w)$, $(M_{\alpha\beta} \text{ or } \phi_{\alpha})$, and $(N_{\alpha\beta} \text{ or } v_{\alpha})$. However, relaxation of differentiability could not be done on both components of a pair. Some possibilities are indicated by (80) through (82). Using these equations to eliminate one or the other of the adjoint pair of operators results in reduction of the differentiability requirement on some of the admissible field variables. This provides a basis for extension of the variational principle to a domain where the differentiability requirements are selectively relaxed. These extended variational formulations also provide the basis for certain useful specializations to reduce the number of field variables. To develop these extensions, it is convenient to rearrange the terms in (86) to write the governing function as:

$$\Omega(u) = 2 \sum_{k=1}^N \{ \langle v_{\alpha}^{(k)}, g^* F_{\alpha}^{(k)} + Y^{(k)} \rangle_{R^{(k)}} + \langle \phi_{\alpha}^{(k)}, g^* G_{\alpha}^{(k)} + Z^{(k)} \rangle_{R^{(k)}} \}$$

$$\begin{aligned}
& + \langle w^{(k)}, g^* F_3^{(k)} + X^{(k)} \rangle_{R^{(k)}} \} \\
& + \sum_{k=1}^N \{ \langle v_\alpha^{(k)}, g^* N_{\alpha\beta,\beta}^{(k)} \rangle_{R^{(k)}} + \langle v_\alpha^{(k)}, -P^{(k)} v_\alpha^{(k)} - R^{(k)} \phi_\alpha^{(k)} \rangle_{R^{(k)}} \\
& + \langle e_{\alpha\beta}^{(k)}, g^* N_{\alpha\beta}^{(k)} - g^* A_{\alpha\beta\gamma\delta}^{(k)} e_{\gamma\delta}^{(k)} - g^* B_{\alpha\beta\gamma\delta}^{(k)} \kappa_{\gamma\delta}^{(k)} \rangle_{R^{(k)}} \\
& + \langle N_{\alpha\beta}^{(k)}, g^* e_{\alpha\beta}^{(k)} - g^* v_{(\alpha,\beta)}^{(k)} \rangle_{R^{(k)}} \\
& + \langle \phi_\alpha^{(k)}, g^* M_{\alpha\beta,\beta}^{(k)} - g^* Q_\alpha^{(k)} - R^{(k)} v_\alpha^{(k)} - I^{(k)} \phi_\alpha^{(k)} \rangle_{R^{(k)}} \\
& + \langle \kappa_{\alpha\beta}^{(k)}, g^* M_{\alpha\beta}^{(k)} - g^* B_{\alpha\beta\gamma\delta}^{(k)} e_{\gamma\delta}^{(k)} - g^* D_{\alpha\beta\gamma\delta}^{(k)} \kappa_{\gamma\delta}^{(k)} \rangle_{R^{(k)}} \\
& + \langle M_{\alpha\beta}^{(k)}, g^* \kappa_{\alpha\beta}^{(k)} - g^* \phi_{(\alpha,\beta)}^{(k)} \rangle_{R^{(k)}} \\
& + \langle w^{(k)}, g^* Q_{\alpha,\alpha}^{(k)} - P^{(k)} w^{(k)} \rangle_{R^{(k)}} \\
& + \langle 2 \epsilon_{\alpha 3}^{(k)}, g^* Q_\alpha^{(k)} - g^* G_{\alpha 3 \gamma 3}^{(k)} (2 \epsilon_{\gamma 3}^{(k)}) \rangle_{R^{(k)}} \\
& + \langle Q_\alpha^{(k)}, g^* (2 \epsilon_{\alpha 3}^{(k)}) - g^* \phi_\alpha^{(k)} - g^* w_{,\alpha}^{(k)} \rangle_{R^{(k)}} \quad (89) \\
& + \sum_{k=1}^{N-1} \{ \langle v_\alpha^{(k)}, g^* \sigma_{\alpha 3}^{+(k)} \rangle_{R^{(k)}} + \langle \phi_\alpha^{(k)}, t_k g^* \sigma_{\alpha 3}^{+(k)} \rangle_{R^{(k)}} + \langle w^{(k)}, g^* \sigma_{33}^{+(k)} \rangle_{R^{(k)}} \} \\
& + \sum_{k=2}^N \{ \langle v_\alpha^{(k)}, -g^* \sigma_{\alpha 3}^{-(k)} \rangle_{R^{(k)}} + \langle w^{(k)}, -g^* \sigma_{33}^{-k} \rangle_{R^{(k)}} \} \\
& + \sum_{k=1}^{N-1} \{ \langle \sigma_{\alpha 3}^{+(k)}, g^* v_\alpha^{(k)} + t_k g^* \phi_\alpha^{(k)} - g^* v_\alpha^{(k+1)} \rangle_{R^{(k)}} + \langle \sigma_{33}^{+(k)}, g^* w^{(k)} - g^* w^{(k+1)} \rangle_{R^{(k)}} \} \\
& - 2 \langle v_\alpha^{(1)}, g^* \sigma_{\alpha 3}^{-(1)} \rangle_{R^1} - 2 \langle w^{(1)}, g^* \sigma_{33}^{-(1)} \rangle_{R^1} \\
& + 2 \langle v_\alpha^{(N)}, g^* \sigma_{\alpha 3}^{+(N)} \rangle_{R^{(N)}} + 2 \langle \phi_\alpha^{(N)}, t_N g^* \sigma_{\alpha 3}^{+(N)} \rangle_{R^{(N)}} + 2 \langle w^{(N)}, g^* \sigma_{33}^{+(N)} \rangle_{R^{(N)}} \\
& + \sum_{k=1}^N \{ \langle v_\alpha^{(k)}, g^* (-N_{\alpha\beta}^{(k)} \eta_\beta + 2 \hat{N}_{\alpha\beta}^{(k)} \eta_\beta) \rangle_{S_1^{(k)}} + \langle N_{\alpha\beta}^{(k)} \eta_\beta, g^* (v_\alpha^{(k)} - 2 \phi_\alpha^{(k)}) \rangle_{S_2^{(k)}} \\
& + \langle \phi_\alpha^{(k)}, g^* (-M_{\alpha\beta}^{(k)} \eta_\beta + 2 \hat{M}_{\alpha\beta}^{(k)} \eta_\beta) \rangle_{S_3^{(k)}} + \langle M_{\alpha\beta}^{(k)} \eta_\beta, g^* (\phi_\alpha^{(k)} - 2 \phi_\alpha^{(k)}) \rangle_{S_4^{(k)}} \}
\end{aligned}$$

$$\begin{aligned}
& + \langle w^{(k)}, g^*(-Q_{\alpha}^{(k)} \eta_{\alpha} + 2 \hat{Q}_{\alpha}^{(k)} \eta_{\alpha}) \rangle_{S_5^{(k)}} + \langle Q_{\alpha}^{(k)} \eta_{\alpha}, g^*(w^{(k)} - 2 \hat{w}^{(k)}) \rangle_{S_6^{(k)}} \\
& + \sum_{k=1}^N \{ \langle v_{\alpha}^{(k)}, g^*(-(N_{\alpha\beta}^{(k)} \eta_{\beta})' + 2(\hat{N}_{\alpha\beta}^{(k)})' \eta_{\beta}) \rangle_{S_{1i}^{(k)}} + \langle N_{\alpha\beta}^{(k)} \eta_{\beta}, g^*((v_{\alpha}^{(k)})' - 2(\hat{v}_{\alpha}^{(k)})') \rangle_{S_{2i}^{(k)}} \\
& + \langle \phi_{\alpha}^{(k)}, g^*(-(M_{\alpha\beta}^{(k)} \eta_{\beta})' + 2(\hat{M}_{\alpha\beta}^{(k)})' \eta_{\beta}) \rangle_{S_{3i}^{(k)}} + \langle M_{\alpha\beta}^{(k)} \eta_{\beta}, g^*((\phi_{\alpha}^{(k)})' - 2(\hat{\phi}_{\alpha}^{(k)})') \rangle_{S_{4i}^{(k)}} \\
& + \langle w^{(k)}, g^*(-(Q_{\alpha}^{(k)} \eta_{\alpha})' + 2(\hat{Q}_{\alpha}^{(k)})' \eta_{\alpha}) \rangle_{S_{5i}^{(k)}} + \langle Q_{\alpha}^{(k)} \eta_{\alpha}, g^*((w^{(k)})' - 2(\hat{w}^{(k)})') \rangle_{S_{6i}^{(k)}} \}
\end{aligned}$$

STEP 1

For example, eliminating $N_{\alpha\beta,\beta}$ in (89) by using (80), the domain of $N_{\alpha\beta}^{(k)}$ is extended from C^1 to C° , and the function has the form

$$\begin{aligned}
\Omega_1(u) = & 2 \sum_{k=1}^N \{ \langle v_{\alpha}^{(k)}, g^* F_{\alpha}^{(k)} + Y^{(k)} \rangle_{R^{(k)}} + \langle \phi_{\alpha}^{(k)}, g^* G_{\alpha}^{(k)} + Z^{(k)} \rangle_{R^{(k)}} \\
& + \langle w^{(k)}, g^* F_3^{(k)} + X^{(k)} \rangle_{R^{(k)}} \} \\
& + \sum_{k=1}^N \{ \langle v_{\alpha}^{(k)}, -P^{(k)} v_{\alpha}^{(k)} - R^{(k)} \phi_{\alpha}^{(k)} \rangle_{R^{(k)}} \\
& + \langle e_{\alpha\beta}^{(k)}, -g^* A_{\alpha\beta\gamma\delta}^{(k)} e_{\gamma\delta}^{(k)} - g^* B_{\alpha\beta\gamma\delta}^{(k)} \kappa_{\gamma\delta}^{(k)} \rangle_{R^{(k)}} \\
& + 2 \langle N_{\alpha\beta}^{(k)}, g^* e_{\alpha\beta}^{(k)} - g^* v_{(\alpha,\beta)}^{(k)} \rangle_{R^{(k)}} \\
& + \langle \phi_{\alpha}^{(k)}, g^* M_{\alpha\beta,\beta}^{(k)} - g^* Q_{\alpha}^{(k)} - R^{(k)} v_{\alpha}^{(k)} - I^{(k)} \phi_{\alpha}^{(k)} \rangle_{R^{(k)}} \\
& + \langle \kappa_{\alpha\beta}^{(k)}, g^* M_{\alpha\beta}^{(k)} - g^* B_{\alpha\beta\gamma\delta}^{(k)} e_{\gamma\delta}^{(k)} - g^* D_{\alpha\beta\gamma\delta}^{(k)} \kappa_{\gamma\delta}^{(k)} \rangle_{R^{(k)}} \\
& + \langle M_{\alpha\beta}^{(k)}, g^* \kappa_{\alpha\beta}^{(k)} - g^* \phi_{(\alpha,\beta)}^{(k)} \rangle_{R^{(k)}} \\
& + \langle w^{(k)}, g^* Q_{\alpha,\alpha}^{(k)} - P^{(k)} w^{(k)} \rangle_{R^{(k)}} \\
& + \langle 2 \epsilon_{\alpha 3}^{(k)}, g^* Q_{\alpha}^{(k)} - g^* G_{\alpha 3 \gamma 3}^{(k)} (2 \epsilon_{\gamma 3}^{(k)}) \rangle_{R^{(k)}} \\
& + \langle Q_{\alpha}^{(k)}, g^* (2 \epsilon_{\alpha 3}^{(k)}) - g^* \phi_{\alpha}^{(k)} - g^* w_{,\alpha}^{(k)} \rangle_{R^{(k)}} \} \tag{90}
\end{aligned}$$

$$\begin{aligned}
& + \sum_{k=1}^{N-1} \{ \langle v_\alpha^{(k)}, g^* \sigma_{\alpha 3}^{+(k)} \rangle_{R^{(k)}} + \langle \phi_\alpha^{(k)}, t_k g^* \sigma_{\alpha 3}^{+(k)} \rangle_{R^{(k)}} + \langle w^{(k)}, g^* \sigma_{33}^{+(k)} \rangle_{R^{(k)}} \} \\
& + \sum_{k=2}^N \{ \langle v_\alpha^{(k)}, -g^* \sigma_{\alpha 3}^{-(k)} \rangle_{R^{(k)}} + \langle w^{(k)}, -g^* \sigma_{33}^{-k} \rangle_{R^{(k)}} \} \\
& + \sum_{k=1}^{N-1} \{ \langle \sigma_{\alpha 3}^{+(k)}, g^* v_\alpha^{(k)} + t_k g^* \phi_\alpha^{(k)} - g^* v_\alpha^{(k+1)} \rangle_{R^{(k)}} + \langle \sigma_{33}^{+(k)}, g^* w^{(k)} - g^* w^{(k+1)} \rangle_{R^{(k)}} \} \\
& - 2 \langle v_\alpha^{(1)}, g^* \sigma_{\alpha 3}^{-(1)} \rangle_{R^1} - 2 \langle w^{(1)}, g^* \sigma_{33}^{-(1)} \rangle_{R^1} \\
& + 2 \langle v_\alpha^{(N)}, g^* \sigma_{\alpha 3}^{+(N)} \rangle_{R^{(N)}} + 2 \langle \phi_\alpha^{(N)}, t_N g^* \sigma_{\alpha 3}^{+(N)} \rangle_{R^{(N)}} + 2 \langle w^{(N)}, g^* \sigma_{33}^{+(N)} \rangle_{R^{(N)}} \\
& + \sum_{k=1}^N \{ \langle v_\alpha^{(k)}, 2 g^* \hat{N}_{\alpha \beta}^{(k)} \eta_\beta \rangle_{S_1^{(k)}} + \langle N_{\alpha \beta}^{(k)} \eta_\beta, 2 g^*(v_\alpha^{(k)} - \vartheta_\alpha^{(k)}) \rangle_{S_2^{(k)}} \\
& + \langle \phi_\alpha^{(k)}, g^*(-M_{\alpha \beta}^{(k)} \eta_\beta + 2 \hat{M}_{\alpha \beta}^{(k)} \eta_\beta) \rangle_{S_3^{(k)}} + \langle M_{\alpha \beta}^{(k)} \eta_\beta, g^*(\phi_\alpha^{(k)} - 2 \phi_\alpha^{(k)}) \rangle_{S_4^{(k)}} \\
& + \langle w^{(k)}, g^*(-Q_\alpha^{(k)} \eta_\alpha + 2 \hat{Q}_\alpha^{(k)} \eta_\alpha) \rangle_{S_5^{(k)}} + \langle Q_\alpha^{(k)} \eta_\alpha, g^*(w^{(k)} - 2 \hat{w}^{(k)}) \rangle_{S_6^{(k)}} \} \\
& + \sum_{k=1}^N \{ \langle v_\alpha^{(k)}, 2 g^* \hat{N}'_{\alpha \beta}^{(k)} \eta_\beta \rangle_{S_{1l}^{(k)}} + \langle N'_{\alpha \beta}^{(k)} \eta_\beta, 2 g^*(v'_\alpha^{(k)} - \vartheta'_\alpha^{(k)}) \rangle_{S_{2l}^{(k)}} \\
& + \langle \phi_\alpha^{(k)}, g^*(-M'_{\alpha \beta}^{(k)} \eta_\beta + 2 \hat{M}'_{\alpha \beta}^{(k)} \eta_\beta) \rangle_{S_{3l}^{(k)}} + \langle M'_{\alpha \beta}^{(k)} \eta_\beta, g^*(\phi'_\alpha^{(k)} - 2 \phi'_\alpha^{(k)}) \rangle_{S_{4l}^{(k)}} \\
& + \langle w^{(k)}, g^*(-Q'_\alpha^{(k)} \eta_\alpha + 2 \hat{Q}'_\alpha^{(k)} \eta_\alpha) \rangle_{S_{5l}^{(k)}} + \langle Q'_\alpha^{(k)} \eta_\alpha, g^*(w'^{(k)} - 2 \hat{w}'^{(k)}) \rangle_{S_{6l}^{(k)}} \}
\end{aligned}$$

STEP 2

Eliminating $M_{\alpha\beta,\beta}^{(k)}$ in (90) using (81) leads to

$$\begin{aligned}
 \Omega_2(u) = & 2 \sum_{k=1}^N \left\{ \langle v_\alpha^{(k)}, g^* F_\alpha^{(k)} + Y^{(k)} \rangle_{R^{(k)}} + \langle \phi_\alpha^{(k)}, g^* G_\alpha^{(k)} + Z^{(k)} \rangle_{R^{(k)}} \right. \\
 & + \langle w^{(k)}, g^* F_3^{(k)} + X^{(k)} \rangle_{R^{(k)}} \} \\
 & + \sum_{k=1}^N \left\{ \langle v_\alpha^{(k)}, -P^{(k)} v_\alpha^{(k)} - R^{(k)} \phi_\alpha^{(k)} \rangle_{R^{(k)}} \right. \\
 & + \langle e_{\alpha\beta}^{(k)}, -g^* A_{\alpha\beta\gamma\delta}^{(k)} g^* e_{\gamma\delta}^{(k)} - g^* B_{\alpha\beta\gamma\delta}^{(k)} \kappa_{\gamma\delta}^{(k)} \rangle_{R^{(k)}} \\
 & + 2 \langle N_{\alpha\beta}^{(k)}, g^* e_{\alpha\beta}^{(k)} - g^* v_{(\alpha,\beta)}^{(k)} \rangle_{R^{(k)}} \\
 & + \langle \phi_\alpha^{(k)}, -g^* Q_\alpha^{(k)} - R^{(k)} v_\alpha^{(k)} - I^{(k)} \phi_\alpha^{(k)} \rangle_{R^{(k)}} \\
 & + \langle \kappa_{\alpha\beta}^{(k)}, -g^* B_{\alpha\beta\gamma\delta}^{(k)} e_{\gamma\delta}^{(k)} - g^* D_{\alpha\beta\gamma\delta}^{(k)} \kappa_{\gamma\delta}^{(k)} \rangle_{R^{(k)}} \\
 & + 2 \langle M_{\alpha\beta}^{(k)}, g^* \kappa_{\alpha\beta}^{(k)} - g^* \phi_{(\alpha,\beta)}^{(k)} \rangle_{R^{(k)}} \\
 & + \langle w^{(k)}, g^* Q_{\alpha,\alpha}^{(k)} - P^{(k)} w^{(k)} \rangle_{R^{(k)}} \\
 & + \langle 2\epsilon_{\alpha 3}^{(k)}, g^* Q_\alpha^{(k)} - g^* G_{\alpha 3 \gamma 3}^{(k)} (2\epsilon_{\gamma 3}^{(k)}) \rangle_{R^{(k)}} \\
 & + \langle Q_\alpha^{(k)}, g^* (2\epsilon_{\alpha 3}^{(k)}) - g^* \phi_\alpha^{(k)} - g^* w_\alpha^{(k)} \rangle_{R^{(k)}} \} \tag{91} \\
 & + \sum_{k=1}^{N-1} \left\{ \langle v_\alpha^{(k)}, g^* \sigma_{\alpha 3}^{+(k)} \rangle_{R^{(k)}} + \langle \phi_\alpha^{(k)}, t_k g^* \sigma_{\alpha 3}^{+(k)} \rangle_{R^{(k)}} + \langle w^{(k)}, g^* \sigma_{33}^{+(k)} \rangle_{R^{(k)}} \right\} \\
 & + \sum_{k=2}^N \left\{ \langle v_\alpha^{(k)}, -g^* \sigma_{\alpha 3}^{-(k)} \rangle_{R^{(k)}} + \langle w^{(k)}, -g^* \sigma_{33}^{-k} \rangle_{R^{(k)}} \right\} \\
 & + \sum_{k=1}^{N-1} \left\{ \langle \sigma_{\alpha 3}^{+(k)}, g^* v_\alpha^{(k)} + t_k g^* \phi_\alpha^{(k)} - g^* v_\alpha^{(k+1)} \rangle_{R^{(k)}} + \langle \sigma_{33}^{+(k)}, g^* w^{(k)} - g^* w^{(k+1)} \rangle_{R^{(k)}} \right\} \\
 & - 2 \langle v_\alpha^{(1)}, g^* \sigma_{\alpha 3}^{-(1)} \rangle_{R^1} - 2 \langle w^{(1)}, g^* \sigma_{33}^{-(1)} \rangle_{R^1}
 \end{aligned}$$

$$\begin{aligned}
& + 2 \langle v_{\alpha}^{(N)}, g^* \sigma_{\alpha 3}^{+(N)} \rangle_{R^{(N)}} + 2 \langle \phi_{\alpha}^{(N)}, t_N g^* \sigma_{\alpha 3}^{+(N)} \rangle_{R^{(N)}} + 2 \langle w^{(N)}, g^* \sigma_{33}^{+(N)} \rangle_{R^{(N)}} \\
& + \sum_{k=1}^N \{ \langle v_{\alpha}^{(k)}, 2g^* \hat{N}_{\alpha \beta}^{(k)} \eta_{\beta} \rangle_{S_1^{(k)}} + \langle N_{\alpha \beta}^{(k)} \eta_{\beta}, 2g^*(v_{\alpha}^{(k)} - \phi_{\alpha}^{(k)}) \rangle_{S_2^{(k)}} \\
& + \langle \phi_{\alpha}^{(k)}, 2g^* \hat{M}_{\alpha \beta}^{(k)} \eta_{\beta} \rangle_{S_3^{(k)}} + \langle M_{\alpha \beta}^{(k)} \eta_{\beta}, 2g^*(\phi_{\alpha}^{(k)} - \phi_{\alpha}^{(k)}) \rangle_{S_4^{(k)}} \\
& + \langle w^{(k)}, g^*(-Q_{\alpha}^{(k)} \eta_{\alpha} + 2Q_{\alpha}^{(k)} \eta_{\alpha}) \rangle_{S_5^{(k)}} + \langle Q_{\alpha}^{(k)} \eta_{\alpha}, g^*(w^{(k)} - 2\hat{w}^{(k)}) \rangle_{S_6^{(k)}} \} \\
& + \sum_{k=1}^N \{ \langle v_{\alpha}^{(k)}, 2g^* \hat{N}_{\alpha \beta}^{(k)} \eta_{\beta} \rangle_{S_1^{(k)}} + \langle N_{\alpha \beta}^{(k)} \eta_{\beta}, 2g^*(v_{\alpha}^{(k)} - \phi_{\alpha}^{(k)}) \rangle_{S_2^{(k)}} \\
& + \langle \phi_{\alpha}^{(k)}, 2g^* \hat{M}_{\alpha \beta}^{(k)} \eta_{\beta} \rangle_{S_3^{(k)}} + \langle M_{\alpha \beta}^{(k)} \eta_{\beta}, 2g^*(\phi_{\alpha}^{(k)} - \phi_{\alpha}^{(k)}) \rangle_{S_4^{(k)}} \\
& + \langle w^{(k)}, g^*(-Q_{\alpha}^{(k)} \eta_{\alpha} + 2Q_{\alpha}^{(k)} \eta_{\alpha}) \rangle_{S_5^{(k)}} + \langle Q_{\alpha}^{(k)} \eta_{\alpha}, g^*(w^{(k)} - 2\hat{w}^{(k)}) \rangle_{S_6^{(k)}} \}
\end{aligned}$$

STEP 3

Eliminating $Q_{\alpha, \mu}^{(k)}$ in (91) using (82) results in:

$$\begin{aligned}
\Omega_3(u) = & 2 \sum_{k=1}^N \{ \langle v_{\alpha}^{(k)}, g^* F_{\alpha}^{(k)} + Y^{(k)} \rangle_{R^{(k)}} + \langle \phi_{\alpha}^{(k)}, g^* G_{\alpha}^{(k)} + Z^{(k)} \rangle_{R^{(k)}} \\
& + \langle w^{(k)}, g^* F_3^{(k)} + X^{(k)} \rangle_{R^{(k)}} \} \\
& + \sum_{k=1}^N \{ \langle v_{\alpha}^{(k)}, -P^{(k)} v_{\alpha}^{(k)} - R^{(k)} \phi_{\alpha}^{(k)} \rangle_{R^{(k)}} \\
& + \langle e_{\alpha \beta}^{(k)}, -g^* A_{\alpha \beta \gamma \delta}^{(k)} e_{\gamma \delta}^{(k)} - g^* B_{\alpha \beta \gamma \delta}^{(k)} \kappa_{\gamma \delta}^{(k)} \rangle_{R^{(k)}} \\
& + 2 \langle N_{\alpha \beta}^{(k)}, g^* e_{\alpha \beta}^{(k)} - g^* v_{(\alpha, \beta)}^{(k)} \rangle_{R^{(k)}} \\
& + \langle \phi_{\alpha}^{(k)}, -R^{(k)} v_{\alpha}^{(k)} - I^{(k)} \phi_{\alpha}^{(k)} \rangle_{R^{(k)}} \\
& + \langle \kappa_{\alpha \beta}^{(k)}, -g^* B_{\alpha \beta \gamma \delta}^{(k)} e_{\gamma \delta}^{(k)} - g^* D_{\alpha \beta \gamma \delta}^{(k)} \kappa_{\gamma \delta}^{(k)} \rangle_{R^{(k)}} \\
& + 2 \langle M_{\alpha \beta}^{(k)}, g^* \kappa_{\alpha \beta}^{(k)} - g^* \phi_{(\alpha, \beta)}^{(k)} \rangle_{R^{(k)}} + \langle w^{(k)}, -P^{(k)} w^{(k)} \rangle_{R^{(k)}}
\end{aligned}$$

$$\begin{aligned}
& + \langle 2\epsilon_{\alpha 3}^{(k)}, -g^* G_{\alpha 3 \gamma 3}^{(k)} g^*(2\epsilon_{\gamma 3}^{(k)}) \rangle_{R^{(k)}} \\
& + 2 \langle Q_\alpha^{(k)}, g^*(2\epsilon_{\alpha 3}^{(k)}) - g^* \phi_\alpha^{(k)} - g^* w_{,\alpha}^{(k)} \rangle_{R^{(k)}} \quad (92)
\end{aligned}$$

$$\begin{aligned}
& + \sum_{k=1}^{N-1} \{ \langle v_\alpha^{(k)}, g^* \sigma_{\alpha 3}^{+(k)} \rangle_{R^{(k)}} + \langle \phi_\alpha^{(k)}, t_k g^* \sigma_{\alpha 3}^{+(k)} \rangle_{R^{(k)}} + \langle w^{(k)}, g^* \sigma_{33}^{+(k)} \rangle_{R^{(k)}} \} \\
& + \sum_{k=2}^N \{ \langle v_\alpha^{(k)}, -g^* \sigma_{\alpha 3}^{-(k)} \rangle_{R^{(k)}} + \langle w^{(k)}, -g^* \sigma_{33}^{-k} \rangle_{R^{(k)}} \} \\
& + \sum_{k=1}^{N-1} \{ \langle \sigma_{\alpha 3}^{+(k)}, g^* v_\alpha^{(k)} + t_k g^* \phi_\alpha^{(k)} - g^* v_\alpha^{(k+1)} \rangle_{R^{(k)}} + \langle \sigma_{33}^{+(k)}, g^* w^{(k)} - g^* w^{(k+1)} \rangle_{R^{(k)}} \} \\
& - 2 \langle v_\alpha^{(1)}, g^* \sigma_{\alpha 3}^{-(1)} \rangle_{R^1} - 2 \langle w^{(1)}, g^* \sigma_{33}^{-(1)} \rangle_{R^1} \\
& + 2 \langle v_\alpha^{(N)}, g^* \sigma_{\alpha 3}^{+(N)} \rangle_{R^{(N)}} + 2 \langle \phi_\alpha^{(N)}, t_N g^* \sigma_{\alpha 3}^{+(N)} \rangle_{R^{(N)}} + 2 \langle w^{(N)}, g^* \sigma_{33}^{+(N)} \rangle_{R^{(N)}} \\
& + \sum_{k=1}^N \{ \langle v_\alpha^{(k)}, 2g^* \hat{N}_{\alpha \beta}^{(k)} \eta_\beta \rangle_{S_1^{(k)}} + \langle N_{\alpha \beta}^{(k)} \eta_\beta, 2g^*(v_\alpha^{(k)} - \phi_\alpha^{(k)}) \rangle_{S_2^{(k)}} \\
& + \langle \phi_\alpha^{(k)}, 2g^* \hat{M}_{\alpha \beta}^{(k)} \eta_\beta \rangle_{S_3^{(k)}} + \langle M_{\alpha \beta}^{(k)} \eta_\beta, 2g^*(\phi_\alpha^{(k)} - \phi_\alpha^{(k)}) \rangle_{S_4^{(k)}} \\
& + \langle w^{(k)}, 2g^* \hat{Q}_\alpha^{(k)} \eta_\alpha \rangle_{S_5^{(k)}} + \langle Q_\alpha^{(k)} \eta_\alpha, 2g^*(w^{(k)} - \hat{w}^{(k)}) \rangle_{S_6^{(k)}} \} \\
& + \sum_{k=1}^N \{ \langle v_\alpha^{(k)}, 2g^* \hat{N}_{\alpha \beta}^{(k)} \eta_\beta \rangle_{S_{1l}^{(k)}} + \langle N_{\alpha \beta}^{(k)} \eta_\beta, 2g^*(v_\alpha^{(k)} - \phi_\alpha^{(k)})' \rangle_{S_{2l}^{(k)}} \\
& + \langle \phi_\alpha^{(k)}, 2g^* \hat{M}_{\alpha \beta}^{(k)} \eta_\beta \rangle_{S_{3l}^{(k)}} + \langle M_{\alpha \beta}^{(k)} \eta_\beta, 2g^*(\phi_\alpha^{(k)} - \phi_\alpha^{(k)})' \rangle_{S_{4l}^{(k)}} \\
& + \langle w^{(k)}, 2g^* \hat{Q}_\alpha^{(k)} \eta_\alpha \rangle_{S_{5l}^{(k)}} + \langle Q_\alpha^{(k)} \eta_\alpha, 2g^*(w^{(k)} - \hat{w}^{(k)})' \rangle_{S_{6l}^{(k)}} \}
\end{aligned}$$

2.3.3 Some Specialization

The function defined by (92) has no differentiability constraints on the stress resultants $N_{\alpha\beta}, M_{\alpha\beta}, Q_\alpha$. This function also leads to certain useful specializations by identically satisfying some of the field equations. Assuming that in (92), continuity of $w^{(k)}$ is identically satisfied i.e. normal displacement is restricted to be constant through the thickness, i.e., $w^{(k)} = w$ for all k (67),

$$\begin{aligned}
 \Omega_4(u) = & 2 \sum_{k=1}^N \left\{ \left\langle v_\alpha^{(k)}, g^* F_\alpha^{(k)} + Y^{(k)} \right\rangle_{R^{(k)}} + \left\langle \phi_\alpha^{(k)}, g^* G_\alpha^{(k)} + Z^{(k)} \right\rangle_{R^{(k)}} \right. \\
 & + \left. \left\langle w^{(k)}, g^* F_3^{(k)} + X^{(k)} \right\rangle_{R^{(k)}} \right\} \\
 & + \sum_{k=1}^N \left\{ \left\langle v_\alpha^{(k)}, -P^{(k)} v_\alpha^{(k)} - R^{(k)} \phi_\alpha^{(k)} \right\rangle_{R^{(k)}} \right. \\
 & + \left. \left\langle e_{\alpha\beta}^{(k)}, -g^* A_{\alpha\beta\gamma\delta}^{(k)} e_{\gamma\delta}^{(k)} - g^* B_{\alpha\beta\gamma\delta}^{(k)} K_{\gamma\delta}^{(k)} \right\rangle_{R^{(k)}} \right. \\
 & + 2 \left\langle N_{\alpha\beta}^{(k)}, g^* e_{\alpha\beta}^{(k)} - g^* v_{(\alpha,\beta)}^{(k)} \right\rangle_{R^{(k)}} \\
 & + \left. \left\langle \phi_\alpha^{(k)}, -R^{(k)} v_\alpha^{(k)} - I^{(k)} \phi_\alpha^{(k)} \right\rangle_{R^{(k)}} \right. \\
 & + \left. \left\langle \kappa_{\alpha\beta}^{(k)}, -g^* B_{\alpha\beta\gamma\delta}^{(k)} e_{\gamma\delta}^{(k)} - g^* D_{\alpha\beta\gamma\delta}^{(k)} K_{\gamma\delta}^{(k)} \right\rangle_{R^{(k)}} \right. \\
 & + 2 \left\langle M_{\alpha\beta}^{(k)}, g^* \kappa_{\alpha\beta}^{(k)} - g^* \phi_{(\alpha,\beta)}^{(k)} \right\rangle_{R^{(k)}} + \left\langle w^{(k)}, -P^{(k)} w^{(k)} \right\rangle_{R^{(k)}} \\
 & + \left. \left\langle 2 \epsilon_{\alpha 3}^{(k)}, -g^* G_{\alpha 3 \gamma 3}^{(k)} (2 \epsilon_{\gamma 3}^{(k)}) \right\rangle_{R^{(k)}} \right. \\
 & + 2 \left\langle Q_\alpha^{(k)}, g^* (2 \epsilon_{\alpha 3}^{(k)}) - g^* \phi_\alpha^{(k)} - g^* w_\alpha^{(k)} \right\rangle_{R^{(k)}} \tag{93} \\
 & + \sum_{k=1}^{N-1} \left\{ \left\langle v_\alpha^{(k)}, g^* \sigma_{\alpha 3}^{+(k)} \right\rangle_{R^{(k)}} + \left\langle \phi_\alpha^{(k)}, t_k g^* \sigma_{\alpha 3}^{+(k)} \right\rangle_{R^{(k)}} + \left\langle w^{(k)}, g^* \sigma_{33}^{+(k)} \right\rangle_{R^{(k)}} \right\} \\
 & + \sum_{k=2}^N \left\{ \left\langle v_\alpha^{(k)}, -g^* \sigma_{\alpha 3}^{-(k)} \right\rangle_{R^{(k)}} + \left\langle w^{(k)}, -g^* \sigma_{33}^{-k} \right\rangle_{R^{(k)}} \right\} \\
 & + \sum_{k=1}^{N-1} \left\{ \left\langle \sigma_{\alpha 3}^{+(k)}, g^* v_\alpha^{(k)} + t_k g^* \phi_\alpha^{(k)} - g^* v_\alpha^{(k+1)} \right\rangle_{R^{(k)}} + \left\langle \sigma_{33}^{+(k)}, g^* w^{(k)} - g^* w^{(k+1)} \right\rangle_{R^{(k)}} \right\}
 \end{aligned}$$

$$\begin{aligned}
& -2 \langle v_{\alpha}^{(1)}, g^* \sigma_{\alpha 3}^{-(1)} \rangle_{R^1} - 2 \langle w^{(1)}, g^* \sigma_{33}^{-(1)} \rangle_{R^1} \\
& + 2 \langle v_{\alpha}^{(N)}, g^* \sigma_{\alpha 3}^{+(N)} \rangle_{R^{(N)}} + 2 \langle \phi_{\alpha}^{(N)}, t_N g^* \sigma_{\alpha 3}^{+(N)} \rangle_{R^{(N)}} + 2 \langle w^{(N)}, g^* \sigma_{33}^{+(N)} \rangle_{R^{(N)}} \\
& + \sum_{k=1}^N \{ \langle v_{\alpha}^{(k)}, 2g^* \hat{N}_{\alpha \beta}^{(k)} \eta_{\beta} \rangle_{S_1^{(k)}} + \langle N_{\alpha \beta}^{(k)} \eta_{\beta}, 2g^*(v_{\alpha}^{(k)} - \phi_{\alpha}^{(k)}) \rangle_{S_2^{(k)}} \\
& + \langle \phi_{\alpha}^{(k)}, 2g^* \hat{M}_{\alpha \beta}^{(k)} \eta_{\beta} \rangle_{S_3^{(k)}} + \langle M_{\alpha \beta}^{(k)} \eta_{\beta}, 2g^*(\phi_{\alpha}^{(k)} - \phi_{\alpha}^{(k)}) \rangle_{S_4^{(k)}} \\
& + \langle w^{(k)}, 2g^* \hat{Q}_{\alpha}^{(k)} \eta_{\alpha} \rangle_{S_5^{(k)}} + \langle Q_{\alpha}^{(k)} \eta_{\alpha}, 2g^*(w^{(k)} - \hat{w}^{(k)}) \rangle_{S_6^{(k)}} \} \\
& + \sum_{k=1}^N \{ \langle v_{\alpha}^{(k)}, 2g^* \hat{N}_{\alpha \beta}^{(k)} \eta_{\beta} \rangle_{S_{11}^{(k)}} + \langle N_{\alpha \beta}^{(k)} \eta_{\beta}, 2g^*(v_{\alpha}^{(k)} - \phi_{\alpha}^{(k)})' \rangle_{S_{21}^{(k)}} \\
& + \langle \phi_{\alpha}^{(k)}, 2g^* \hat{M}_{\alpha \beta}^{(k)} \eta_{\beta} \rangle_{S_{31}^{(k)}} + \langle M_{\alpha \beta}^{(k)} \eta_{\beta}, 2g^*(\phi_{\alpha}^{(k)} - \phi_{\alpha}^{(k)})' \rangle_{S_{41}^{(k)}} \\
& + \langle w^{(k)}, 2g^* \hat{Q}_{\alpha}^{(k)} \eta_{\alpha} \rangle_{S_{51}^{(k)}} + \langle Q_{\alpha}^{(k)} \eta_{\alpha}, 2g^*(w^{(k)} - \hat{w}^{(k)})' \rangle_{S_{61}^{(k)}} \}
\end{aligned}$$

If the kinematic relations (59) through (61) are identically satisfied, equation (93) leads to:

$$\begin{aligned}
\Omega_5(u) = & 2 \sum_{k=1}^N \{ \langle v_{\alpha}^{(k)}, g^* F_{\alpha}^{(k)} + Y^{(k)} \rangle_{R^{(k)}} + \langle \phi_{\alpha}^{(k)}, g^* G_{\alpha}^{(k)} + Z^{(k)} \rangle_{R^{(k)}} \\
& + \langle w^{(k)}, g^* F_3^{(k)} + X^{(k)} \rangle_{R^{(k)}} \} \\
& + \sum_{k=1}^N \{ \langle v_{\alpha}^{(k)}, -P^{(k)} v_{\alpha}^{(k)} - R^{(k)} \phi_{\alpha}^{(k)} \rangle_{R^{(k)}} \\
& + \langle e_{\alpha \beta}^{(k)}, -g^* A_{\alpha \beta \gamma \delta}^{(k)} e_{\gamma \delta}^{(k)} - g^* B_{\alpha \beta \gamma \delta}^{(k)} \kappa_{\gamma \delta}^{(k)} \rangle_{R^{(k)}} \\
& + \langle \phi_{\alpha}^{(k)}, -R^{(k)} v_{\alpha}^{(k)} - I^{(k)} \phi_{\alpha}^{(k)} \rangle_{R^{(k)}} \\
& + \langle \kappa_{\alpha \beta}^{(k)}, -g^* B_{\alpha \beta \gamma \delta}^{(k)} e_{\gamma \delta}^{(k)} - g^* D_{\alpha \beta \gamma \delta}^{(k)} \kappa_{\gamma \delta}^{(k)} \rangle_{R^{(k)}} \\
& + \langle 2 \epsilon_{\alpha 3}^{(k)}, -g^* G_{\alpha 3 \gamma 3}^{(k)} (2 \epsilon_{\gamma 3}^{(k)}) \rangle_{R^{(k)}} + \langle w, -P^{(k)} w \rangle_{R^{(k)}} \} \tag{94}
\end{aligned}$$

$$\begin{aligned}
& + \sum_{k=1}^{N-1} \{ \langle v_\alpha^{(k)}, g^* \sigma_{\alpha 3}^{+(k)} \rangle_{R^{(k)}} + \langle \phi_\alpha^{(k)}, t_k g^* \sigma_{\alpha 3}^{+(k)} \rangle_{R^{(k)}} + \langle w^{(k)}, g^* \sigma_{33}^{+(k)} \rangle_{R^{(k)}} \} \\
& + \sum_{k=2}^N \{ \langle v_\alpha^{(k)}, -g^* \sigma_{\alpha 3}^{-(k)} \rangle_{R^{(k)}} + \langle w^{(k)}, -g^* \sigma_{33}^{-k} \rangle_{R^{(k)}} \} \\
& + \sum_{k=1}^{N-1} \{ \langle \sigma_{\alpha 3}^{+(k)}, g^* v_\alpha^{(k)} + t_k g^* \phi_\alpha^{(k)} - g^* v_\alpha^{(k+1)} \rangle_{R^{(k)}} + \langle \sigma_{33}^{+(k)}, g^* w^{(k)} - g^* w^{(k+1)} \rangle_{R^{(k)}} \} \\
& - 2 \langle v_\alpha^{(1)}, g^* \sigma_{\alpha 3}^{-(1)} \rangle_{R^1} - 2 \langle w^{(1)}, g^* \sigma_{33}^{-(1)} \rangle_{R^1} \\
& + 2 \langle v_\alpha^{(N)}, g^* \sigma_{\alpha 3}^{+(N)} \rangle_{R^{(N)}} + 2 \langle \phi_\alpha^{(N)}, t_N g^* \sigma_{\alpha 3}^{+(N)} \rangle_{R^{(N)}} + 2 \langle w^{(N)}, g^* \sigma_{33}^{+(N)} \rangle_{R^{(N)}} \\
& + \sum_{k=1}^N \{ \langle v_\alpha^{(k)}, 2g^* \hat{N}_{\alpha \beta}^{(k)} \eta_\beta \rangle_{S_1^{(k)}} + \langle N_{\alpha \beta}^{(k)} \eta_\beta, 2g^*(v_\alpha^{(k)} - \hat{v}_\alpha^{(k)}) \rangle_{S_2^{(k)}} \\
& + \langle \phi_\alpha^{(k)}, 2g^* \hat{M}_{\alpha \beta}^{(k)} \eta_\beta \rangle_{S_3^{(k)}} + \langle M_{\alpha \beta}^{(k)} \eta_\beta, 2g^*(\phi_\alpha^{(k)} - \hat{\phi}_\alpha^{(k)}) \rangle_{S_4^{(k)}} \\
& + \langle w^{(k)}, 2g^* \hat{Q}_\alpha^{(k)} \eta_\alpha \rangle_{S_5^{(k)}} + \langle Q_\alpha^{(k)} \eta_\alpha, 2g^*(w^{(k)} - \hat{w}^{(k)}) \rangle_{S_6^{(k)}} \} \\
& + \sum_{k=1}^N \{ \langle v_\alpha^{(k)}, 2g^* \hat{N}'_{\alpha \beta}^{(k)} \eta_\beta \rangle_{S_{11}^{(k)}} + \langle N'_{\alpha \beta} \eta_\beta, 2g^*(v_\alpha^{(k)} - \hat{v}_\alpha^{(k)})' \rangle_{S_{21}^{(k)}} \\
& + \langle \phi_\alpha^{(k)}, 2g^* \hat{M}'_{\alpha \beta}^{(k)} \eta_\beta \rangle_{S_{31}^{(k)}} + \langle M'_{\alpha \beta} \eta_\beta, 2g^*(\phi_\alpha^{(k)} - \hat{\phi}_\alpha^{(k)})' \rangle_{S_{41}^{(k)}} \\
& + \langle w^{(k)}, 2g^* \hat{Q}'_\alpha^{(k)} \eta_\alpha \rangle_{S_{51}^{(k)}} + \langle Q'_\alpha \eta_\alpha, 2g^*(w^{(k)} - \hat{w}^{(k)})' \rangle_{S_{61}^{(k)}} \}
\end{aligned}$$

If the kinematic boundary conditions in (83) and (84) are identically satisfied, equation (94) reduces to

$$\begin{aligned}
\Omega_6(u) = & 2 \sum_{k=1}^N \{ \langle v_\alpha^{(k)}, g^* F_\alpha^{(k)} + Y^{(k)} \rangle_{R^{(k)}} + \langle \phi_\alpha^{(k)}, g^* G_\alpha^{(k)} + Z^{(k)} \rangle_{R^{(k)}} \\
& + \langle w^{(k)}, g^* F_3^{(k)} + X^{(k)} \rangle_{R^{(k)}} \} \\
& + \sum_{k=1}^N \{ \langle v_\alpha^{(k)}, -P^{(k)} v_\alpha^{(k)} - R^{(k)} \phi_\alpha^{(k)} \rangle_{R^{(k)}}
\end{aligned}$$

$$+ \langle e_{\alpha\beta}^{(k)}, -g^* A_{\alpha\beta\gamma\delta}^{(k)} e_{\gamma\delta}^{(k)} - g^* B_{\alpha\beta\gamma\delta}^{(k)} \kappa_{\gamma\delta}^{(k)} \rangle_{R^{(k)}}$$

$$+ \langle \phi_{\alpha}^{(k)}, -R_{\alpha}^{(k)} v_{\alpha}^{(k)} - I_{\alpha}^{(k)} \phi_{\alpha}^{(k)} \rangle_{R^{(k)}}$$

$$+ \langle \kappa_{\alpha\beta}^{(k)}, -g^* B_{\alpha\beta\gamma\delta}^{(k)} e_{\gamma\delta}^{(k)} - g^* D_{\alpha\beta\gamma\delta}^{(k)} \kappa_{\gamma\delta}^{(k)} \rangle_{R^{(k)}}$$

$$+ \langle 2\epsilon_{\alpha 3}^{(k)}, -g^* G_{\alpha 3\gamma 3}^{(k)} (2\epsilon_{\gamma 3}^{(k)}) \rangle_{R^{(k)}} + \langle w, -P^{(k)} w \rangle_{R^{(k)}} \} \quad (95)$$

$$+ \sum_{k=1}^{N-1} \{ \langle v_{\alpha}^{(k)}, g^* \sigma_{\alpha 3}^{+(k)} \rangle_{R^{(k)}} + \langle \phi_{\alpha}^{(k)}, t_k g^* \sigma_{\alpha 3}^{+(k)} \rangle_{R^{(k)}} + \langle w^{(k)}, g^* \sigma_{33}^{+(k)} \rangle_{R^{(k)}} \}$$

$$+ \sum_{k=2}^N \{ \langle v_{\alpha}^{(k)}, -g^* \sigma_{\alpha 3}^{-(k)} \rangle_{R^{(k)}} + \langle w^{(k)}, -g^* \sigma_{33}^{-(k)} \rangle_{R^{(k)}} \}$$

$$+ \sum_{k=1}^{N-1} \{ \langle \sigma_{\alpha 3}^{+(k)}, g^* v_{\alpha}^{(k)} + t_k g^* \phi_{\alpha}^{(k)} - g^* v_{\alpha}^{(k+1)} \rangle_{R^{(k)}} + \langle \sigma_{33}^{+(k)}, g^* w^{(k)} - g^* w^{(k+1)} \rangle_{R^{(k)}} \}$$

$$- 2 \langle v_{\alpha}^{(1)}, g^* \sigma_{\alpha 3}^{-(1)} \rangle_{R^1} - 2 \langle w^{(1)}, g^* \sigma_{33}^{-(1)} \rangle_{R^1}$$

$$+ 2 \langle v_{\alpha}^{(N)}, g^* \sigma_{\alpha 3}^{+(N)} \rangle_{R^{(N)}} + 2 \langle \phi_{\alpha}^{(N)}, t_N g^* \sigma_{\alpha 3}^{+(N)} \rangle_{R^{(N)}} + 2 \langle w^{(N)}, g^* \sigma_{33}^{+(N)} \rangle_{R^{(N)}}$$

$$+ 2 \sum_{k=1}^N \{ \langle v_{\alpha}^{(k)}, g^* \hat{N}_{\alpha\beta}^{(k)} \eta_{\beta} \rangle_{S_1^{(k)}} + \langle \phi_{\alpha}^{(k)}, g^* \hat{M}_{\alpha\beta}^{(k)} \eta_{\beta} \rangle_{S_3^{(k)}} + \langle w^{(k)}, g^* \hat{Q}_{\alpha}^{(k)} \eta_{\alpha} \rangle_{S_5^{(k)}} \}$$

$$+ 2 \sum_{k=1}^N \{ \langle v_{\alpha}^{(k)}, g^* \hat{N}'_{\alpha\beta}^{(k)} \eta_{\beta} \rangle_{S_{1l}^{(k)}} + \langle \phi_{\alpha}^{(k)}, g^* \hat{M}'_{\alpha\beta}^{(k)} \eta_{\beta} \rangle_{S_{3l}^{(k)}} + \langle w^{(k)}, 2g^* \hat{Q}'_{\alpha}^{(k)} \eta_{\alpha} \rangle_{S_{5l}^{(k)}} \}$$

Let

$$P_3 = \sigma_{33}^{+(N)} - \sigma_{33}^{-(1)}$$

Then, if the constitutive relations (62) through (64) are identically satisfied, $\Omega_6(u)$ specializes to

$$\begin{aligned} \Omega_7(u) = 2 \sum_{k=1}^N & \{ \langle v_{\alpha}^{(k)}, g^* F_{\alpha}^{(k)} + Y^{(k)} \rangle_{R^{(k)}} + \langle \phi_{\alpha}^{(k)}, g^* G_{\alpha}^{(k)} + Z^{(k)} \rangle_{R^{(k)}} \\ & + \langle w, g^* F_3^{(k)} + X^{(k)} \rangle_{R^{(k)}} \} \end{aligned}$$

$$\begin{aligned}
& + \sum_{k=1}^N \{ - \langle N_{\alpha\beta}^{(k)}, g^* v_{(\gamma,\delta)}^{(k)} \rangle_{R^{(k)}} - \langle M_{\alpha\beta}^{(k)}, g^* \phi_{(\gamma,\delta)}^{(k)} \rangle_{R^{(k)}} \\
& - \langle Q_\alpha^{(k)}, g^* w_\alpha \rangle_{R^{(k)}} + \langle v_\alpha^{(k)}, -P^{(k)} v_\alpha^{(k)} - R^{(k)} \phi_\alpha^{(k)} \rangle_{R^{(k)}} \\
& + \langle \phi_\alpha^{(k)}, -g^* Q_\alpha^{(k)} - R^{(k)} v_\alpha^{(k)} - I^{(k)} \phi_\alpha^{(k)} \rangle_{R^{(k)}} + \langle w, -P^{(k)} w \rangle_{R^{(k)}} \quad (96) \\
& + \sum_{k=1}^{N-1} \{ \langle v_\alpha^{(k)}, g^* \sigma_{\alpha 3}^{+(k)} \rangle_{R^{(k)}} + \langle \phi_\alpha^{(k)}, t_k g^* \sigma_{\alpha 3}^{+(k)} \rangle_{R^{(k)}} + \langle w, g^* \sigma_{33}^{+(k)} \rangle_{R^{(k)}} \} \\
& + \sum_{k=2}^N \{ \langle v_\alpha^{(k)}, -g^* \sigma_{\alpha 3}^{-(k)} \rangle_{R^{(k)}} + \langle w, -g^* \sigma_{33}^{-k} \rangle_{R^{(k)}} \} \\
& + \sum_{k=1}^{N-1} \{ \langle \sigma_{\alpha 3}^{+(k)}, g^* v_\alpha^{(k)} + t_k g^* \phi_\alpha^{(k)} - g^* v_\alpha^{(k+1)} \rangle_{R^{(k)}} \} \\
& - 2 \langle v_\alpha^{(1)}, g^* \sigma_{\alpha 3}^{-(1)} \rangle_{R^1} + 2 \langle v_\alpha^{(N)}, g^* \sigma_{\alpha 3}^{+(N)} \rangle_{R^{(N)}} \\
& + 2 \langle \phi_\alpha^{(N)}, t_N g^* \sigma_{\alpha 3}^{+(N)} \rangle_{R^{(N)}} + 2 \langle w, g^* P_3 \rangle_R \\
& + 2 \sum_{k=1}^N \{ \langle v_\alpha^{(k)}, g^* \hat{N}_{\alpha\beta}^{(k)} \eta_\beta \rangle_{S_1^{(k)}} + \langle \phi_\alpha^{(k)}, g^* \hat{M}_{\alpha\beta}^{(k)} \eta_\beta \rangle_{S_3^{(k)}} + \langle w, g^* \hat{Q}_\alpha \eta_\alpha \rangle_{S_5^{(k)}} \} \\
& + 2 \sum_{k=1}^N \{ \langle v_\alpha^{(k)}, g^* \hat{N}'_{\alpha\beta}^{(k)} \eta_\beta \rangle_{S_{1l}^{(k)}} + \langle \phi_\alpha^{(k)}, g^* \hat{M}'_{\alpha\beta}^{(k)} \eta_\beta \rangle_{S_{3l}^{(k)}} + \langle w, g^* \hat{Q}'_\alpha \eta_\alpha \rangle_{S_{5l}^{(k)}} \}
\end{aligned}$$

If the interlaminar displacement continuity, (66), is identically satisfied, (96) reduces to:

$$\begin{aligned}
\Omega_8(u) = & 2 \sum_{k=1}^N \{ \langle v_\alpha^{(k)}, g^* F_\alpha^{(k)} + Y^{(k)} \rangle_{R^{(k)}} + \langle \phi_\alpha^{(k)}, g^* G_\alpha^{(k)} + Z^{(k)} \rangle_{R^{(k)}} \\
& + \langle w, g^* F_3^{(k)} + X^{(k)} \rangle_{R^{(k)}} \} \\
& + \sum_{k=1}^N \{ - \langle N_{\alpha\beta}^{(k)}, g^* v_{(\gamma,\delta)}^{(k)} \rangle_{R^{(k)}} - \langle M_{\alpha\beta}^{(k)}, g^* \phi_{(\gamma,\delta)}^{(k)} \rangle_{R^{(k)}} \\
& - \langle Q_\alpha^{(k)}, g^* w_\alpha \rangle_{R^{(k)}} + \langle v_\alpha^{(k)}, -P^{(k)} v_\alpha^{(k)} - R^{(k)} \phi_\alpha^{(k)} \rangle_{R^{(k)}} \\
& + \langle \phi_\alpha^{(k)}, -g^* Q_\alpha^{(k)} - R^{(k)} v_\alpha^{(k)} - I^{(k)} \phi_\alpha^{(k)} \rangle_{R^{(k)}}
\end{aligned}$$

$$- \langle w, P^{(k)} w \rangle_{R^{(k)}} \} \quad (97)$$

$$\begin{aligned} & -2 \langle v_\alpha^{(1)}, g^* \sigma_{\alpha 3}^{-(1)} \rangle_{R^1} + 2 \langle v_\alpha^{(N)}, g^* \sigma_{\alpha 3}^{+(N)} \rangle_{R^{(N)}} \\ & + 2 \langle \phi_\alpha^{(N)}, t_N g^* \sigma_{\alpha 3}^{+(N)} \rangle_{R^{(N)}} + 2 \langle w, g^* P_3 \rangle_R \\ & + 2 \sum_{k=1}^N \{ \langle v_\alpha^{(k)}, g^* \hat{N}_{\alpha \beta}^{(k)} \eta_\beta \rangle_{S_1^{(k)}} + \langle \phi_\alpha^{(k)}, g^* \hat{M}_{\alpha \beta}^{(k)} \eta_\beta \rangle_{S_3^{(k)}} + \langle w, g^* \hat{Q}_\alpha \eta_\alpha \rangle_{S_5^{(k)}} \} \\ & + 2 \sum_{k=1}^N \{ \langle v_\alpha^{(k)}, g^* \hat{N}'_{\alpha \beta}^{(k)} \eta_\beta \rangle_{S_{1l}^{(k)}} + \langle \phi_\alpha^{(k)}, g^* \hat{M}'_{\alpha \beta}^{(k)} \eta_\beta \rangle_{S_{3l}^{(k)}} + \langle w, g^* \hat{Q}'_\alpha \eta_\alpha \rangle_{S_{5l}^{(k)}} \} \end{aligned}$$

Here, $v_\alpha^{(k)}$ is no longer independent for $k = 1, 2, \dots, n$. Furthermore, if surface shear tractions, surface shear couples, body forces, and body couples are neglected, i.e., $\sigma_{\alpha 3}^{(1)} = \sigma_{\alpha 3}^{(N)} = F_\alpha^{(k)} = F_3^{(k)} = G_\alpha^{(k)} = 0$ then (97) reduces to:

$$\begin{aligned} \Omega_9(\mu) = & 2 \sum_{k=1}^N \{ \langle v_\alpha^{(k)}, Y^{(k)} \rangle_{R^{(k)}} + \langle \phi_\alpha^{(k)}, Z^{(k)} \rangle_{R^{(k)}} + \langle w, X^{(k)} \rangle_{R^{(k)}} \} \\ & + \sum_{k=1}^N \{ - \langle N_{\alpha \beta}^{(k)}, g^* v_{(\gamma, \delta)}^{(k)} \rangle_{R^{(k)}} - \langle M_{\alpha \beta}^{(k)}, g^* \phi_{\gamma \delta(k)} \rangle_{R^{(k)}} \\ & - \langle Q_\alpha^{(k)}, g^* w_{,\alpha} \rangle_{R^{(k)}} + \langle v_\alpha^{(k)}, -P^{(k)} v_\alpha^{(k)} - R^{(k)} \phi_\alpha^{(k)} \rangle_{R^{(k)}} \\ & + \langle \phi_\alpha^{(k)}, -g^* Q_\alpha^{(k)} - R^{(k)} v_\alpha^{(k)} - I^{(k)} \phi_\alpha^{(k)} \rangle_{R^{(k)}} \\ & - \langle w, P^{(k)} w \rangle_{R^{(k)}} \} \quad (98) \end{aligned}$$

$$\begin{aligned} & + 2 \langle w, g^* P_3 \rangle_R \\ & + 2 \sum_{k=1}^N \{ \langle v_\alpha^{(k)}, g^* \hat{N}_{\alpha \beta}^{(k)} \eta_\beta \rangle_{S_1^{(k)}} + \langle \phi_\alpha^{(k)}, g^* \hat{M}_{\alpha \beta}^{(k)} \eta_\beta \rangle_{S_3^{(k)}} + \langle w, g^* \hat{Q}_\alpha \eta_\alpha \rangle_{S_5^{(k)}} \} \\ & + 2 \sum_{k=1}^N \{ \langle v_\alpha^{(k)}, g^* \hat{N}'_{\alpha \beta}^{(k)} \eta_\beta \rangle_{S_{1l}^{(k)}} + \langle \phi_\alpha^{(k)}, g^* \hat{M}'_{\alpha \beta}^{(k)} \eta_\beta \rangle_{S_{3l}^{(k)}} + \langle w, g^* \hat{Q}'_\alpha \eta_\alpha \rangle_{S_{5l}^{(k)}} \} \end{aligned}$$

Explicitly, replacing, $v_\alpha^{(k)}$ using the continuity of the displacements across the interface, by $v_\alpha^{(1)}$ and $\phi_\alpha^{(k)}$, Ω_{10} is written as:

$$\begin{aligned}
\Omega_{10}(u) = & 2 \sum_{k=1}^N \left\{ \langle v_\alpha^{(1)}, Y^{(k)} \rangle_{R^{(k)}} + \left\langle \sum_{i=1}^{k-1} t_i \phi_\alpha^{(i)}, Y^{(k)} \right\rangle_{R^{(k)}} + \langle \phi_\alpha^{(k)}, Z^{(k)} \rangle_{R^{(k)}} + \langle w, X^{(k)} \rangle_{R^{(k)}} \right\} \\
& - \sum_{k=1}^N \left\{ \langle N_{\alpha\beta}^{(k)}, g^* v_{(\gamma,\delta)}^{(1)} \rangle_{R^{(k)}} + \langle N_{\alpha\beta}^{(k)}, g^* \sum_{i=1}^{k-1} t_i \phi_{(\gamma,\delta)}^{(i)} \rangle_{R^{(k)}} \right. \\
& \quad \left. + \langle M_{\alpha\beta}^{(k)}, g^* \phi_{(\gamma,\delta)}^{(k)} \rangle_{R^{(k)}} + \langle Q_\alpha^{(k)}, g^* w_\alpha \rangle_{R^{(k)}} \right. \\
& \quad \left. + 2 \langle v_\alpha^{(1)}, R^{(k)} \phi_\alpha^{(k)} \rangle_{R^{(k)}} + 2 \langle \phi_\alpha^{(k)}, R^{(k)} \sum_{i=1}^{k-1} t_i \phi_\alpha^{(i)} \rangle_{R^{(k)}} \right. \\
& \quad \left. + \langle v_\alpha^{(1)}, P^{(k)} v_\alpha^{(1)} \rangle_{R^{(k)}} + 2 \langle v_\alpha^{(1)}, P^{(k)} \sum_{i=1}^{k-1} t_i \phi_\alpha^{(i)} \rangle_{R^{(k)}} \right. \\
& \quad \left. + \langle \sum_{i=1}^{k-1} t_i \phi_\alpha^{(i)}, P^{(k)} \sum_{i=1}^{k-1} t_i \phi_\alpha^{(i)} \rangle_{R^{(k)}} \right. \\
& \quad \left. + \langle \phi_\alpha^{(k)}, g^* Q_\alpha^{(k)} + I^{(k)} \phi_\alpha^{(k)} \rangle_{R^{(k)}} \right\} \\
& + 2 \langle w, g^* P_3 \rangle_R \\
& + 2 \sum_{k=1}^N \left\{ \langle v_\alpha^{(1)}, g^* \hat{N}_{\alpha\beta}^k \eta_\beta \rangle_{S_1^{(k)}} + \langle \sum_{i=1}^{k-1} t_i \phi_\alpha^{(i)}, g^* \hat{N}_{\alpha\beta}^k \eta_\beta \rangle_{S_1^{(k)}} \right. \\
& \quad \left. + \langle \phi_\alpha^{(k)}, g^* \hat{M}_{\alpha\beta}^{(k)} \eta_\beta \rangle_{S_3^{(k)}} + \langle w, g^* \hat{Q}_\alpha \eta_\alpha \rangle_{S_5^{(k)}} \right\} \\
& + 2 \sum_{k=1}^N \left\{ \langle v_\alpha^{(1)}, g^* \hat{N}'_{\alpha\beta}^k \eta_\beta \rangle_{S_{11}^{(k)}} + \langle \sum_{i=1}^{k-1} t_i \phi_\alpha^{(i)}, g^* \hat{N}'_{\alpha\beta}^k \eta_\beta \rangle_{S_{11}^{(k)}} \right. \\
& \quad \left. + \langle \phi_\alpha^{(k)}, g^* \hat{M}'_{\alpha\beta}^{(k)} \eta_\beta \rangle_{S_{31}^{(k)}} + \langle w, g^* \hat{Q}'_\alpha \eta_\alpha \rangle_{S_{51}^{(k)}} \right\}
\end{aligned} \tag{99}$$

If inertia terms are ignored i.e. for the static problem, it is not necessary to take convolution. Then, the governing function is the functional:

$$\Omega_{11}(u) = - \sum_{k=1}^N \left\{ \langle N_{\alpha\beta}^{(k)}, g^* v_{(\gamma,\delta)}^{(1)} \rangle_{R^{(k)}} + \langle N_{\alpha\beta}^{(k)}, g^* \sum_{i=1}^{k-1} t_i \phi_{(\gamma,\delta)}^{(i)} \rangle_{R^{(k)}} \right.$$

$$\begin{aligned}
& + \langle M_{\alpha\beta}^{(k)}, g^* \phi_{(\gamma,\delta)}^{(k)} \rangle_{R^{(k)}} + \langle Q_\alpha^{(k)}, g^* w_{,\alpha} \rangle_{R^{(k)}} + \langle \phi_\alpha^{(k)}, g^* Q_\alpha^{(k)} \rangle_{R^{(k)}} \} \\
& + 2 \langle w, g^* P_3 \rangle_R
\end{aligned} \tag{100}$$

$$\begin{aligned}
& + 2 \sum_{k=1}^N \{ \langle v_\alpha^{(1)}, g^* \hat{N}_{\alpha\beta}^{(k)} \eta_\beta \rangle_{S_1^{(k)}} + \langle \sum_{i=1}^{k-1} t_i \phi_\alpha^{(i)}, g^* \hat{N}_{\alpha\beta}^{(k)} \eta_\beta \rangle_{S_1^{(k)}} \\
& + \langle \phi_\alpha^{(k)}, g^* \hat{M}_{\alpha\beta}^{(k)} \eta_\beta \rangle_{S_3^{(k)}} + \langle w, g^* \hat{Q}_\alpha \eta_\alpha \rangle_{S_5^{(k)}} \} \\
& + 2 \sum_{k=1}^N \{ \langle v_\alpha^{(1)}, g^* \hat{N}_{\alpha\beta}^{(k)} \eta_\beta \rangle_{S_{1i}^{(k)}} + \langle \sum_{i=1}^{k-1} t_i \phi_\alpha^{(i)}, g^* \hat{N}_{\alpha\beta}^{(k)} \eta_\beta \rangle_{S_{1i}^{(k)}} \\
& + \langle \phi_\alpha^{(k)}, g^* \hat{M}_{\alpha\beta}^{(k)} \eta_\beta \rangle_{S_{3i}^{(k)}} + \langle w, g^* \hat{Q}_\alpha \eta_\alpha \rangle_{S_{5i}^{(k)}} \}
\end{aligned}$$

If the physical problem does not have line loads or couples applied to surfaces in the interior, $\hat{N}_{\alpha\beta}$, $\hat{M}_{\alpha\beta}$ and \hat{Q}_α vanish. This gives the governing functional as

$$\begin{aligned}
\Omega_{12}(u) = & - \sum_{k=1}^N \{ \langle N_{\alpha\beta}^{(k)}, g^* v_{(\gamma,\delta)}^{(1)} \rangle_{R^{(k)}} + \langle N_{\alpha\beta}^{(k)}, g^* \sum_{i=1}^{k-1} t_i \phi_{(\gamma,\delta)}^{(i)} \rangle_{R^{(k)}} \\
& + \langle M_{\alpha\beta}^{(k)}, g^* \phi_{(\gamma,\delta)}^{(k)} \rangle_{R^{(k)}} + \langle Q_\alpha^{(k)}, g^* w_{,\alpha} \rangle_{R^{(k)}} + \langle \phi_\alpha^{(k)}, g^* Q_\alpha^{(k)} \rangle_{R^{(k)}} \} \\
& + 2 \langle w, g^* P_3 \rangle_R
\end{aligned} \tag{101}$$

This specialization, dropping the convolution with $g(t)$, was used to set up the finite element approximation discussed in the next section.

Section III

FINITE ELEMENT FORMULATION

3.1 INTRODUCTION

The finite element method subdivides a given region R in an n -dimensional euclidean space into a number of disjoint open subregion (elements) $R^e, e = 1, 2, \dots, m$ such that

$$\bar{R} = \lim_{m \rightarrow \infty} \bigcup R^e \quad (102)$$

Here a superscripted bar over a quantity denotes its 'closure' i.e.

$$\bar{R}^e = R^e \cup \partial R^e \quad (103)$$

where ∂R^e is the boundary of R^e . Disjointness of these elements implies

$$R^e \cap R^f = \emptyset \quad \text{if } e \neq f \quad (104)$$

A set of nodal points in Ω defines the geometry of the elements. In the following section a discretization of the domain by the finite element method is presented. The formulation of the finite element is based on the variational principle governed by the specialized functional Ω_{12} .

3.2 FINITE ELEMENT DISCRETIZATION

Let the field variables at any point within an element be represented by:

$$\begin{aligned} v_\alpha^{(1)}(x_\beta) &= \{H_v^T(x_\beta)\} \{V_\alpha^{(1)}\} \\ \phi_\alpha^{(k)}(x_\beta) &= \{H_\phi^T(x_\beta)\} \{\Phi_\alpha^{(k)}\} \\ w(x_\beta) &= \{H_w^T(x_\beta)\} \{W\} \end{aligned} \quad (105)$$

Here $\{H_v\}$, $\{H_\phi\}$, $\{H_w\}$ are sets of interpolation functions relating the values of the corresponding variable at the nodal points to an arbitrary point within the element and $\{V_\alpha^{(1)}\}$, $\{\Phi_\alpha^{(k)}\}$, and $\{W\}$ are vectors of the apriori unknown values of $v_\alpha^{(1)}, \phi_\alpha^{(k)}$, w at the nodal points. Substitution of (105) into the governing functional (101) yields the spatially discretized functional as:

$$\Omega = \sum_{e=1}^m \Omega_e$$

where, for N layers in the laminate:

$$\begin{aligned}
\Omega_e = & - \sum_{k=1}^K \left\{ \int_{R^e} \{V_\alpha^{(1)}\}^T \{DH_v\} [A^{(k)}] \{DH_v\}^T \{V_\gamma^{(1)}\} dR^e \right. \\
& + 2 \int_{R^e} \{V_\alpha^{(1)}\}^T \{DH_v\} [A^{(k)}] \left(\sum_{i=1}^{k-1} t_i \{DH_\phi\}^T \{\Phi_\gamma^i\} \right) dR^e \\
& + \int_{R^e} \left(\sum_{i=1}^{k-1} \{\Phi_\alpha^i\}^T t_i \{DH_\phi\} \right) [A^{(k)}] \left(\sum_{i=1}^{k-1} t_i \{DH_\phi\}^T \{\Phi_\gamma^i\} \right) dR^e \\
& + 2 \int_{R^e} \{V_\alpha^{(1)}\}^T \{DH_v\} [B^{(k)}] \{DH_\phi\}^T \{\Phi_\gamma^{(k)}\} dR^e \\
& + 2 \int_{R^e} \{\Phi_\alpha^{(k)}\}^T \{DH_\phi\} [B^{(k)}] \left(\sum_{i=1}^{k-1} t_i \{DH_\phi\}^T \{\Phi_\gamma^i\} \right) dR^e \\
& + \int_{R^e} \{\Phi_\alpha^{(k)}\}^T \{DH_\phi\} [D^{(k)}] \{DH_\phi\}^T \{\Phi_\gamma^{(k)}\} dR^e \\
& + \int_{R^e} \langle \{W\}^T, \{\Phi_\alpha^{(k)}\}^T \rangle \begin{bmatrix} \{DH_w\} \\ \{H_\phi\} \end{bmatrix} [G^{(k)}] \{ \{DH_w\}^T, \{H_\phi\}^T \} \begin{bmatrix} \{W\} \\ \{\Phi_\gamma^{(k)}\} \end{bmatrix} dR^e \} \\
& + 2 \int_{R^e} \{W\}^T \{H_w\} P_3 dR^e
\end{aligned} \tag{106}$$

Here the symbol D associated with H denotes appropriate differentiations; $[A^{(k)}]$, $[B^{(k)}]$ and $[D^{(k)}]$ represent constitutive relations; and

$$K_{vva}^{(k)} = \int_{R_e^{(k)}} \{DH_v\} [A^{(k)}] \{DH_v\}^T dR^c$$

$$K_{v\phi a}^{(k)} = \int_{R^e} \{DH_v\} [A^{(k)}] \{DH_\phi\}^T dR^c$$

$$K_{\phi\phi a}^{(k)} = \int_{R^e} \{DH_\phi\} [A^{(k)}] \{DH_\phi\}^T dR^c$$

$$K_{v\phi b}^{(k)} = \int_{R_v^{(k)}} \{DH_v\} [B^{(k)}] \{DH_\phi\}^T dR^c$$

$$K_{\phi\phi b}^{(k)} = \int_{R_\phi^{(k)}} \{DH_\phi\} [B^{(k)}] \{DH_\phi\}^T dR^c$$

$$K_{\phi\psi f}^{(k)} = \int_{R_\phi^{(k)}} \{DH_\phi\} [D^{(k)}] \{DH_\psi\}^T dR^c$$

$$K_{w w G}^{(k)} = \int_{R_w^{(k)}} \{DH_w\} [G^{(k)}] \{DH_w\}^T dR^c$$

$$K_{w\phi G}^{(k)} = \int_{R_\phi^{(k)}} \{DH_w\} [G^{(k)}] \{H_\phi\}^T dR^c$$

$$K_{\phi\phi G}^{(k)} = \int_{R_\phi^{(k)}} \{H_\phi\} [G^{(k)}] \{H_\phi\}^T dR^c$$

$$R_{wp} = \int_{R^e} \{H_w\} P_3 dR^c$$

where

$$\{DH_v\}^T = \begin{pmatrix} H_{v,x}^T & 0 \\ 0 & H_{v,y}^T \\ H_{v,y}^T & H_{v,x}^T \end{pmatrix}$$

$$\{DH_\phi\}^T = \begin{pmatrix} H_{\phi,x}^T & 0 \\ 0 & H_{\phi,y}^T \\ H_{\phi,y}^T & H_{\phi,x}^T \end{pmatrix}$$

$$[DH_w]^T = \begin{pmatrix} H_{w,x}^T \\ H_{w,y}^T \end{pmatrix}$$

$$[H_\phi]^T = \begin{pmatrix} H_\phi^T & 0 \\ 0 & H_\phi^T \end{pmatrix}$$

$$\{H_w\} = \{H_w\}$$

Using the above definitions, equation (106) can be written as:

$$\begin{aligned} \Omega_e = & - \sum_{k=1}^N \{ \{V_\alpha^{(1)}\}^T [K_{vv\sigma}^{(k)}] \{V_\gamma^{(1)}\} + 2 \{V_\alpha^{(1)}\}^T [K_{v\phi\sigma}^{(k)}] (\sum_{i=1}^{k-1} t_i \{\Phi_\gamma^i\}) \\ & + \sum_{i=1}^{k-1} t_i \{\Phi_\alpha^i\}^T [K_{\phi\phi\sigma}^{(k)}] \sum_{j=1}^{k-1} t_j \{\Phi_\gamma^j\} \\ & + 2 \{V_\alpha^{(1)}\}^T [K_{v\phi b}^{(k)}] \{\Phi_\gamma^{(k)}\} + 2 \{\Phi_\alpha^{(k)}\}^T [K_{\phi\phi b}^{(k)}] (\sum_{i=1}^{k-1} t_i \{\Phi_\gamma^i\}) \\ & + \{\Phi_\alpha^{(k)}\}^T [K_{\phi\phi d}^{(k)}] \{\Phi_\gamma^{(k)}\} + \{W\}^T [K_{wwG}^{(k)}] \{W\} \\ & + \{\Phi_\alpha^{(k)}\}^T [K_{w\phi G}^{(k)}] \{W\} + \{W\}^T [K_{w\phi G}^{(k)}] \{\Phi_\gamma^{(k)}\} \\ & + \{\Phi_\alpha^{(k)}\}^T [K_{\phi\phi G}^{(k)}] \{\Phi_\gamma^{(k)}\} \} \\ & + 2 \{W\}^T R_{wp} \end{aligned} \quad (107)$$

Gateaux differential of the governing functional (107), denoting by $\{\bar{V}_\alpha\}$, $\{\bar{\Phi}_\alpha\}$, $\{\bar{W}\}$ the path of variations in $\{V_\alpha\}$, $\{\Phi_\alpha\}$, $\{W\}$ respectively, is:

$$\begin{aligned} \delta_{\bar{u}} \Omega_e = & - 2 \sum_{k=1}^N \{ \{\bar{V}_\alpha^{(1)}\}^T [K_{vv\sigma}^{(k)}] \{V_\gamma^{(1)}\} + \{\bar{V}_\alpha^{(1)}\}^T [K_{v\phi\sigma}^{(k)}] (\sum_{i=1}^{k-1} t_i \{\Phi_\gamma^i\}) \\ & + \sum_{i=1}^{k-1} t_i \{\bar{\Phi}_\alpha^i\}^T [K_{\phi\phi\sigma}^{(k)}] \{V_\gamma^{(1)}\} + \sum_{i=1}^{k-1} t_i \{\bar{\Phi}_\alpha^i\}^T [K_{\phi\phi\sigma}^{(k)}] \sum_{j=1}^{k-1} t_j \{\Phi_\gamma^j\} \\ & + \{\bar{V}_\alpha^{(1)}\}^T [K_{v\phi b}^{(k)}] \{\Phi_\gamma^{(k)}\} + \{\bar{\Phi}_\alpha^{(k)}\}^T [K_{\phi\phi b}^{(k)}] \{V_\gamma^{(1)}\} \\ & + \{\bar{\Phi}_\alpha^{(k)}\}^T [K_{\phi\phi d}^{(k)}] \{\Phi_\gamma^{(k)}\} + \{\bar{W}\}^T [K_{wwG}^{(k)}] \{W\} \\ & + \{\bar{W}\}^T [K_{w\phi G}^{(k)}] \{W\} + \{W\}^T [K_{w\phi G}^{(k)}] \{\bar{\Phi}_\gamma^{(k)}\} \\ & + \{\bar{W}\}^T [K_{\phi\phi G}^{(k)}] \{\Phi_\gamma^{(k)}\} \} \end{aligned}$$

$$\begin{aligned}
& + \{\Phi_{\alpha}^{(k)}\}^T [K_{\phi\phi h}^{(k)}] \left(\sum_{i=1}^{k-1} t_i \{\Phi_{\gamma}^i\} \right) + \left(\sum_{i=1}^{k-1} t_i \{\Phi_{\gamma}^i\} \right) [K_{\phi\phi h}^{(k)}] \{\Phi_{\gamma}^{(k)}\} \\
& + \{\Phi_{\alpha}^{(k)}\}^T [K_{\phi\phi d}^{(k)}] \{\Phi_{\gamma}^{(k)}\} + \{W\}^T [K_{w\phi G}^{(k)}] \{W\} \\
& + \{\Phi_{\alpha}^{(k)}\}^T [K_{w\phi G}^{(k)}]^T \{W\} + \{W\}^T [K_{w\phi G}^{(k)}] \{\Phi_{\gamma}^{(k)}\} \\
& + \{\Phi_{\alpha}^{(k)}\}^T [K_{\phi\phi G}^{(k)}] \{\Phi_{\gamma}^{(k)}\} \\
& + 2 \{W\}^T R_{wp}
\end{aligned} \tag{108}$$

The vanishing of the Gateaux differential $\delta_u \Omega$ (108) for arbitrary $\{\nabla_{\alpha}\}, \{\Phi_{\alpha}\}, \{W\}$ yields the following equations.

$$\sum_{e=1}^m \left[\sum_{k=1}^N \left\{ -[K_{vva}^{(k)}] \{V_{\gamma}^{(1)}\} - [K_{v\phi a}^{(k)}] \left(\sum_{i=1}^{k-1} t_i \{\Phi_{\gamma}^i\} \right) - [K_{v\phi b}^{(k)}] \{\Phi_{\gamma}^{(k)}\} \right\} \right] = 0 \tag{109}$$

$$\begin{aligned}
& \sum_{e=1}^m \left[\sum_{k=1}^N \left\{ -[K_{v\phi b}^{(k)}]^T \{V_{\gamma}^{(1)}\} - [K_{\phi\phi b}^{(k)}] \left(\sum_{i=1}^k t_i \{\Phi_{\gamma}^i\} \right) - [K_{\phi\phi d}^{(k)}] \{\Phi_{\gamma}^{(k)}\} \right. \right. \\
& \quad \left. \left. - [K_{w\phi G}^{(k)}]^T \{W\} - [K_{\phi\phi G}^{(k)}] \{\Phi_{\gamma}^{(k)}\} \right\} \right. \\
& \quad \left. + \sum_{k=1}^N \left\{ - \sum_{i=1}^{k-1} t_i [K_{v\phi a}^{(k)}]^T \{V_{\gamma}^{(1)}\} - \sum_{i=1}^{k-1} t_i [K_{\phi\phi a}^{(k)}] \sum_{i=1}^{k-1} t_i \{\Phi_{\gamma}^i\} - \sum_{i=1}^{k-1} t_i [K_{\phi\phi b}^{(k)}] \{\Phi_{\gamma}^{(k)}\} \right\} \right] = 0
\end{aligned} \tag{110}$$

and

$$\sum_{e=1}^m \left[\sum_{k=1}^N \left\{ -[K_{w\phi G}^{(k)}] \{W\} - [K_{w\phi G}^{(k)}] \{\Phi_{\gamma}^{(k)}\} + \{R_{wp}\} \right\} \right] = 0 \tag{111}$$

Where the $\sum_{e=1}^m$ denotes the "direct stiffness" addition of contributions of all elements.

Equations (109) through (111) can be written collectively in the following matrix form.

$$[K]\{U\} = \{R\}$$

Here

$$[K] = \sum_{e=1}^m [K]^e$$

$$\{R\} = \begin{bmatrix} R_1 \\ R_2 \\ \vdots \\ R_n \end{bmatrix}$$

and

$$\{u\} = \begin{bmatrix} u_1 \\ u_2 \\ \vdots \\ u_n \end{bmatrix}$$

where n is the total number of nodal points in the system and we identify:

$$[K] = \left(\begin{array}{ccccccccc} K_{11} & K_{12} & K_{13} & K_{14} & \cdots & K_{1,i+1} & \cdots & K_{1,N} & K_{1,N+1} & K_{1,N+2} \\ K_{21} & K_{22} & K_{23} & K_{24} & \cdots & K_{2,i+1} & \cdots & K_{2,N} & K_{2,N+1} & K_{2,N+2} \\ K_{31} & K_{32} & K_{33} & K_{34} & \cdots & K_{3,i+1} & \cdots & K_{3,N} & K_{3,N+1} & K_{3,N+2} \\ K_{41} & K_{42} & K_{43} & K_{44} & \cdots & K_{4,i+1} & \cdots & K_{4,N} & K_{4,N+1} & K_{4,N+2} \\ & \ddots & & \ddots & & \ddots & & \ddots & & \ddots \\ & & & \ddots & & \ddots & & \ddots & & \ddots \\ & & & & K_{i+1,i+1} & & \ddots & & \ddots & \\ & & & & & \ddots & & \ddots & & \ddots \\ & & & & & & \ddots & & \ddots & \\ & & & & & & & \ddots & & \ddots \\ & & & & & & & & K_{N,N} & K_{N,N+1} & K_{N,N+2} \\ & & & & & & & & K_{N+1,N+1} & K_{N+1,N+2} & \\ & & & & & & & & & K_{N+2,N+2} \end{array} \right)$$

symmetric

where

$$K_{11} = \sum_{k=1}^N [K_{vva}^{(k)}]$$

$$K_{12} = 0$$

$$K_{13} = [K_{v\phi b}^{(1)}] + t_1 \sum_{l=2}^N [K_{v\phi a}^{(l)}]$$

$$K_{14} = [K_{v\phi b}^{(2)}] + t_2 \sum_{l=3}^N [K_{v\phi a}^{(l)}]$$

$$K_{1,i+1} = [K_{v\phi b}^{(i-1)}] + t_{i-1} \sum_{l=i}^N [K_{v\phi a}^{(l)}]$$

$$K_{1,N} = [K_{v\phi b}^{(N-2)}] + t_{N-2} \sum_{l=N-1}^N [K_{v\phi a}^{(l)}]$$

$$K_{1,N+1} = [K_{v\phi b}^{(N-1)}] + t_{N-1} \sum_{l=N}^N [K_{v\phi a}^{(l)}]$$

$$K_{1,N+2} = [K_{v\phi b}^{(N)}]$$

$$K_{22} = \sum_{l=1}^N [K_{w\phi G}^{(l)}]$$

$$K_{23} = [K_{w\phi G}^{(1)}]$$

$$K_{24} = [K_{w\phi G}^{(i-1)}]$$

$$K_{2,i+1} = [K_{w\phi G}^{(i-1)}]$$

$$K_{2,N} = [K_{w\phi G}^{(N-2)}]$$

$$K_{2,N+1} = [K_{w\phi G}^{(N-1)}]$$

$$K_{2,N+2} = [K_{w\phi G}^{(N)}]$$

$$K_{33} = [K_{\phi\phi b}^{(1)}] + [K_{\phi\phi G}^{(1)}] + t_1^2 \sum_{l=2}^N [K_{\phi\phi a}^{(l)}]$$

$$K_{34} = t_1 [K_{\phi\phi b}^{(2)}] + t_1 t_2 \sum_{l=3}^N [K_{\phi\phi a}^{(l)}]$$

$$K_{3,i+1} = t_1 [K_{\phi\phi b}^{(i-1)}] + t_1 t_{i-1} \sum_{l=i}^N [K_{\phi\phi a}^{(l)}]$$

$$K_{3,N} = t_1 [K_{\phi\phi b}^{(N-2)}] + t_1 t_{N-2} \sum_{l=N-1}^N [K_{\phi\phi a}^{(l)}]$$

$$K_{3,N+1} = t_1 [K_{\phi\phi b}^{(N-1)}] + t_1 t_{N-1} \sum_{l=N}^N [K_{\phi\phi a}^{(l)}]$$

$$K_{3,N+2} = t_1 [K_{\phi\phi b}^{(N)}]$$

$$K_{44} = [K_{\phi\phi d}^{(2)}] + [K_{\phi\phi G}^{(2)}] + t_2^2 \sum_{l=3}^N [K_{\phi\phi a}^{(l)}]$$

$$K_{4,i+1} = t_2 [K_{\phi\phi b}^{(i-1)}] + t_2 t_{i-1} \sum_{l=i}^N [K_{\phi\phi a}^{(l)}]$$

$$K_{4,N} = t_2 [K_{\phi\phi b}^{(N-2)}] + t_2 t_{N-2} \sum_{l=N-1}^N [K_{\phi\phi a}^{(l)}]$$

$$K_{4,N+1} = t_2 [K_{\phi\phi b}^{(N-1)}] + t_2 t_{N-1} \sum_{l=N}^N [K_{\phi\phi a}^{(l)}]$$

$$K_{4,N+2} = t_2 [K_{\phi\phi b}^{(N)}]$$

$$K_{i+1,i+1} = [K_{\phi\phi d}^{(i-1)}] + [K_{\phi\phi G}^{(i-1)}] + t_{i-1}^2 \sum_{l=i}^N [K_{\phi\phi a}^{(l)}]$$

$$K_{i+1,N} = t_{i-1} [K_{\phi\phi b}^{(N-2)}] + t_{i-1,N-2} \sum_{l=N-1}^N [K_{\phi\phi a}^{(l)}]$$

$$K_{i+1,N+1} = t_{i-1} [K_{\phi\phi b}^{(N-1)}] + t_{i-1,N-1} \sum_{l=N}^N [K_{\phi\phi a}^{(l)}]$$

$$K_{i+1,N+2} = t_{i-1} [K_{\phi\phi b}^{(N)}]$$

$$K_{N,N} = [K_{\phi\phi d}^{(N-2)}] + [K_{\phi\phi G}^{(N-2)}] + t_{N-2}^2 \sum_{l=N-1}^N [K_{\phi\phi a}^{(l)}]$$

$$K_{N,N+1} = t_{N-2} [K_{\phi\phi b}^{(N-1)}] + t_{N-2,N-1} \sum_{l=N}^N [K_{\phi\phi a}^{(l)}]$$

$$K_{N,N+2} = t_{N-2} [K_{\phi\phi b}^{(N)}]$$

$$K_{N+1,N+1} = [K_{\phi\phi d}^{(N-1)}] + [K_{\phi\phi G}^{(N-1)}] + t_{N-1}^2 \sum_{l=N}^N [K_{\phi\phi a}^{(l)}]$$

$$K_{N+1,N+2} = t_{N-1} [K_{\phi\phi b}^{(N)}]$$

$$K_{N+2,N+2} = [K_{\phi\phi\phi}^{(N)}] + [K_{\phi\phi G}^{(N)}]$$

$$\{U\}_j^T = \langle v_a^1, w, \phi_a^1, \phi_a^2, \dots, \phi_a^i, \dots, \phi_a^n \rangle_j$$

and

$$\{R\}_j = \begin{pmatrix} 0 \\ 0 \\ R_w \\ 0 \\ \vdots \\ \vdots \\ 0 \end{pmatrix}_j \quad (112)$$

where the subscript j denotes the j th node.

3.3 SOLUTION PROCESS

Since the stiffness matrix is symmetric and banded, only the above-diagonal terms in the global stiffness matrix are stored in the form of a rectangular matrix. The first column of this matrix is the diagonal of the original matrix. The load vector is set up according to (112). After the global stiffness matrix and load vectors are assembled, the system of simultaneous equations is solved for the displacement degrees of freedom using the Gaussian elimination process. The solution for nodal displacements (δ^e) of an element along with $[B]$ matrix which is the element strain-displacement relation are used to calculate the stresses at the desired points of the element. i.e.,

$$\epsilon_i = B \delta^e = \sum_{i=1}^n B_i \delta_i$$

where n represents number of nodal points in the element.

$$\sigma = \bar{Q} B \delta^e$$

and $[Q]$ contains the elastic constants of the specific lamina. In (106) the specific $[B]$ is denoted by $[DH]^T$

Section IV

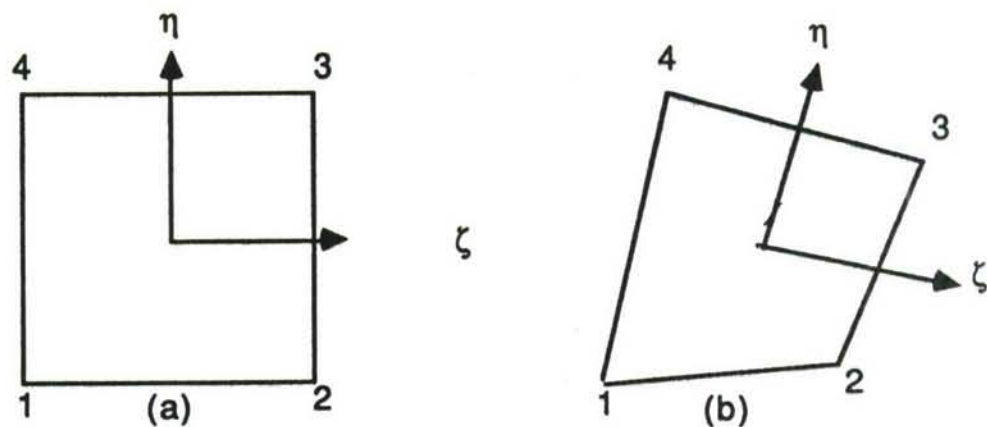
VERIFICATION AND APPLICATIONS

4.1 PROBLEM DESCRIPTION

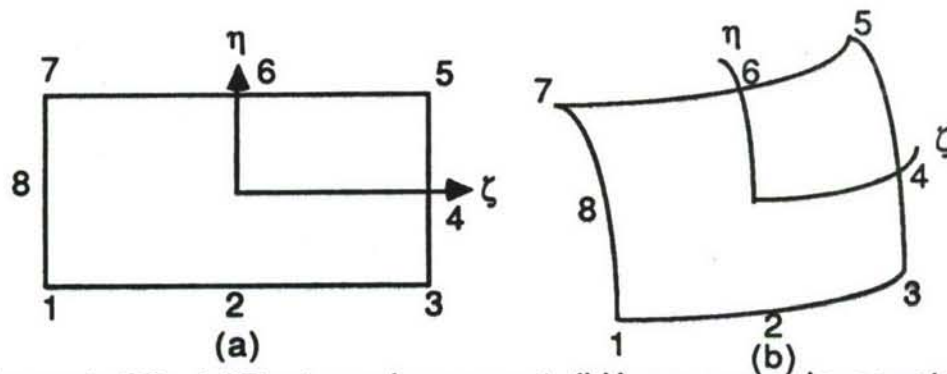
The theory discussed in Sections II and III was implemented in a computer program. The computer program was written in Fortran and designed to run on the IBM3081 main-frame.

Eight-noded serendipity, nine-noded Lagrangian, and four-noded Lagrangian quadrilateral isoparametric plate elements were used (Fig. 2). The nodal degrees of freedom (the number of unknowns associated with each nodal point) depend upon the number of layers in the laminate. If the number of layers is m , then the degree of freedom is $(2m+3)$ for each nodal point. This consists of three displacement components (u, v, w) for a reference point on the 'through the thickness' nodal point and rotations (ϕ_x, ϕ_y) of each layer to describe completely the deformed geometry. Two versions of the program were prepared. The first was an "incore" program wherein all the matrices were generated and stored in core and the solution process did not require auxiliary storage. This version was adequate for solution of example problems and verification of the general approach. Later, a version was developed where the algebraic equations were assembled and stored in blocks. This version was used for solution of a 22-laminae problem using the CRAY-XMP computer at the Ohio Supercomputer Center. This implementation was verified by application to several example problems. These examples included:

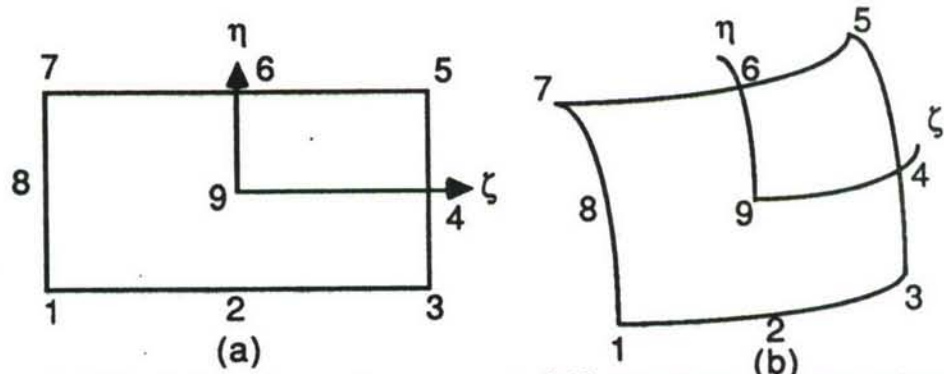
1. A simply supported square sandwich plate made of isotropic/orthotropic surface layers. The core was assumed to have a finite shear modulus but zero elastic



1. Element Q4: (a)Rectangular parent (b)Isoparametric counterpart



2. Element Q8: (a)Rectangular parent (b)Isoparametric counterpart



3. Element Q9: (a)Rectangular parent (b)Isoparametric counterpart

Figure 2: Four, eight, and nine-noded quadrilateral element used.

modulus in extension.

2. Free-edge delamination specimens

a. Angle-ply [$\pm 45^\circ$]

b. Cross-ply [0/90]

The results were compared with available solutions. The effect upon the accuracy of the results of mesh refinement and sublayers subdivision was studied. The code was used to determine stresses and deformations in a multi-ply free-edge delamination specimen.

4.1.1 Analysis of Plates

The multilayer plate finite element method was used to analyze a three layer, square, simply supported sandwich plate uniformly loaded in the transverse direction. The geometrical and material properties of the plates were (the top and bottom layers are denoted by subscripts 1 and 3, the core by 2). This example was the same as used by [5]

Plate dimensions;

Length of each side = 10 inches.

Thickness t_1 and t_3 of surface layers = 0.028 in

Thickness of core t_2 = 0.75 in

Material properties

a. Stiff layers are isotropic elastic.

$$E_1 = E_3 = 10^7 \text{ lb/in}^2$$

$$\nu_1 = \nu_3 = 0.3$$

$$G_2 = 3 \times 10^4 \text{ lb/in}^2$$

b. Stiff layers are orthotropic elastic.

$$E_{11} = E_{33} = 10^7 \text{ lb/in}^2$$

$$E_{y1} = E_{y3} = 4 \times 10^6 \text{ lb/in}^2$$

$$G_{xy1} = G_{iy3} = 1.875 \times 10^6 \text{ lb/in}^2$$

$$\nu_{x1} = \nu_{x3} = 0.3$$

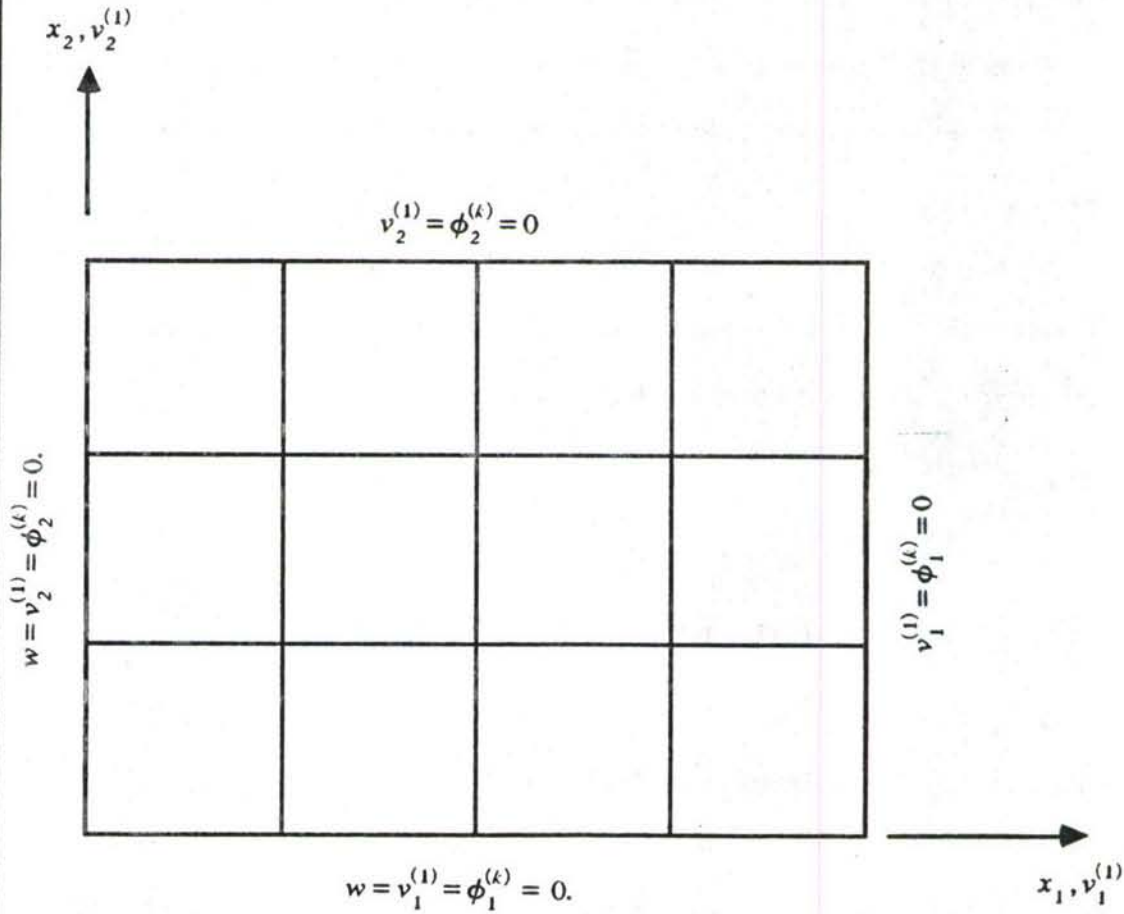
$$G_{xz2} = 3 \times 10^4 \text{ lb/in}^2$$

$$G_{yz2} = 1.2 \times 10^4 \text{ lb/in}^2$$

Loading

$$q=1 \text{ lb/in}^2$$

Due to double symmetry, only one quarter of the plate was analyzed in each case (Fig. 3). When eight- and nine-noded elements were used four mesh discretizations viz., (1x1), (2X2), (4X4), and (8X8) were used. In the case of four-noded element, the discretization for the quarter of the plate was extended to a finer (16x16) mesh.



(One quarter of the plate)

Figure 3: Mesh configuration and boundary conditions for a quarter plate.

4.1.2 Analysis of Four-Ply Free-Edge Delamination Specimens

The free-edge delamination specimen was treated as a special case of a plate Fig.(4). The boundary conditions considered were: fixed-fixed (longitudinal displacement specified) at the longitudinal ends and free-free at the transverse edges. The results for four-ply symmetric laminate with stacking [$\pm 45^\circ$], and [0/90]₂ were compared with Pagano's solution [10] which is based on a generalization of Reissner's theory. The comparison covered only σ_{zz} , σ_{z3} , and u_z because Pagano's solutions were available only for these quantities.

The dimensions were specified as $a/b \geq 7$ and $b = 8h$, where a , b , and h are length, width, and thickness of each lamina, respectively. For proper comparison, the material properties assumed were the same as in [10].

$$E_{11} = 20 \times 10^6 \text{ psi}$$

$$E_{22} = E_{33} = 2.1 \times 10^6 \text{ psi}$$

$$G_{12} = G_{13} = G_{23} = .85 \times 10^6 \text{ psi}$$

$$\nu_{12} = \nu_{13} = \nu_{23} = 0.21$$

Following Pagano, $N=2$ indicates each lamina is treated as a single layer, and $N=6$ indicates that each lamina of thickness h is modeled by three sublayers with thicknesses of $h/3$. For $N=10$ each lamina with thickness h is subdivided into five sublayers. In going from three sublayers to five, only one of the sublayers was subdivided into three new sublayers with thickness of $h/9$.

Two different types of mesh refinement were considered. In both types, refinement was carried out in a manner such that the nodal points of the previous, coarser mesh were a subset of the finer mesh. Refinement associated with longitudinal direction was performed by dividing the domain in the longitudinal direction into the stated number of equal length elements. In the case of the transverse direction, the

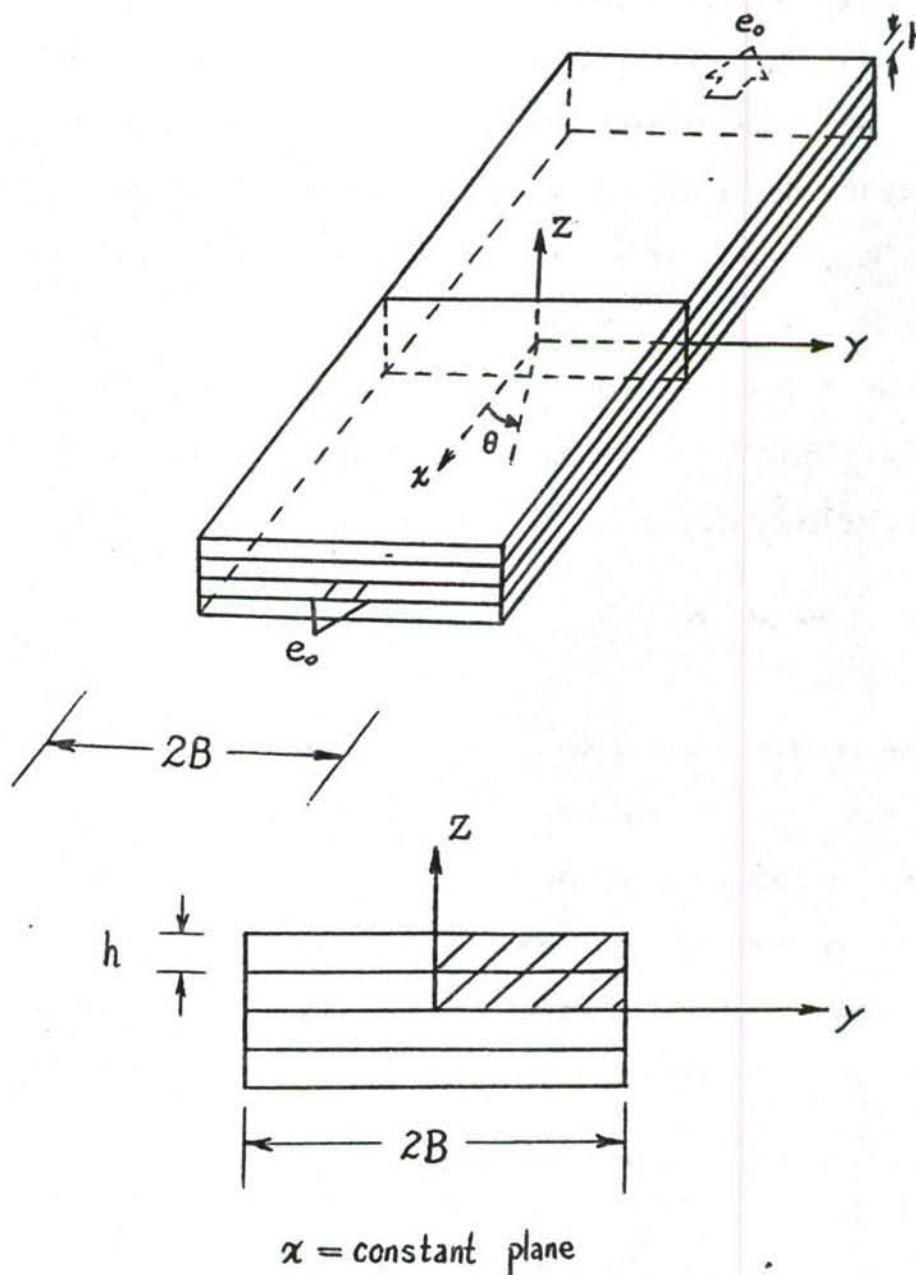


Figure 4: Configuration for laminated coupon under uniaxial tension.

refinement was in the form shown in Figs.(5) and (6), to minimize the required storage. In one sequence of refinements, shown in Fig.(5), the width of the specimen was first divided into five equal-width elements. Only the edge elements were refined further, each time the edge elements being subdivided into three elements. This process was continued. In the other sequence illustrated by Fig.(6), an edge element was used such that the (y/b) ratio for its center was 0.995. The remaining interior domain was discretized into three strips. Refinement over the thickness was done on the central sublayer while changing from $N=6$ to $N=10$, Fig.(7c) in order to get good estimates for τ_{xy} and σ_{xx} . On the other hand, to evaluate τ_{xz} at the interface, discretization was performed on the sublayer next to the interface, Fig.(7d). Because of symmetric stacking sequence, only two layers were used in the analysis.

4.1.3 Results of the Analysis

a. Rectangular Plates

Figs.(8) through (11) show a comparison of the approximate solution with that of the sandwich plate theory as presented in [5]. Fig.(8) shows the convergence of the central deflection of a sandwich plate with isotropic layers. Results using the Q8 and the Q9 elements converge to the exact solution more rapidly than those from the Q4 element. The results obtained for one element, in the case of Q9 element, or four elements in the case of Q8 elements, are superior to results obtained from 256 (16x16) Q4 elements. Fig.(9) shows that, for a given error limit, the amount of time needed for Q8 and Q9 elements is considerably smaller than for Q4 elements. Results for a sandwich plate with orthotropic layers are presented in Figs.(10) and (11). The same observation, can be made as in the case of isotropic plates. The numerical results for isotropic and orthotropic cases are presented in Tables (1) and (2), respectively.

The program was also used to solve the isotropic problem where the shear correction factor was ignored. The maximum central deflection for an 8x8 mesh, using

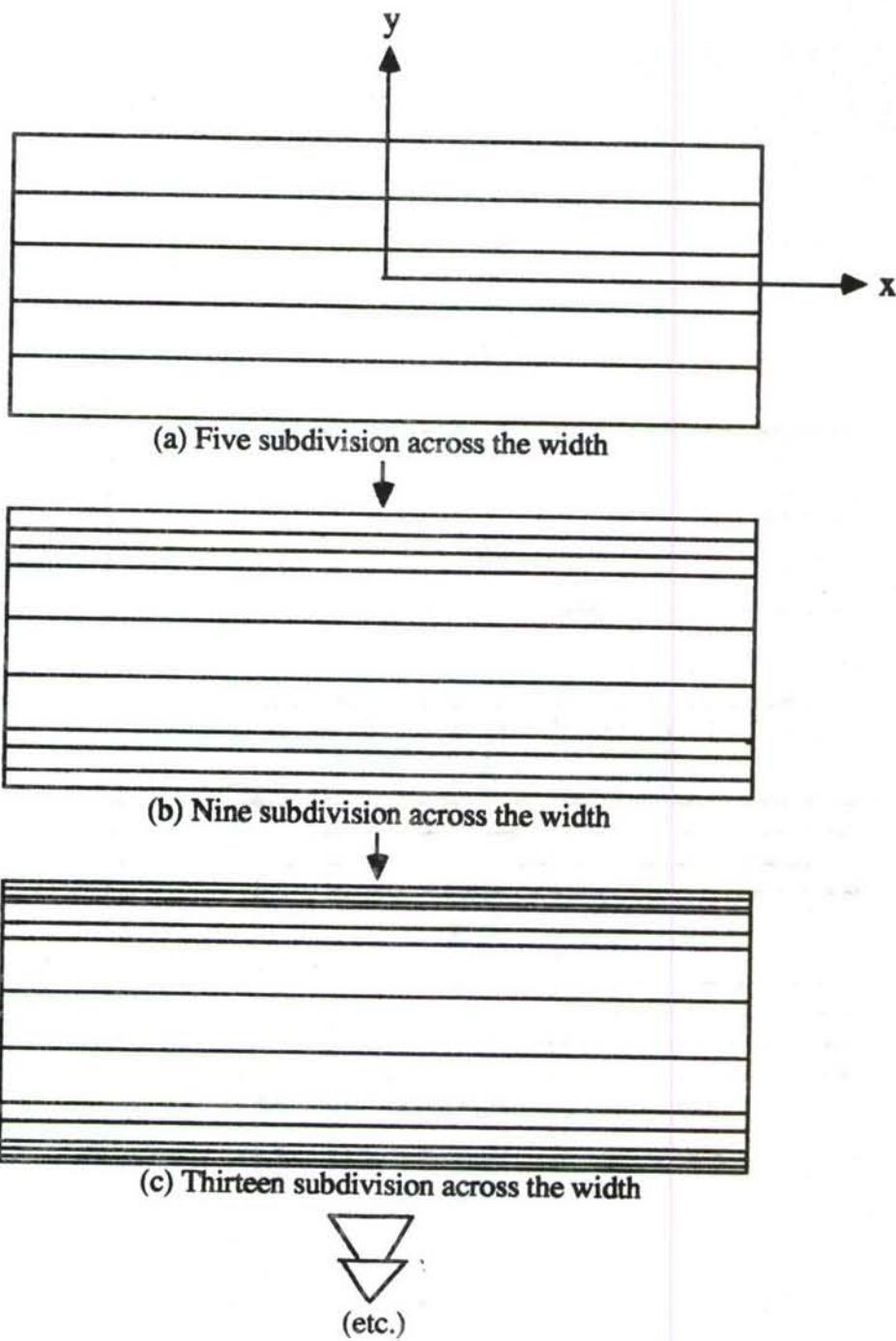


Figure 5: Sequence of mesh refinement across the width.

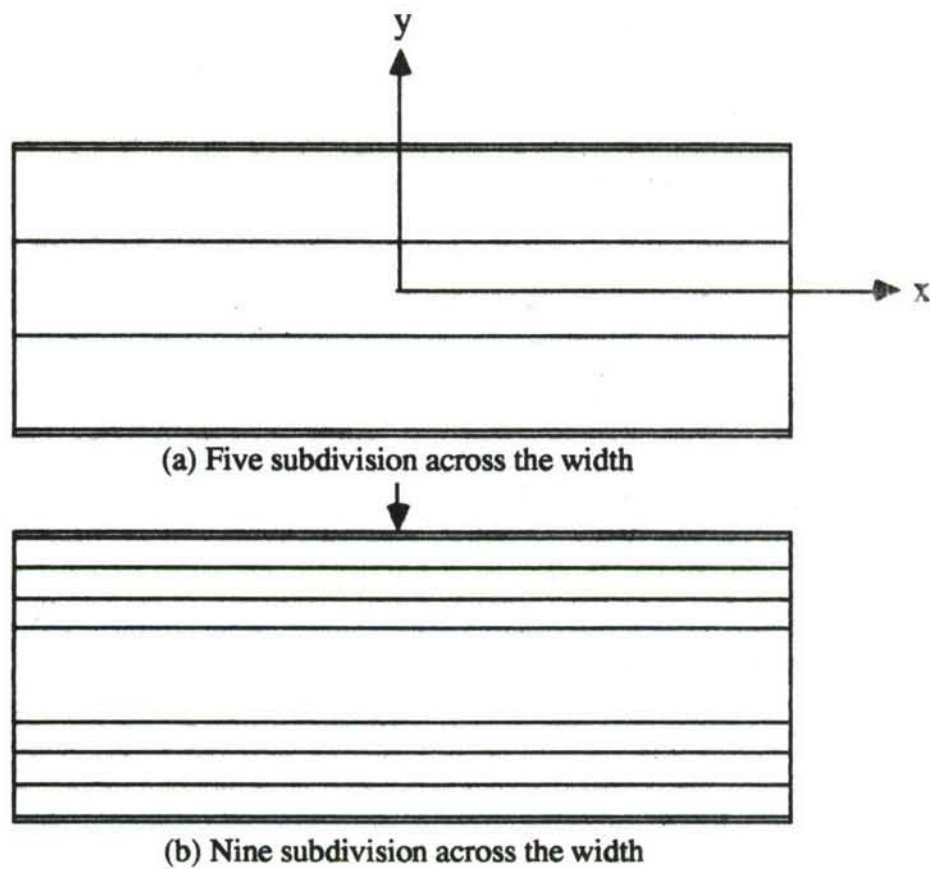


Figure 6: Sequence of refinement across the width with a thinner edge element.

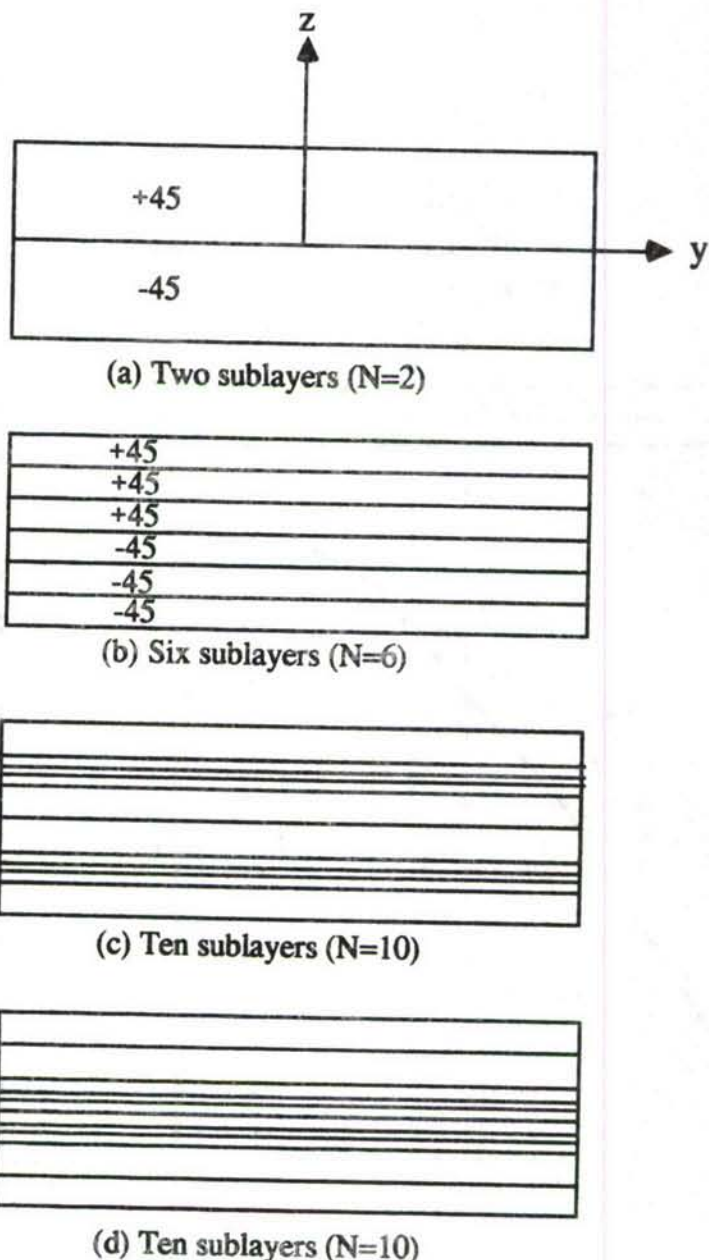


Figure 7: Sequence of refinements over the thickness.

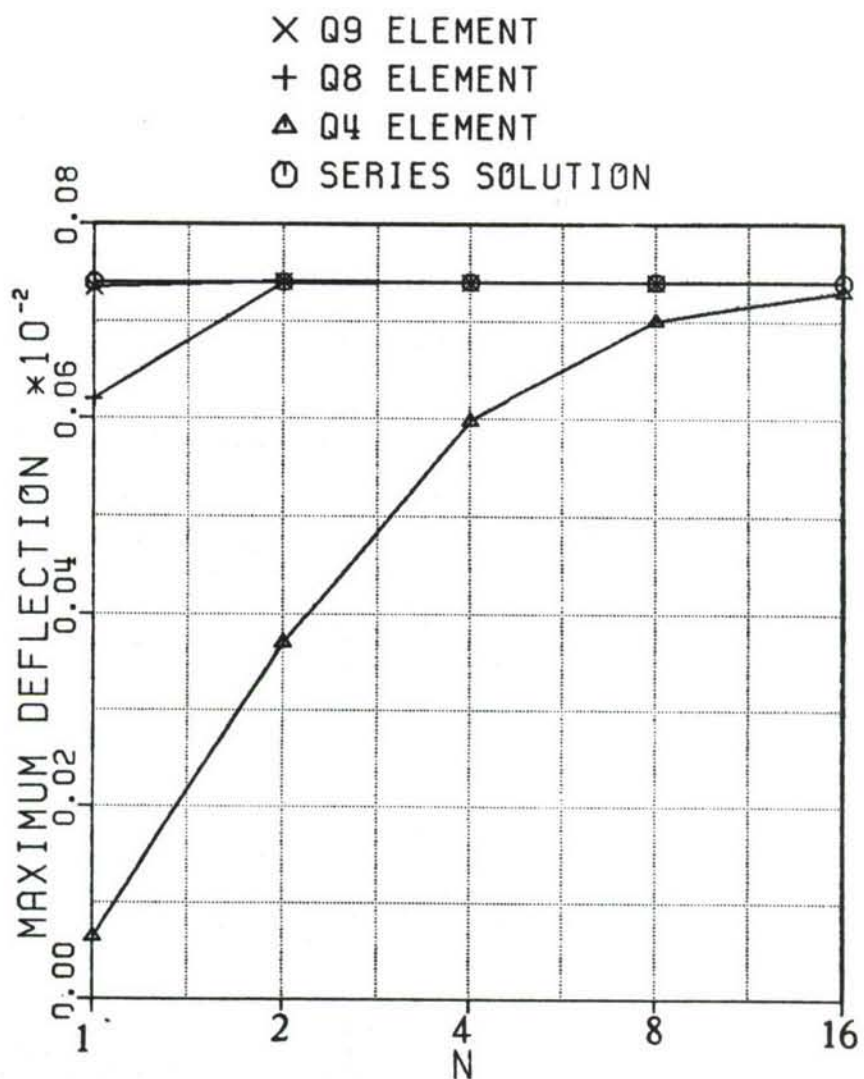


Figure 8: Number of subdomains along each side vs central deflection of a square isotropic simply supported plate with No. of elements = N^2 .

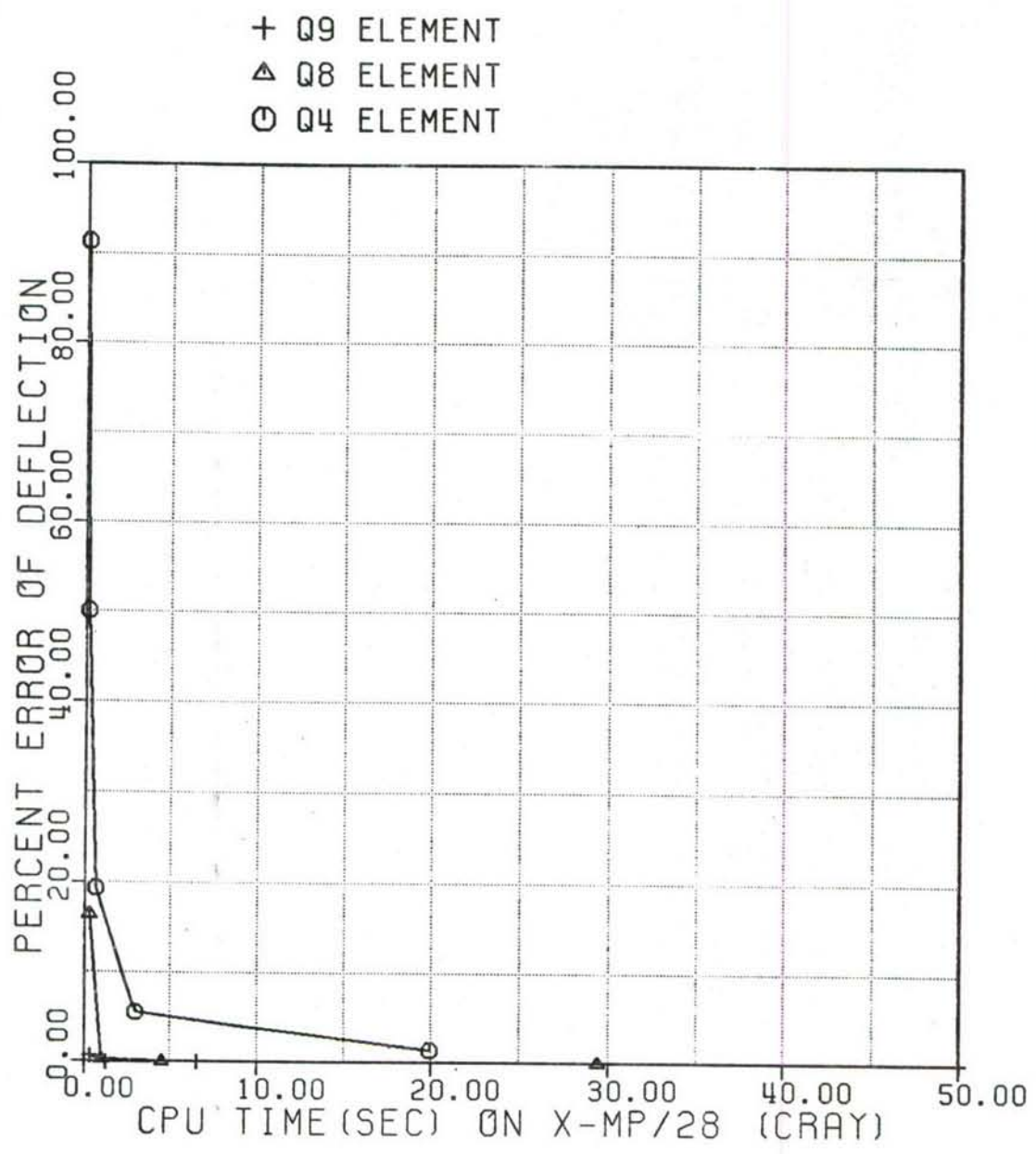


Figure 9: CPU time vs error in central deflection with mesh refinement-isotropic layers.

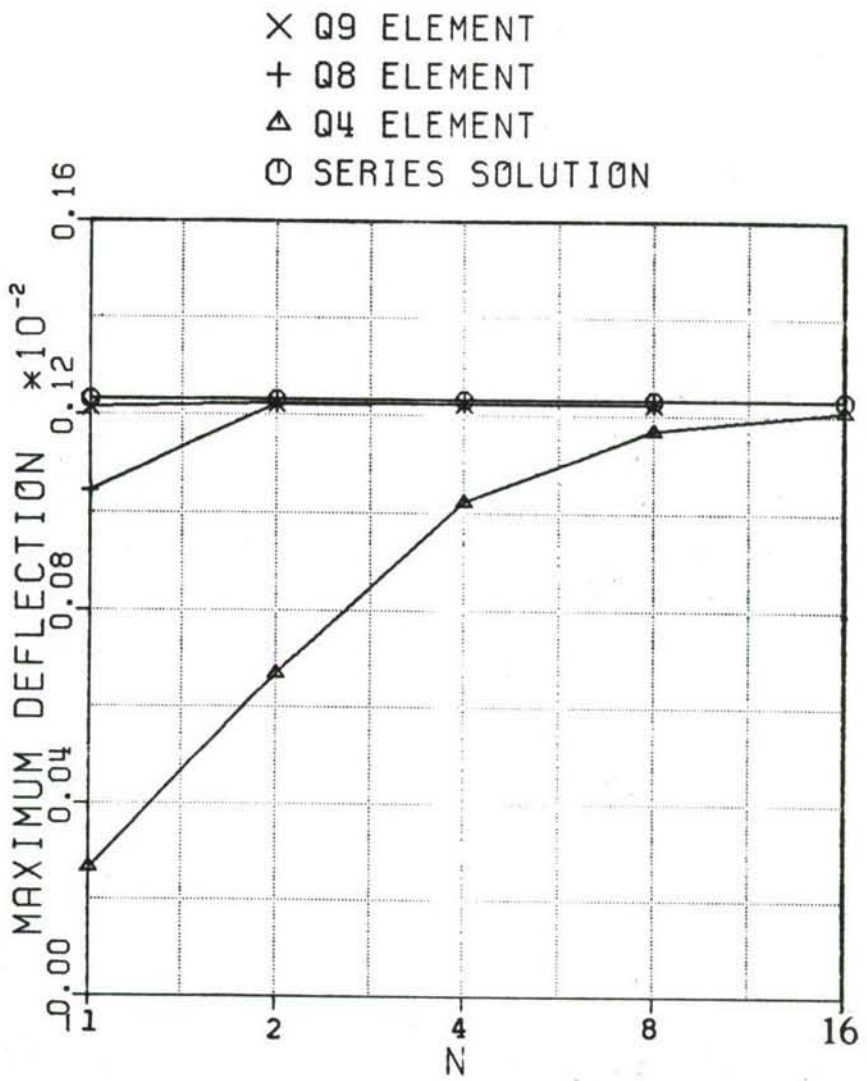


Figure 10: Central deflection of a square orthotropic simply supported sandwich plate.

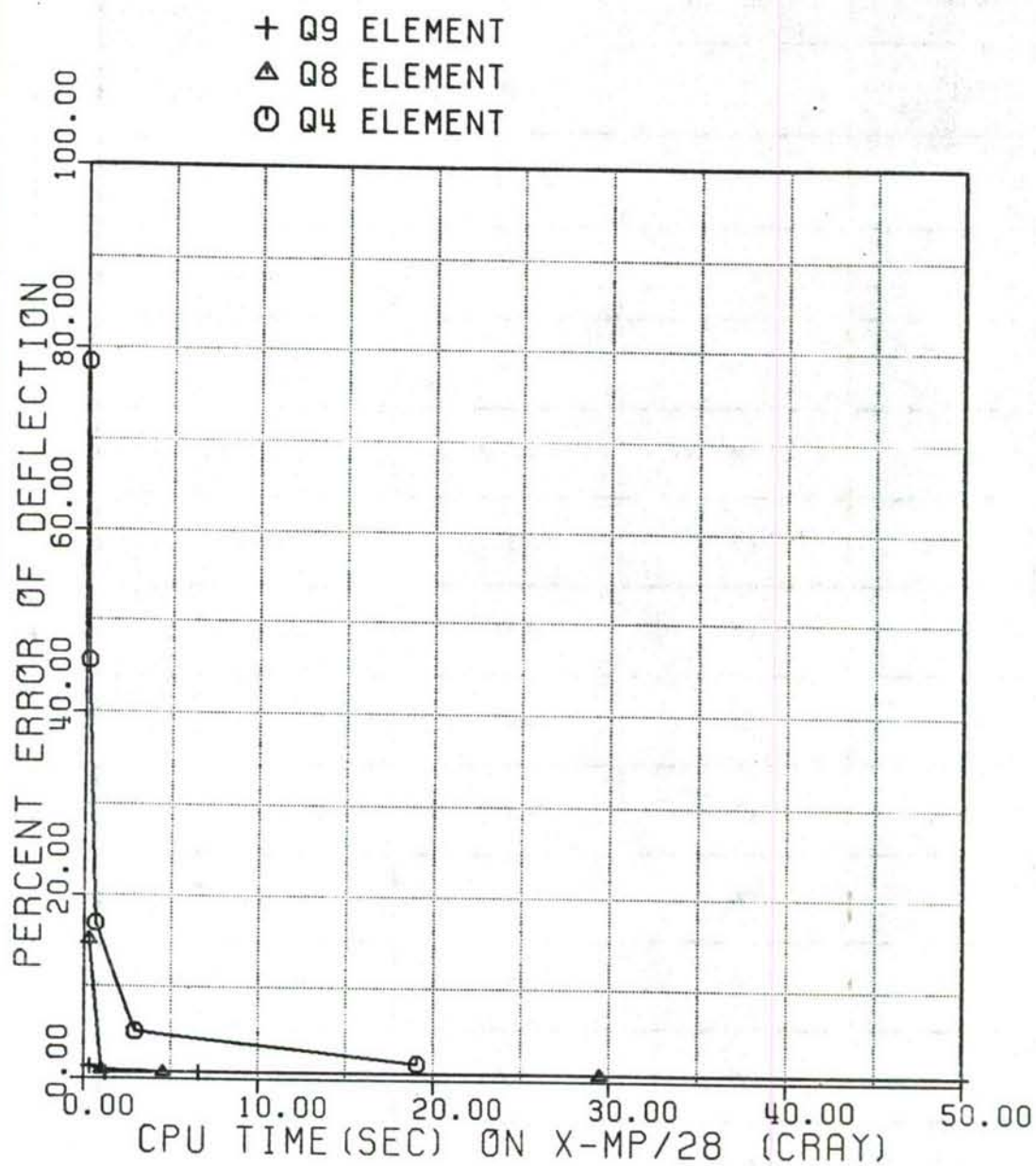


Figure 11: CPU time vs error in central deflection with mesh refinement-orthotropic layers.

Table 1: Numerical values for maximum deflection and the corresponding CPU time for different types of elements.(Isotropic case)

Number of Elements	Element Type	CPU (Sec)	Maximum deflection
1x1	Q4	0.046	0.000054402
2x2	Q4	0.154	0.00036986
4x4	Q4	0.605	0.00059685
8x8	Q4	2.918	0.00069959
16x16	Q4	19.897	0.00072964
1x1	Q8	0.232	0.0006189
2x2	Q8	0.934	0.00073851
4x4	Q8	4.492	0.00073997
8x8	Q8	29.377	0.00074005
1x1	Q9	0.287	0.00073539
2x2	Q9	1.221	0.00074087
4x4	Q9	6.516	0.00074008
8x8	Q9	50.446	0.00074006
Series Solution			0.00074

Table 2: Numerical values for maximum deflection and the corresponding CPU time for different types of elements.(Orthotropic case)

Number of Elements	Element Type	CPU (Sec)	Maximum deflection
1x1	Q4	0.046	0.00026536
2x2	Q4	0.146	0.00066988
4x4	Q4	0.591	0.0010218
8x8	Q4	2.851	0.0011671
16x16	Q4	19.071	0.0012078
1x1	Q8	0.228	0.0010439
2x2	Q8	0.954	0.0012194
4x4	Q8	4.497	0.0012215
8x8	Q8	29.467	0.0012216
1x1	Q9	0.286	0.0012140
2x2	Q9	1.224	0.0012224
4x4	Q9	6.545	0.0012216
8x8	Q9	50.267	0.0012216
Series Solution			0.00123

Q8 element, was $W_{\max} = 0.00043601$. The series solution for same problem gave almost identical value. $W_{\max} = 0.00043605$. Therefore, maximum deflection due to shear for this plate would be:

$$W_{S_{\max}} = 0.000740 - 0.0004360 = 0.000304$$

b. Four-Ply Free-Edge Delamination Specimen

Values of σ_{3z} presented in the subsequent sections were determined based on the constitutive equations (36) and (37). Determination of these stress components is also possible through the use of the equilibrium equations. However, inplane strain is linear over an element and discontinuous at the nodal points, resulting in a discontinuous set of inplane stresses. Furthermore, the numerical evaluation of σ_{33} needs one numerical differentiation, and σ_{33} needs two numerical differentiation. Therefore, the use of numerical differentiation would not result in a satisfactory estimate unless the number of elements in the y-direction is increased to a point where the discontinuity of σ_{ab} is reduced considerably. This would result in a very expensive computational analysis. Therefore, it was more convenient to determine σ_{3z} from the constitutive relations.

i. Angle-ply Laminate [± 45]

Since the stresses were determined at the center of the elements, to determine the predicted results at the center of the longitudinal dimension ($x = L/2$), an odd number of elements were used when using Q8 or Q9 element. Because these elements have midside nodes, displacements were also directly available at $x = \frac{L}{2}$. In the case of Q4 element, two analyses had to be carried out. To obtain the solution for stresses, an odd number of elements were used. However, as for the Q8 and Q9 elements, to obtain the displacement results at $(L/2)$, it was necessary to discretize the longitudinal direction into an even number of elements, (odd number of nodal points) so that a

set of nodal points would be located at $x = \frac{L}{2}$.

Q4 element

Fig. (12), shows plots of values of σ_x at mid-surface of the top lamina for mesh refinement in the y-direction. The number of elements in the x-direction was kept constant at 11 and over the thickness, each layer had constant rotation about the x- and y-axes. As observed from the figure, accuracy of the axial stress is unaffected by refinement in the y direction. However, the values do improve somewhat with refinement in the longitudinal (x) direction (Figs. 13 and 14). Fig. (13) shows the effect of refinement along x into 21 and 31 elements with the number of elements along y kept constant at 17. Fig. (14) shows the effect of refinement along x for 9 elements in the y-direction. Fig. (15) shows the effect of thickness refinement on σ_x . The results improve significantly with refinement near the free-edge. The same observation can be made for τ_{xy} in Figs. (16) through (18) respectively. The calculated values of σ_x improve slightly with refinement in the x-direction but are unaffected by the refinement along the y and z-directions. Accuracy of τ_{xz} is not affected by refinement in the longitudinal or the transverse directions, Figs. (19) through (21).

Accuracy of the stresses at the free-edge improves significantly with refinement over the thickness, i.e. as N is increased from 2 to 6. This refinement does not introduce additional elements but increases the degree of freedom at each of the nodal points by assuming rotation to be constant over a smaller portion of the thickness. Comparison of results for different values of N indicates that N=6, in comparison to N=2 and N=10, gives more accurate prediction for σ_x Fig. (15). Further refinement to N=10, in comparison to N=2 and N=6, leads to better estimation of τ_{xy} Fig. (22) and τ_{xz} Fig. (23). It should be mentioned that thickness refinement does not influence the accuracy of stresses near $Y/b=0$. Stresses at the free-edge, however, are greatly influenced.

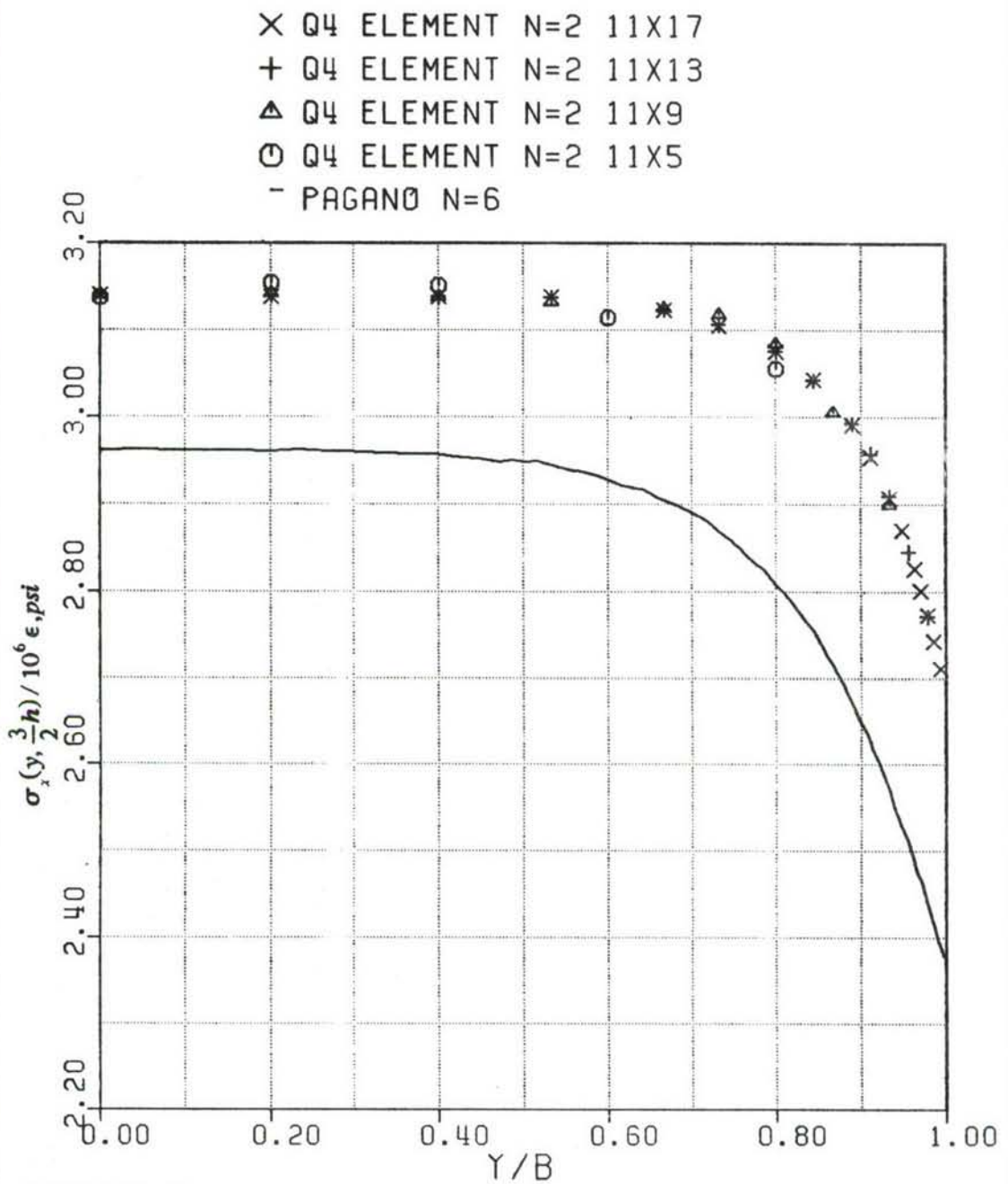


Figure 12: X-stress at the mid-surface of the top lamina with refinement in y-direction; Angle-ply specimen.

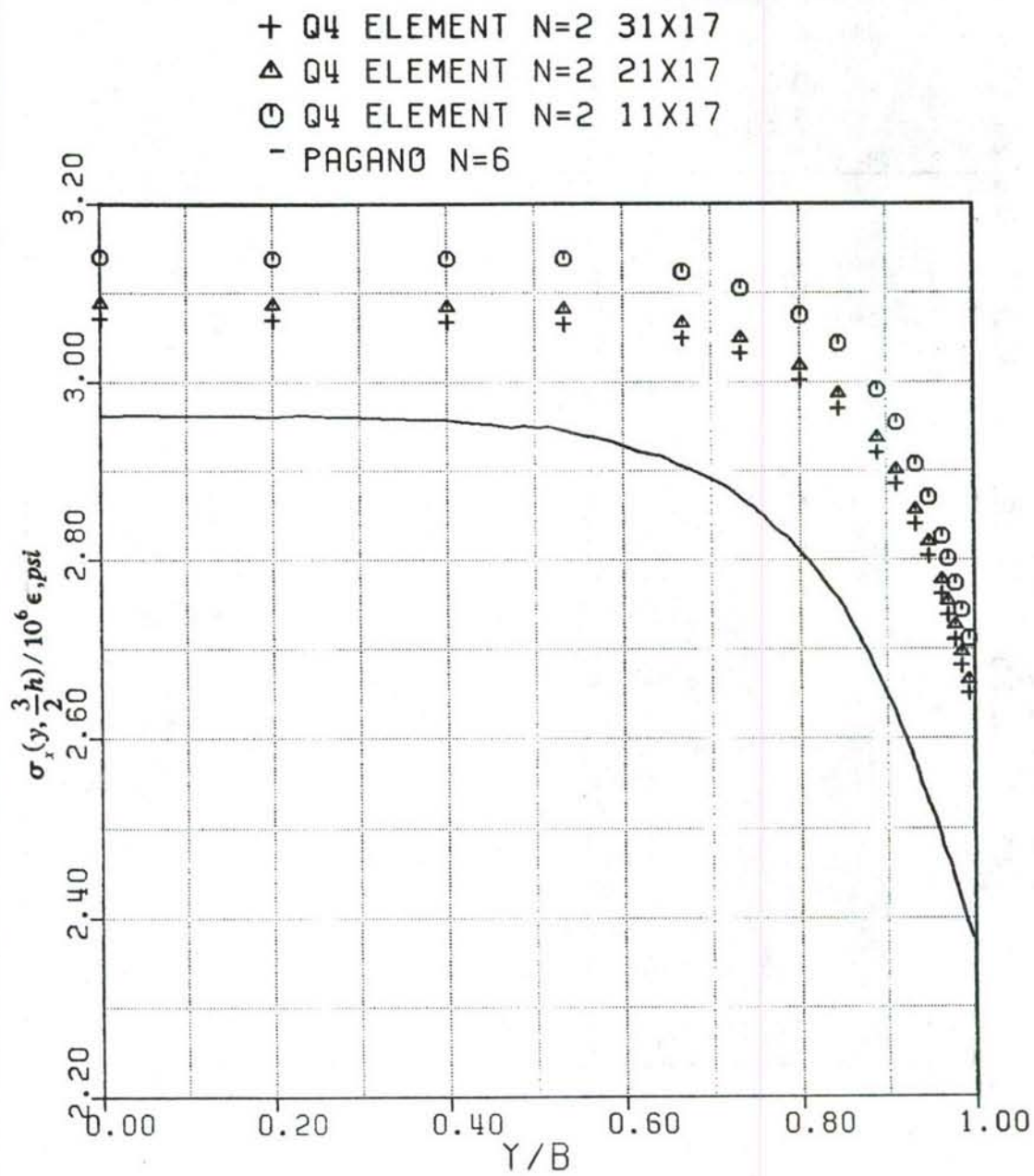


Figure 13: X-stress at the mid-surface of the top lamina with refinement in x-direction; Angle-ply specimen.

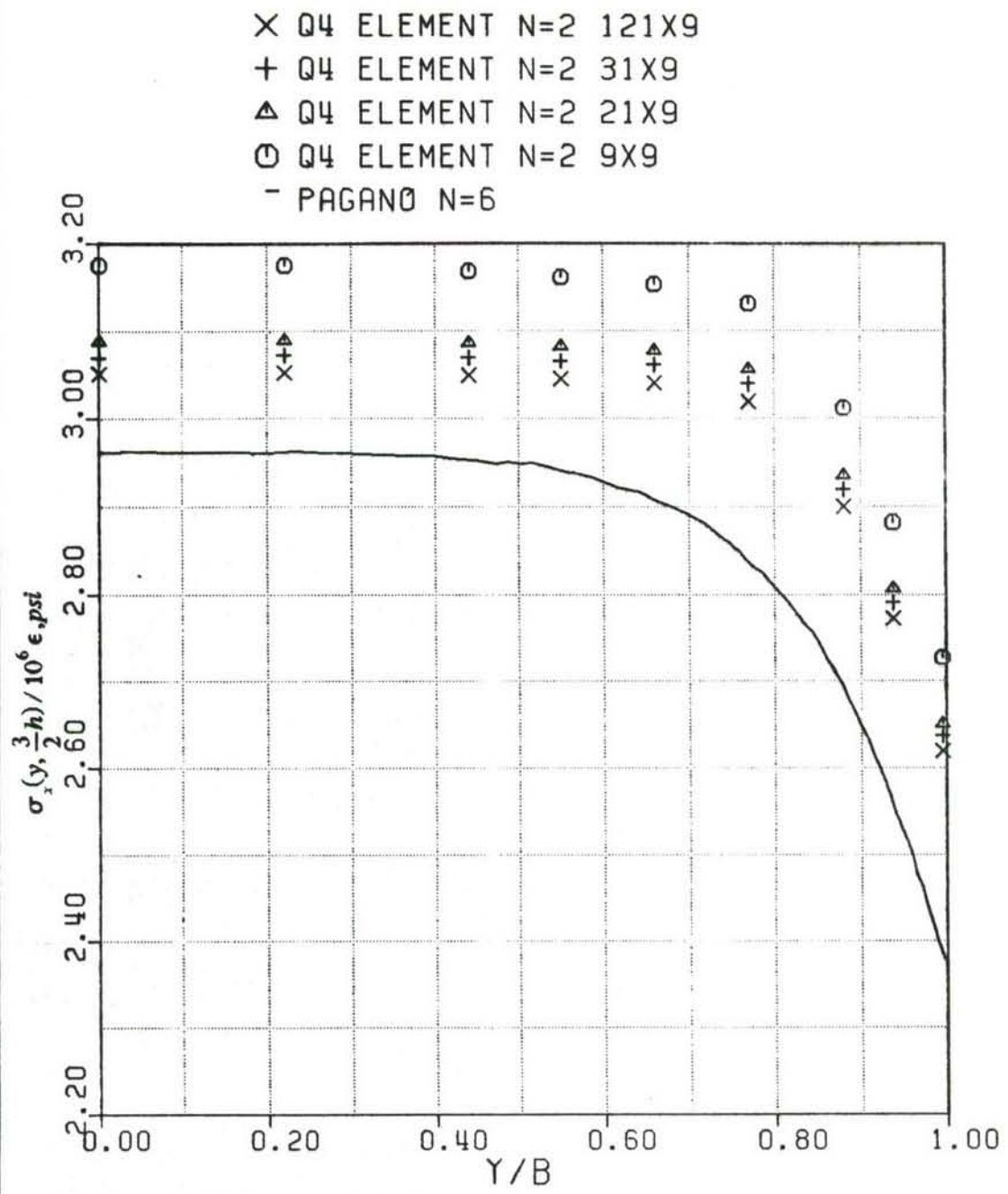


Figure 14: X-stress at midsurface of the top layer with refinement in x-direction; Angle-ply specimen, using edge elements.

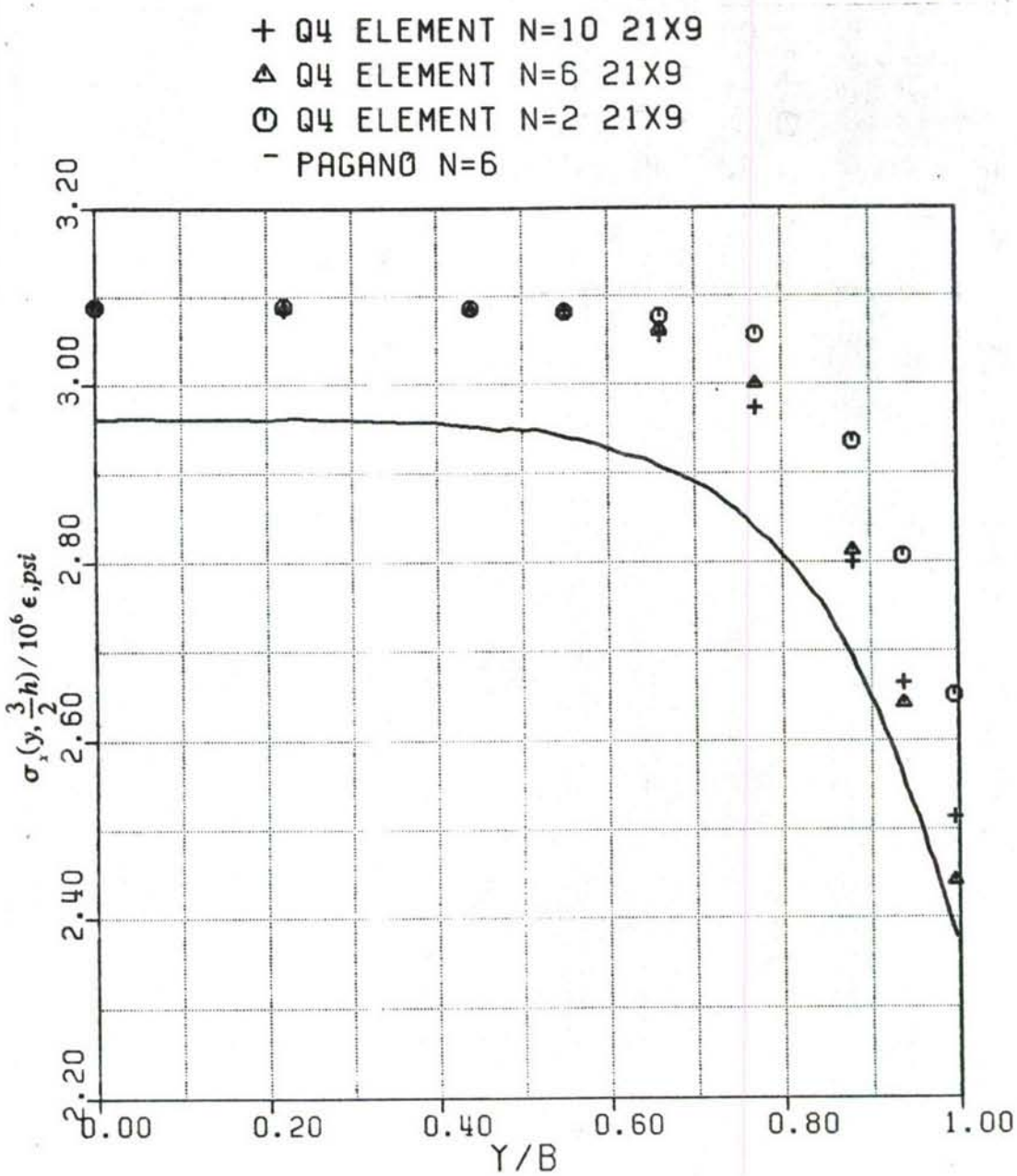


Figure 15: X-stress at midsurface of top layer with thickness refinement; Angle-ply specimen.

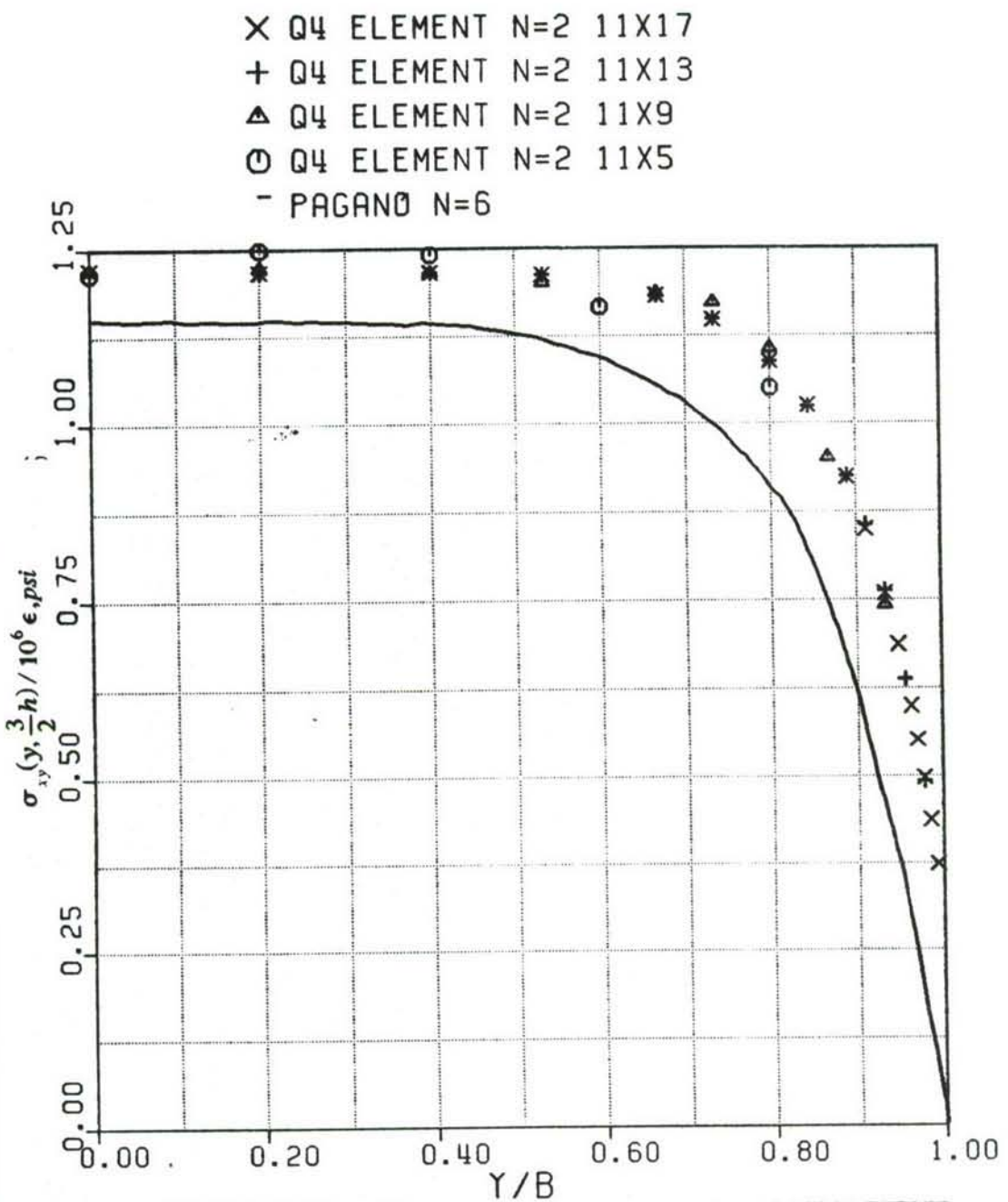


Figure 16: XY-stress at midsurface of top layer with refinement in y-direction; Angle-ply specimen.

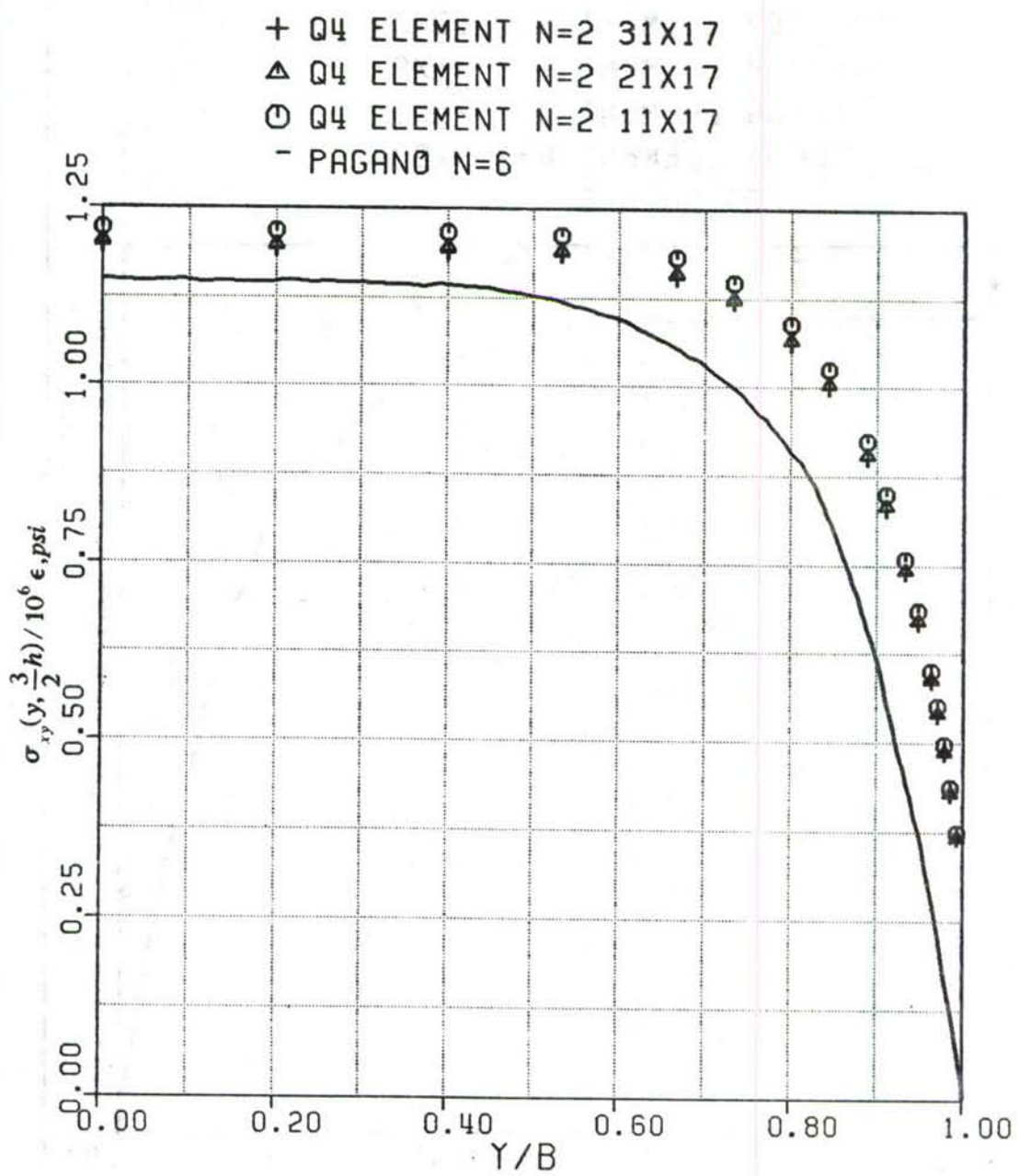


Figure 17: XY-stress at midsurface of top layer with refinement in x-direction; Angle-ply specimen.

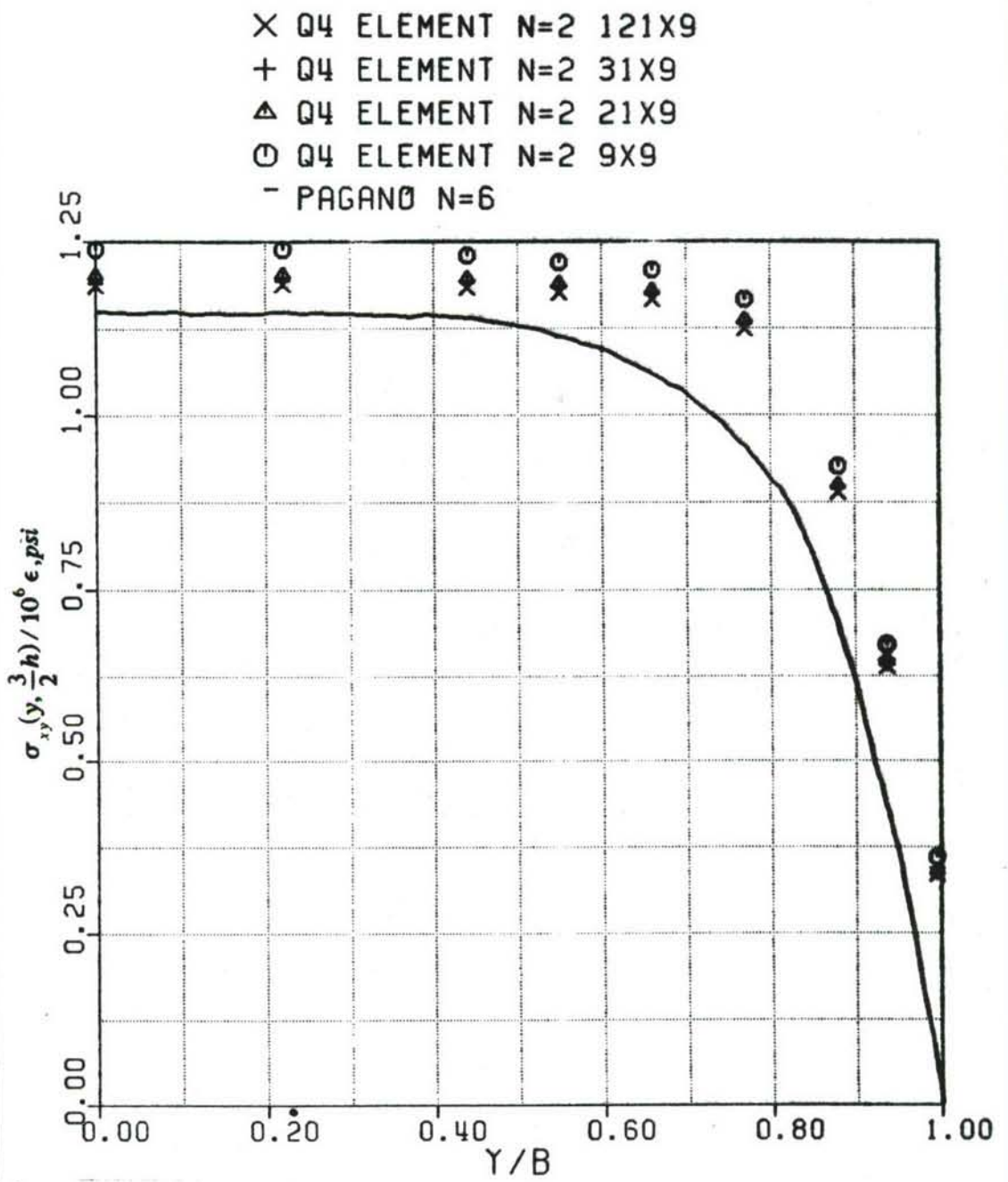


Figure 18: XY-stress at midsurface of top layer with refinement in x-direction; Angle-ply specimen.

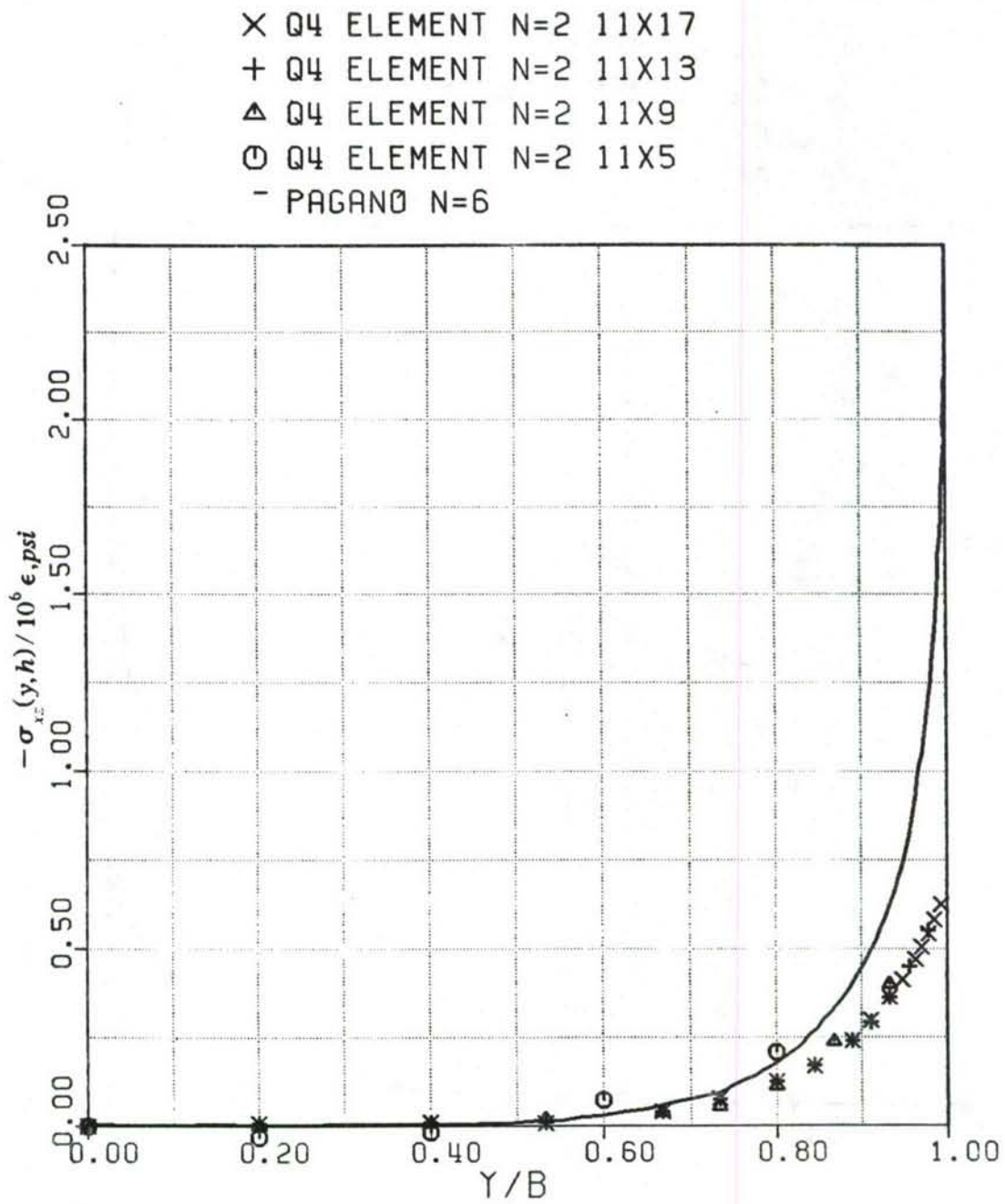


Figure 19: XZ-stress at $z=h$ with refinement in y -direction; Angle-ply specimen.

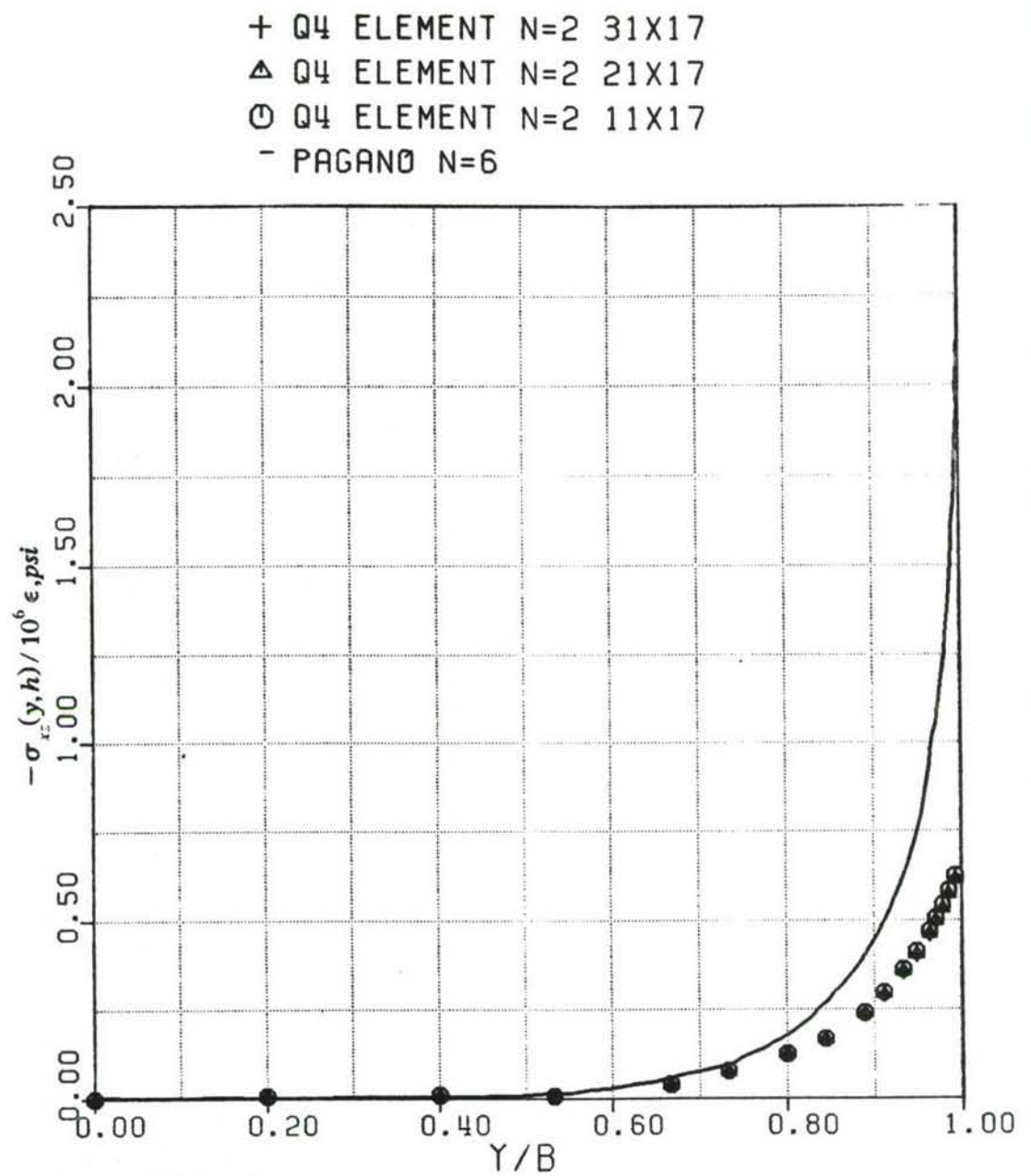


Figure 20: XZ-stress at $z=h$ with refinement in x-direction; Angle-ply specimen.

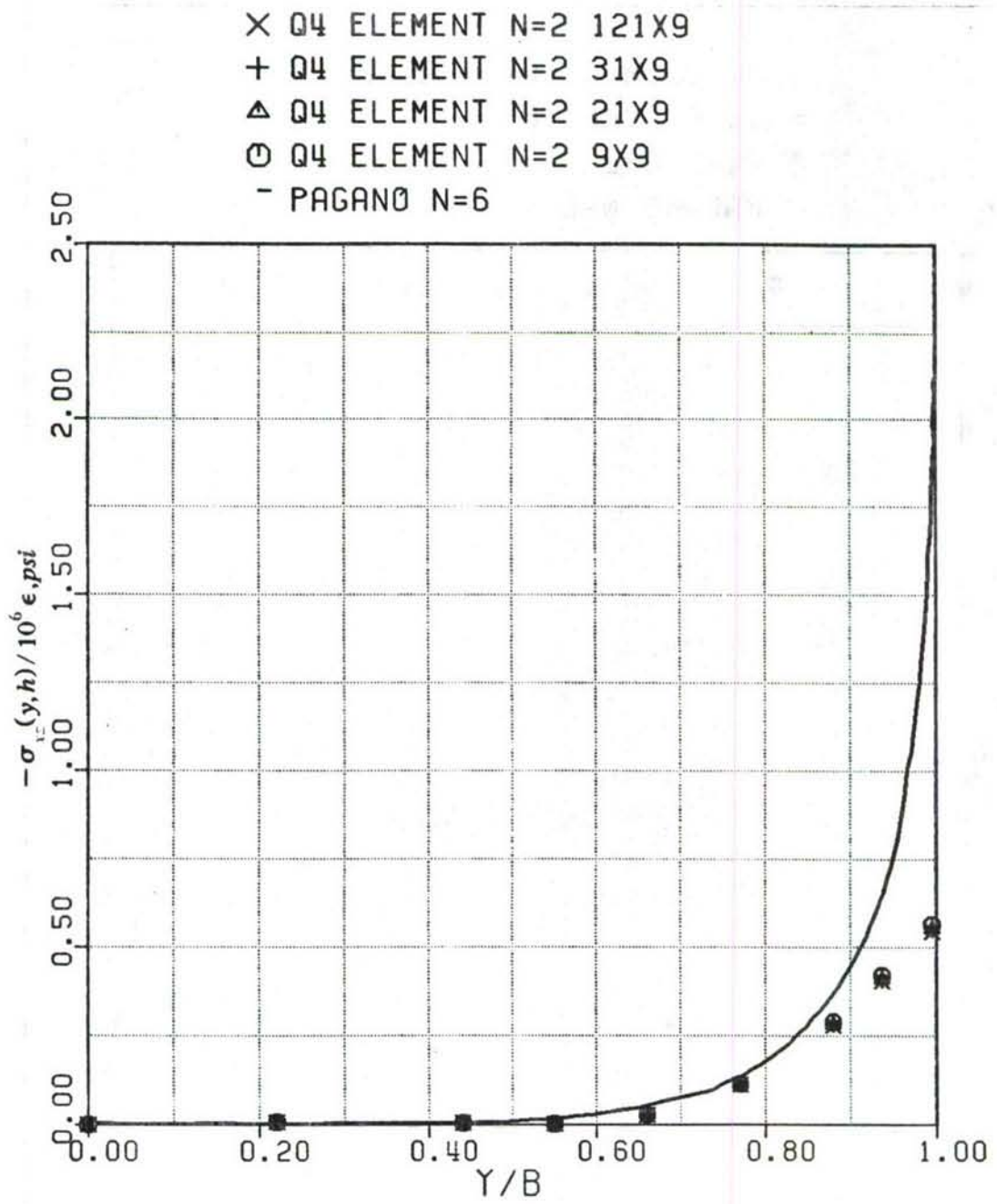


Figure 21: XZ-stress at $z=h$ with refinement in x-direction; Angle-ply specimen.

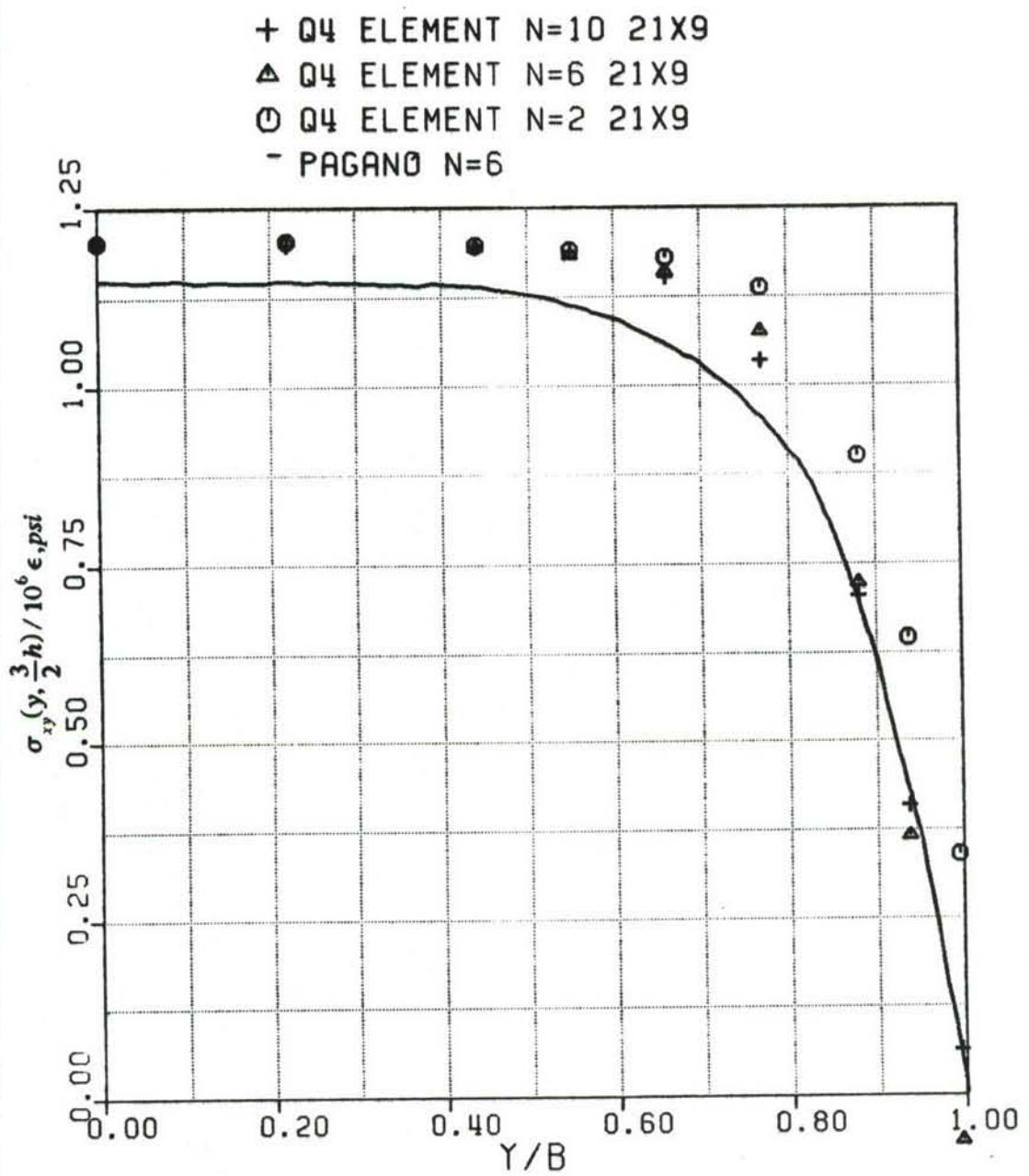


Figure 22: XY-stress at the mid-surface of the top layer with thickness refinement; Angle-ply specimen.

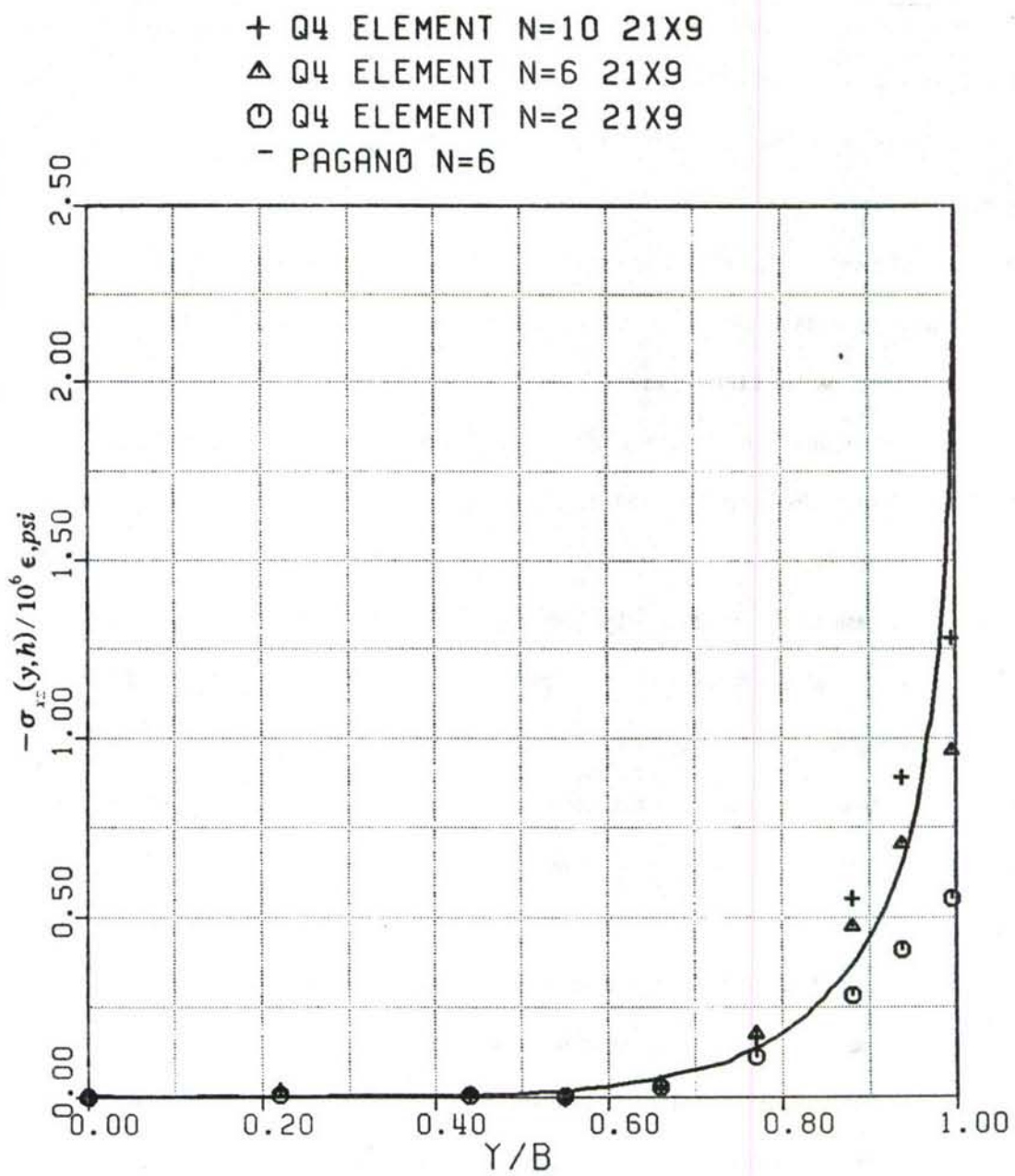


Figure 23: XZ-stress at $z=h$ with thickness refinement; Angle-ply specimen.

Comparison of accuracy for different types of elements

Accuracy of the stresses calculated using different types of elements was compared and the execution time for each case noted. Four, eight, and nine-noded elements were used. Two different mesh sizes viz. 9x9 and 21x9, with edge elements were used with four-noded elements (Fig. 6). For eight and nine-noded elements only a 9x9 mesh with 'edge elements', i.e. elements along the edge having very small dimension in the y-direction, was used. The CPU times on the Cray X-MP/28 for this set of problems are shown in Table (3). Fig. (24), for N=2, shows that the Q4 element with the 21x9 mesh predicts the axial stress at the free edge with 11.47% error as compared to the Q8 element with 11.09% and Q9 element with 10.99%. For N=6, Fig. (25), the error for the Q4 element reduced to 2.68%, for Q8 to 2.22%, and for Q9 to 2.12%. In Fig. (26), for N=10, the error for Q4 is 5.72% and for Q8 is 5.11%. Throughout, the Q4 element gives significant error near $Y/b=0$. Comparison of inplane shear stress shows that the results at the free edge are predicted with approximately same accuracy (Fig. (27) through (29)) by all the elements. In the case of τ_{xz} (Fig. (30) through (32)), Q4 with 9x9 and 21x9 mesh refinement gave practically the same results throughout the width of the specimen showing that the system is rather insensitive to refinement along the length of the specimen.

Further, Q8 and Q9 gave the same result at the free edge but were more accurate than Q4. In Fig. (33), the longitudinal displacement predicted at $X=L/2$ and the top surface of the specimen using Q8 element is shown for N=2, N=6, and N=10. In Fig. (34) and (35) corresponding results are shown for N=2 and N=6 in the case of Q9 and Q4 elements. It is seen, Fig. (33), that for N=2 the displacements are slightly overpredicted at the free edge and for N=6 and N=10 displacements are slightly underpredicted. Though the results improve with refinement from N=2 to N=6, further improvement with refinement to N=10 is not realized.

Table 3: Comparison of CPU time on X-MP/28 for Q4, Q8, and Q9 elements.

N	Element	Mesh	CPU on X-MP/28 (SEC)
2	Q4	9X9	1.82
		21X9	4.479
	Q8	9X9	16.555
		9X9	28.181
6	Q4	9X9	16.961
		21X9	40.279
	Q8	9X9	190.222
		9X9	323.116
10	Q4	9X9	60.755
		21X9	145.421
	Q8	9X9	704.333

X Q9 ELEMENT N=2 9X9
 + Q8 ELEMENT N=2 9X9
 ▲ Q4 ELEMENT N=2 21X9
 ○ Q4 ELEMENT N=2 9X9
 - PAGANO N=6

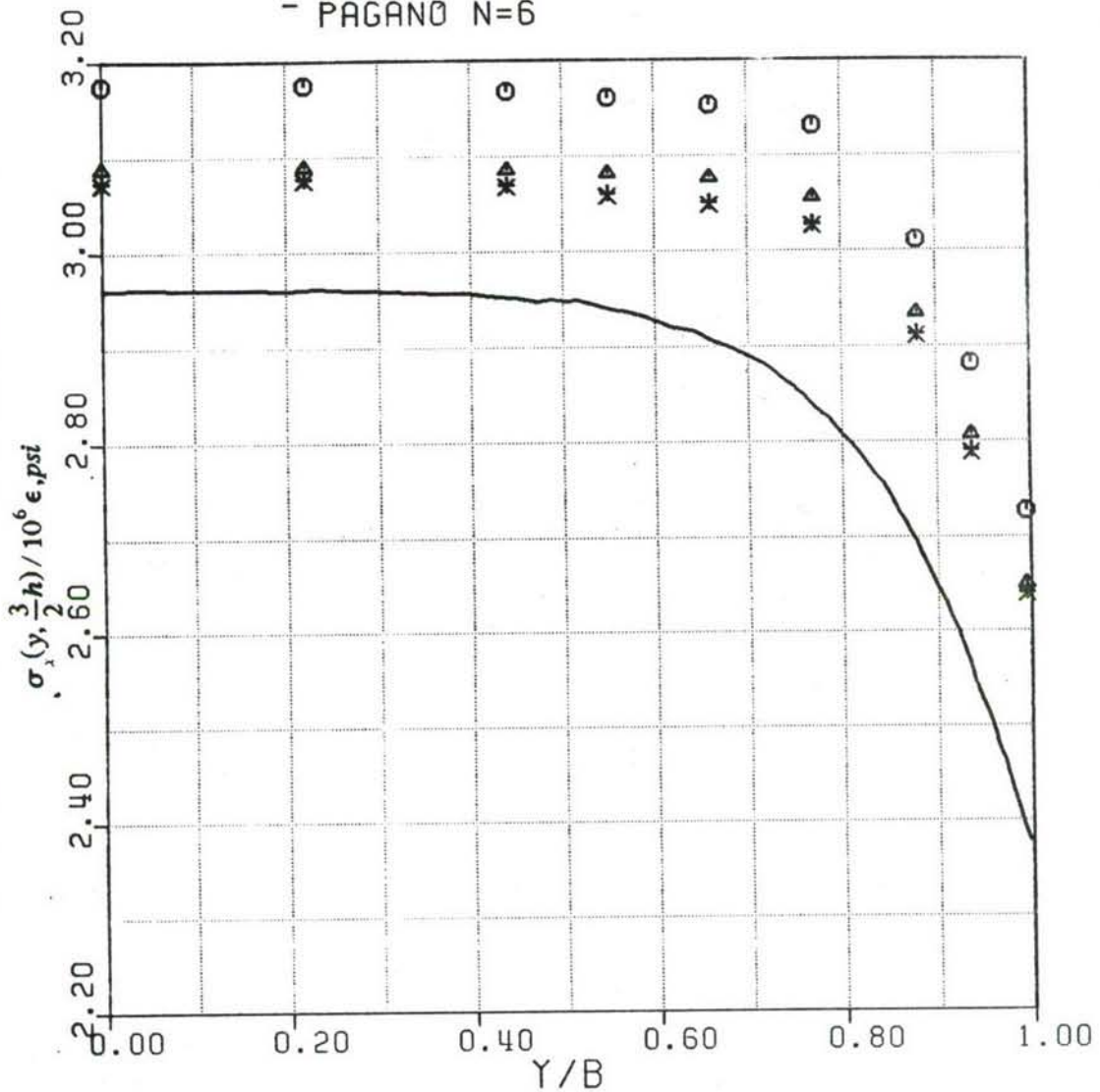


Figure 24: X-stress for N=2, Q4, Q8, and Q9 elements.

X Q9 ELEMENT N=6 9X9
 + Q8 ELEMENT N=6 9X9
 △ Q4 ELEMENT N=6 21X9
 ○ Q4 ELEMENT N=6 9X9
 - PAGANO N=6

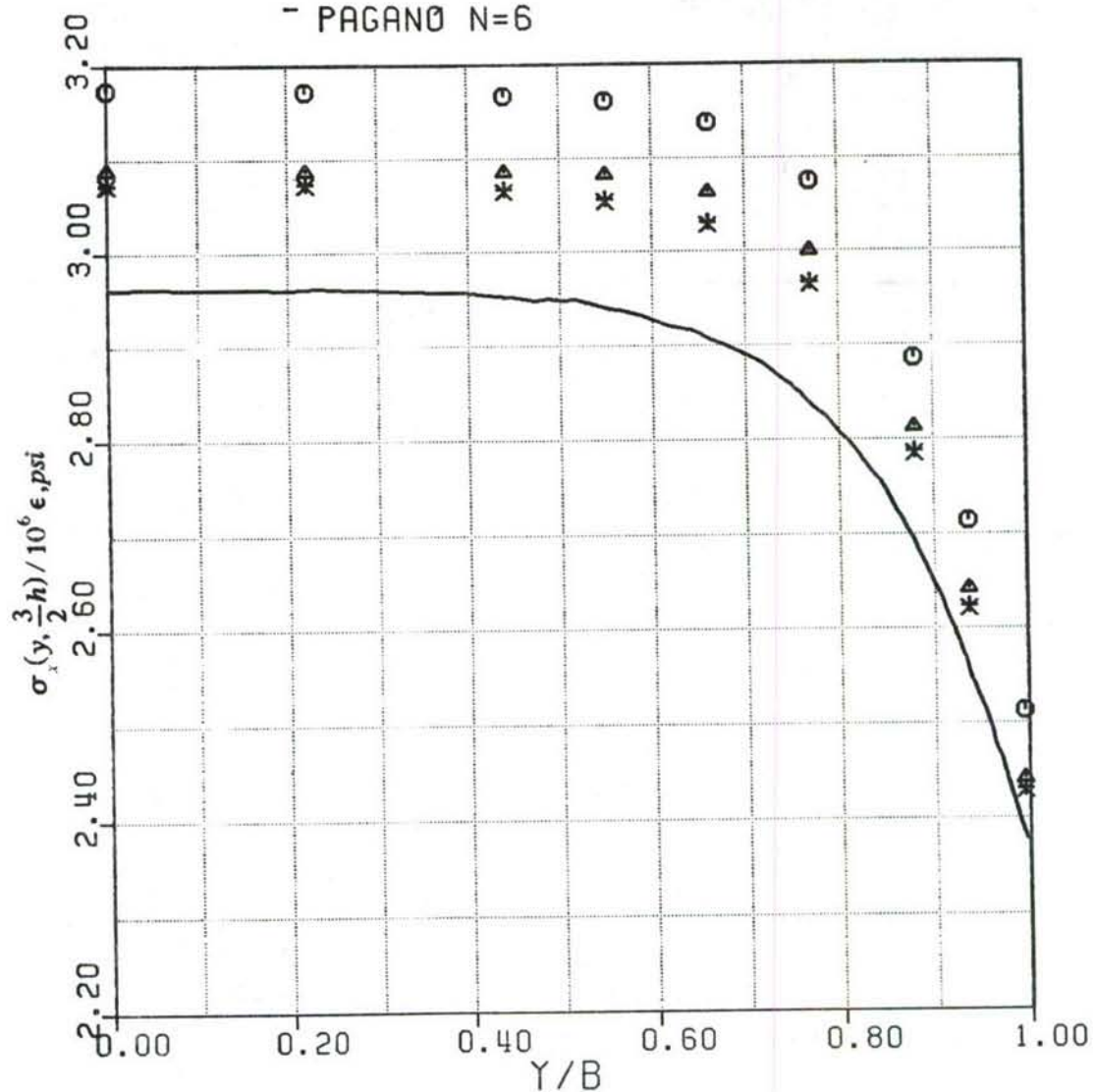
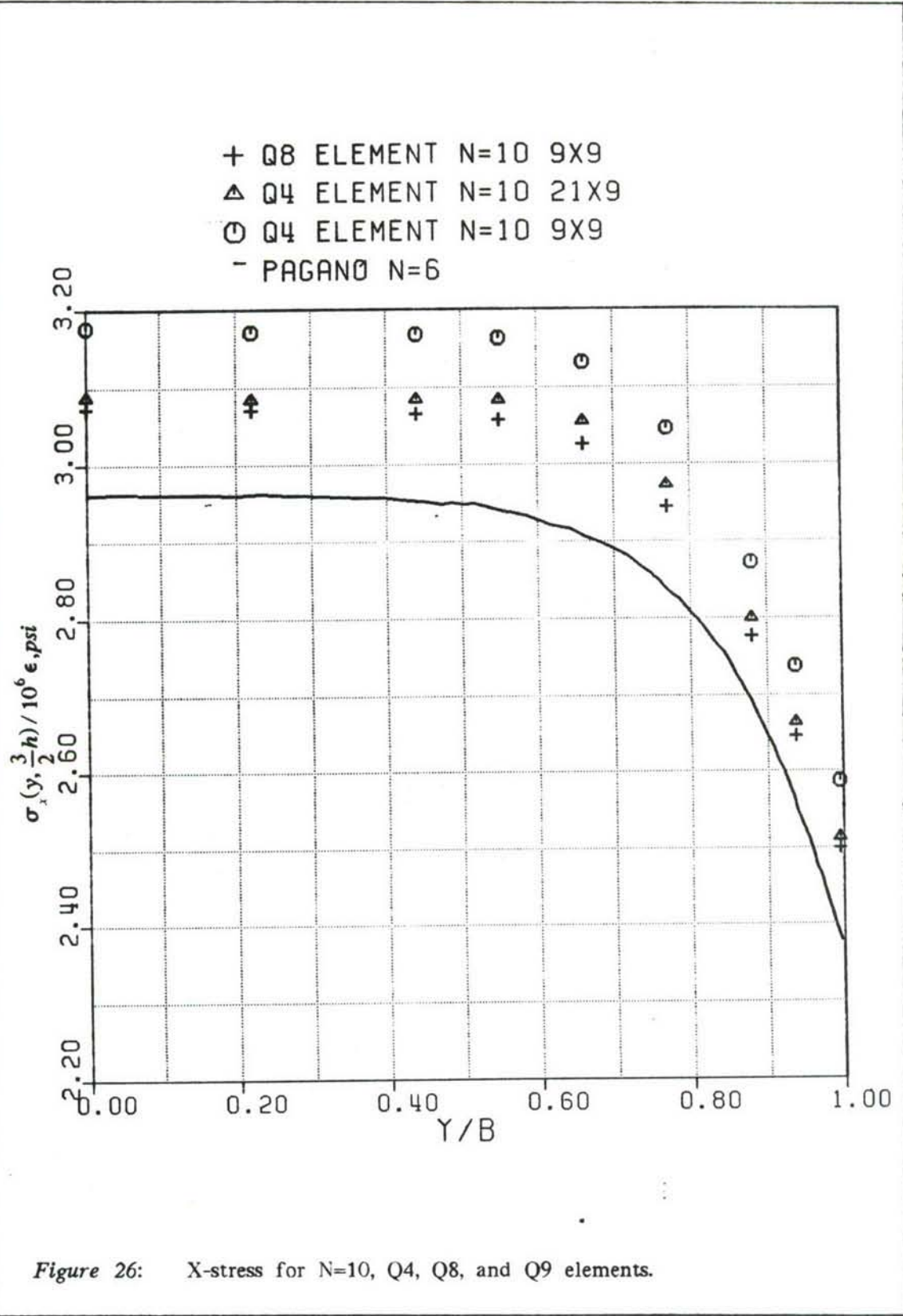


Figure 25: X-stress for N=6, Q4, Q8, and Q9 elements.



X Q9 ELEMENT N=2 9X9
 + Q8 ELEMENT N=2 9X9
 ▲ Q4 ELEMENT N=2 21X9
 ○ Q4 ELEMENT N=2 9X9
 - PAGANO N=6

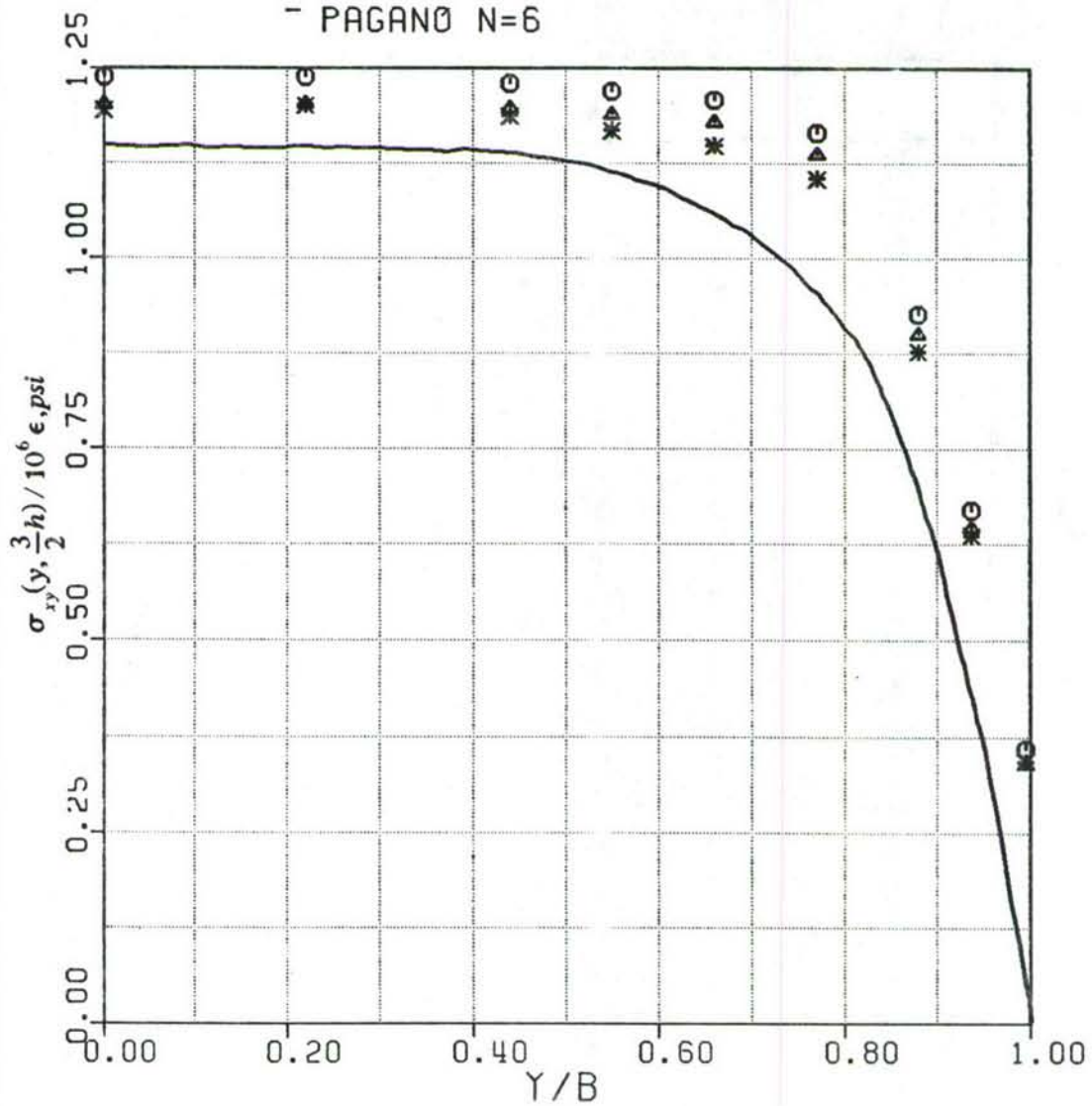


Figure 27: XY-stress for N=2, Q4, Q8, and Q9 elements.

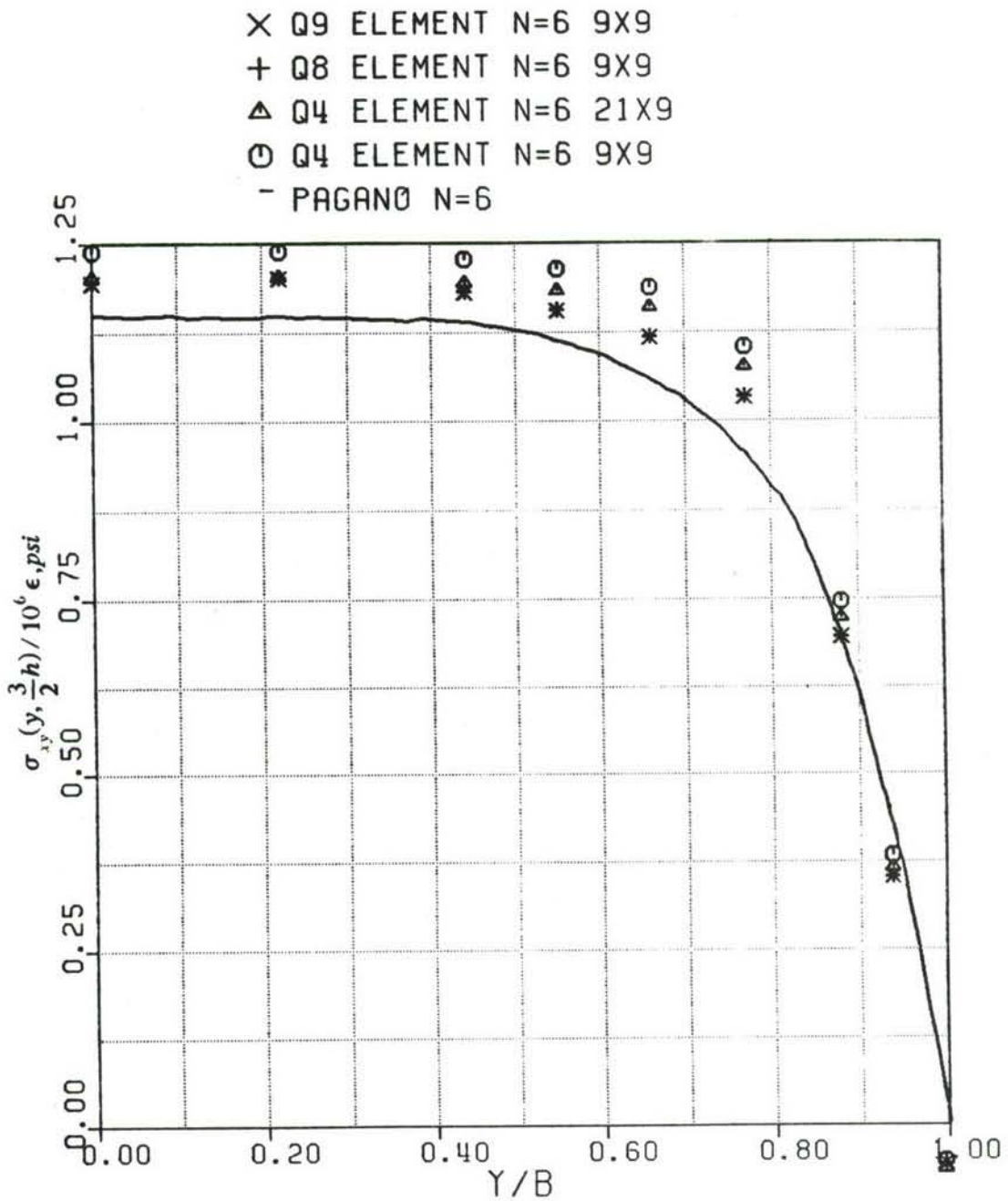


Figure 28: XY-stress for N=6, Q4, Q8, and Q9 elements.

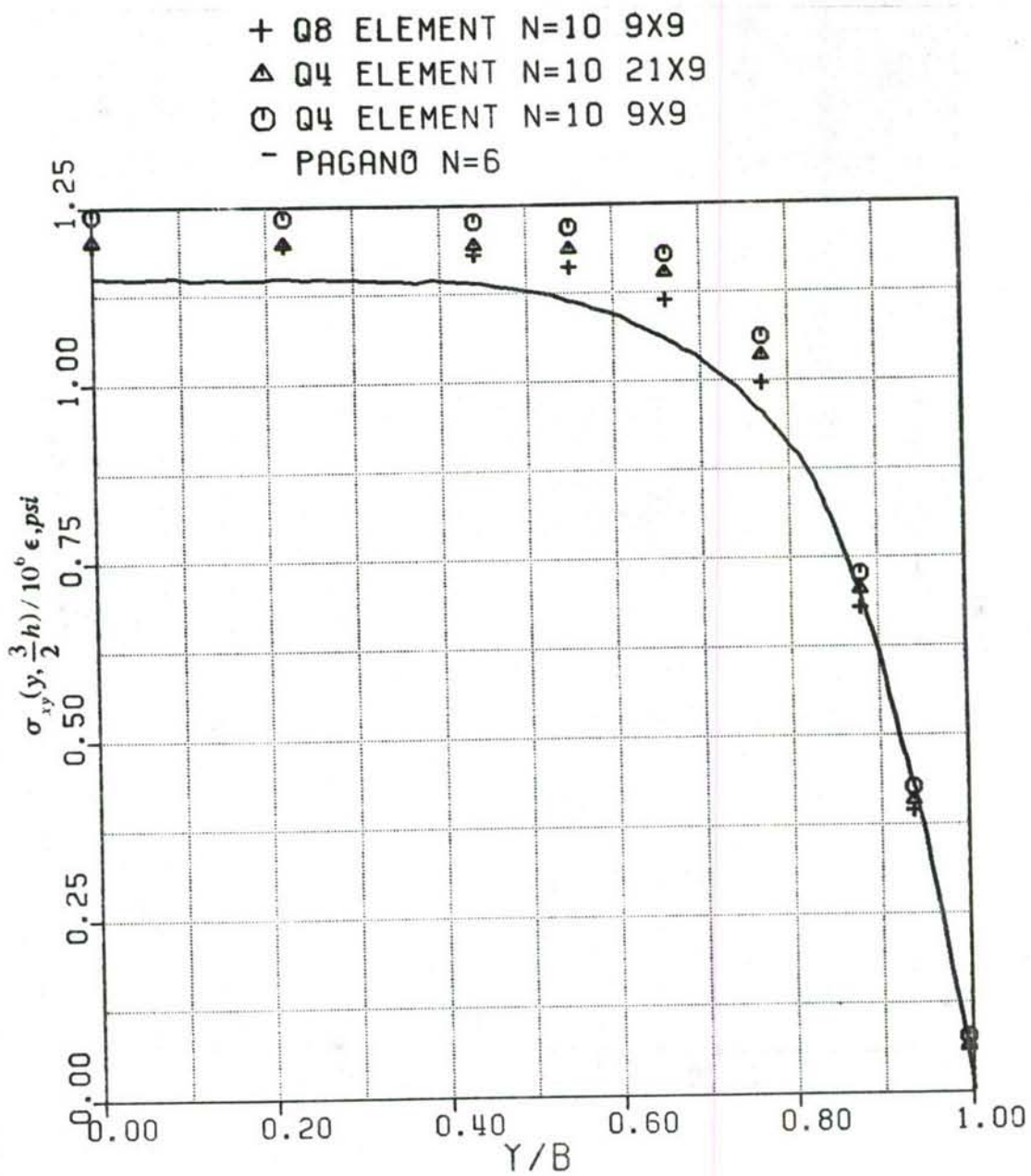


Figure 29: XY-stress for N=10, Q4, Q8, and Q9 elements.

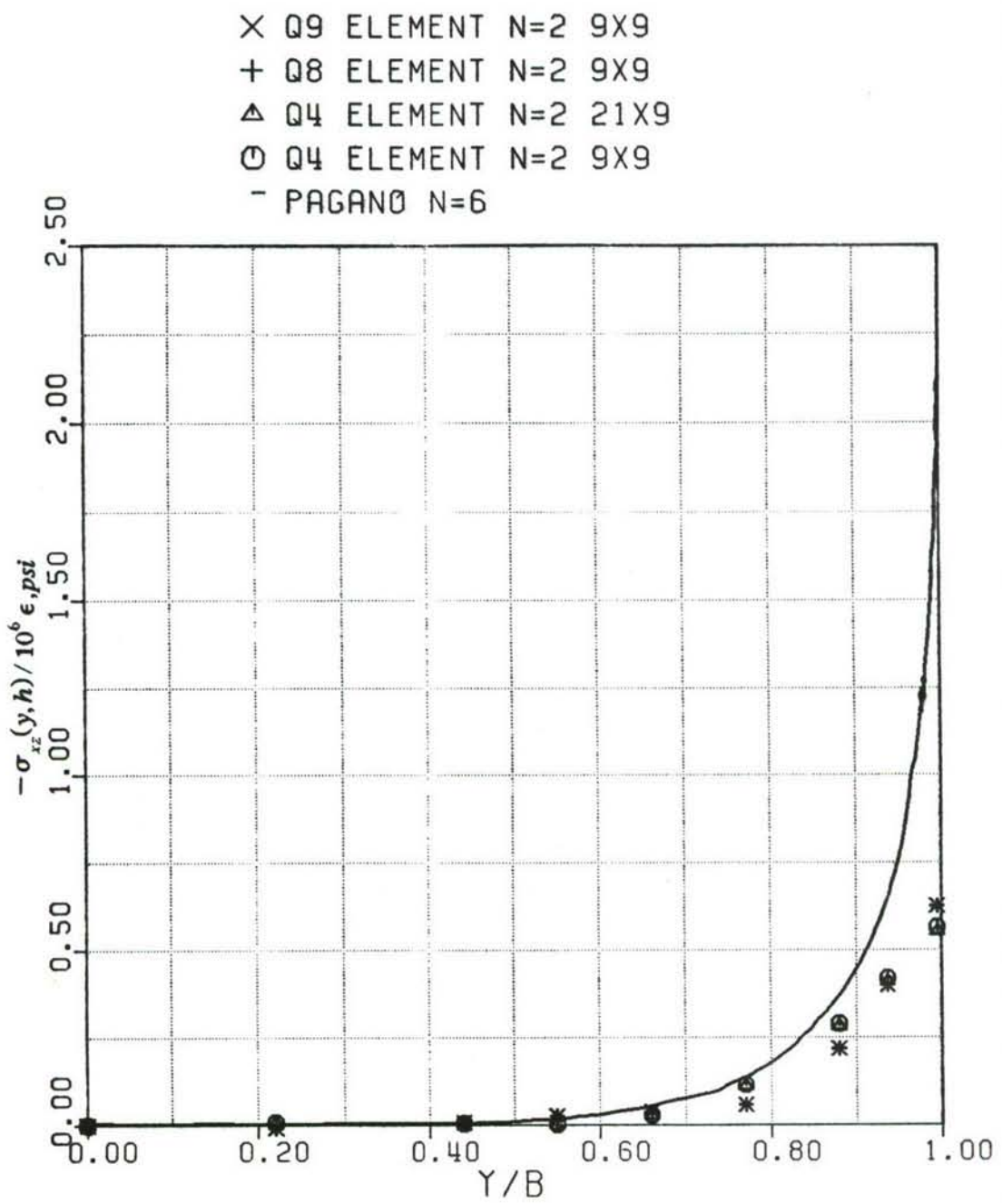


Figure 30: XZ-stress at $z=h$ for $N=2$, Q4, Q8, and Q9 elements.

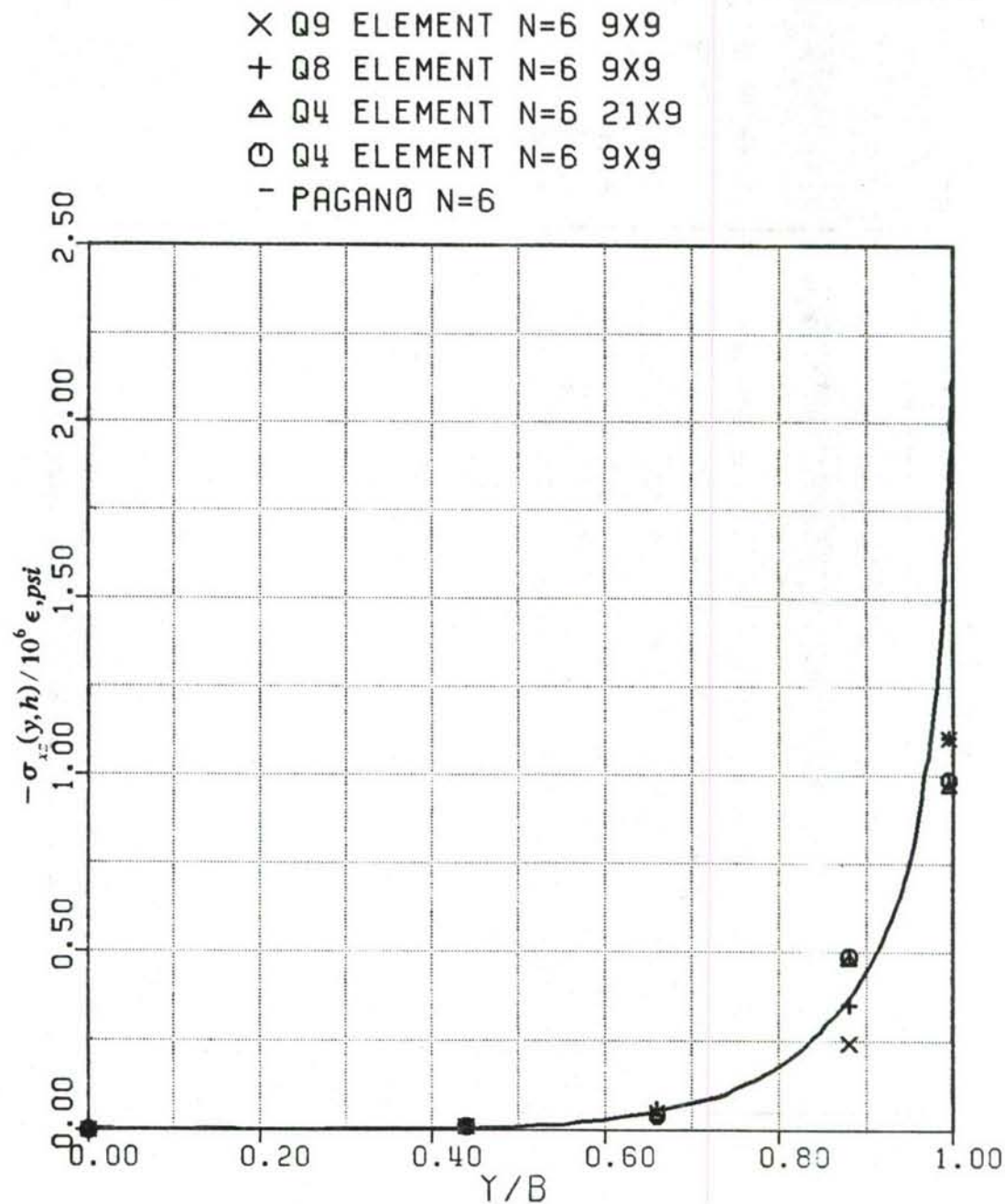


Figure 31: XZ-stress at $z=h$ for $N=6$, Q4, Q8, and Q9 elements.

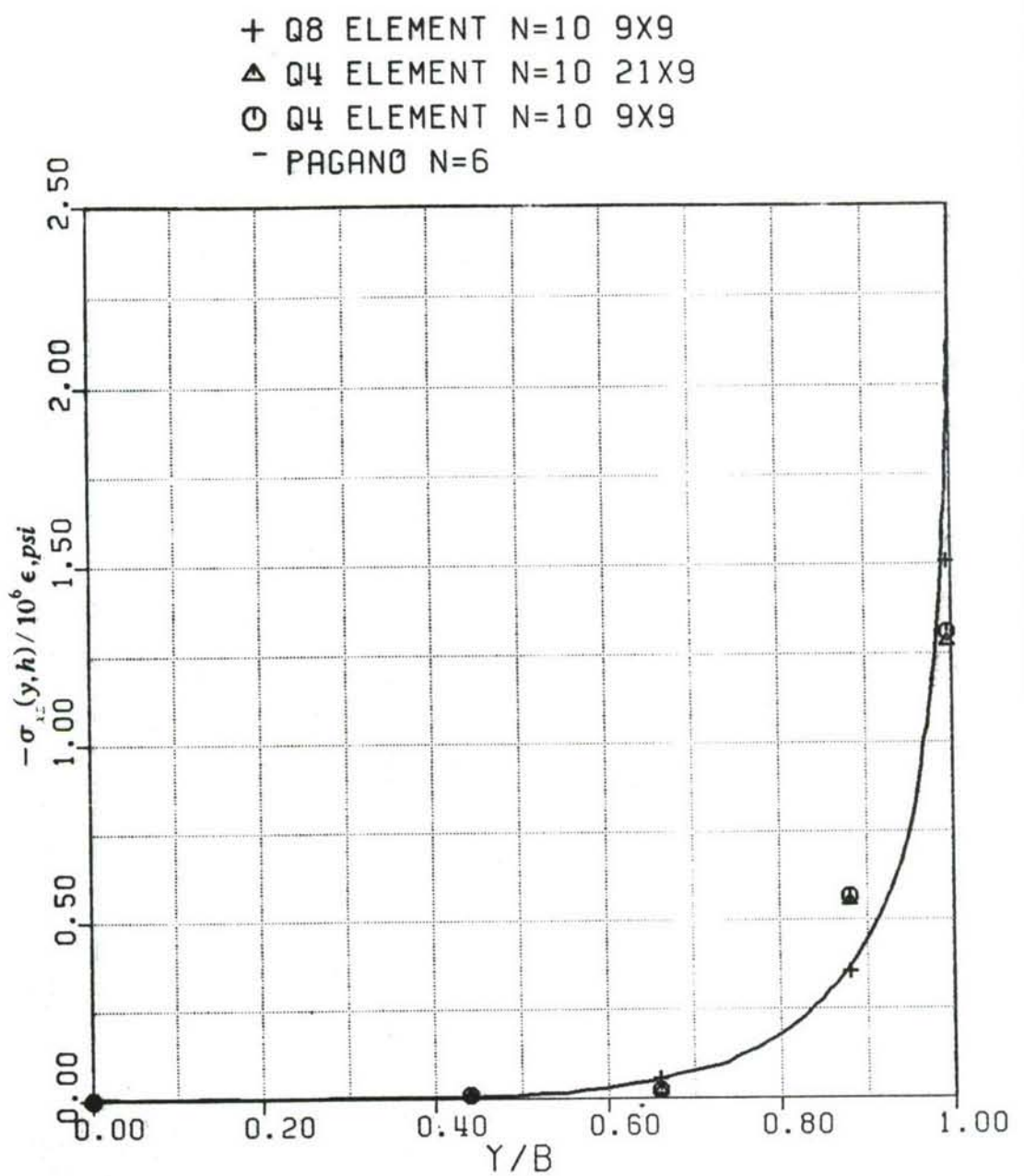


Figure 32: XZ-stress at $z=h$ for $N=10$, Q4, Q8, and Q9 elements.

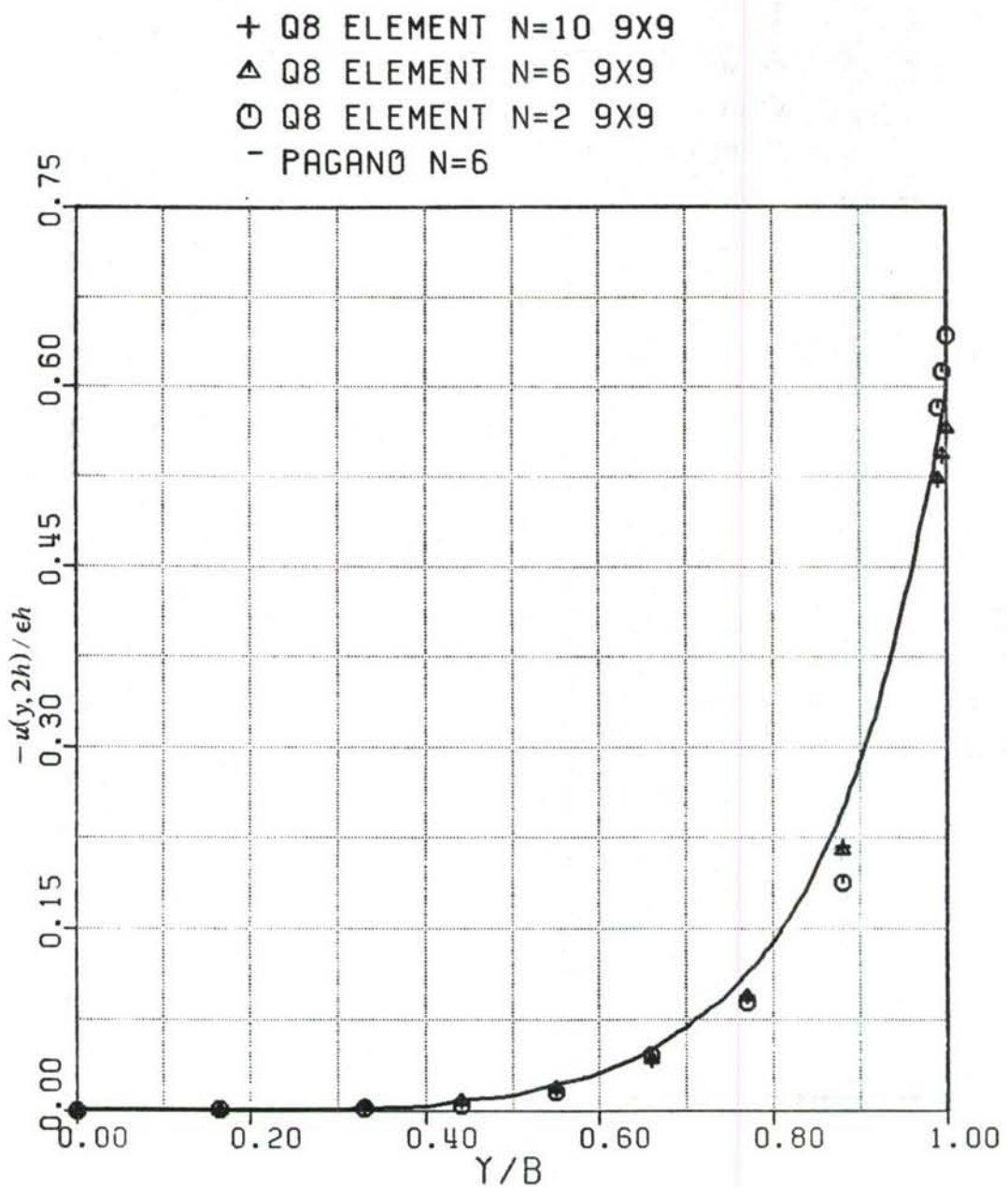


Figure 33: Longitudinal displacement at $U(L/2, y, 2h)$ of Q8 element, N=2,6 and 10.

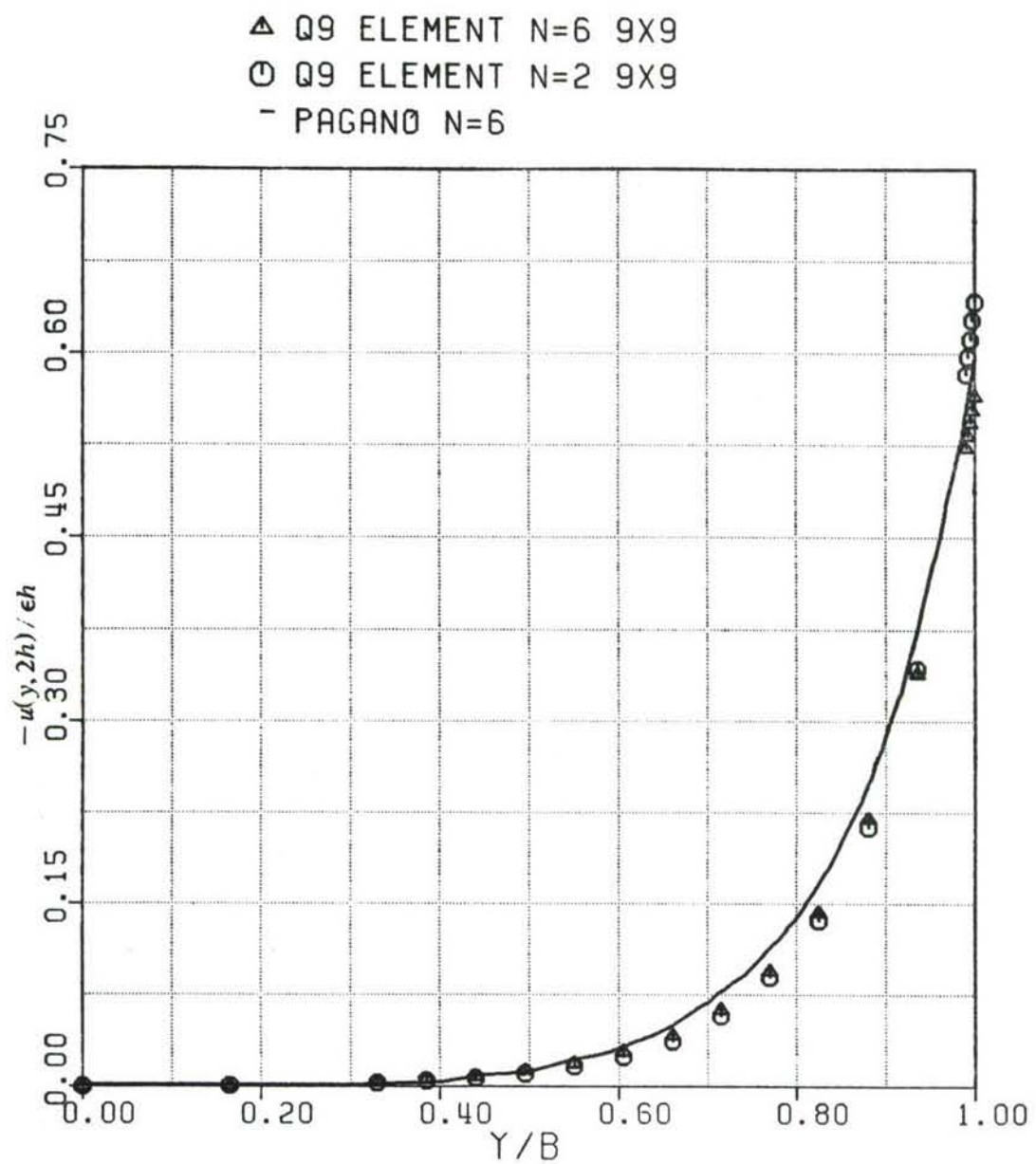


Figure 34: Longitudinal displacement at $U(L/2,y,2h)$ of Q9 element, $N=2$, and 6 .

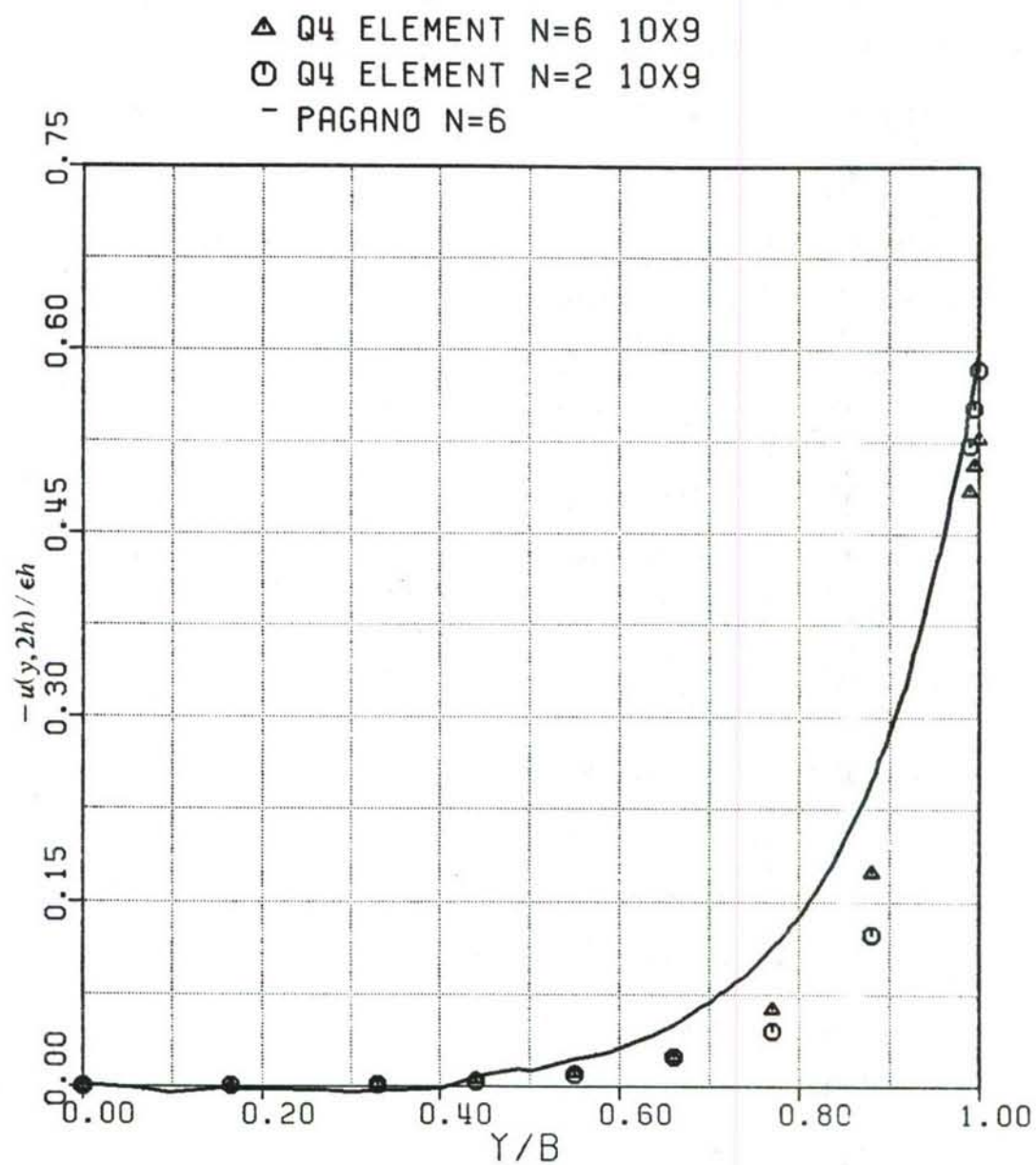


Figure 35: Longitudinal displacement at $U(L/2, y, 2h)$ of Q4 element, N=2, and 6.

ii. Cross-ply laminate [0/90]

Values of τ_{yz} and σ_{zz} were calculated for four-layer cross-ply [0/90], using equations (2.33) and (2.34) as was done in the case of τ_{xz} for the angle-ply laminate [± 45].

As shown in Fig. (36) mesh refinement in the y-direction does not lead to any noticeable improvement in the calculated values of τ_{yz} . Fig. (37) indicates that approximation of τ_{yz} is not dependent on axial refinement either. Results obtained for refinement through the thickness, Fig. (38), for 11x17 mesh, 17 being the number of elements along the y-direction, indicate that this refinement profoundly influences the results. However, the traction-free boundary condition at the free edge is not satisfied and, therefore, the solution does not match Pagano's results. The calculated values of σ_{yz} are in error up to 30% even with refinement, for y/b equal to 0.8. Near the free-edge, the error is quite large. The values of σ_{33} determined from equation (37) were either exactly zero or close to zero. This is clearly wrong and represents a serious limitation of the theory.

4.1.4 Analysis of 22-Layer Free-Edge Delamination Specimen

The procedure developed was applied to a 22-layer coupon with fiber orientation of [(25.5/-25.5)_s/90], which was previously solved by Chang [11] and Dandan [12]. The laminate width and ply thickness were taken as 1.0 inch and 0.00505 inch, respectively. The material properties of a lamina were the same as used in previous investigations [11], [12].

$$E_{11} = 19.26 * 10^6 \text{ (psi)}$$

$$E_{22} = E_{33} = 1.32 * 10^6 \text{ (psi)}$$

$$G_{12} = G_{13} = G_{23} = 0.83 * 10^6 \text{ (psi)}$$

$$\nu_{12} = \nu_{13} = \nu_{23} = 0.35$$

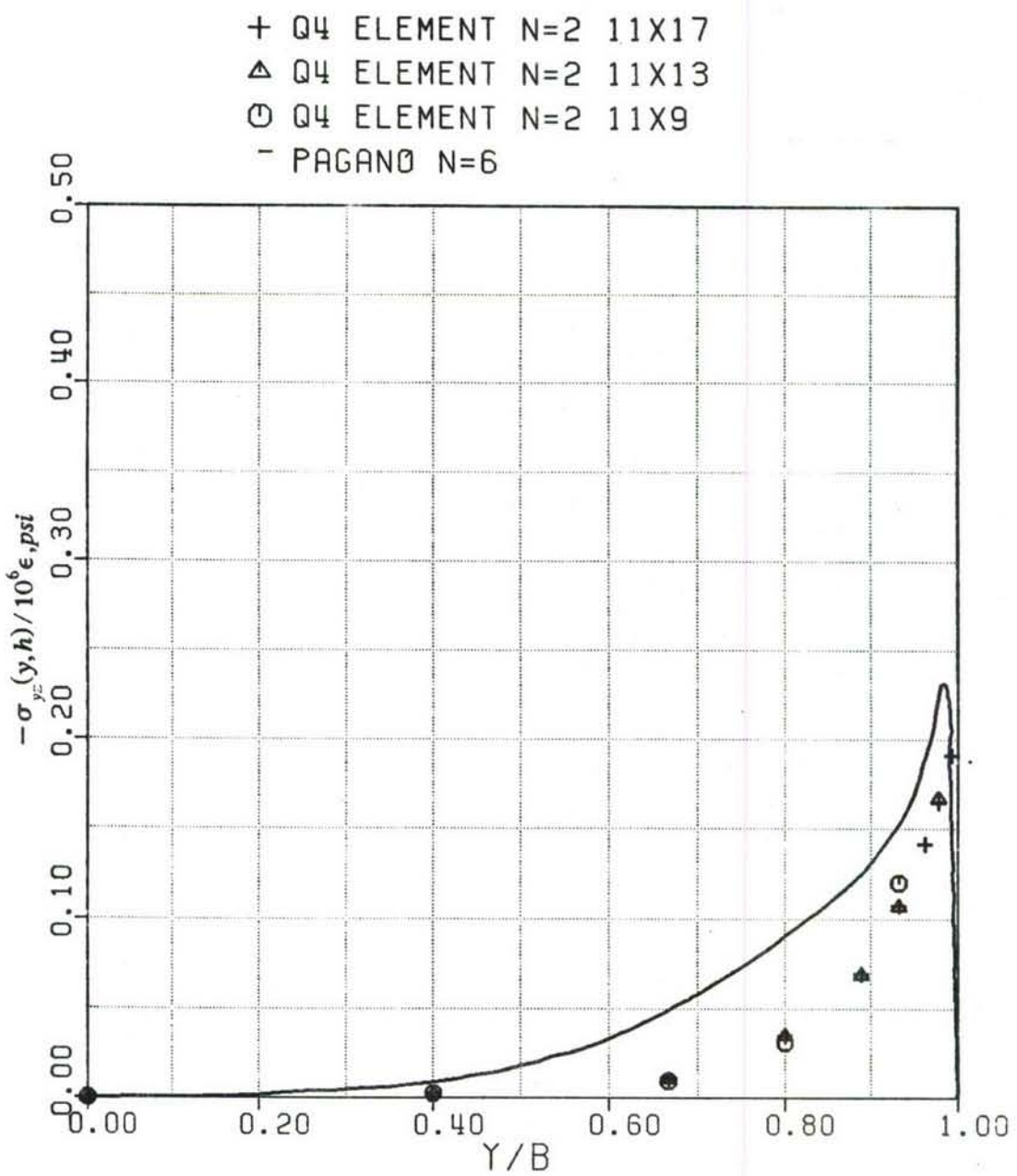


Figure 36: YZ-stress at $z=h$ with mesh refinement in y -direction; Cross-ply specimen.

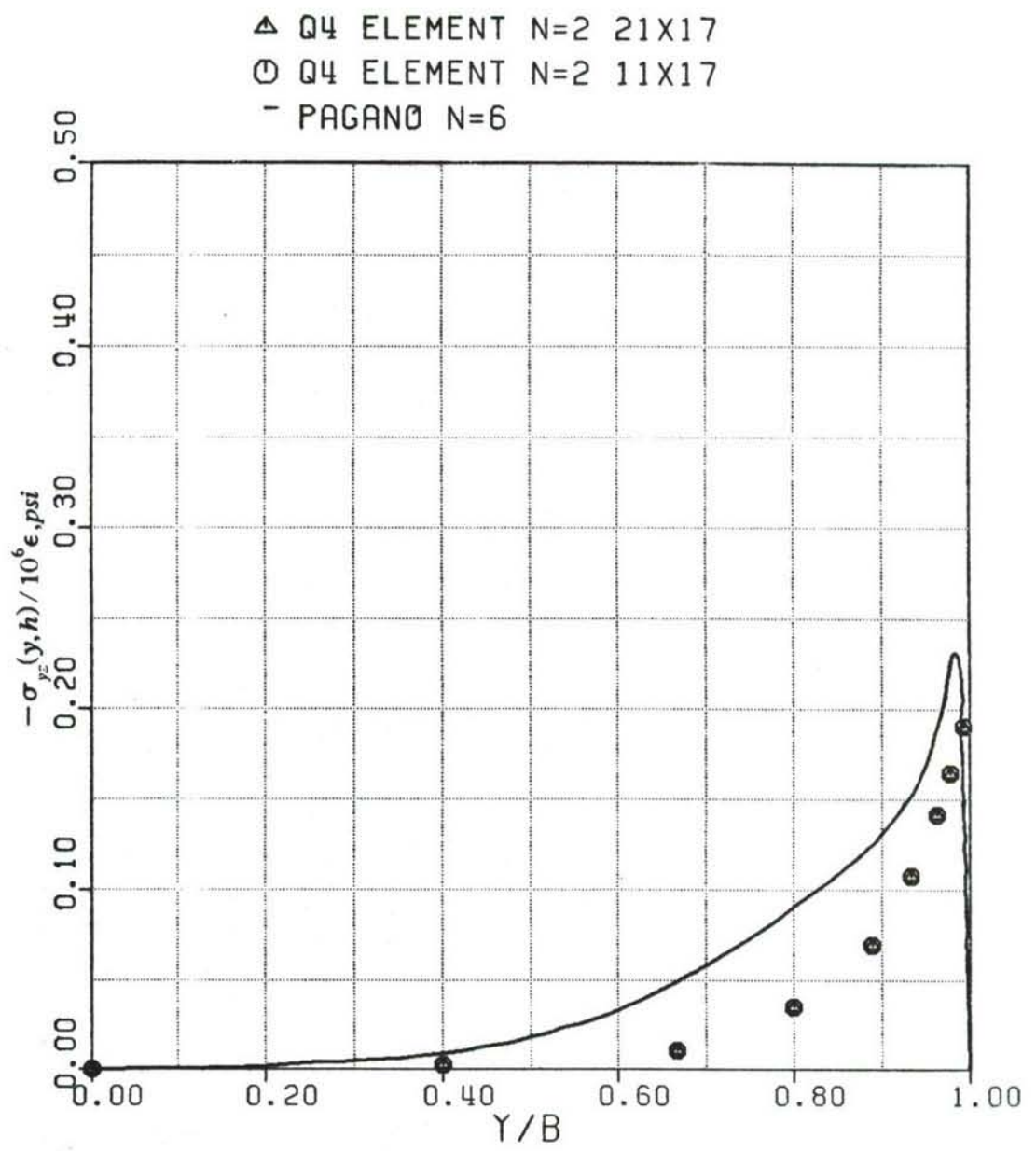


Figure 37: YZ-stress at $z=h$ with mesh refinement in x-direction; Cross-ply specimen.

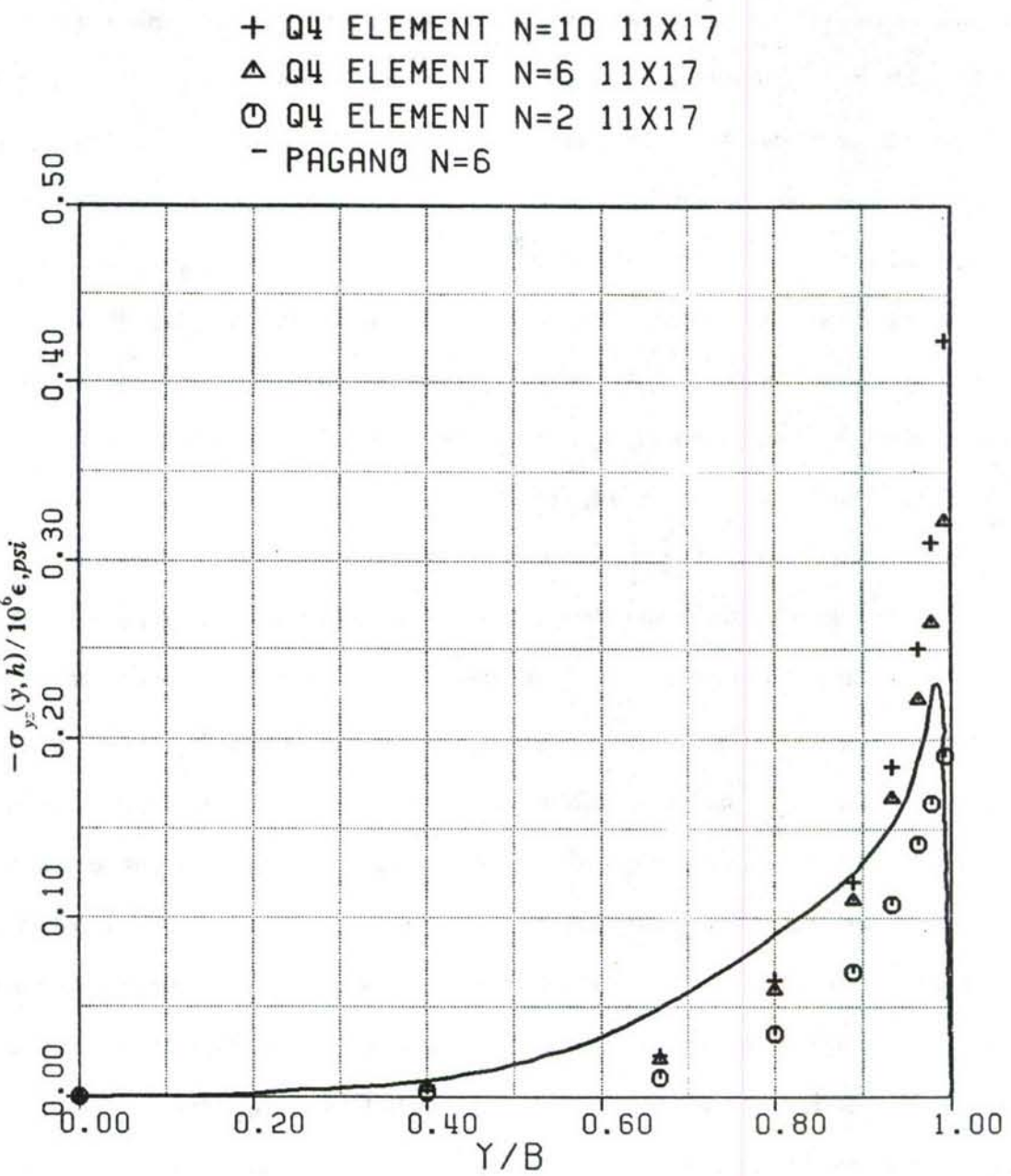


Figure 38: YZ-stress at $z=h$ for (11x17) mesh in case of $N=2$, $N=6$, and $N=10$; Cross-ply specimen.

Due to the symmetry of the laminate, it was only necessary to consider 11 lamina in the analysis. Based on the analysis performed on the four-layer coupon specimen, it was concluded that refinement along the x-direction improves the accuracy of the results more effectively than the refinement along the y-direction. For this reason, the 22-layer specimen was discretized into 22 elements in the x-direction and 13 in the y-direction. All elements have the same dimensions in the x-direction. However, in the y-direction, the edge elements have a width of 0.005 inch, with the remaining portion discretized shown in Fig. (6). The formulations in [11] and [12] were based on a two-dimensional model dependent on y- and z- coordinates only. In [12], 22 elements were used in the z-direction and 14 in the y-direction. In the present investigation, the discretization is along the x- and y-coordinates. Therefore, it was not feasible to match the mesh with that used in [11] and [12].

To compare the results with those given in [12] and [11], two different analyses were performed. In [12] the results are given at the center of each layers. In the present investigation, $\sigma_{\alpha\beta}$ components are calculated at the centers of the laminae, and based upon the effectiveness of the refinement over the thickness noticed in the analysis of the four-layer specimen, each layer is divided into three sublayers, forming a total of 33 layers. σ_3 is calculated at the interface in the present investigation. However, in order that these results be comparable to those obtained in [12] and [11] at the center of the lamina, each layer must be subdivided into two sublayers, forming a total of 22 layers, producing the necessary interfaces. An average axial strain of (0.95414×10^{-5}) was applied, which is the same as applied by Chang [11].

Fig. (39) shows the cross-section of the upper half of the symmetric laminate and defines the location for plotting of results. Fig. (40) and Fig. (41) show the distribution of σ_y along the center of the 11th and the 5th layer for different (y/B) ratios. The results obtained from FSDT match those obtained from the higher order

element [11] and the axisymmetric model [12]. Similarly, Fig. (42) shows that σ_x at the center of the 11th layer can be obtained accurately, though the concentration of the stress at the free-edge does not match that obtained by the higher order element [11]. Distribution of σ_{xy} along R_{11} , as shown in Fig. (43), closely follows the result given in [11]. However, the σ_{xz} stresses determined from the FSDT are in considerable error near the free edge. Figs. (44) to (47) show the plots for σ_{xz} along R1, R5, R6, R11, and Figs. (48) to (50) indicate the σ_{yz} along R5, R6, and R11. It is evident that both σ_{xz} and σ_{yz} are predicted reasonably well by the FSDT in the regions $y/B < 0.7$. However, for $y/B > 0.9$, the predicted stresses for σ_{xz} even result in signs different from those in [11]. Results for σ_{yz} do not satisfy the free-edge stress at $y/B = 1.0$. Figures (51) through (53) show the through-the-thickness distribution of σ_{zz} , σ_{xz} , and σ_{yz} along the free-edge. The results from the FSDT do not agree with those from [11] and [12] and are, apparently, quite wrong. Furthermore, Figs. (54) to (57) show the distribution of σ_{zz} along R1, R5, R6, and R11. The stress distribution obtained from the present approach is quite different from that given by [12].

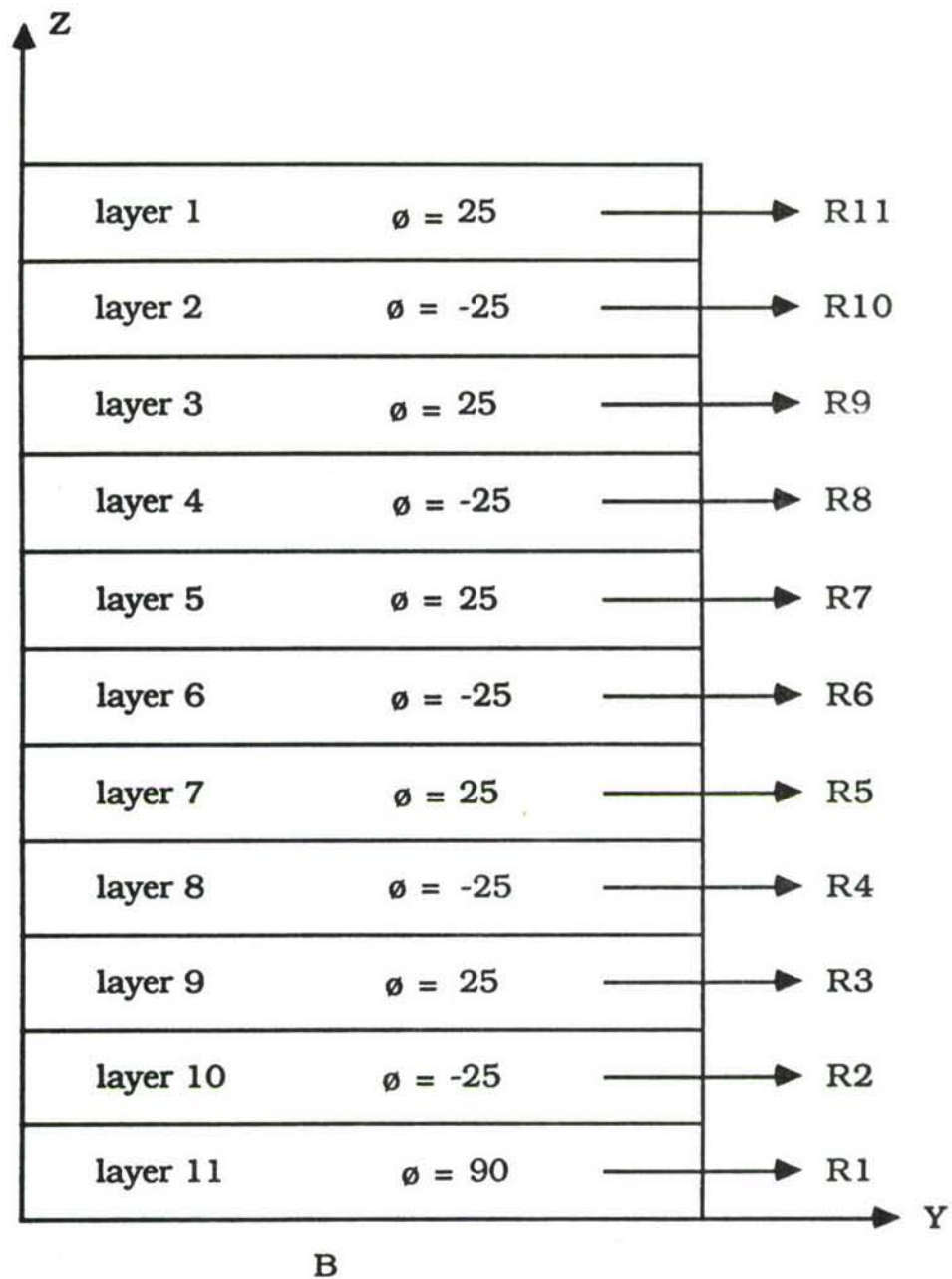


Figure 39: Cross-section of the upper half of the 22-layer coupon.

22 LAYERS Y STRESS AT R1

Δ 23X13 N=33
 - CHANG
 O DANDAN

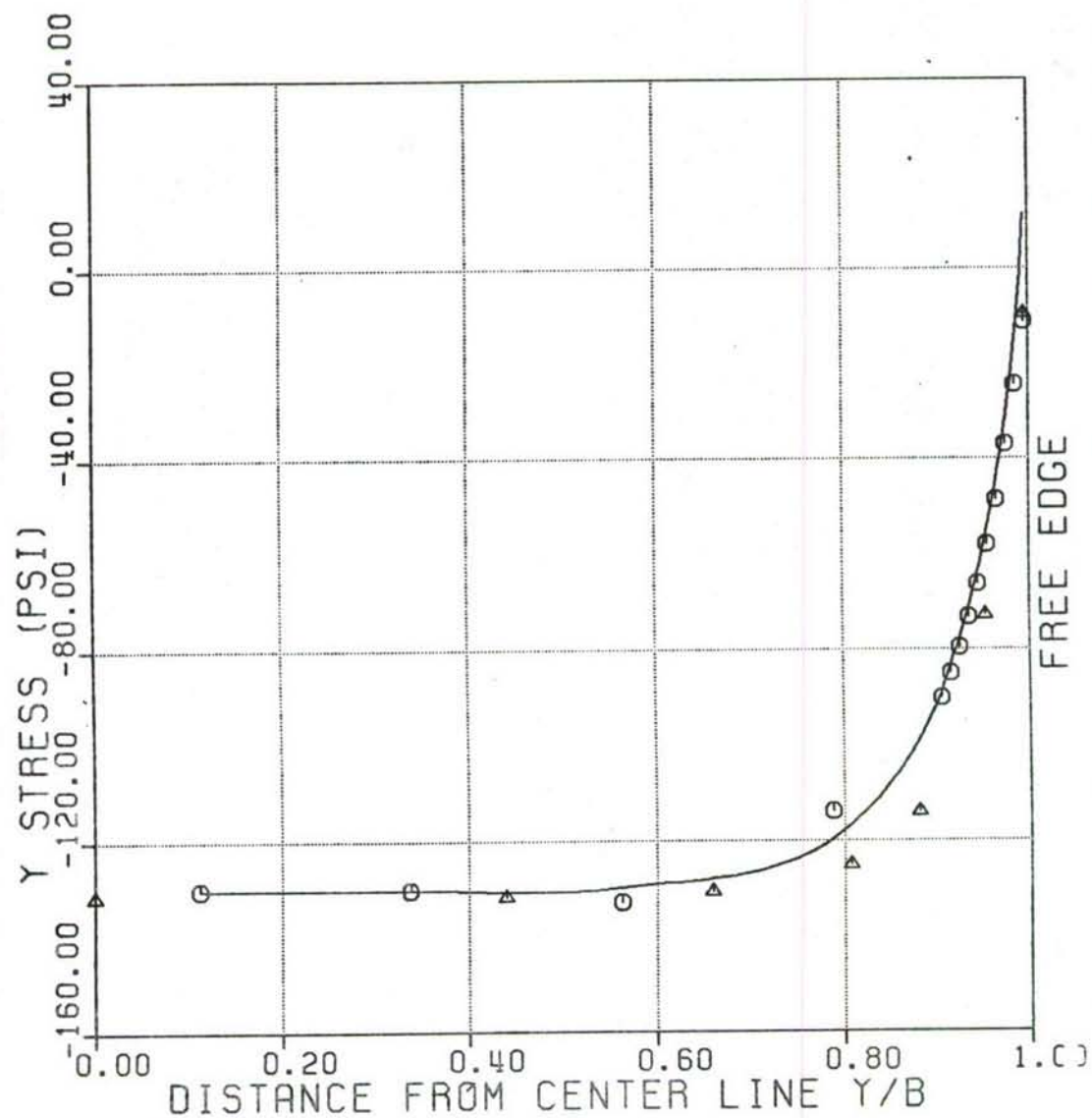


Figure 40: Y-stress at R1 for 22-layer coupon.

22 LAYERS Y STRESS AT R5

▲ 23X13 N=33
 - CHANG
 ○ DANDAN

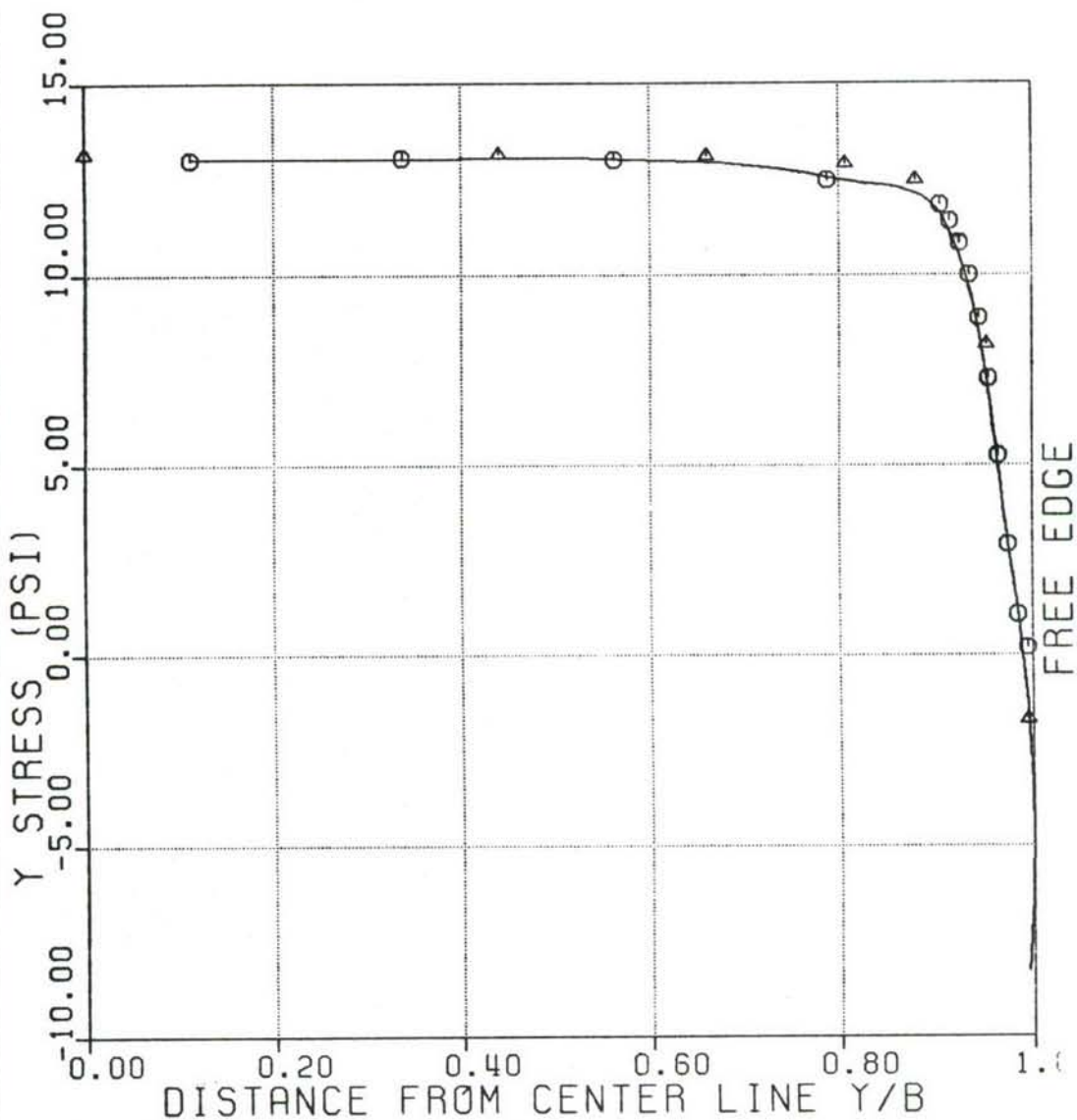


Figure 41: Y-stress at R5 for 22-layer coupon.

22 LAYERS X STRESS AT R1

▲ 23X13 N=33
 - CHANG
 ○ DANDAN

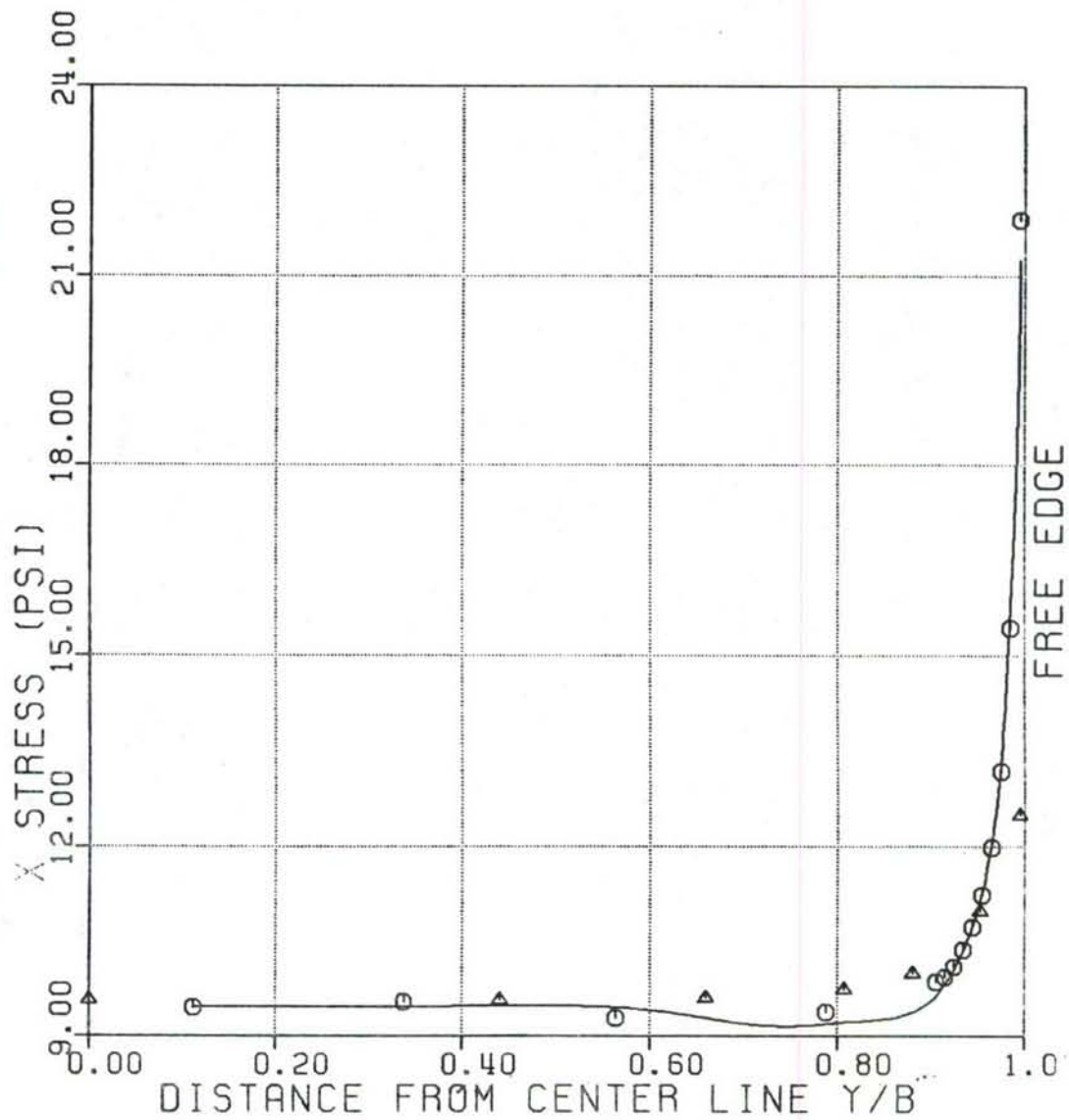


Figure 42: X-stress at R1 for 22-layer coupon.

22 LAYERS XY STRESS AT R11

▲ 23X13 N=33
 - CHANG
 ○ DANDAN

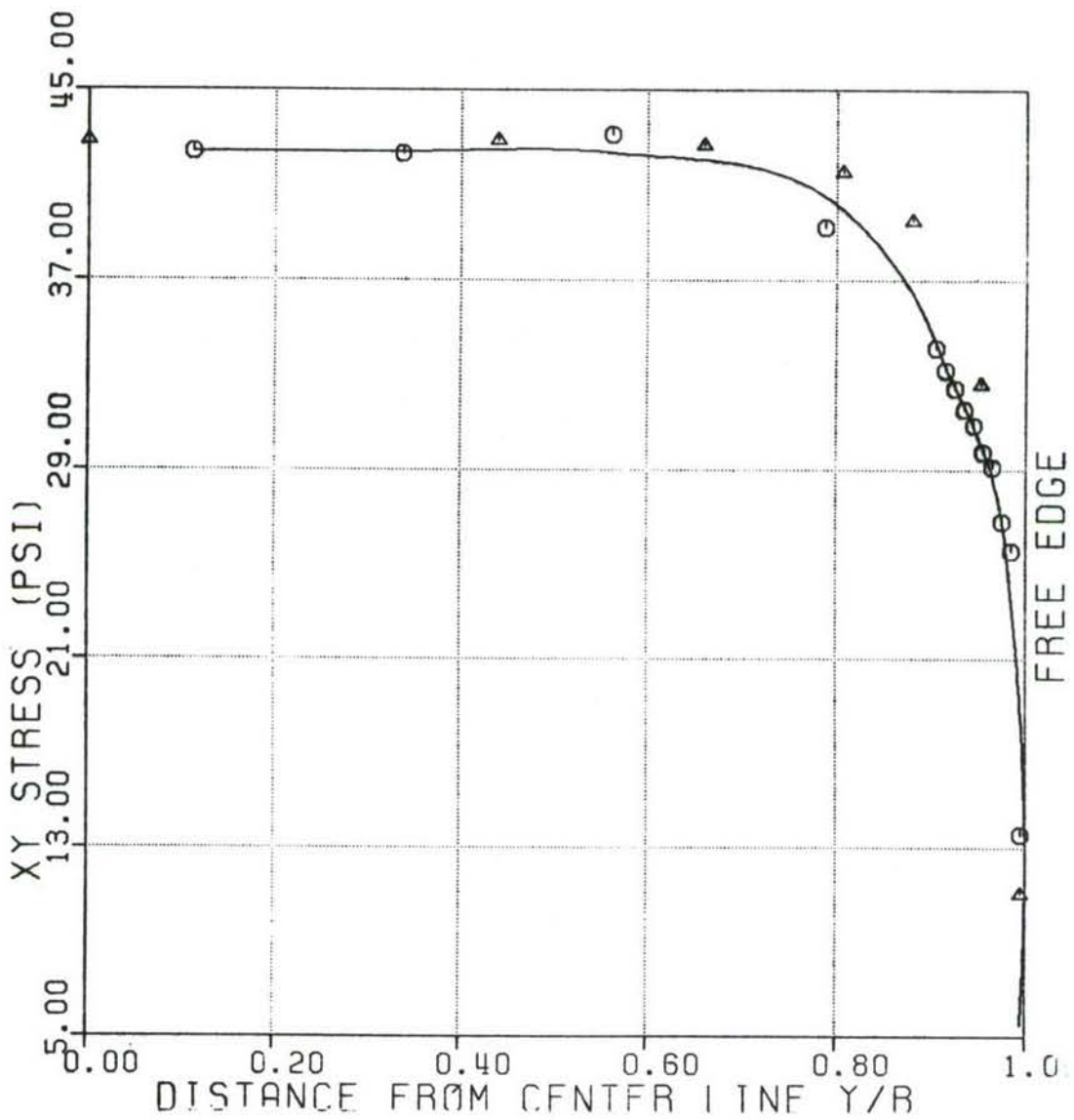


Figure 43: XY-stress at R11 for 22-layer coupon.

22 LAYERS XZ STRESS AT R1

△ 23X13 N=22

- CHANG

○ DANDAN

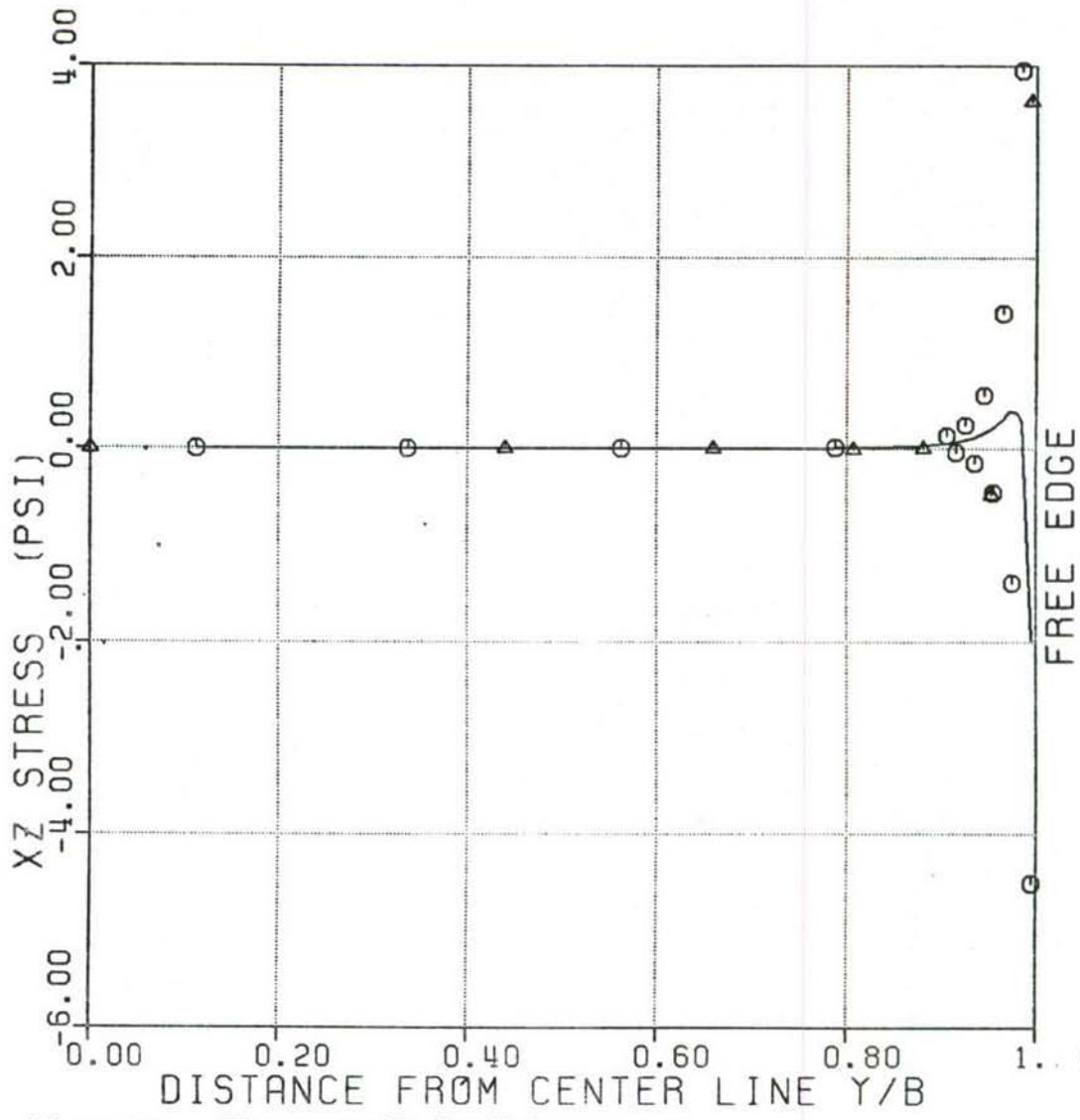


Figure 44: ZX-stress at R1 for 22-layer coupon.

22 LAYERS XZ STRESS AT R5

▲ 23X13 N=22
 - CHANG
 ○ DANDAN

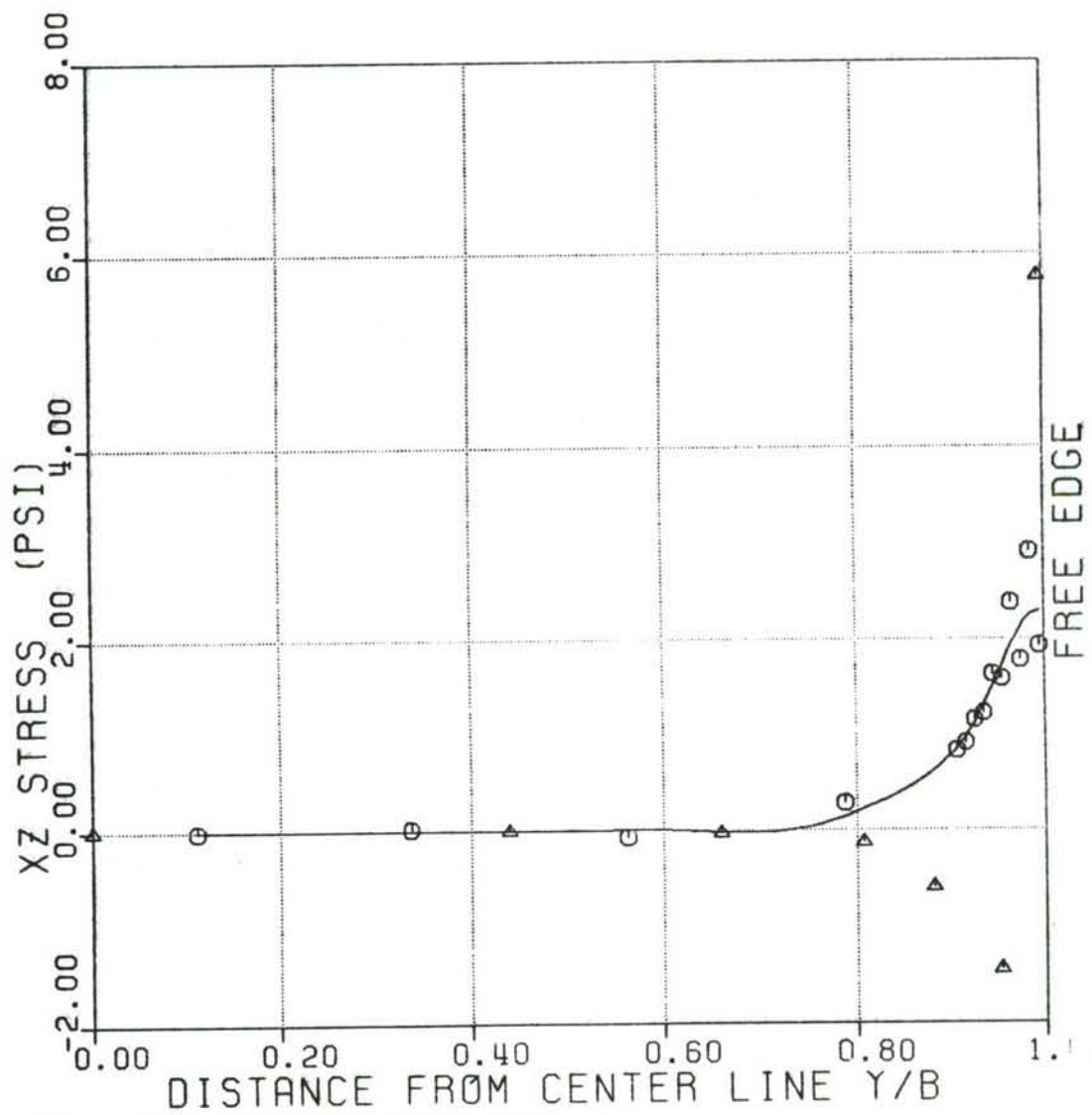


Figure 45: ZX-stress at R5 for 22-layer coupon.

22 LAYERS XZ STRESS AT R6

Δ 23X13 N=22
 - CHANG
 O DANDAN

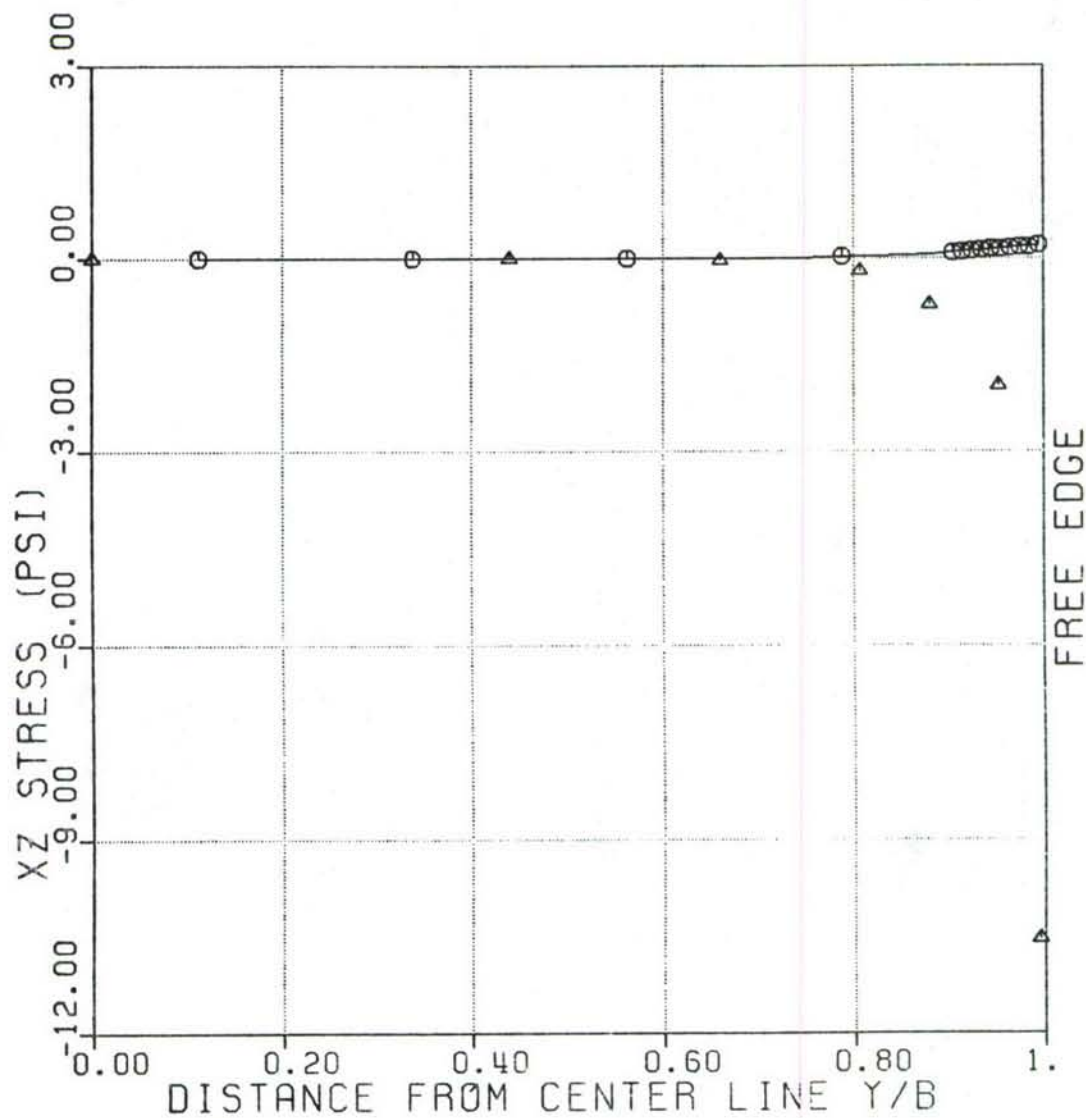


Figure 46: ZX-stress at R6 for 22-layer coupon.

22 LAYERS XZ STRESS AT R11

△ 23X13 N=22
 - CHANG
 ○ DANDAN

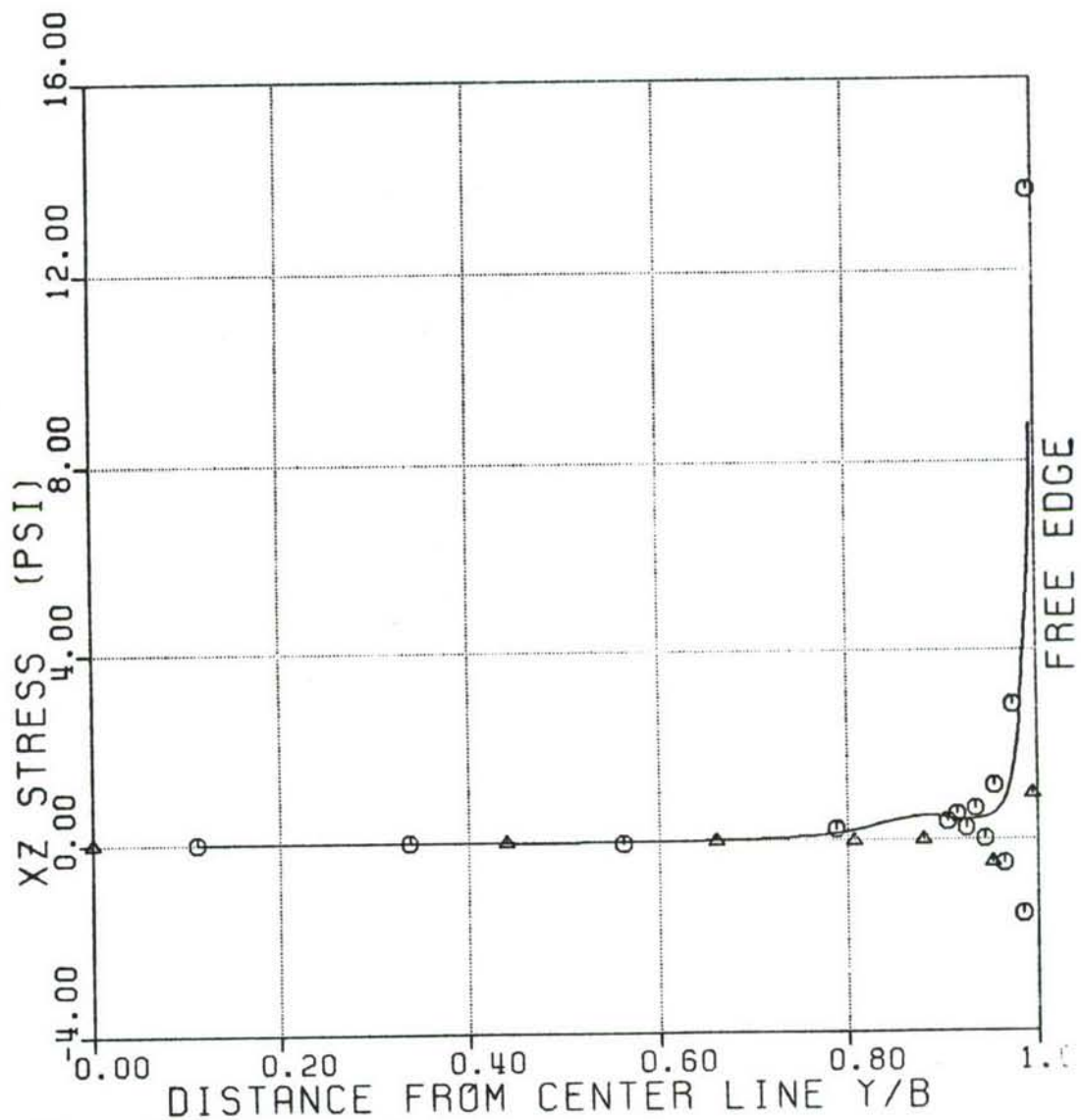


Figure 47: ZX-stress at R11 for 22-layer coupon.

22 LAYERS YZ STRESS AT R5

Δ 23X13 N=22
 - CHANG
 O DANDAN

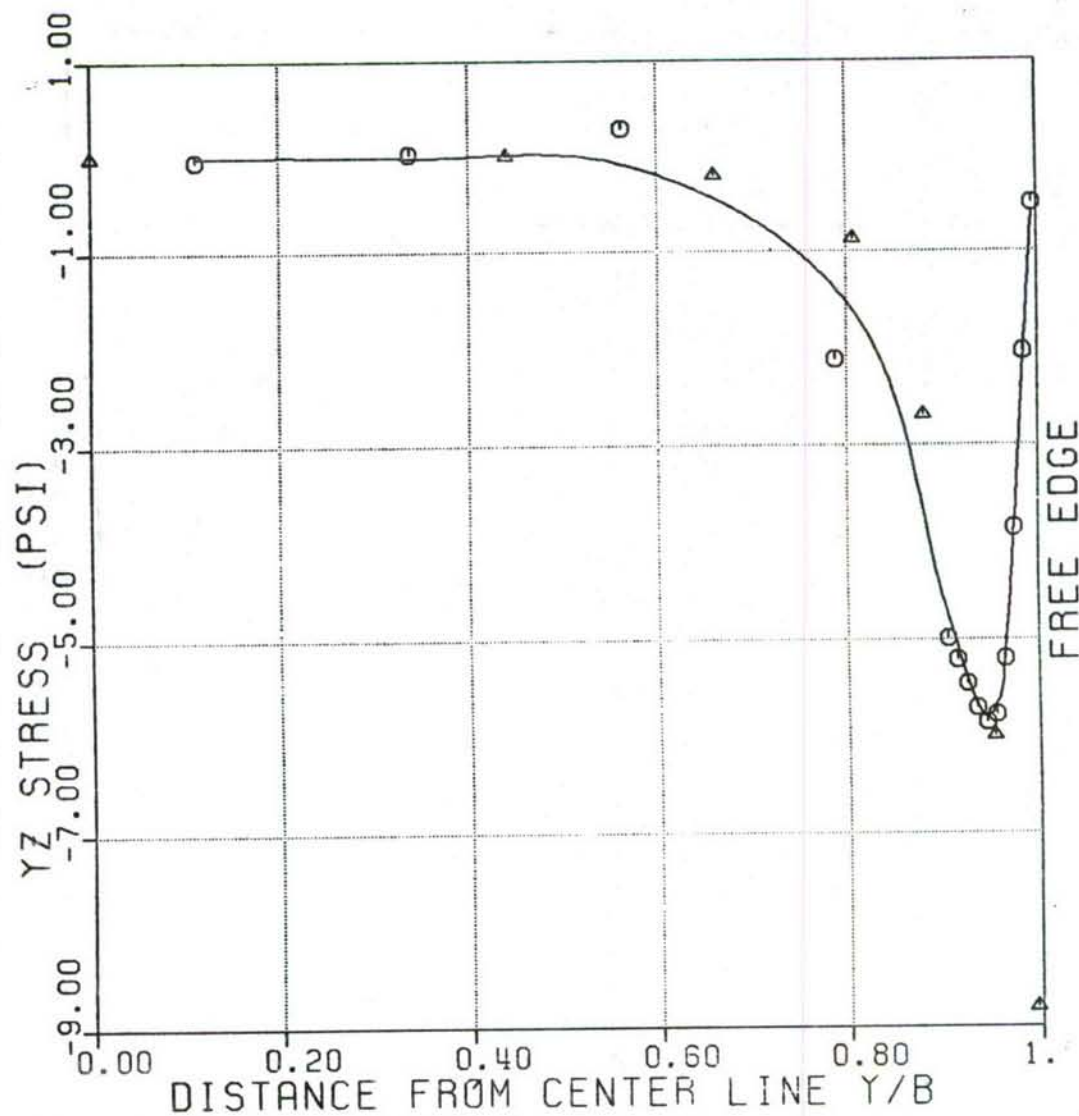


Figure 48: YZ-stress at R5 for 22-layer coupon.

22 LAYERS YZ STRESS AT R6

▲ 23X13 N=22
 - CHANG
 ○ DANDAN

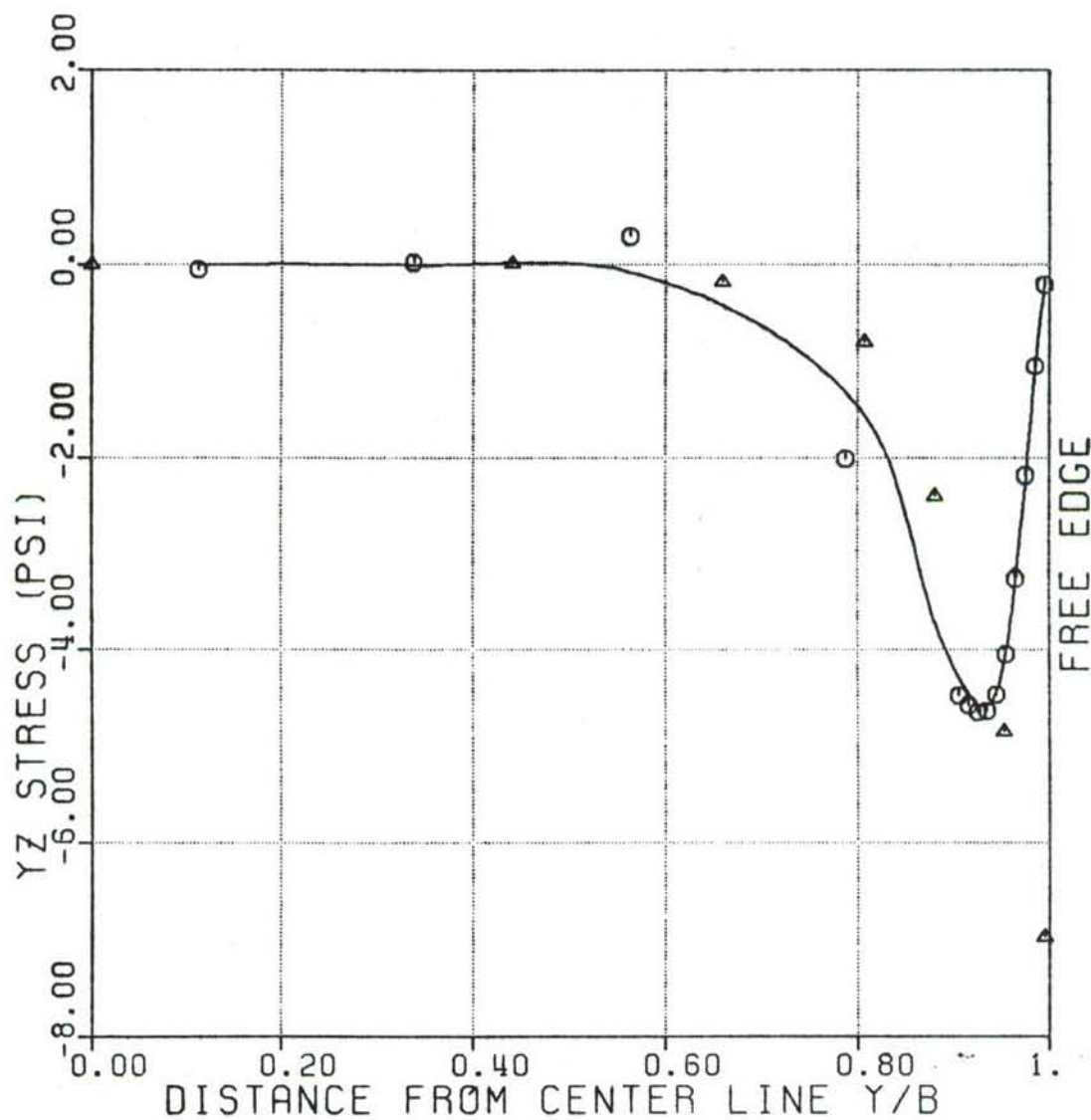


Figure 49: YZ-stress at R6 for 22-layer coupon.

22 LAYERS YZ STRESS AT R11

Δ 23X13 N=22
 - CHANG
 \circ DANDAN

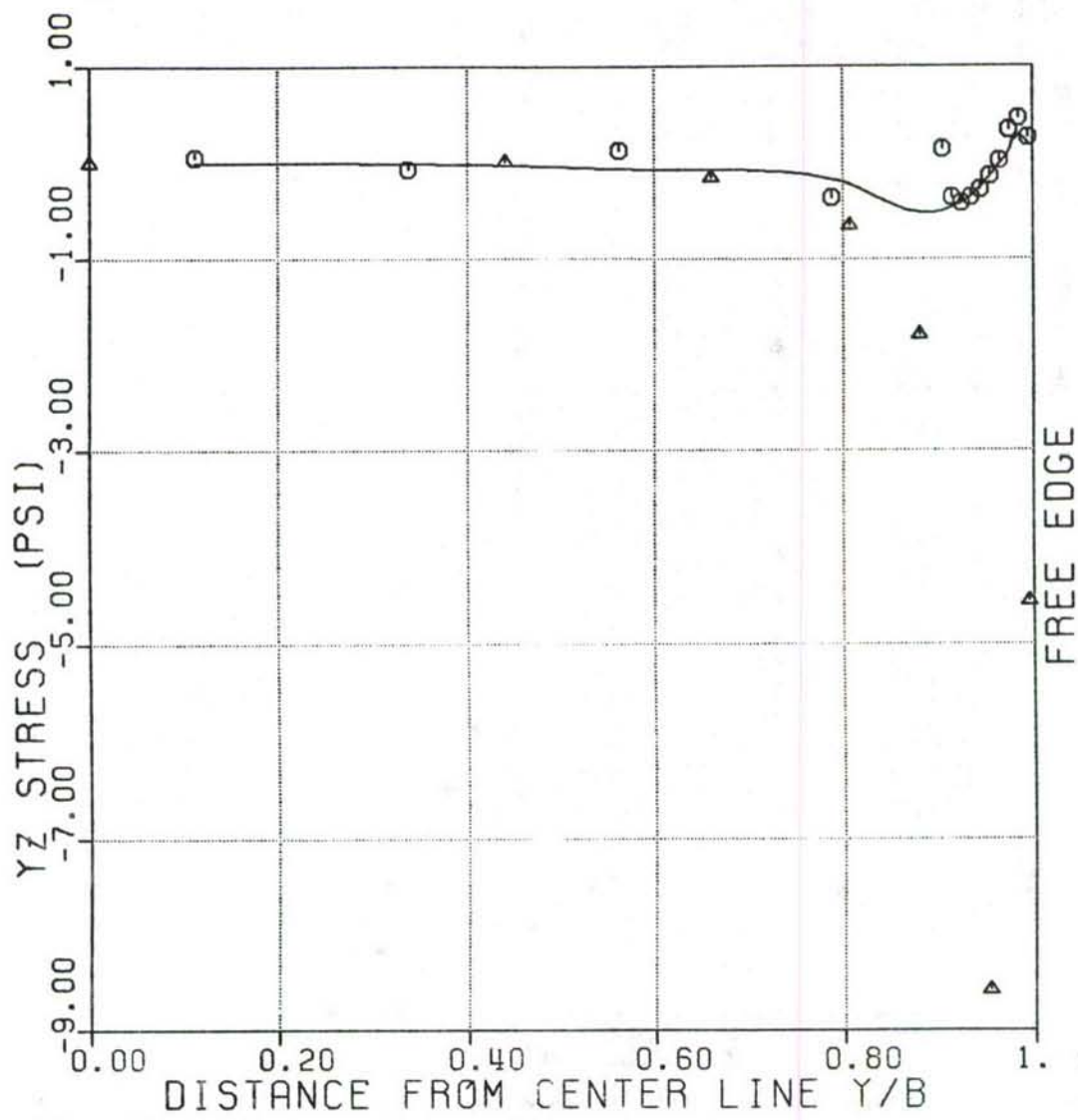


Figure 50: YZ-stress at R11 for 22-layer coupon.

□ N=33, 23X13
 ↑ CHANG 1987
 ★ DANDAN
 - SPLINE FIT OF DATA INDICATED BY ★

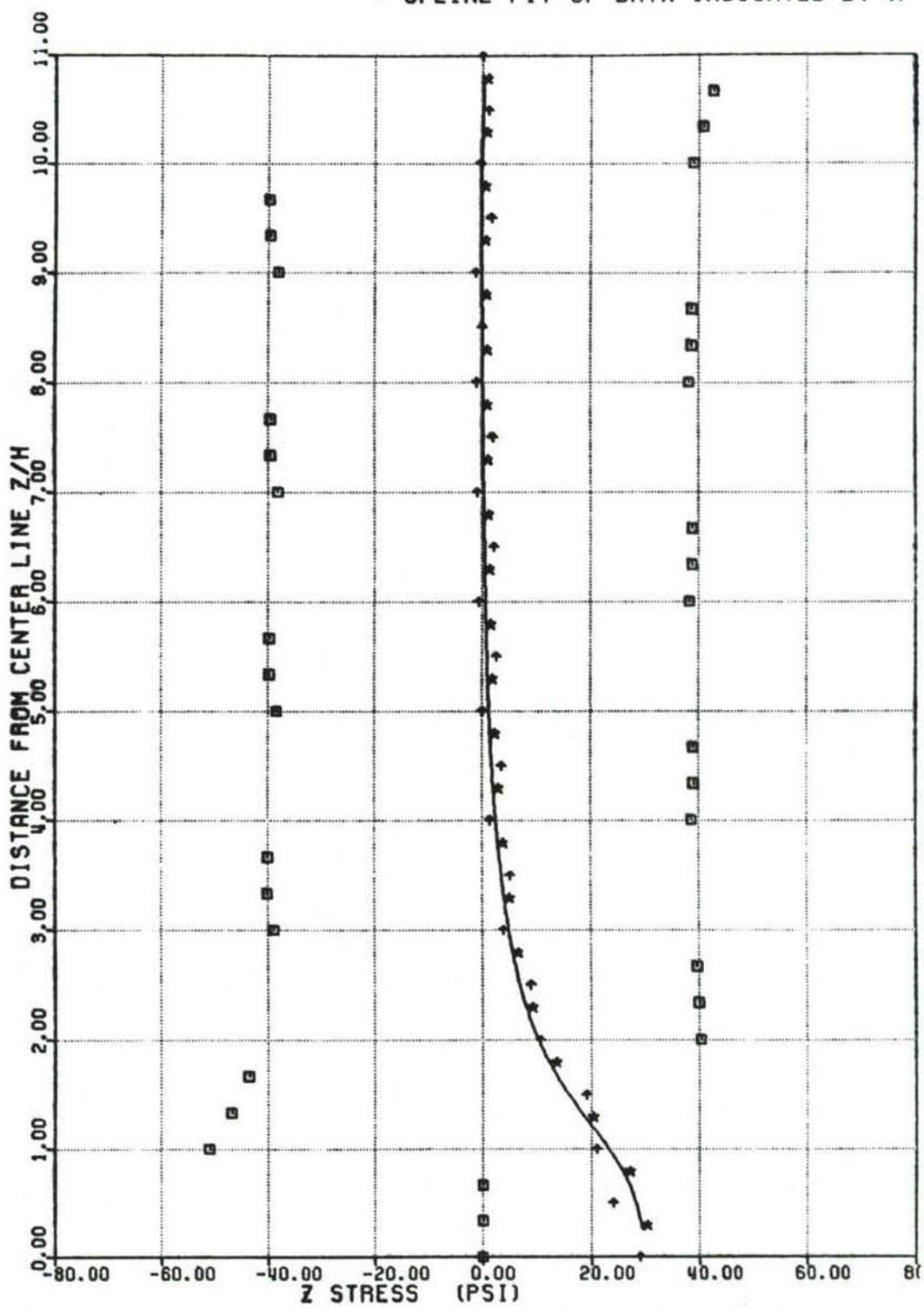


Figure 51: Through the thickness distribution of Z-stress at $y/b=0.995$ for the 22-layer coupon.

□ N=33, 23X13
 ↑ CHANG 1987
 ★ DANDAN
 - SPLINE FIT OF DATA INDICATED BY ★

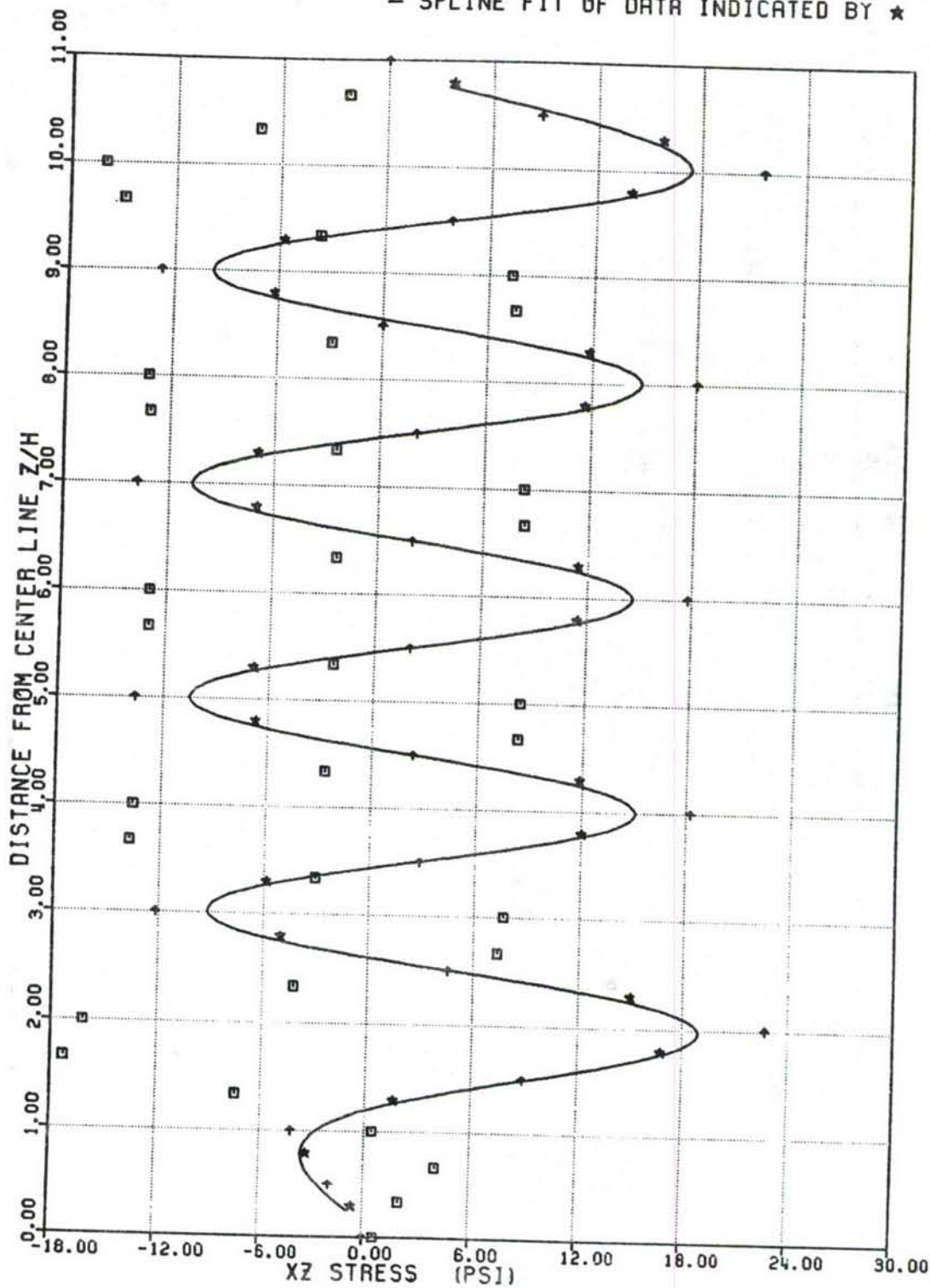


Figure 52: Through the thickness distribution of XZ-stress at $y/b=0.995$ for the 22-layer coupon.

□ N=33, 23X13
 ↑ CHANG 1987
 ★ DANDAN
 - SPLINE FIT OF DATA INDICATED BY ★

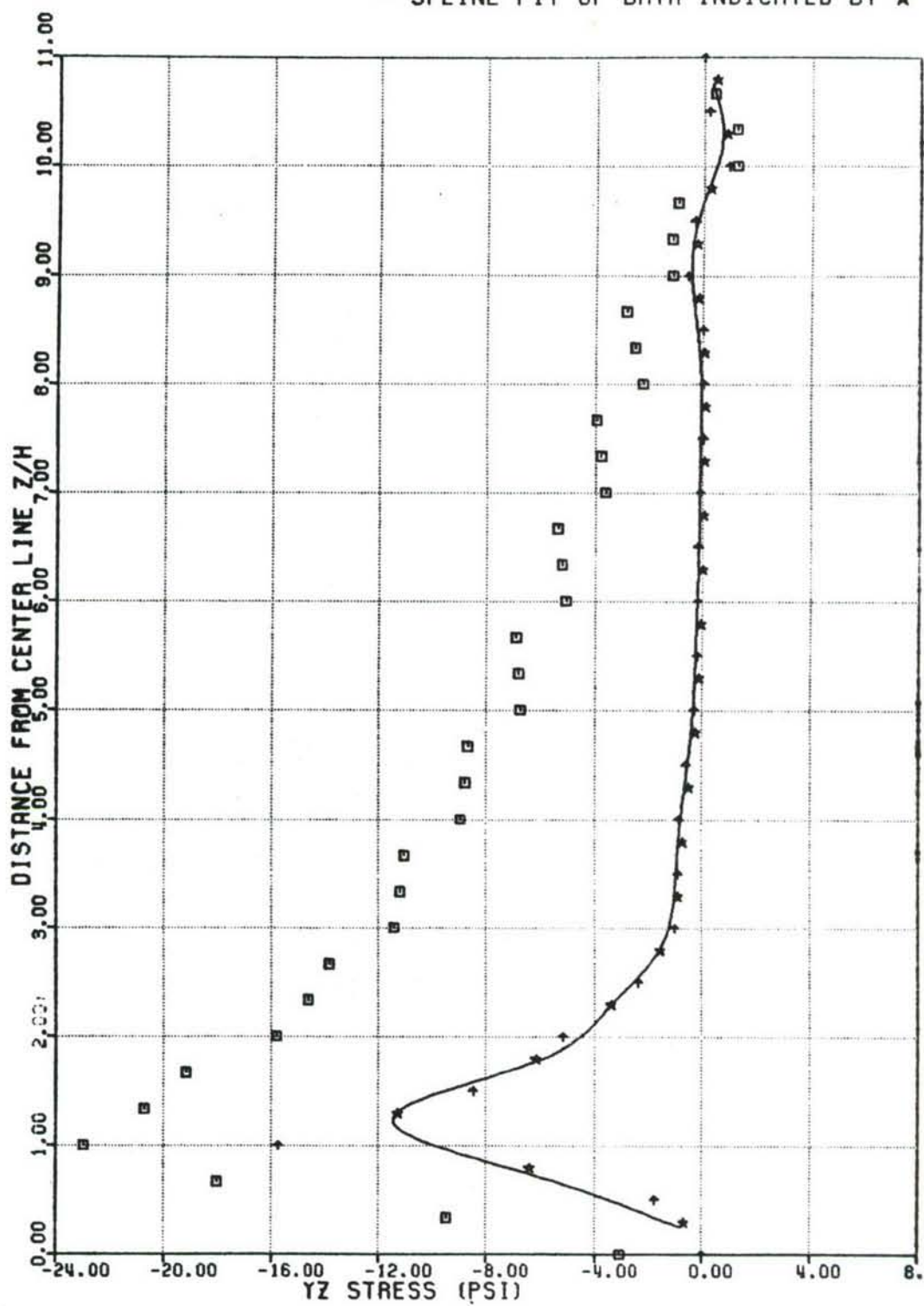


Figure 53: Through the thickness distribution of YZ-stress at $y/b=0.995$ for the 22-layer coupon.

22 LAYERS ZZ-STRESS AT R1

△ DANDAN
○ 23X13 N=22

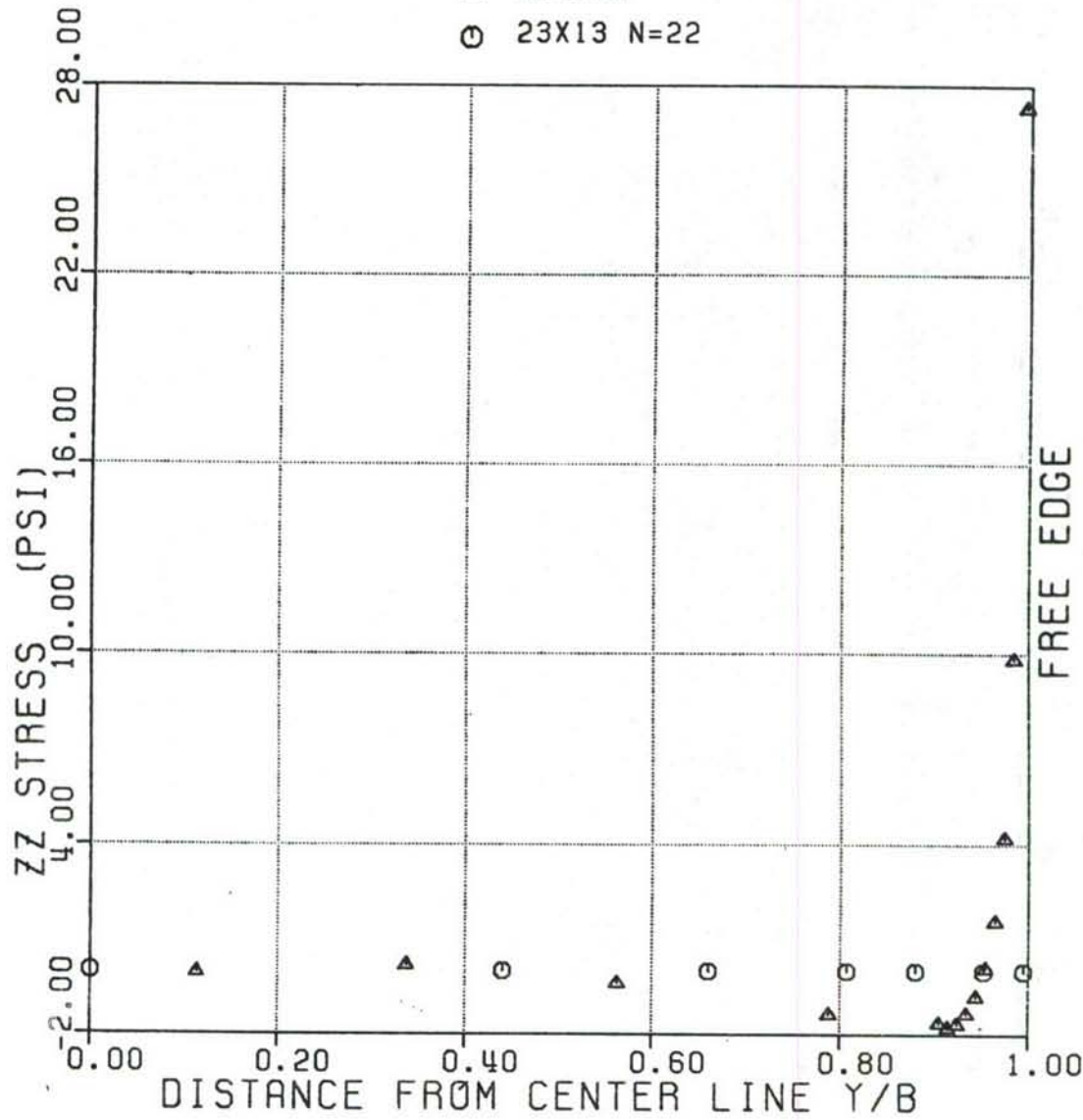


Figure 54: Z-stress at R1 for 22-layer coupon.

22 LAYERS ZZ-STRESS AT R5

△ DANDAN
○ 23X13 N=22

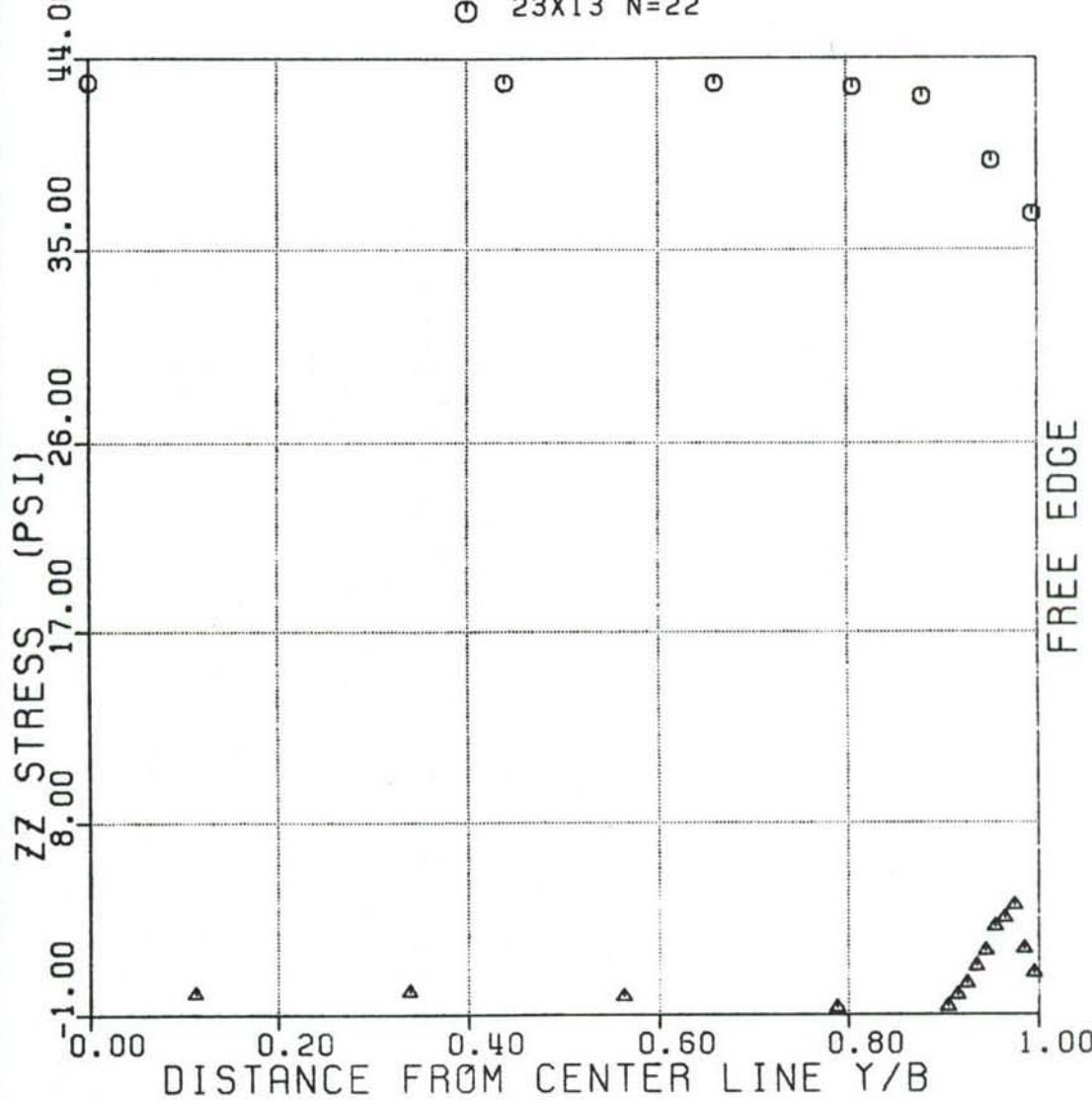


Figure 55: Z-stress at R5 for 22-layer coupon.

22 LAYERS ZZ-STRESS AT R6

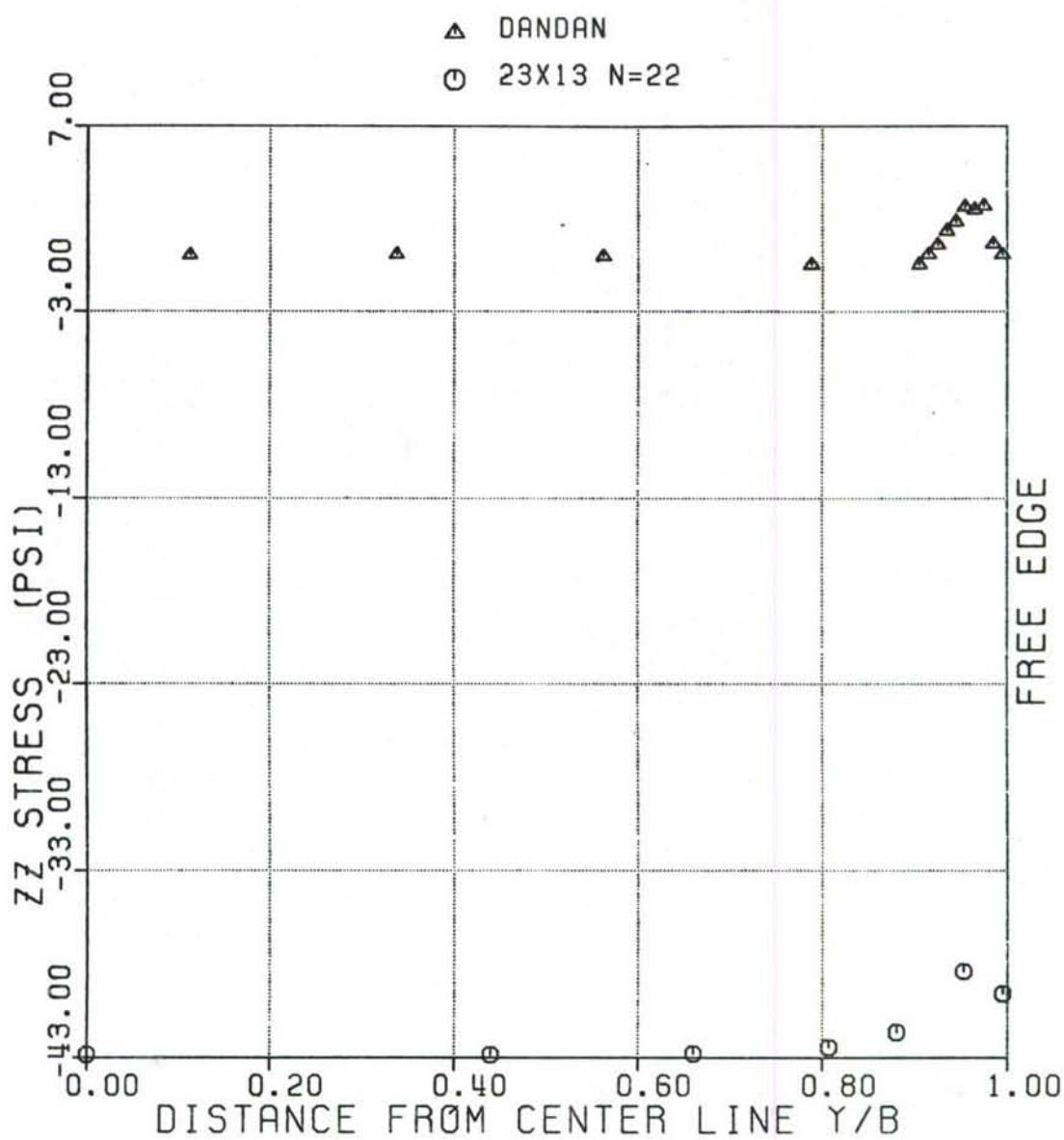


Figure 56: Z-stress at R6 for 22-layer coupon.

22 LAYERS ZZ-STRESS AT R11

△ DANDAN

○ 23X13 N=22

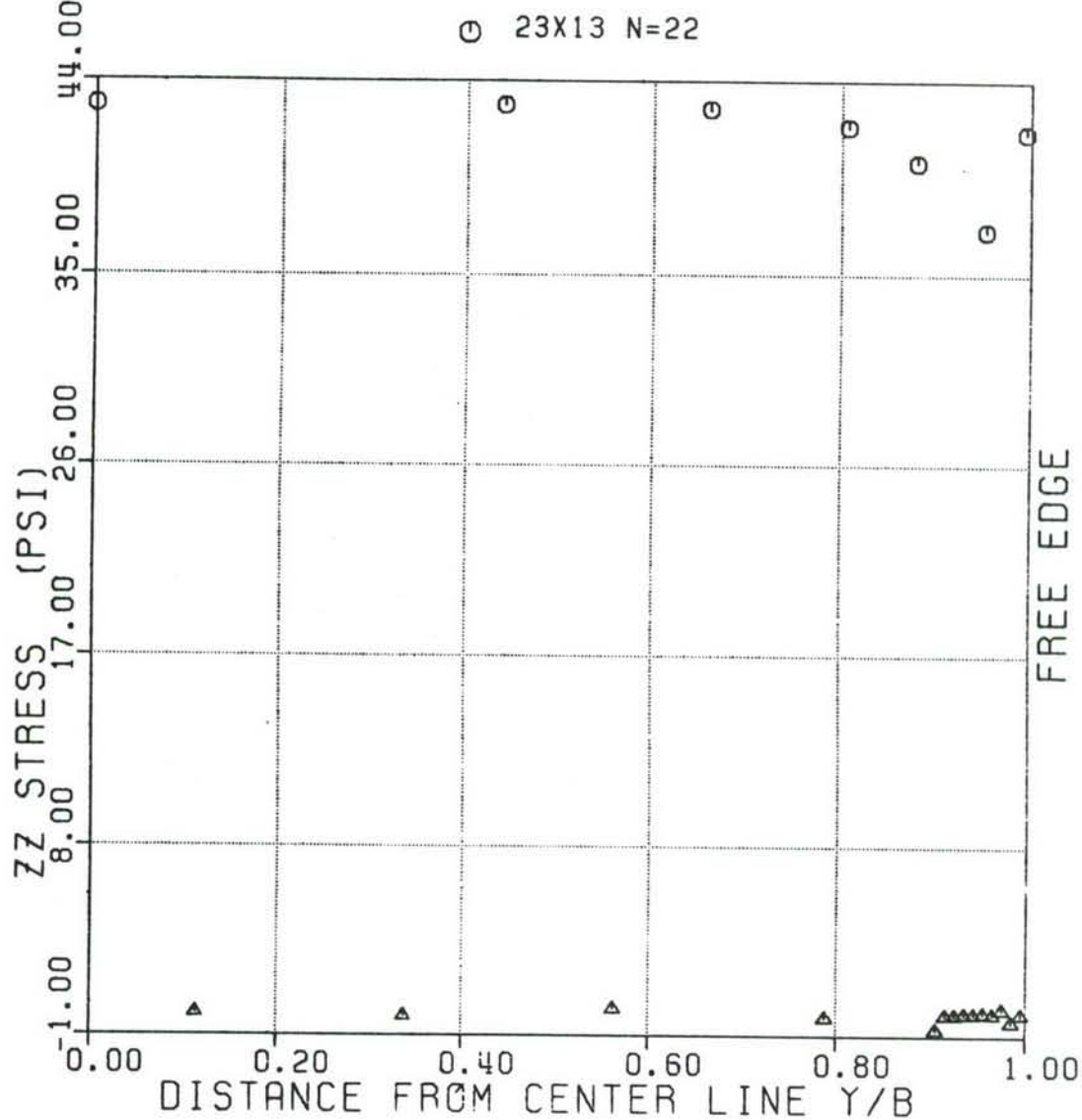


Figure 57: Z-stress at R11 for 22-layer coupon.

4.1.5 Summary and Conclusions

1. The Q8 and Q9 elements are superior to the Q4 element for the analysis of plates. However, for analysis of coupons under uniform extension, the performance of the Q8 and Q9 elements was comparable to the Q4 element. The CPU times needed for the Q8 and Q9 were much greater than required for the analysis using Q4 elements. Thus, the Q4 element appears to give the better combination of accuracy and economy of computational effort for coupons.
2. To improve the predicted results for σ_x and τ_{xy} at $y/b=0$, refinement along the longitudinal direction seems to be most effective. However, the solution at the free-edge depended upon thickness refinement. The best results at the free-edge for σ_x were for $N=6$, while for τ_{xy} they were for $N=10$.
3. The results for τ_{xz} and τ_{yz} did not improve significantly with refinement in x- or y-directions. The thickness refinement improved the predicted results at the free-edge for τ_{xz} , but did not satisfy the traction-free boundary condition at the free-edge for τ_{yz} .
4. The predicted results for σ_z are all either zero or close to zero for the four-layer delamination specimens. However, for the 22-layer delamination specimen, they were oscillatory along the z-coordinate and quite different from the results obtained by Chang [11] and Dandan [12].
5. The predicted displacements for free-edge delamination specimens are close to Pagano's results. For $N=2$ the displacement results are slightly overpredicted, and for $N=6$ and $N=10$, the displacements are slightly underpredicted.

Section V

DISCUSSION

In the present research program, the theoretical studies carried out have included two distinct approaches to the problem of stress analysis of composite laminates. One approach consisted of a specialization of the three-dimensional elastostatics theory to the case of free-edge delamination specimens under uniform axial strain in which the stress field is independent of the longitudinal coordinate. The other approach consisted of development and application of theories of laminated plates to the problem of free-edge delamination. The present report covers study of the applicability of the existing "discrete laminate theory" as one of the first steps in the research program. This investigation has served to establish the pattern for later efforts on improved theories for study of free-edge delamination of composite laminates.

The equations of the discrete laminate theory are well known. These have been included in this report for completeness and for the purpose of pointing out the theoretical assumptions inherent in the theory. Mawenya and Davis [5] had previously presented a finite element implementation of the theory, but they provided no details and did not apply the theory to free-edge delamination.

The equations of the discrete laminate theory, essentially treating a laminate plate as a stacking of Mindlin plates, assumes linear variation of the in-plane displacements over the thickness of each layer ensuring continuity of displacements at the interfaces. As part of the present research effort, the equations have been written in matrix form such that the matrix of operators is self-adjoint in an appropriate linear vector space. The general formulation was written for the dynamic problem in the convolution

product space and then, for the elastostatic problem, a special form was defined in the inner product space. For such systems of equations, standard techniques are available for the construction of variational principles and for identification of consistent boundary operators. General variational formulations with extensions and useful specializations have been explicitly developed for the problem. One specialized variational formulation, corresponding to the popular potential energy theory, has been used to develop finite element procedures.

Three different isoparametric finite element interpolation schemes viz., the four-point Lagrangian, the nine-point Lagrangian, and the eight-point serendipity, have been implemented in a computer program written initially for an IBM 3081 mainframe computer and later modified to run on a CRAY-XMP/28. These finite element procedures were verified through application to homogeneous as well as sandwich plate problems for which solutions are available. Their effectiveness in modelling the stress-distribution in free-edge delamination specimens has been examined.

The present investigation indicated that the discrete laminate theory of laminated plates is quite effective in modelling displacements in plates subjected to arbitrary transverse loads. The shear effects can be allowed for satisfactorily. For such problems, the higher order elements viz., the nine-point Lagrangian and the eight-point serendipity, performed better than the simple four-point Lagrangian element. However, for application to free-edge delamination, the entire approach is inadequate. The stress distribution obtained for the example problems was reasonably good with respect to in-plane stresses, but the theory could not give reasonable estimates of the other three components of stress. The traction-free edge condition could not be modelled. The stresses had to be calculated directly from the stress-strain relationships because use of equilibrium equations for determination of shear stress and transverse stress would involve numerical differentiation of quantities for which estimates only at a finite

number of points were available. Mesh refinement to get a sufficiently large number of points would make the cost of analysis prohibitive.

The studies showed that refinement along the length or the width of the specimen had relatively little effect on the quality of results. Refinement over the thickness i.e., subdivision of each lamina into a number of sublayers, helped improve accuracy. This suggests that a distribution of in-plane stresses of an order higher than linear over the thickness of each lamina might represent the actual stress distribution more closely.

In order to satisfy the traction-free conditions along the free-edges, it is necessary that edge tractions appear as field variables in the set of field equations. An alternative, of course, is to use Lagrange multiplier techniques to enforce constraints

For direct use of equilibrium equations to determine the shear stresses and the direct transverse stress, explicit introduction of interface tractions as field variables in the theory would avoid the need for expensive numerical differentiations. Also this would ensure continuity of traction across interfaces and perhaps yield better approximation for the interfacial stresses.

The discrete laminate theory discussed in this report is based on assumptions regarding transverse and in-plane displacements. An alternative is to assume variation of in-plane stresses and to derive the other stress components through equilibrium equations. If force resultants appear in the expressions for stresses, and are regarded as field variables of the problem, the constitutive relationships for these need to be established. If it is assumed that there is no interfacial slip, it would be impossible for any layer to deform independently of the others. This would necessarily lead to a coupling in the constitutive relations for the force resultants of individual layers.

Pagano's [10] theory which uses the assumption of linear variation of in-plane stress components over the thickness of each layer or sublayer, satisfies equilibrium

pointwise, satisfies constitutive equations and interfacial continuity of tractions as well as displacements, and can satisfy traction boundary conditions for free-edge delamination specimens exactly, appears to be an appropriate approach for determination of stress fields in composite laminate plates with natural boundary conditions. The case of free-edge delamination specimens is a specialization of the general theory. The theory has been difficult to use because of the large number of field variables involved and limitations on computational capabilities. A research effort directed towards development of finite element models based on Pagano's theory or development of other methods of solution of the set of differential equations could be useful.

REFERENCES

1. Srinivas, S., *A Refined Analysis of Composite Laminates*, J. Sound & Vib., Vol. 30, No. 4, 495-507, 1973.
2. Sun, C.T. and Whitney, J.M., *Theories for the Dynamic Response of Laminated Plates*, AIAA J., Vol. 11, 178-183, 1973.
3. Reddy, J. N., *A Penalty Plate-Bending Element for the Analysis of Laminated Anisotropic Composite Plates*, Int. J. Numer. Methods in Engrg., Vol. 15, pp. 1187-1206, 1980.
4. Reddy, J. N., *Dynamic (Transient) Analysis of Layered Anisotropic Composite Material Plates*, Int. J. Numer. Methods in Engrg., Vol. 19, 237-255, 1983.
5. Mawenya, A.S. and Davis, J.D., Finite element bending analysis of *Finite Element Bending Analysis of Multilayer Plates*, Int. J. Numer. Methods in Engrg., Vol. 8, 215-225, 1974.
6. Sandhu, R. S., and Pister, K. S., *A Variational Principle for Linear Coupled Field Problems*, Int. J. Eng. Sci., Vol. 8, 986-999, 1970.
7. Sandhu, R. S., and Pister, K. S., *Variational Principles for Boundary Value and Initial Boundary Value Problems*, Int. J. Solids Struct., Vol. 7, 639-654, 1971.
8. Sandhu, R. S., and Salaam, U., *Variational Formulation of Linear Problems with Nonhomogenous Boundary Conditions and Internal Discontinuities*, Comp. Meth. Appl. Mech. Eng., Vol. 7, 75-91, 1975.
9. Sandhu, R. S., *Variational Principles for Finite Element Approximations in Finite Elements in Water Resources Engineering*, G. F. Pinder and C. A. Brebbia (eds.), Pentech Press, 1976.

10. Pagano N.J., *Stress Fields In Composite Laminates*, Int. J. Solids Structures, Vol. 14, 385-400, 1978.
11. Chang, C. C., *Finite Element Analysis of Laminated Composite Free-Edge Delamination Specimens*, Ph.D. Dissertation, The Ohio State University, 1987.
12. Sandhu, R. S., Sierakowski, R. L., Wolfe, W. E., and Dandan, R. A., *Finite Element Analysis of Laminated Composite Axisymmetric Solids, Vol. I - Theory and Applications*, Wright Laboratory Technical Report WL-TR-91-3020, Vol. 1, Wright-Patterson Air Force Base, Ohio, 1991.
13. Mikhlin, S. C., *The Problem of the Minimum of a Quadratic Functional*, Holden-Day, San Francisco, 1965.
14. Plantema, F.J., *Sandwich Construction*, John Wiley and Sons, 1966.
15. Khatua T.P and Cheung Y.K, *Bending and Vibration of Multilayer Sandwich Beams and Plates*, Int. J. Numer. Methods in Engrg., Vol. 6, 11-24, 1973.
16. Pagano N.J. and Hatfield S.J, *Elastic Behaviour of Multilayered Bidirectional Sandwich Beam and Plates*, AIAA J., Vol. 10, 931-933, 1972.
17. Pagano N.J., *Exact Solution for Rectangular Bidirectional Composites and Sandwich Plates*, J. Composite Matls., Vol. 4, 20-24, 1970.
18. Zienkiewicz, O.C., *The Finite Element Method*, 3rd edition, McGraw-Hill, 1977.
19. Ugural, A.C., *Stresses in Plates and Shells*, McGraw-Hill, 1981.
20. Azar, J. J., *Bending theory of multilayer sandwich plates*, AIAA J., Vol. 6, 2166-2169, 1969.

Appendix A

VARIATIONAL FORMULATION

Often, obtaining an approximate solution to a coupled boundary value problem relies on appropriate variational formulation. Following Sandhu's [6] [7] [8] [9], extension of Mikhlin's [13] basic variational theorem to coupled linear boundary value problems including nonhomogenous boundary condition, we present here a summary of the basic concepts for setting up the variational formulation applicable to the problem of laminated plates.

A.1 PRELIMINARIES

A.1.1 Boundary Value Problem

Consider the boundary value problem

$$Au = f \quad \text{on } R \tag{A.1}$$

$$Cu = g \quad \text{on } \partial R \tag{A.2}$$

where ∂R is the boundary of the open connected region R in an euclidean space. \bar{R} is the closure of R . A and C are linear bounded operators. Let V_R and $V_{\partial R}$ be linear vector spaces defined on the regions indicated by the subscripts, and $W_R, W_{\partial R}$ be dense subsets in V_R and $V_{\partial R}$, respectively. Then the differential operators A and C can be regarded as the transformations

$$A: W_R \rightarrow V_R \tag{A.3}$$

$$C: W_{\partial R} \rightarrow V_{\partial R}$$

A.1.2 Bilinear Mapping

Let V and S be linear vector spaces. A bilinear mapping $B:V \times V \rightarrow S$ assigns to each ordered pair of vectors $u, v \in V$ an element in S . Furthermore, bilinearity is satisfied for $u_1, u_2, v_1, v_2, u, v \in V$, if

$$B(\alpha u_1 + u_2, v) = \alpha B(u_1, v) + B(u_2, v) \quad (\text{A.4})$$

$$B(u, \alpha v_1 + v_2) = \alpha B(u, v_1) + B(u, v_2) \quad (\text{A.5})$$

where α is scalar. For convenience, we shall use the notation.

$$B_R(u, v) = \langle u, v \rangle_R \quad (\text{A.6})$$

To set up a variational formulation, symmetric, nondegenerate bilinear mappings are used, i.e.,

$$\langle u, v \rangle_R = \langle v, u \rangle_R \quad (\text{A.7})$$

and

$$\langle u, v \rangle = 0 \quad \text{for all } v \text{ if and only if } u = 0 \quad (\text{A.8})$$

A.1.3 Self-Adjoint Operator

An operator A^* on V is said to be the adjoint of A with respect to symmetric bilinear mapping $B_R:V \times V \rightarrow S$, where S is a linear vector space, if

$$\langle u, Av \rangle_R = \langle v, A^*u \rangle_R + D_{\partial R}(v, u) \quad (\text{A.9})$$

for all u and $v \in V$ and where $D_{\partial R}(u, v)$ represents quantities associated with boundary ∂R of R . If $A = A^*$, then A is said to be self-adjoint. If A is a self-adjoint operator, then $D_{\partial R}(v, u)$ is antisymmetric, i.e.,

$$D_{\partial R}(v, u) = -D_{\partial R}(u, v) \quad (\text{A.10})$$

Furthermore, A is said to be symmetric with respect to the bilinear mapping, if

$$\langle u, Av \rangle_R = \langle v, Au \rangle_R \quad (\text{A.11})$$

The boundary operator C is said to be consistent with the self-adjoint operator A if

$$D_{\partial^R}(v, u) = \langle u, Cv \rangle_{\partial^R} - \langle v, Cu \rangle_{\partial^R} \quad (\text{A.12})$$

A.1.4 Gateaux Differential

If $\Omega: V \rightarrow S$, where V is such that if $u, \bar{u} \in V$, $u + \lambda \bar{u} \in V$ for scalar λ ,

the Gateaux differential of $\Omega(u)$ along a path \bar{u} is defined by

$$\delta_{\bar{u}} \Omega(u) = \lim_{\lambda \rightarrow 0} \frac{\Omega(u + \lambda \bar{u}) - \Omega(u)}{\lambda} \quad (\text{A.13})$$

where \bar{u} is referred to as the path.

A.2 THEOREM

For the field equations (A.1) we define

$$\Omega(u) = \langle u, Au \rangle_R - 2 \langle u, f \rangle_R \quad (\text{A.14})$$

The Gateaux differential of Ω is:

$$\begin{aligned} \delta_{\bar{u}} \Omega(u) &= \lim_{\lambda \rightarrow 0} \frac{\langle u + \lambda \bar{u}, A(u + \lambda \bar{u}) \rangle - 2 \langle u + \lambda \bar{u}, f \rangle - \langle u, Au \rangle + 2 \langle u, f \rangle}{\lambda} \quad (\text{A.15}) \\ &= \langle u, A\bar{u} \rangle + \langle \bar{u}, Au \rangle - 2 \langle \bar{u}, f \rangle \\ &= 2 \langle \bar{u}, Au - f \rangle \end{aligned}$$

The Gateaux differential vanishes at the solution $u = u_0$ where $Au_0 - f = 0$. Conversely, if $\delta_{\bar{u}} \Omega(u)$ vanishes for all \bar{u} , nondegeneracy of \langle , \rangle implies $Au_0 - f = 0$. If the range of the bilinear mapping is the real line, vanishing of the function Ω would imply its minimum, maximum, or stationary value, depending upon the operator A being positive, negative or semi-definite.

A.3 LINEAR COUPLED PROBLEMS

The above discussion for a single-valued function u can be extended to the case of several variables. If there are n variables, V is defined as the direct sum

$$V = V_1 + V_2 + \dots + V_n \quad (\text{A.16})$$

and an element $u \in V$ is an n -tuple (u_1, u_2, \dots, u_n) with $u_i \in V_i$ for $i=1, 2, \dots, n$. A bilinear mapping on V is defined as

$$\langle u, v \rangle = \langle u_1, v_1 \rangle_{R^1} + \langle u_2, v_2 \rangle_{R^2} + \dots + \langle u_n, v_n \rangle_{R^n} \quad (\text{A.17})$$

where $\langle \cdot, \cdot \rangle_{R^i}$ is defined for components u_i, v_i of $\{u\}, \{v\}$ respectively.

If the field and boundary condition of a linear coupled boundary value problem are:

$$\sum_{j=1}^n A_{ij} u_j = f_i \quad \text{on } R \quad (\text{A.18})$$

$$\sum_{j=1}^n C_{ij} u_j = g_i \quad \text{on } \partial R \quad i=1, 2, \dots, n \quad (\text{A.19})$$

the governing functional based on Eqs. (A.18) and (A.19) is

$$\Omega(u) = \sum_{i=1}^n \left\langle u_i, \sum_{j=1}^n A_{ij} u_j - 2f_i \right\rangle_R + \sum_{i=1}^n \left\langle u_i, \sum_{j=1}^n C_{ij} u_j - 2g_i \right\rangle_{\partial R} \quad (\text{A.20})$$

The set of operators A_{ij} is said to be self-adjoint with respect to the bilinear mapping, if

$$\left\langle v_i, \sum_{j=1}^n A_{ij} u_j \right\rangle_R = \left\langle \sum_{j=1}^n u_j, A_{ji} v_i \right\rangle_R + D_{\partial R}(u_j, v_i) \quad (\text{A.21})$$

where $D_{\partial R}(u_j, v_i)$ represents quantities associated with boundary ∂R of R . The boundary operators C_{ij} are said to be consistent with the field operator A_{ij} if

$$D_{\partial R}(u_j, v_i) = \sum_{j=1}^n \left\langle u_j, C_{ji} v_i \right\rangle_{\partial R} - \left\langle v_i, \sum_{j=1}^n C_{ij} u_j \right\rangle_{\partial R} \quad (\text{A.22})$$

Appendix B

SOLUTION OF SANDWICH PLATE

B.1 PRELIMINARIES

Based on Plantema [14], the series solution for sandwich plate was calculated. In this case, the bending of plates is assumed to be due to bending of stiff layers and the shear deformation of the core layer, so that

$$w = w_b + w_s \quad (B.1)$$

where the transverse load is the only applied load and the stiff layers are isotropic. w_b satisfies the equation:

$$D \nabla^4 w_b = q \quad (B.2)$$

where

$$D = \frac{E t_1^3}{12(1 - \nu^2)}$$

and w_s satisfies the equation:

$$-S \nabla^2 w_s = q \quad (B.3)$$

where

$$S = \frac{(t_2 + t_1)^2}{t_2} G_2$$

B.2 METHOD OF SOLUTION

For a simply supported rectangular plate the transverse displacement due to bending may be represented by Fourier series in the form:

$$w(x,y) = \sum_{m=1}^{\infty} \sum_{n=1}^{\infty} a_{mn} \sin \frac{m\pi x}{a} \sin \frac{n\pi y}{b} \quad (\text{B.4})$$

and corresponding load by:

$$q(x,y) = \sum_{m=1}^{\infty} \sum_{n=1}^{\infty} q_{mn} \sin \frac{m\pi x}{a} \sin \frac{n\pi y}{b} \quad (\text{B.5})$$

Multiplying both sides of (B.5) by $\sin \frac{m'\pi x}{a} \sin \frac{n'\pi y}{b}$ and integrating over the domain,

for $q(x,y) = q_o$,

$$q_{mn} = \frac{16q_o}{\pi^2 mn}$$

Substituting (B.4) and (B.5) into (B.2) and evaluating a_{mn} , $w_b(x,y)$ is:

$$w_b(x,y) = \frac{16q_o}{\pi^6 D} \sum_m^{\infty} \sum_n^{\infty} \frac{\sin(m\pi x/a) \sin(n\pi y/b)}{mn[(m/a)^2 + (n/b)^2]^2} \quad (m, n = 1, 3, \dots) \quad (\text{B.6})$$

Similarly, (B.3) can be solved to yield:

$$w_s(x,y) = \frac{16q_o}{\pi^4 S} \sum_m^{\infty} \sum_n^{\infty} \frac{\sin(m\pi x/a) \sin(n\pi y/b)}{mn[(m/a)^2 + (n/b)^2]} \quad (m, n = 1, 3, \dots)$$

The series solution was obtained through summation of 151 terms in the case of isotropic sandwich plate for $a=b=10$ inches and $q_o = 1.0 \text{ lb/in}^2$. In the orthotropic case the results given by Mawenya and Davis [5] were used for comparison purposes.